A STUDY OF THE SURFACE FINISH PRODUCED BY GRINDING. PART 2. (Part 1. M. Tech - 1972)

A thesis submitted for the degree of Doctor of Philosophy

by

Gordon John Jones

Department of Production Technology, Brunel University

April 1985

Part one of this thesis is the author’s masters thesis

ABSTRACT

A survey of the literature of grinding and surface texture shows the influence of dressing and wear on surfaces involved in the process and the advantages of stylus profilometry for data collection from both grinding wheels and ground surfaces. Statistical analysis is favoured for surface profile characterization and, of the various parameters used, power spectral density alone offers some prospect of effective comparison between these surfaces.

Work on grinding with single crystals of natural corundum was eventually discontinued in favour of experiments with conventional bonded grinding wheels subjected to a dressing operation and some wear in grinding steel surfaces. Statistical parameters representing the surfaces are computed using data obtained from profilograms. Results in terms of power spectral density are presented showing progressive improvement following upon developments in apparatus and methods which facilitated the use of larger surface profile samples. Transfer functions are used to relate power spectra representing corresponding pairs of surfaces.

The significance of power spectral density applied to surface profile characterization is discussed and, in this context, it is suggested that these should be described as variance spectra. Attention is drawn to certain disadvantages of variance spectra applied to grinding wheel and ground surface profiles.

Methods designed to improve presentation of variance spectra lead to development of a proposed new and more suitable spectrum in which density of standard deviation of surface profile ordinates with respect to frequency is plotted against frequency. Transfer functions calculated from related pairs of these standard deviation spectra show a strong linear correlation with frequency and offer prospects of convenient comparison between the profiles of the various surfaces involved in grinding.

CONTENTS

Chapters and pages are numbered to follow consecutively from Part 1 in order to facilitate reference to the earlier work and to avoid possible confusion between the two parts. Figures are numbered to identify them with Chapters and Appendices to correspond with those Chapters to which their contents primarily relate

Acknowledgements

This work has been made possible through the co-operation of the following members of staff of Brunel University and Willesden College of Technology. The help and advice of these and others whose names are recorded in Part 1 is acknowledged with gratitude.

Mr. R. Bulpett

Mr. E. Cave

Mr. E. H. Cittern

Mr. R. Duggan

Dr. B. F. Figgins

Mr. S. J. Humphrys

Mr. J. McMenemy

Prof. R. W. New

Mr. R. Radford

Mr. D. C. Scrimshaw

Mr. G. W. Smith

INTRODUCTION

This work is concerned with the finish or surface texture produced on the workpiece as a result of grinding. Grinding, in the context of this study, refers to operations carried out on machine tools with provision for controlling the geometry and dimensions of the workpiece, such as cylindrical and surface grinders. The object of the investigation is to obtain better understanding of the influence on the surface texture of the ground surface exerted by the surface of the grinding wheel.

The nature of the grinding wheel surface is determined not only by the structure of the wheel but, to a considerable extent by dressing carried out preparatory to grinding and also by wear during a grinding operation.

A study of the relationship between the ground surface and that of the grinding wheel requires means for characterizing both surfaces in terms suitable for quantitative comparison. Standardized surface texture parameters are calculated on the basis of a continuous surface profile. Also, numerical assessment by means of such parameters does not uniquely represent a surface profile and is therefore unreliable for detailed study or accurate comparisons.

Furthermore such parameters are unsuitable for application to a discontinuous profile such as that of a grinding wheel.

In order to relate the surface profile of workpiece and grinding wheel it is necessary to identify some parameter or parameters applicable to both types of surface and capable of effectively comparing them. Meaningful comparison indicates the need for better surface characterization than that provided by any standard surface texture parameter such as the arithmetical average roughness value R_a. Also the method or methods adopted must be applicable to a pair of surfaces one of which has a discontinuous profile.

Some preliminary work, devoted mainly to surface relationships in grinding has already been carried out by the author. This was submitted for the award of an M Tech degree and,since the same title is used, this earlier thesis will be referred to as Part 1 and the present work as Part 2.

Part 1 contains an outline history of the grinding process. This includes notes on the abrasive and other materials used in grinding and the composition of bonded grinding wheels currently in use. Vitreous bonded grinding wheels containing aluminium oxide abrasive synthesized in the electric furnace were found to have been is use since about 1900. These represent the type of wheel in most widespread use for the grinding of ferrous materials and were used exclusively throughout the investigation.

In Part 1 the mechanism of dressing and wear of grinding wheels is discussed with some emphasis on the facts, not then universally recognized, that asperities of different heights exist in the active zone of a grinding wheel and that there are a number of such asperities on that surface of a grit interacting with the workpiece. Since these asperities are involved in the process of removing material from the workpiece and are also affected by wear of the grinding wheel their number and distribution has to be considered in studying the surfaces concerned in the process.

One of the objectives formulated in Part 1 was to repeat experiments described in an earlier publication, designed to estimate the heights of asperities by measurement of scratches produced on the ground workpiece by the action of the grinding wheel. These experiments provided some idea of the probable nature of the distribution of asperities with respect to height and confirmed the need for methods capable of measuring the heights of asperities directly from the grinding wheel.

Most of the papers examined during the Part 1 invest--igation were published during the nineteen-fifties and early nineteen-sixties. These contain much information on the mechanics of grinding but relatively few deal in any detail with surface texture of the ground workpiece. However, some information was found on obtaining traces, by means of a stylus, from the surface of a grinding wheel rotated at extremely low speed, and in presenting the distribution of heights in histogram form. Developments of the first method were later used by the author for experiments carried out in Part 2 while histograms had been used in Part 1 to represent profile height distribution.

In part 1 asperity heights were determined by measurement of profilograms obtained from the surfaces of grinding wheels. From these measurements relative frequencies were calculated and plotted to define the corresponding distribution curves. These distributions are compared with their counterparts obtained from the corresponding ground surfaces and a measure of correlation is demonstrated.

Profile height distribution curves were recognised as providing a limited description of any surface whether of the grinding wheel or the ground workpiece. Once again, attention was directed to the fact that not only was it necessary to cope with problems peculiar to the grinding process but also to seek parameters capable of more completely describing the surfaces, which might also be useful in investigating the nature of any relationship between grinding wheel and workpiece surfaces.

Average roughness parameters such as R_a, sometimes failed to differentiate between surfaces with very different characteristics, mainly by reason of relative insensitivity to the frequency of surface features, and were probably of less value, for the purposes envisaged, than profile height distribution curves.

Some use was also made in Part 1 of scanning electron microscopy in order to provide visual evidence of the nature of grinding wheel surfaces. For this purpose, specimens were taken from the periphery of grinding wheels which had previously been subjected to dressing and grinding operations.

Since these results were obtained at a late stage of the Part 1 investigation, they were presented in an appendix showing the effects of wear on grit surfaces. Preparation of each specimen for examination necessitated its removal from and destruction of a grinding wheel.

At this point it is appropriate to explain the numbering system adopted in Part 2 which follows consecutively from Part 1 to facilitate reference to the earlier work and to avoid possible confusion between the two parts. Chapters in Part 2 are therefore numbered from 8 to 13, pages from 90 to 261, and the bibliographical references (20) to (42). Illustrations and tables are numbered to identify them with chapters, and appendices to correspond with those chapters to which their content primarily relates.

Apart from the wastage of grinding wheels resulting from the procedure adopted in Part 1 for the preparation of specimens for electron microscopy, cutting specimens from a bonded grinding wheel excluded the possibility of re-examining the same grits, or the same area of wheel surface at, for example, a more advanced stage of wear. A further point in favour of some alternative to the use of a bonded grinding wheel was the need to facilitate identification of individual grits in the surface under scrutiny. These considerations led, in the Part 2 investigation, to design and construction of the composite grinding wheel described in Chapter 8.

In the event, work with this composite grinding wheel was confined to its use with large single grits of natural corundum. The results were regarded as somewhat unreliable by reason of problems with the apparatus, some of which remained unsolved.

There is reason to believe that further development of composite grinding wheel methods could yield worth--while results and the justification for not pursuing this line of investigation is that information and facilities became available for profile measurement and statistical characterisation of surface profiles which appeared more likely to yield applicable quantitative results than electron microscopy.

Of the twenty-two published papers dealt with in Chapter 7 a high proportion consider grinding wheel surface profile and contain results obtained from actual grinding operations. Surprisingly few take account of the effects of grinding wheel dressing and wear on the surface concerned, despite the fact that dressing is always necessary and wheel wear inevitably takes place in grinding operations.

Stylus profilometry was apparently used for some aspect of surface measurement in eighteen of the papers examined. Descriptions of two versions of an oscillating stylus profilometer were found in the literature and a further two papers dealing with oscillating stylus profilometry applied to grinding wheels.

Encouraging results had been obtained in Part 1 using stylus profilometry applied to both ground surface and grinding wheel. Also not only did recent publications indicate widespread use and further development of stylus profilometry but also provided evidence that its capacity for resolution of surface detail is more than adequate for the study of surface texture (40). On the basis of this published information and the experience gained in Part 1 it was concluded that stylus profilometry would be the most adaptable and potentially informative method of studying the surfaces involved in the grinding process.

In the present work considerable effort has perforce been concentrated on the grinding wheel: due solely to the special problems met with in the production of profilograms from its surface and their subsequent characterisation. Since the ground surface has a continuous profile the production of profilograms is straightforward and although some aspects of the characterisation problem are common to both surfaces those relating to the grinding wheel present greater difficulty because of its discontinuity. As a result the text contains relatively little on the subject of the ground surface notwithstanding that its roughness represents that output of the process with which this work is primarily concerned.

Reference has already been made to those applications of oscillating stylus profilometry to grinding wheel surfaces found in the literature. The oscillating stylus could penetrate deeply into the voids and more accurately follow the steeply sloping outer sides of grits than the conventional stylus with its large included angle. However, these deeper levels within the grinding wheel obviously did not interact with the workpiece and it was decided that profilometry using more conventional non-oscillating stylus equipment was adequate for the purpose of the current investigation.

The optimum choice of means to analyse and present surface profile data is by no means immediately apparent from the literature. In addition to standardised measures of surface texture such as arithmetical average (R_a) a variety of alternative parameters for surface characterisation are to be found. These include the first and second derivatives of R_a, surface density, height distribution, mean radius of curvature of asperities, slope variance, second-order autoregressive models, and bearing area curves. Shinaishin (27) makes use of power spectral density curves for surface and grinding force analysis while Peklenik (21), (22), (24), (25) employs autocorrelograms and power spectra for surface profile analysis and introduces slope variance in the same context.

Particular interest on the part of the author in power spectra for the study of surfaces was first stimulated by information in one of these papers (21) on the use of autocorrelation functions and dispersion spectra for characterisation of grinding wheel profiles. In later papers by the same author, 'dispersion spectrum' is replaced by 'power spectrum' in reference to the same function: described as the Fourier transform of the autocorrelation function.

In the author's opinion, and in the context of surface profile analysis, the earlier terminology is preferable because 'dispersion' being synonymous with 'variance' has self evident relevance to the description of a profile defined by ordinates while 'power' has no such apparent relevance. Furthermore the use of variance explicitly defines the meaning of a spectrum in which variance density is plotted against frequency of surface profile heights, as in Fig 7.1.

The total area beneath a curve such as that of Fig 7.1 represents the variance of the profile for the total range of frequencies considered; assuming this curve to be a good estimate of some true spectrum. The variance associated with particular frequency bands can also obviously be obtained from such a curve.

In the same paper (21) transfer functions are used to compare surfaces (Fig 7.2) the points defining these curves being the ratios of corresponding pairs of variance density ordinates. Each point on such a curve is a transfer coefficient obtained by dividing the ordinate of the spectral density curve representing the output surface by the corresponding spectral density ordinate for the input surface: corresponding in the sense that both ordinates relate to the same frequency.

These transfer functions represented the most explicit attempt found in the literature to demonstrate the relationship between the roughness of different surfaces: complementary perhaps to comparison of average roughness values but providing significant additional information in graphical form on frequency relationships.

Meaningful comparison of dissimilar surfaces is clearly essential to the present investigation and transfer functions were potentially suitable for this purpose. The fact that they were derived from dispersion spectra provided an incentive to further study of spectral density as a means of surface description. However, the nature of the associated problems were by no means apparent at this stage because the available publications gave little information on the techniques of surface measurement and computation used.

More recently, surface profile ordinate distribution, autocorrelation, and spectral density have again been used as parameters for surface characterisation. Some adverse criticism has been levlled at the last two, by the same author, including statements to the effect that computation of both autocorrelation and spectral density functions is slow and that interpretation requires special abilities; these features rendering the functions unsuitable for practical measurement. However, no information is provided as to the equipment used or the time taken.

Despite the criticisms, information obtained from published data was interpreted as encouragement to proceed further with autocorrelation and spectral density functions as parameters applicable to the investigation of both ground surfaces and grinding wheel surfaces. Spectral density was particularly favoured from the outset because interpretation of the curve appeared more straightforward than for the autocorrelogram and there was the additional prospect of useful comparison by means of transfer functions.

From the foregoing it will be evident that the decison to concentrate on profilometry for surface measurement was influenced by a number of publications while the strongest influence towards spectral analysis is derived from Peklenik's work.

Chapter 9 contains some information relating to the statistical parameters; the apparatus and methods used to obtain profilograms. A brief account of abortive attempts to produce autocorrelograms using a 'package' program is followed by the writing of programs for computing various parameters including power spectral density.

Chapter 10 contains results obtained from surface profile samples defined by 1000 ordinates presented in the form of power spectral density curves. The greatly increased sample size resulted in spectral curves with a much higher standard of smoothness and consistency than those previously obtained from samples of only 100 ordinates. Comparisons between spectra obtained from different surfaces are presented in the form of transfer function curves defined by ordinates calculated as the ratio of corresponding pairs of ordinates from the spectra representing the input and output surfaces.

It will be seen that power spectral density plotted on a natural scale does not provide for effective visual comparison between those parts of the two curves associated with the shorter wavelengths. This is seen, for example, in Fig 10.20. However, the transfer function curve in the associated Fig 10.21 does provide an informative visual comparison between the profiles of a ground surface and the corresponding grinding wheel.

Plotting power spectral density on a logarithmic scale resulted in improved differentiation between spectral density curves. The same technique applied to the transfer function curves indicated that the shape of these for the pairs of surface profiles considered is fairly constant.

Material presented in Chapter 10 includes initial attempts to present results in terms of what were now considered to be good estimates of the power spectra representing surface profiles. It also contains the first attempts to establish the nature of any relationship which might exist between input and output profiles.

As indicated by the title, Chapter 11 is concerned with the search for some alternative presentation of spectral density curves in a form better adapted to the purposes of the investigation. The first step taken in this direction was to consider the units in which the parameter known as power spectral density should be expressed; having regard to the fact that in the context of surface profile study, it is computed from an array of ordinates measured in units of length.

On the basis that the area beneath the power spectral density curve represents variance expressed in linear units to the second power, the horizontal axis may be scaled in terms of frequency expressed as the reciprocal of the unit of length. From this it follows that power spectral density ordinates will be in length units to the third power.

More detailed discussion in Chapter 11 along the lines indicated is followed by results expressed in appropriate units (Table 11.1). Examples of spectral curves scaled in terms of these units are shown as Figs 11.10 and 11.11 and it will be seen that these are described as variance spectra: 'power spectral density' and 'power spectrum' having been discarded as inappropriate terminology for use in the context of surface profile measurement.

The remainder of Chapter 11 is devoted to presentation of results in the form of spectral curves obtained by plotting the square root of 'variance spectra density' as defined above, versus frequency. These modified spectra are better differentiated than their variance spectral counterparts and transfer functions calculated from pairs of these modified curves are nearly linear. However, further examination reveals that the units relating to the area beneath the curve are inconsistent with any recognised parameter of variability. Recognition of this shortcoming led to formulation of the alternative spectrum proposed in Chapter 12.

All results given in Chapter 12 are presented in terms of a new spectrum, the area beneath this curve representing standard deviation expressed in units of length appropriate to the surface profile data from which the spectrum is computed. These will be referred to as standard deviation spectra.

Standard deviation spectra representing related surfaces differ more, one from another, than variance spectra particularly in respect of the higher frequencies. This is seen to particular effect in the case of those representing rather similar surfaces as for example Figs 12.3, 12.5 and 12.7.

In order to demsonstrate the extent to which transfer functions relating surface profiles may appropriately be represented by straight line graphs, linear regression and 95 per cent confidence limits are applied to those obtained from several pairs of profiles. Finally these regression lines are compared in order to show that they clearly distinguish not only between profiles differing considerably in character but also between very similar profiles. These transfer functions are therefore suitable for comparing the widely differing surfaces typical of grinding wheel and ground surface and also the more similar surfaces typical, for example, of the grinding wheel surface at different stages of wear.

The effects of grinding wheel wear on the transfer functions relating the standard deviation spectra for pairs of profiles are discussed in Chapter 13.

The simplest interpretation of the change due to wear being that it results in a diminution in the standard deviation of profile heights. This also applies to the change in the ground surface associated with grinding wheel wear. This simple conclusion provides confirmation of similar results in Part 1 using estimates of standard deviation obtained from asperity distribution curves.

Detailed interpretation of standard deviation spectra and the transfer functions relating these provides considerably more information as follows.

(a) In addition to providing an estimate of standard deviation the proposed spectra also show the distribution of this parameter in relation to frequency for a given profile.

(b) Transfer functions obtained from comparable spectra, for example those associated with a specified amount of grinding wheel wear, provide an estimate of the change in standard deviation associated with this wear and also the change in distribution of this parameter, with respect to frequency, as a result of wear. Similar remarks apply to comparison in the same terms between the profiles of ground surface and grinding wheel.

Descriptive treatment of the conclusions reached from this investigation has caused problems in the choice of terminology, particularly that applicable to the original methods of presentation. However, results expressed in graphical form are believed to be explicit and, when the work was undertaken, this was the first time a detailed set of data connecting the surface profiles involved in the grinding process had been evolved.

PAGE NUMBERING AS IN THE ORIGINAL THESIS

CHAPTER 7. LITERATURE SURVEY

In order to investigate the ground surface as a function of grinding wheel surface topography it is necessary to describe and compare two very different surfaces. The usual means of characterizing surfaces are not sufficiently comprehensive for this purpose. For instance, the arithmetical average value (R_a) defines a surface in terms of a single number which must be supplemented by additional information in order to provide a more adequate description. For specification purposes it may suffice to state the manufacturing process and the required R_a value. Alternatively a surface profilogram may be used in conjunction with R_a. In either case the characterization is part quantitative and part descriptive.

Similar limitations apply to surface texture parameters alternative to R_a, none of which provide a surface description suitable for an investigation of this type. Therefore the assistance of the literature was sought to find the extent to which more suitable parameters and methods existed or could be developed. These had to be applicable on the one hand to the ground surface and on the other to the grinding wheel with its characteristic features including structural voids of such depth as virtually to represent discontinuities in the surface. The need for effective quantitative comparison of these dissimilar surfaces had to be considered and therefore most of the papers examined deal with some aspect of finishing surfaces by grinding although material on the wider treatment of surface measurement is also included.

In the following pages twenty-two papers (excluding Part 1 of this Thesis) are considered, approximately in order of publication date. Extracts are used to facilitate discussion and the survey is summarized at the end of the chapter.

The earliest paper examined, due to Myers (20) is devoted to surface roughness characterization and therefore appeared likely to contribute to solution of the problems which have been outlined. This author dismisses autocorrelation techniques as inadequate for surface characterization but adds that power spectrum analysis would collect most of the information necessary to describe a surface. On the latter point the meaning of this statement is obscure since in both cases the input information is identical, namely a series of ordinates, and the difference lies in the subsequent mathematical processing and presentation of data.

Myers next outlines what is described as a more straight-forward procedure in terms of three new mathematical characteristics of a surface profile. These are respect-ively the first and second derivatives (designated Z_2 and Z_3) of the standard r.m.s. surface texture parameter (Z_1) while the third is defined as

$$Z_4 = \frac{\Sigma(\Delta X_i)p - \Sigma(\Delta X_i)n}{L}$$

where $L = (\Delta X_i)p + \Sigma(\Delta X_i)$ = total profile distance

X_i = segment of L

p = positive slope

n = negative slope

Examples are given of the application of Z_1, Z_2, Z_3 and Z_4 to hypothetical surface profiles and it is shown that certain features are emphasised by one or other of these parameters. However, all the profiles are based upon regular waveforms and no account is taken of the random character of real surface profiles. Comparisons are made in general terms between two of the hypothetical profiles and real surfaces but these appear to be conjectural. The only experimental verification offered is obtained by plotting experimental values of frictional coefficient against Z_1, Z_2 and Z_3. All three diagrams show consider-able scatter but rather less in the case of Z_2 than for Z_1 and Z_3. Regression lines are drawn for each of the three plots and correlation coefficients calculated. The largest correlation coefficient (0.84) occurs for Z_2 and from this it is concluded that slope of the surface profile is most important in influencing friction and that friction can best be predicted by Z_2. This conclusion is self evident since Z_2 being the first derivative of the r.m.s. surface parameter does in fact represent its average slope.

This treatment of surface texture in terms of a frictional characteristic is of interest but apart from the above result the paper contains no information on the roughness of real machined surfaces. Also the methods described did not appear to be applicable to ground surfaces because the 'characteristics' employed take little account of the predominantly random nature of such surfaces.

A more revealing paper is provided by Peklenik (21) who defines the random input of a grinding process as the cutting elements of the grinding wheel and its outputs as surface roughness of the workpiece and grinding wheel wear. The influence of the physical properties and geometry of grinding wheel for the dressed and worn cutting space is determined in terms of averages, correlation functions, and dispersion spectra. The transfer function of the grinding process in terms of surface roughness of the workpiece and wear of the grinding wheel is developed, and the cutting ability of the grinding wheel is defined and investigated.

The elementary cutting profile is defined as the profile obtained in the cross-section of the cutting surface perpendicular to the cutting speed vector. The grinding process results from the interaction between the work--piece and a succession of elementary cutting profiles. The shape of such a profile can be expressed as a random function X(b) capable of being defined by its average and autocorrelation function.

Investigation of cutting profiles for grinding wheels having abrasive grains of different materials, size, and hardness show that X(b) is stationary and ergodic and therefore one elementary cutting profile is representative of the random function in a certain section of the cutting surface.

For the cutting profile to be ergodic the cutting surface must be produced without systematic errors which implies optimum dressing conditions.

The average value of an elementary profile is given by

$$m_x(b) = \frac{1}{b}\int_0^b x(b)\,d\,b$$

where b = width of the cutting space.

The random shape of an elementary cutting profile is characterized by the autocorrelation function $K_x(\beta)$

$$k_x(\beta)=\frac{1}{b-\beta}\int_{b}^{b-\beta} x(b)x(b+\beta)db$$

where β=b-b' (lag) between ordinates x(b) and x(b+β)

If $\beta=0$ $K_x(0) = D_x(b)$

where K_x = number of cutting edges per unit length and D_x = dispersion of the elementary profile considered as a random process.

The average value $m_x(b)$ and dispersion D_x are the characteristics of the elementary profile of a grinding wheel.

Individual profiles may be obtained by scanning methods which were developed in conjunction with methods to determine the number of cutting edges on the cutting surface.

The average value m_x and the dispersion D_x were calculated for the following values of grinding wheel depth of cut: 2.5, 5, 10 and 15μm. Results showed that the averages of the elementary cutting profiles were influenced by the hardness and grain size of the grinding wheel.

Three graphs representing the computed autocorrelation functions for grinding wheel surfaces are presented and it is mentioned that for convenient analysis it is necessary to normalize these curves (divide by the dispersion). Autocorrelation functions for the three different grinding wheels are shown to be quite different.

Characterization of the grinding wheel surface in terms of the average and autocorrelation function derived from the elementary cutting profile is said to include all features which must be considered in investigation of the cutting process. Characteristics previously used, namely the number of cutting edges per unit length and the shape factor are included in the mean and autocorrelation function.

Frequency characteristics of the elementary cutting profile are defined by the dispersion spectrum or spectral density which can be obtained when the correlation function is known. Figure 7.1 shows the dispersion spectrum for a specified grinding wheel. It is stated that dispersion spectra for other wheels were found to be of similar form and that the relation--ship between dispersion and frequency depends strongly on the geometrical and physical properties of the cutting space of the grinding wheel. Also the dispersion spectrum may be used to determine the wear and roughness transfer functions for the grinding process.

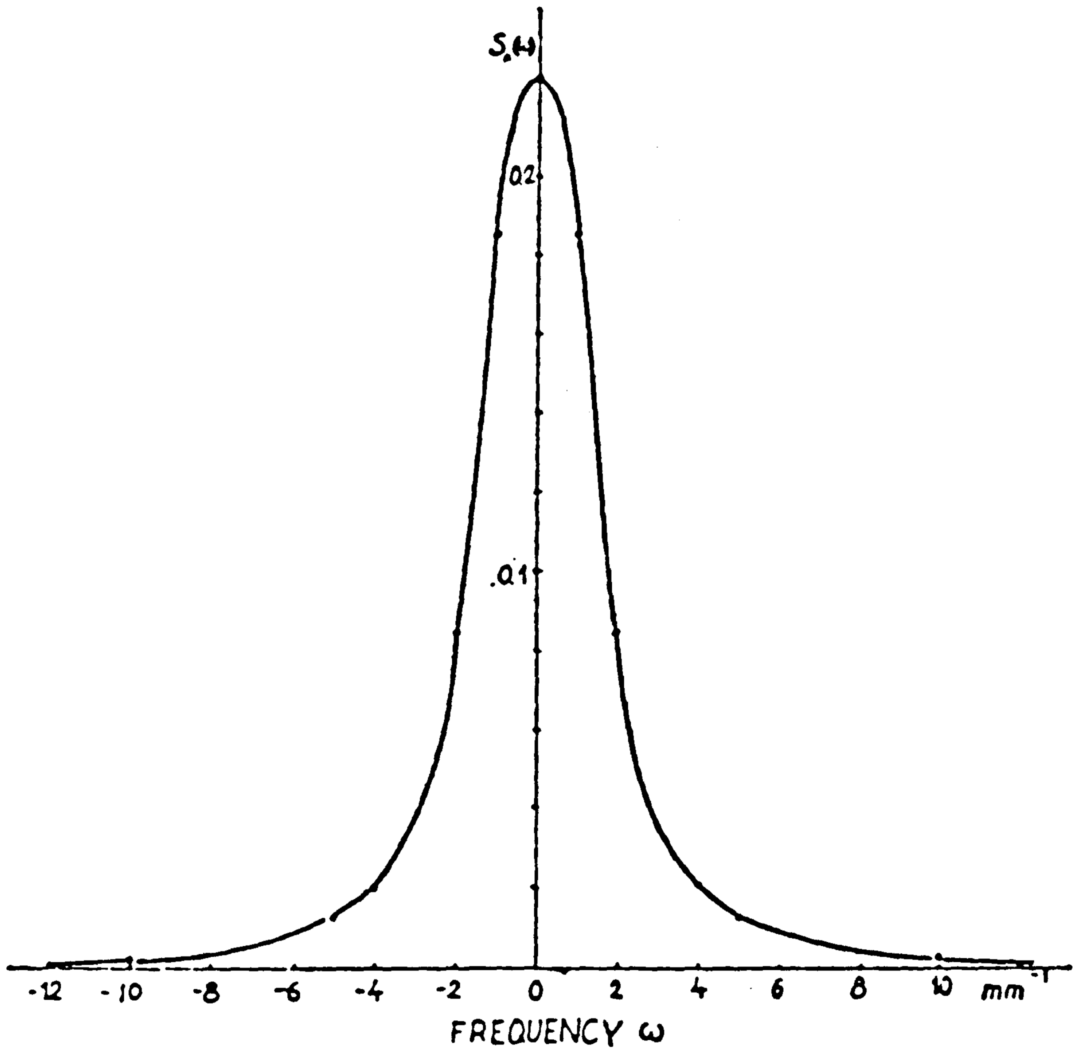

Fig 7.1 Dispersion spectrum of aluminium-oxide grinding wheels; grain size 60, hardness P_b = 1.35 kg, level a = 10μm (after Peklenik).

Cross correlation applied to successive elementary cutting profiles indicates very weak correlation between individual profiles which means that these are statistic--ally independent for the cases investigated.

Surface roughness of the workpiece and wear of the grinding wheel are said to be the important outputs of plunge grinding without spark-out. The grinding process being represented as a linear transfer system which creates the surface on the workpiece and on the cutting space of the grinding wheel.

The input of the grinding process is a stationary random process representing the cutting space of the grinding wheel characterized in terms of its mean level and autocorrelation function or dispersion spectrum. Corresponding outputs are surface roughness of the workpiece and change in shape of the elementary cutting profiles as a result of wear and brittle fracture. Both of these are also stationary stochastic processes capable of being described by the same characteristics as the inputs.

The transfer function represented by the ratio between output and input dispersion spectra serves to character--ize the grinding process in relation to frequency.

When a grinding process generates a surface roughness or a wear pattern it follows that some frequencies will be amplified and others will be reduced or attenuated. Actually it is necessary to establish the interactions of the grinding wheel and the workpiece material and the grinding conditions. Solution of this problem should make effective control of the grinding process possible.

Correlation functions representing input and output surfaces for a specified set of conditions are presented and also surface roughness and wear transfer functions (Fig. 7.2) derived from the corresponding dispersion spectra together with the transformation coefficient representing the ratio of the averages for the two surfaces.

The cutting ability of the grinding wheel decreases with wear and can be defined as the inverse of the wear transfer function. Cutting ability is a maximum if the spectral characteristics of the cutting profile remain constant over the whole frequency range. The use of worn cutting profiles which have changed in these terms by reason of wear causes the cutting ability to fall below unity.

One of the future problems is to determine which factors influence the surface roughness and wear transfer functions respectively.

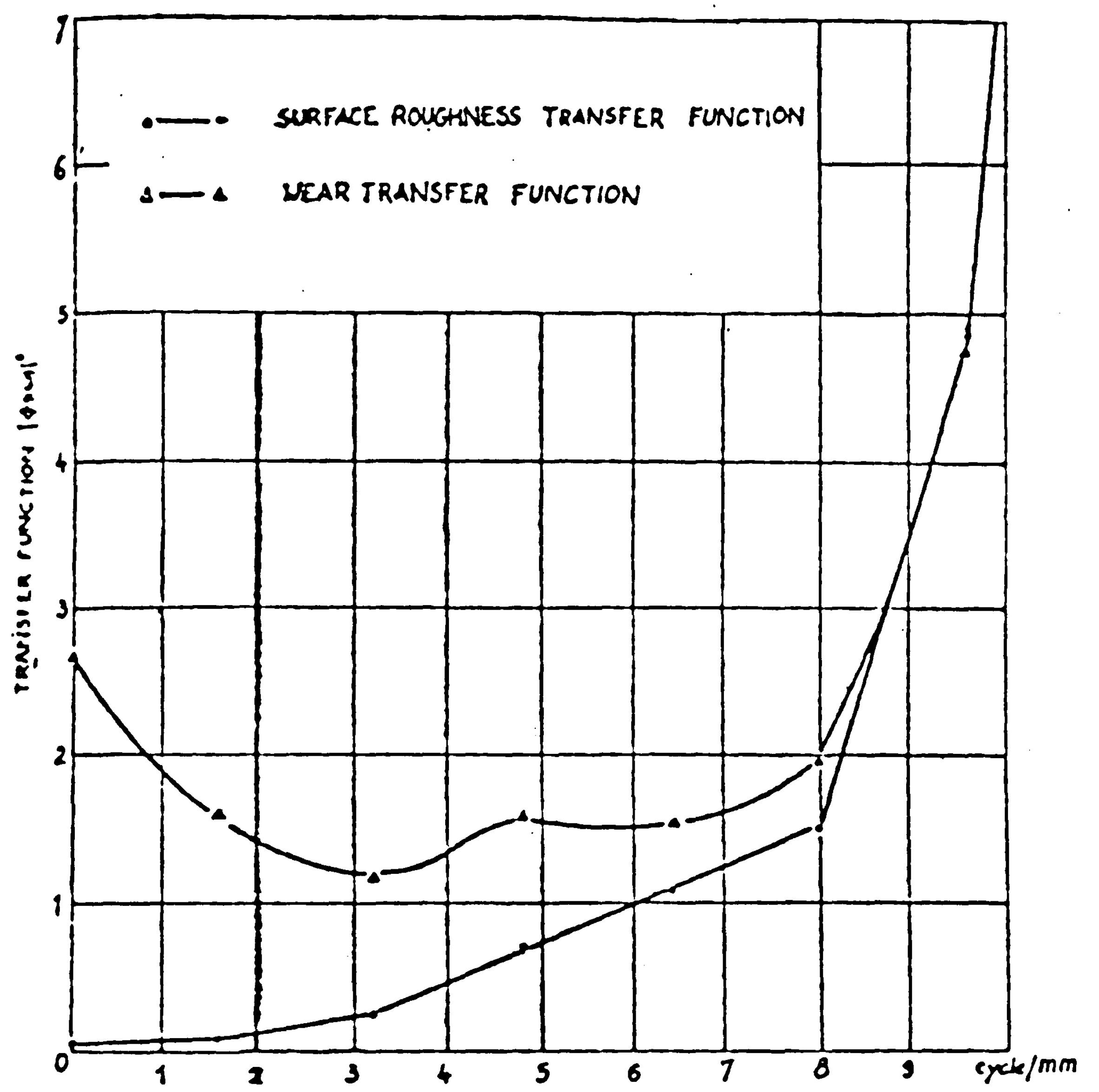

Fig 7.2 Surface roughness and wear transfer function of grinding process (after Peklenik)

The foregoing summarizes a paper of some complexity which on close examination reveals an underlying pattern of concepts for characterizing and relating the surfaces of grinding wheels and workpieces which appear relatively simple. In order to appreciate this an understanding of

the information contained in a dispersion spectrum is necessary. Such a graph (known alternatively as a power spectrum or power spectral density curve) can be obtained when the correlation function is known, although it may also be directly computed. Figure 7.1 shows such a spectrum on which areas beneath the curve represent the distribution of dispersion or variance with respect to angular frequency. Any ordinate therefore represents the density of variance associated with the corresponding frequency.

For the purpose of characterizing a surface profile it is convenient to plot spectral density against frequency f (cycles/mm) instead of the angular frequency ω where $f = \frac{\omega}{2\pi}$ and to show only that part of the spectrum corresponding to positive values of f.

Peklenik's paper tends to emphasise the validity of representing physical and geometrical properties of grinding wheel and workpiece surfaces in terms of averages and autocorrelation functions together with dispersion spectra, the last named being given rather less prominence. It is clearly indicated that the autocorrelogram and dispersion spectrum are represented as alternatives. Both are calculated from the same data and one is a Fourier transform of the other.

Of the two parameters the dispersion spectrum appears to offer a more explicit description of surface profile than the autocorrelogram. However Peklenik implies a preference, not clearly accounted for in the author's view, for the autocorrelogram while mentioning the need for an additional calculation (dividing the auto--correlogram ordinate by the dispersion) to facilitate analysis.

In the author's experience, calculation of power spectral densities occupied significantly more computer time than autocorrelation but presented no additional problems. The overall result was a preference for power spectral analysis based to some extent on the following reasoning.

It is generally accepted that a population may be described in terms of the average level and dispersion (variance) of the random variate. If the ordinates defining a surface profile form a distribution subject to random variation with respect to height that profile may similarly be defined in terms of its mean level and dispersion about that level but such a description is clearly inadequate because it takes no account of the distribution of heights with respect to frequency or spacing of the features making up the profile.

The information which variance fails to express in the context of surface profile characterization is precisely that which is contained additionally in the dispersion spectrum. It therefore appears that a surface profile can be adequately and explicitly characterized in terms of its average and dispersion spectrum with respect to frequency.

The relationship between the grinding wheel cutting zone and the elementary surface profile of the work--piece is expressed in terms of the transfer function and transfer coefficient. The first of these takes the form of a curve Figure 7.2 obtained by dividing the output dispersion spectrum by the corresponding input dispersion spectrum; the second is the ratio of the two averages. Similar transfer curves are used to express wear and cutting ability of the grinding wheel. Clearly these transfer curves and coefficients may provide potential means for prediction of output surface characteristics and this throws light on the concluding remarks in the paper.

Conclusions are drawn to the effect that the method of analysis makes it possible to define the grinding process mathematically and that one of the future problems in grinding is to determine which factors influence the transfer functions.

Peklenik's paper of 1965 (22) has some relevance to the present investigation since it deals with the characterization of various machined surfaces including some finished by grinding. Unlike the paper previously discussed (21) it contains no information on the surface of the grinding wheel. The structure of surfaces produced by different processes but having equal roughness characteristics is investigated as a two-dimensional problem.

The practise of categorising the components of surface texture as roughness and waviness is said to be at least questionable because its properties and behaviour cannot be allocated to these two arbitrarily defined types of deviation. Profiles can however be classified in accord--ance with two characteristic forms, which may be regarded as limiting types, as follows.

1. The periodic profile comprised of one or several cosine or sine functions.

2. The purely stochastic profile containing only random components and no periodic components.

Surface profiles rarely correspond with type 1 but purely stochastic profiles, as defined under 2, do occur under certain conditions, mainly on polished surfaces.

The majority of surface profiles are said to lie between the two types and it is therefore necessary to consider the whole profile spectrum. Composite profiles can be defined as periodic carrier profiles on which are super--imposed stochastic components, the latter exhibiting no clear periodicities.

It was considered necessary to establish whether a given profile is (a) stationary, (b) ergodic and (c) whether it is normal or otherwise.

Tests were said to have confirmed that the mean level of the profile and its variance were statistically constant confirming that the measured results did not depend on the commencement of reading.

It is stated that a single scan of the surface is representative only when the profile can be termed ergodic. This condition was shown to be fulfilled since the correlation functions of the profiles approach zero as β (the lag) approaches infinity.

Carrier profiles with superimposed stochastic components are said to be stationary and ergodic except when defects of shape affect the random profile.

Recent investigations had shown that surfaces with only random components, ground surfaces in particular, exhibit a normal distribution while turned, milled, honed, and lapped surfaces did not.

A series of parameters widely used in connection with surface measurements are listed in a table together with their formulae. These include the mean value, arithmetical deviation (R_a), geometrical mean rough--ness value (R_s), and peak to valley height. It is pointed out that these describe the profiles only in the ordinate direction and surfaces with equal values of R_a, R_s etc. may differ widely in structure.

In the last few years there had been attempts to find new parameters providing a more complete description of surface profiles including those proposed by Myers (20).

In this paper surfaces are characterized in terms of the normalized autocorrelation function computed from a two-dimensional surface profile and unlike the earlier work (21) no mention is made of the mean and dispersion spectrum as parameters for surface characterization.

It is pointed out that surfaces with equal roughness value in terms of R_a, R_s, R_z etc. may differ widely in structure. Differentiation of such surfaces by means of autocorrelation functions is shown to be possible. However this does not necessarily show autocorrelation functions to be superior because all the ground surfaces had widely differing values of mean and standard deviation, these being the only parameters previously recorded for comparing these surfaces.

Expressions representing the autocorrelation functions for two ground surfaces are tabulated. The first of these relates to a ground surface described as having only random components:

$$k_x(\beta) = e^{-16\beta}$$

while the second has periodicity due to the dressing feed

$$k_x(\beta) = 0{\cdot}93\,e^{-0{\cdot}525\beta} - 0{\cdot}005\,e^{-100\beta} + 0{\cdot}075\,e^{-1{\cdot}01\beta}\cos 40{\cdot}5\beta$$

where β = the 'lag' or displacement measured parallel to the surface for the purpose of calculating the series of correlation coefficients which constitute ordinates defining the autocorrelogram.

In conclusion, Peklenik mentions practical limitations on the use of autocorrelation functions but adds that they are indispensable because they provide important information about surface structure.

The profile of a ground surface free from periodic components can, apparently, be represented by the simple exponential expression of which an example taken from the paper appears on the previous page. However, the complexity of the corresponding expression for a ground surface with random and periodic components is such as to convey no impression of surface profile or shape of the correlation function representing that profile. Nonetheless the validity of the information contained in the expression seems unquestionable and any lingering doubts relate to the practical usefulness of expressing a surface characterization in such terms.

Both the papers by Peklenik so far considered contain information of direct relevance to the present study. The earlier paper (21) in particular demonstrated that it is practicable to compare the roughness of two ground surfaces, or of two grinding wheel surfaces worn to a different extent, by means of transfer functions. These transfer functions were derived from power spectra and in view of this the greater emphasis accorded to the autocorrelation function appears somewhat anomalous. However, the overall impression remained that here was material with potential for further development directly applicable to the problems of this investigation.

A paper on surface microtopography by Williamson (23) is included because it contains material on various methods of surface measurement and surface texture parameters. The author's summary is as follows.

> This paper describes an approach to the study of surfaces based on the digital analysis of data obtained from profilo--metric examination. This technique is used to determine several new surface texture parameters including the surface density, height distribution, and mean radius of curvature of the asperities. Recnt theories have shown that these are the parameters which control the nature of surface contact. The implications which these ideas have for the science of metrology are discussed.
>
> The study also shows that many surfaces have height distributions which are Gaussian, and in particular that the heights of the upper half of most surfaces closely follow a Gaussian distribution.

By combining data from many closely spaced parallel profiles it has been possible to reconstruct detailed maps of the surface texture. Two examples are discussed: bead-blasted aluminium, and a glass surface lightly blasted with alumina. One of the advantages of microcartography is that it permits the geometry of the contact between rough surfaces to be studied in detail. A map is given showing the manner in which the contact area between two bead-blasted aluminium surfaces splits into sub-areas and how these sub-areas are distributed with respect to the surface features of the contact--ing solids.

Although the summary refers to only two surfaces the paper includes results derived from a third, namely, a surface finished by abrading a mild steel specimen on 400 grade carborundum paper and then sliding this against a copper block flooded with oleic acid at approximately 10kg force and 130cm/s velocity for 30s.

It is stated that cumulative height distribution curves such as those in Figures 7.3 and 7.4 are a particularly helpful method of describing a surface. The author quotes authorities in support of his contention that such curves represent 'bearing area curves', i.e. the contact areas which would exist if

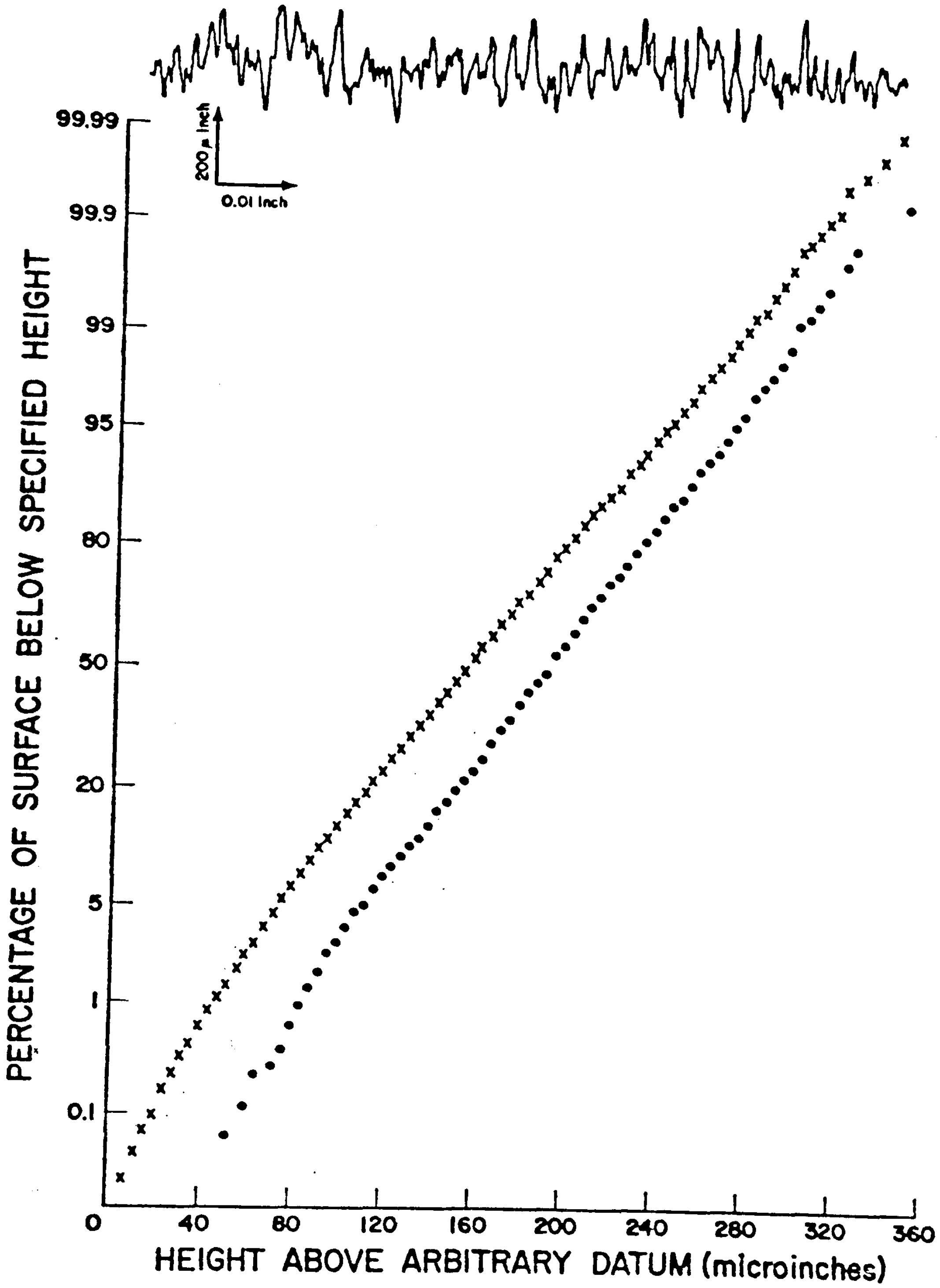

Fig 7.3 Cumulative height distribution of bead-blasted aluminium (diagram and the following note after Williamson) Both the distributions of all heights (×) and of peaks (•) are Gaussian. The profile of the same surface is shown in the upper diagram: the vertical magnification is 50 times the horizontal magnification.

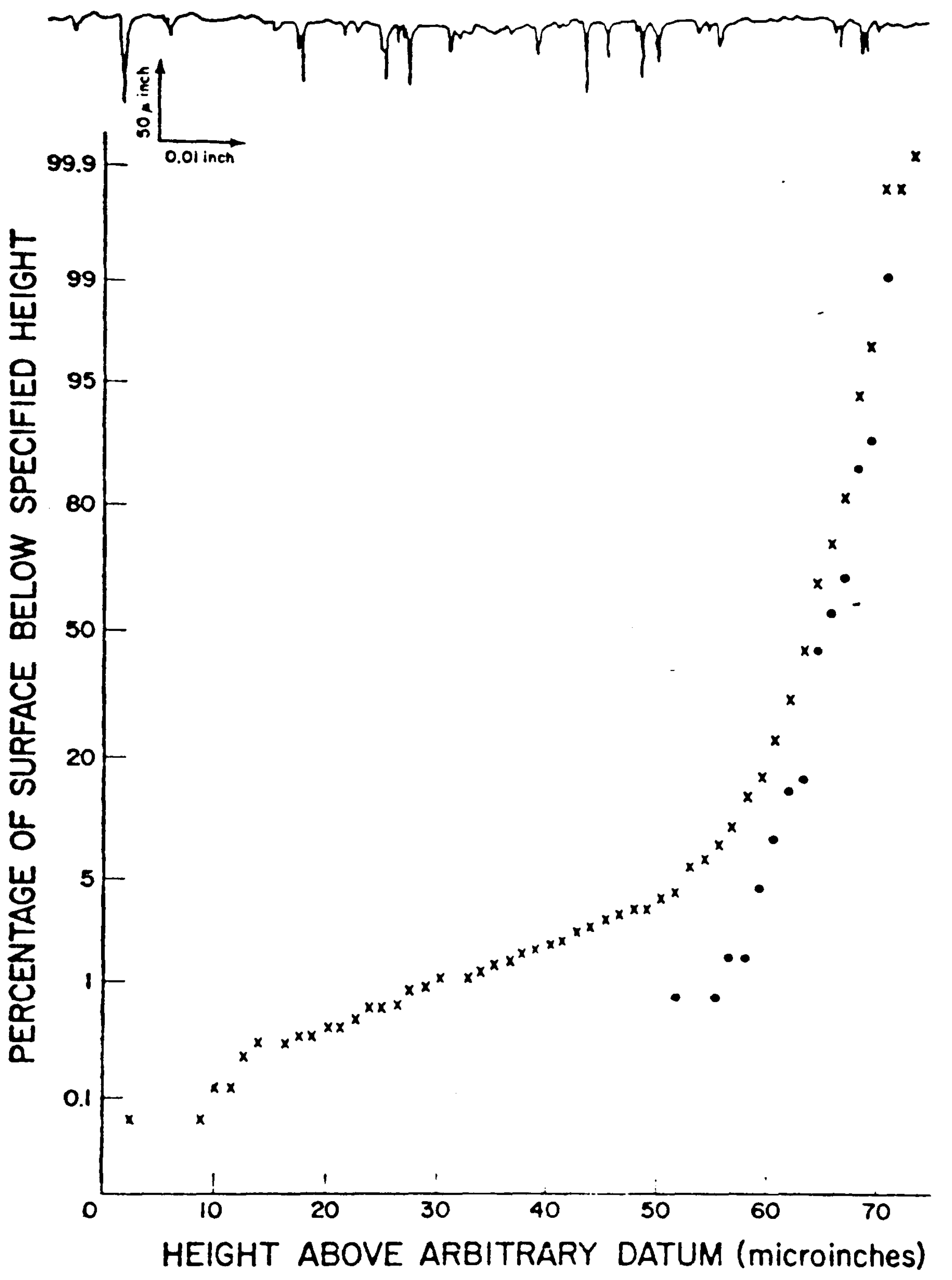

Fig 7.4 Cumulative height distribution of mild steel specimen (diagram and notes below after Williamson) Distribution of all heights×. Distribution of peaks•.

This specimen was abraded on 400 grade carborundum paper, then slid against a copper block flooded with oleic acid at approximately 10kg, 130cm/s for 30s.

the surface was worn down to a certain height. He also mentions suggestions of others to the effect that these are only 'bearing line curves' and that two such distributions from perpendicular profiles must be 'multiplied together' to produce a genuine height distribution for a surface. He adds that the latter suggestion is misleading and that a height distribution can, in principle, be obtained from an infinite number of closely spaced parallel sections - the usual process of integration over a surface.

For the purpose of producing maps representing the microtopography of surfaces 25 parellel profiles were recorded and synchronized by methods described in the text. The author adds that it is relatively easy to programme the computer to search such data for true summits: a summit being defined for this purpose as a spot height higher than its eight nearest neighbours. Results are presented in the form of these maps and a table based apparently upon the height distributions.

Williamson's dismissal of the suggestion made by other investigators to the effect that two distributions from perpendicular surface profiles must be 'multiplied together' to produce a genuine height distribution is not easily reconciled with other information contained in the paper. Figures 7.3 & 7.4 show different distributions for 'peaks only' and 'all heights'.

In the terminology of the paper 'peaks' appear to be synonymous with 'true summits' and the latter are arbitrarily defined as points higher then their eight nearest neighbours. Since there is no evidence that any one profile contains real maximum heights or summits it follows that the 'peaks only' distribution is also arbitrary and perhaps less accurately represent--ative of the surface than the alternative idea of a distribution based upon two perpendicular profiles.

The second paragraph of the author's introduction states that the study shows that many surfaces have Gaussian height distributions and that in particular the heights of the upper half of most surfaces closely follow a gaussian distribution. These statements clearly cannot be justified on the unsupported evidence of this paper in isolation which certainly includes Gaussian distributions on the lines indicated but for only three types of surface one of these being produced by the rather unusual method of abrasion with coated abrasive paper followed by frictional wear.

It would be invidious to detail other less obvious discrepancies between introductory claims and the results presented. Some claims may be based upon results from the author's earlier joint publications two of which are mentioned in the bibliography but, if so, the facts are not clear from the text of this paper.

Nonetheless inclusion of this paper is justified on the basis that results presented in the form of cumulative distributions provide an interesting comparison with results similarly presented in Part 1 of this investigation. The surfaces were produced by different methods but there are similarities between the distributions and, at this stage, profile height distribution curves were still being considered for possible future use.

Two further papers by Peklenik were next considered. The first of these (24) proposed a surface classification system outlined in the following terms.

> After at least three or four decades of intensive research into surface description, we are still not in a position to provide the designer with comprehensive information about surfaces.
>
> Previous investigations (3) show that quite different surface profiles may have similar values of R_a or other parameters. The recent introduction of the random function approach for characterizing surface profiles yields new techniques for a more comprehensive statistical description of the surface.

Correlation functions or their Fourier transforms, the power spectra, provide an excellent new tool for the fundamental investigation of surfaces.

It is well known that in many cases the surface profile contains periodicities together with random components. One of the prerequisites for accurate surface characterization is the detection of this deterministic component and that portion which is random noise.

The concept on which the present investigation and the proposed typology is based, has been developed from the premise that every surface profile may be described by basic autocorrelation functions and/or a combination of these functions.

In what follows some attempt has been made to clarify the content of this paper in terms of arrangement and emphasis. Autocorrelation functions are used throughout as the basis of surface classification but in the terminology of the original text correlation and autocorrelation are synonymous.

Investigation of a large number of surfaces has shown that their correlation functions can be divided into five groups. The first and fifth groups are defined as follows.

Profiles considered in Group 1 are the straight line and sine wave without any random distortions. These do not occur in practice but their correlation functions are defined since these represent elements for inclusion in Groups 2, 3, and 4.

Group 5 represents wide band random noise. Its correlation function approximates to an exponential function which simulates the delta function corresponding with the autocorrelogram

$$r_{xx}(\beta)=e^{-\alpha\beta}$$

The surface correlation length β_o is defined as the average length of the surface over which the correlation moment is at least 0.05; for machined surfaces this is usually about $\beta_{o\,min}$ = 0.05mm. Smaller values are taken to indicate that no correlation exists in the surface. The α value defines the decay of the $r_{xx}(\beta)$ function and is one of the parameters which characterize the type of random profile. If α decreases the correlation length β_o increases, the limiting case being a straight line (Group 1) for which $\alpha = 0$ and the correlation function is constant.

In Group 2 are classified surfaces in which a random wave is superimposed on a sine wave or other determin--istic function. The autocorrelation function of Group 2 is defined as the sum of two $r_{xx}(\beta)$ functions and an example is given based upon the combination of a sine wave and a random wave.

$$r_{xx}(\beta) = e^{-\alpha\beta} + \cos\Omega\beta$$

Correlation functions of this type do not decay to zero.

Group 3 is described as a carrier profile with super--imposed random function and is said to represent the most common type of surface. It's autocorrelation function is a product of the autocorrelation functions of the carrier profile $r_1(\beta)$ and the superimposed random profile $r_0(\beta)$. Numerous surface measurements have shown that the carrier profile is a harmonic wave of frequency Ω. It's autocorrelation function is expressed by

$$r_{xx}(\beta) = \cos\Omega\beta$$

and falls within Group 1. The $r_0(\beta)$ of the random component corresponds with the approxiamte formula for Group 5. Therefore the autocorrelation function for Group 3 is given by

$$r_{xx}(\beta) = e^{-\alpha\beta}\cos\Omega\beta$$

The shape of the function depends on the ratio $\mu = \frac{\alpha}{\Omega}$
If $\mu \rightarrow 0$ the function $r_{xx}(\beta)$ approaches $\cos \Omega \beta$.
If μ increases the function tends to the shape expressed by the formula for Group 3. The decay of correlation with increasing profile length is a characteristic of this surface type and the correlation length β_0 defines basic surface elements.

Group 4 is introduced to provide for surfaces which cannot be described by elementary autocorrelation functions and therefore cannot be assigned to the groups already defined. The autocorrelation function of Group 4 consists of the sum of the elementary correlation functions of Groups 1, 2, 3, and 5.

The provision of five groups for classification of the surfaces under consideration is clearly unnecessary because, as the author points out, machined surfaces corresponding with Group 1 do not arise in practice. Also it is stated that Group 4 has been introduced because real surfaces cannot always be described by elementary correlation functions. In other words, surfaces exist which do not fall within Groups 2, 3, or 5. However, none of the 34 surfaces considered are assigned to Group 4 and for the purposes of this study it may be neglected.

Correlation analysis of a wide range of machined surfaces yields two unique parameters, the correlation length and/or the periodicity.

The correlation length β_0 and the correlation wavelength β_w represent additional information which provides for classification into sub-groups.

A surface profile will be classified first into one of the basic groups 1 - 5 on the basis of the shape of it's autocorrelation function. Further classification within the group involves estimation of β_o and β_w. Numerical evaluation of β_o and β_w for a large number of surfaces shows that β_o varies between 0.05 and 2.5mm and β_w between 0 and 1mm. To establish reasonable intervals for the sub-groups the R5 series of preferred numbers (DIN 323) were applied.

Numerical values for the surfaces classified have the following meaning e.g. 3/0.1/0.04 = basic group No 3, $\beta_o = 0.1$, and $\beta_w = 0.04$. The numerical classification for 34 surfaces is set out in three tables. Three of these surfaces are assigned to Group 5, five to Group 2 and the remaining 26 to Group 3.

Finally it is pointed out that analysis of the surfaces classified within each group shows that surfaces manufactured by different methods may be classified as the same type even though their R_a or σ_x values differ. Also, surfaces with similar R_a or σ_x values differ in their type classification, as characterized by different β_0 and β_w values.

Of the 34 surfaces considered ten were produced by grinding and a further six by honing, lapping, or linishing. Eight of the ground surfaces are assigned to Group 3 while Groups 2 and 5 each contain one of the remaining cylindrically ground surfaces. The six surfaces produced by abrasive processes other than grinding are in Group 3.

Group 3 is said to represent the most common type of surface and, of the eighteen surfaces produced by abrasive processes considered in the paper, sixteen fall into this category.

The foregoing paper is of interest as providing for effective classification of ground surfaces in terms of autocorrelation theory. In effect it represents a continuation of an earlier work by the same author (22) which has already been considered. However, these two papers appeared to have less direct relevance to the present study than the first of this author's papers to be examined (21). These works are followed in 1968 by a fourth contribution (25) on surface characterization which includes power spectra as one of the statistical parameters for surface profile description along with profile height distribution curves and autocorrelograms. As in the earlier paper (21) the use of transfer functions for comparison of surface profiles represented by power spectra is envisaged.

The summary of this paper (25) restates that statistical description of a surface by means of the first and second moments of the ordinate probability density distribution such as R_a or R_s is inadequate. The paper also deals with a number of aspects of surface characterization already outlined in this survey and the author claims priority in introducing the concept of identifying the manufacturing process from the surface using correlation theory.

The introduction includes a statement to the effect that the grinding process may be defined by a transfer function computed from power spectra representing the cutting surface of the grinding wheel as the input of the system and the generated surface as the output.

Because the generated surface represents the output of the manufacturing system it is conceivable that this surface reflects the dynamic behaviour of the machine tool under actual cutting conditions and may also serve to characterize this dynamic behaviour.

The author enumerates surface quality parameters and states that from a geometrical viewpoint a surface represents a three-dimensional random structure.

Autocorrelation and cross-correlation functions, power spectra, and slope probability distribution parameters are applied to surface characterization considered as a two-dimensional and/or three-dimensional random process. Surfaces manufactured by a variety of metal-removal processes were investigated in order to differentiate between surfaces with the same R_a and R_s values, and secondly, to separate the periodic and random components in the surfaces.

The actual configuration of real surfaces extracted by two-dimensional surface measurement reveals the probabil--istic characteristic for surface deviations of both

large and small orders of magnitude. The measured profiles represent random functions $X_1(\ell)$, $X_2(\ell)$, $\ldots X_n(\ell)$ as indicated in Figure 7.5

A real surface, however, represents a three-dimensional random structure characterized by a system of inter--related random functions $X_1(\ell)$, $X_2(\ell)\ldots,X_n(\ell)$ designated as a vector random function, Figure 7.6

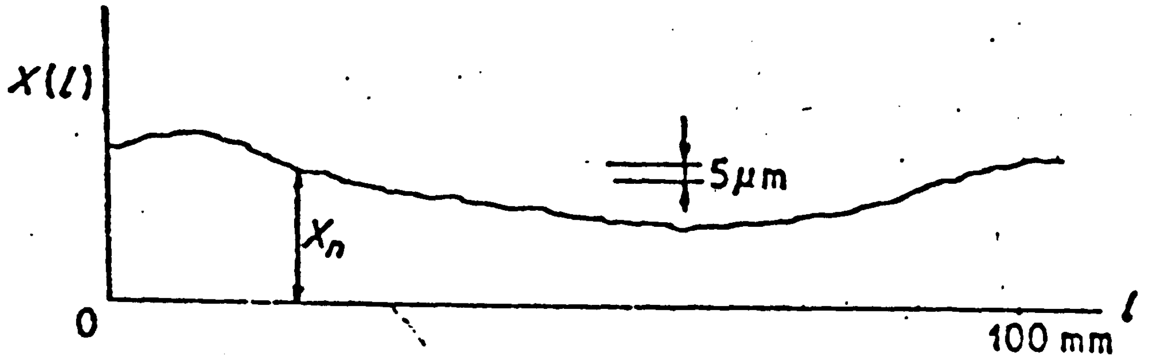

a

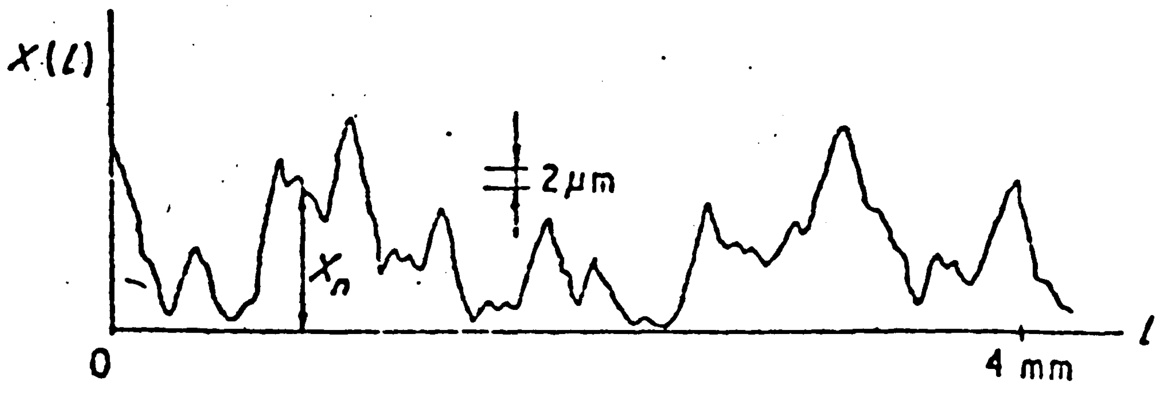

b

Fig 7.5 Large- and small-scale deviations in the two-dimensional case (after Peklenik)

a Large-scale deviations

b Small-scale deviations

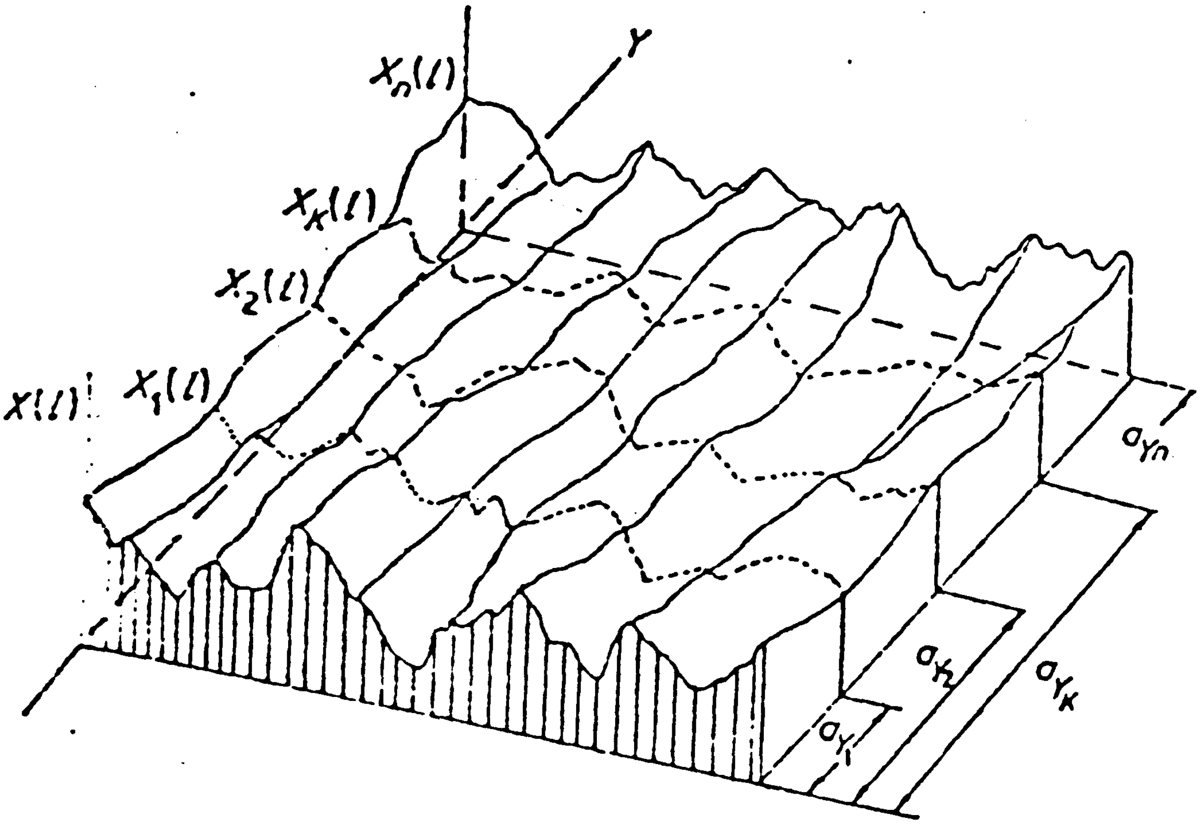

Fig 7.6 Three-dimensional concept of a surface of inter-related profiles representing the random functions $X_1(\ell)$, $X_2(\ell)$,...... $X_n(\ell)$ (after Peklenik)

A three-dimensional flatness measuring machine by Peklenik is illustrated and a brief description indicates that by means of this it was possible to explore a surface of maximum size 150mm × 150mm; heights being determined by a pick-up interposed between a reference plane and the surface under examination.

Surface characterization is said to be incomplete unless the third dimension of the surface is considered. Reference is made to a concept for three-dimensional assessment using cross correlation analysis. The paper then proceeds to deal with two-dimensional analysis of surface texture.

> The autocorrelation function $R_{xx}(\lambda)$ of a surface profile $X(\ell)$ involves the coherences which could not be derived from the distribution function. one of the major problems in surface texture identification is the separation of the periodic and random content in a profile. Considering the surface profile $X(\ell)$ as a stationary and ergodic random function it's autocorrelation function $R_{xx}(\lambda)$ is generally estimated as follows:
>
> $$R_{xx}(\lambda) = \frac{1}{N-\lambda} \sum_{i=1}^{N=\lambda} \overset{\circ}{X}(\ell_1) \overset{\circ}{X}(\ell_1 + \lambda)$$

where $\overset{\circ}{X}(\ell_1)$ is equal to $X_i - m_x$, N is the number of sampled data, and λ is the displacement between two ordinates $X(\ell)$ necessary for computing the correlation function.

The $R_{xx}(0)$ value represents the variance D_x of the surface profile $X(\ell)$ that is

$$R_{x\cdot}(0) = D$$

$$\text{and } \sqrt{D_x} \equiv \sigma_x = R$$

It is convenient to normalize the autocorrelation function

$$r_{xx}(\lambda) = \frac{R_{xx}(\lambda)}{D_x}$$

and all experimental results will be discussed in the normalized form.

In some cases it is more convenient and desirable to present the surface profile $X(\ell)$ in frequency domain. Using the correlation function the power spectrum is expressed as

$$S_x(\omega) = \frac{2}{\pi}\int_0^{\infty} R_{xx}(\lambda) \cos \omega\lambda \, d\lambda$$

The relationship between the power spectrum $S_x(\omega)$ and the variance D_x of a stationary surface profile $X(\ell)$ is given by

$$D = \int_0^{\infty} S_x(\omega)\, d\omega = R_{xx}(0)$$

where $\omega = 2\pi f$ is the angular frequency and f is the frequency (cycles/mm or cycles/cm)

Analysis of experimental results follows and this relates to surfaces produced by shaping, spark erosion, electrolytic machining, milling, fine turning, surface grinding, and superfinishing. Computed results are summarized in terms of statistical characteristics of which the following result relating to surface grinding is an example (Figure 7.7).

This shows (a) the surface profile $X(\ell)$, (b) the distrib--ution function $f(x)$, (c) the autocorrelation function $r_{xx}(\lambda)$ and (d) the power spectrum $S_x(\omega)$. Statistical moments are tabulated for the various surfaces and for the ground surface these include the following values: R_a = 1.0μm, $\sigma_x (R_s)$ = 1.3μm, peak to valley height = 15.0μm. The correlation length λ_0 = 0.15mm, and the correlation wavelength $\bar{\lambda}_w$ = 0.2mm.

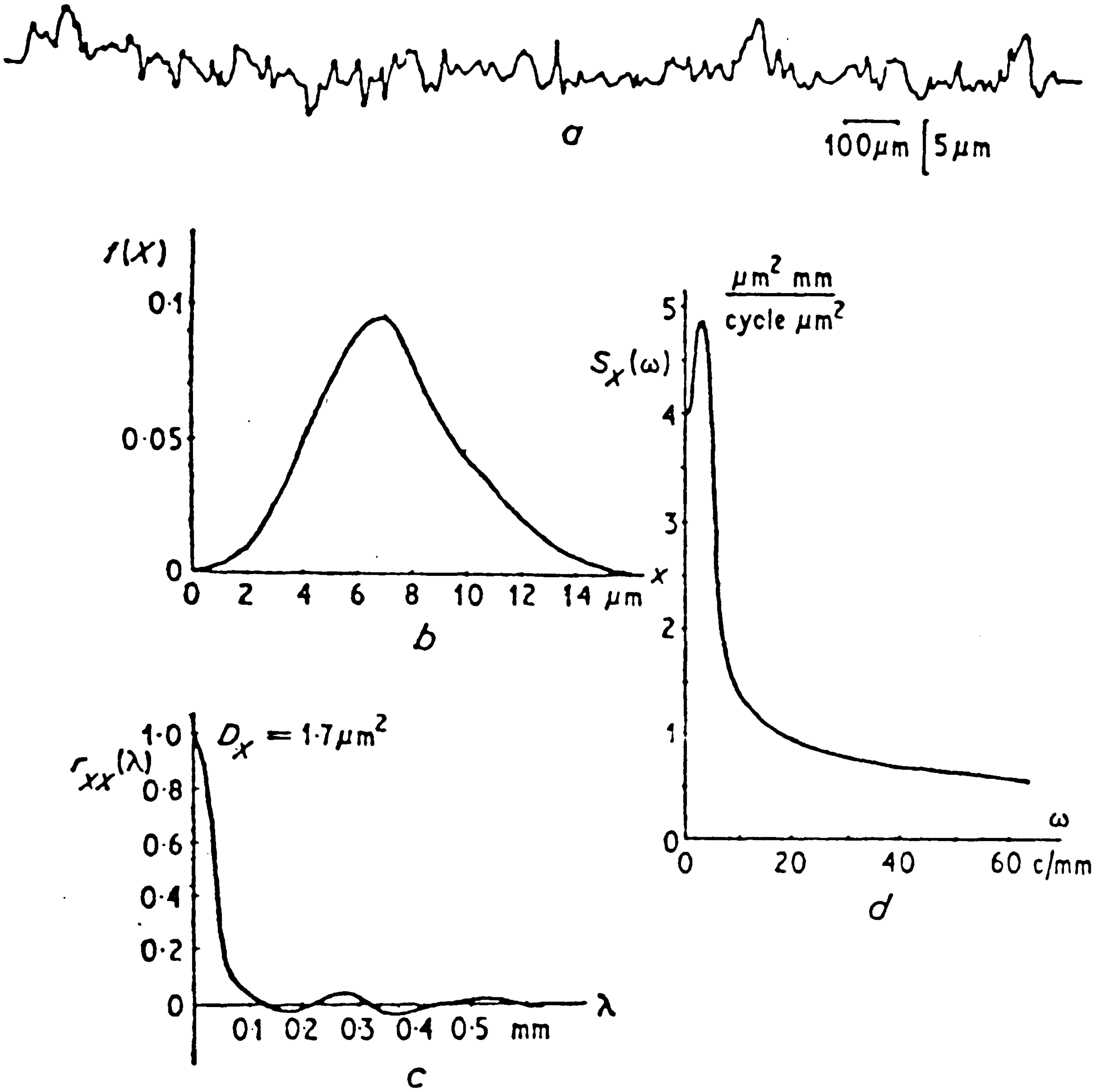

Fig 7.7 Profilogram and characteristics of a surface ground surface, c.l.a. = 1.0μm (after Peklenik)

The distribution function for the ground surface is described as having ordinates x forming a Gaussian distribution. The normalized correlation function is said to be of the type represented by the equation

$$r_{xx}(\lambda) = e^{-\alpha x}$$

Where investigation of surface systems by means of transfer functions is envisaged the surfaces are represented in frequency domain. The Fourier transforms of the experiment--ally determined correlation functions were calculated using the expression

$$S_x(\omega) = \frac{2}{\pi}\int_0^\infty R_{xx}(\lambda)\ \cos\omega\lambda\, d\lambda$$

The characteristic carrier frequency of a given profile is represented by the pronounced peak of the function $S_x(\omega)$.

The disadvantage of frequency analysis is that there is no possibility of determining the correlation length of the surface from the power spectrum.

The introduction of correlation functions, or power spectra, as practical measurements is limited for two reasons. First, compututation by analogue or digital computer takes too long, and second, interpretation of these functions requires skill and understanding not necessar--ily available at shop floor level.

As an additional parameter to existing R_a and R_s values the slope standard deviation $\dot{x}$ was proposed in an earlier paper. The slope of the profile changes randomly at every point owing to the stochastic nature of the process. It is assumed that surface profiles having the same arithmetic average m_x ($m_x = R_a$) and variance D_x ($\sigma_x^2 = D_x = R_s^2$) may have quite different values of average $m_{\dot{x}}$ and variance $D_{\dot{x}}$ for the slope. This property of the profile is expressed in the shape of the autocorrelation function $R_{xx}(\lambda)$ by stronger or weaker correlation moments between the profile ordinates.

From the theory of random functions the second derivative of $R_{xx}(\lambda)$ for a random process $X(\ell)$ yields the slope variance $D_{\dot{x}}$ if $\lambda = 0$

$$D_{\dot{x}} = - \frac{d^2}{d\lambda^2} R_{xx}(\lambda) \Big|_{\lambda=0}$$

This equation enables the $D_{\dot{x}}$ parameter to be introduced. this fulfils two of the important requirements in characterization and practical application.

(i) $D_{\dot{x}}$ is directly connected with the autocorrelation function $R_{xx}(\lambda)$ and

(ii) $D_{\dot{x}}$ is a number and not a function and is therefore easy to understand at shop floor level.

Three-dimensional surface texture assessment is next considered. In principle, only a numerical assessment in all three dimensions can provide comprehensive descriptions of surfaces for fundamental investigation of the various problems mentioned at the beginning of the paper.

Figure 7.8 shows various directional patterns of surfaces resulting from different manufacturing processes classified as follows:

(i) pronounced direction a, b, and c,
(ii) less pronounced direction d, and
(iii) without any or with very weak directional pattern e.

Two measuring methods were developed to obtain the necessary information as follows.

First, parallel tracing in which the surface should be traced twice, the distance a_Y between the surface profile $X_1(\ell)$ and $X_2(\ell)$ being chosen according to requirements a condition being that both traces should have the same starting axis.

Secondly, radial tracing in which the number of profiles are taken, originating from a point O on the surface, at various angles $\pm\phi_1$, $\pm\phi_2 \cdots \pm\phi_n$ in relation to the coordinate axis OY.

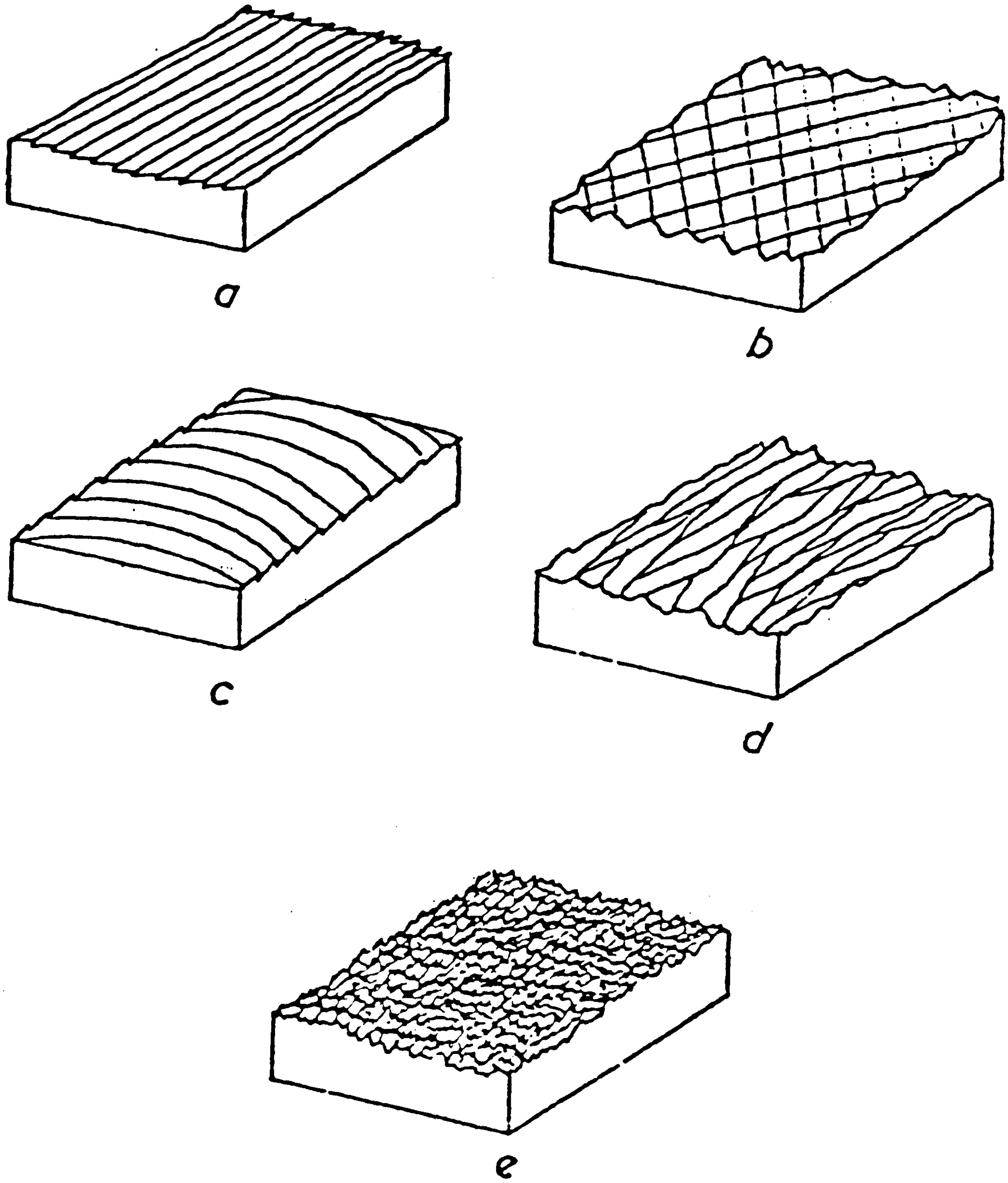

a, *b* Shaping. *c* Milling.
d Grinding. *e* Spark erosion.

Fig 7.8 Directional pattern of surfaces generated in various manufacturing processes (after Peklenik)

The micro-geometrical isotropy is characteristic of the surface under investigation. The directional pattern which characterizes the third dimension of a surface may be expressed analytically by the cross-correlation function $R_{1,2}(\lambda)$ as follows

$$R_{1,2}(\lambda) = \frac{1}{N-\lambda}\sum_{i=1}^{N=\lambda}\mathring{X}_1(\ell)\,\mathring{X}_2(\ell+\lambda)$$

where $\mathring{X}_1 = X_{i1} - m_x$; $\mathring{X}_2 = X_{i2} - m_x$

The peak value of the cross-correlation function $R_{ij}(\lambda)$ related to the distance a_Y between the two parallel traces is convenient for the evaluation of the directional surface pattern. It is therefore

$$R_{ij}(\lambda)_{max} = f(a_Y)$$

For surfaces with pronounced parallel directional pattern the cross-correlation function $R_{ij}(\lambda)$ should correspond to the autocorrelation functions $R_{ii}(\lambda)$ or $R_{jj}(\lambda)$ within the confidence limits. The peak values of $R_{ij}(\lambda)$ are, in this case over the whole range of profile distances a near unity. In a theoretical surface with strictly deterministic characteristics and absolutely parallel directional pattern, the following condition must be fulfilled.

$$R_{if}(\lambda)_{max} = R_{ii}(0) = R_{jj}(0) = 1$$

Consequently the functional relation between the distance a_Y and $R_{if}(\lambda)_{max}$ is a straight line parallel to the a_Y axis.

Experimental results are given for milled, shaped, ground, and spark eroded surfaces and the degree of anisotropy found in the surfaces is expressed in polar coordinate form.

It is suggested that the radial tracing method proposed for three-dimensional assessment of surface structure may be suitable for surfaces with weak or non-directional patterns. The method may also be applied to surfaces with circular or spiral patterns produced by plain turning, face milling etc. where the parellel tracing method would not provide meaningful results.

One of the basic problems in surface identification, apart from those already discussed, is the determination of the type or family to which the generated surface belongs. The following topography system has been developed from the premise that every surface profile may be described by a basic autocorrelation function. These functions have previously been shown to have the ability to separate the random and periodic components in a surface.

Investigations on a large number of surfaces indicate that the autocorrelation function generated by various stock removal processes may be classified in five groups. Graphical representations of the autocorrelation functions and their analytical formulae for the proposed froups I - V are summarized in Table 7.1

Furthermore, a classification system based on estimates of the correlation length λ_o and the correlation wavelength λ_w has been developed and incorporated within the framework of the topographical surface system. In other words, a surface profile will be classified first into one of the basic groups (I - V) on the basis of the shape of the autocorrelation function. Further classification within the group involves estimation of the correlation length λ_o and the wavelength λ_w. Details and results of this investigation are given in (24).

Group	Formula	Correlation function shape
I	$r_{xx}(\lambda) = \text{const.}$ $r_{xx}(\lambda) = \cos \Omega\lambda$	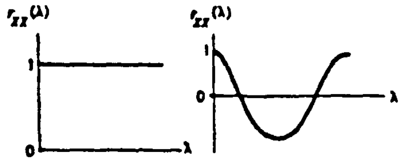
II	$r_{xx}(\lambda) = e^{-\alpha\lambda} + \cos \Omega\lambda$	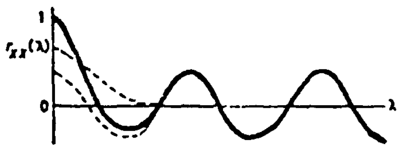
III	$r_{xx}(\lambda) = e^{-\alpha\lambda} \cos \Omega\lambda$	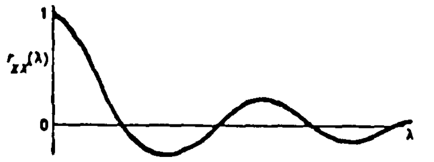
IV	$r_{xx}(\lambda) = \sum_{k=0}^{m} A_k e^{-\alpha_k\lambda} + \sum_{m=0}^{p} A_m e^{-\alpha_m\lambda} \cos \Omega_m \lambda + \sum_{r=0}^{m} A_r e^{-\alpha_r\lambda} \sin \Omega_r\lambda + C$	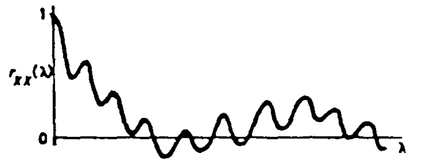
V	$r_{xx}(\lambda) = e^{-\alpha\lambda}$	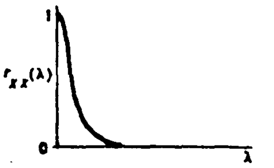

Table 7.1 (after Peklenik)

Peklenik states that in some cases it is desirable to represent the surface profile in frequency domain making use of the Fourier transform of the autocorrelation function. Use of the resulting power spectrum is proposed for the purpose of investigating surface systems as transfer functions. In the context of grinding, this refers to relating the surfaces of grinding wheel and workpiece or alternatively, to the comparison of surfaces representing different stages of grinding wheel wear. The author mentions, as disadvantages of frequency analysis, that it is impossible to determine the correlation length of the surface from the power spectrum, that computation of power spectra takes too long, and also that interpretation of these functions presents difficulty for shop floor personnel.

Peklenik apparently considers the separation of random and periodic elements in a profile to be essential in characterizing the corresponding surface. He also appears to have considered the autocorrelation function to have advantages over the power spectrum for the purpose of this separation. Attention is also drawn to difficulties associated with producing and interpreting both correlation functions and power spectra. However the following notes attempt to show that the justification for these views is not entirely adequate.

Separation of periodic and random elements in a surface does not appear to be fundamentally necessary for it's characterization, although it is to some extent, practicable. From results presented in the paper it is clear that the characteristic carrier frequency in a surface profile gives rise to a pronounced 'peak' in the power spectral density curve while the corresponding autocorrelogram shows a periodicity of the same wavelength as that present in the profile. As means of identifying periodicity in a profile it seems therefore that there is little to choose between the autocorrelation and power spectral density functions.

The random content of a profile is characterized by the correlation length which, as the author points out, is obtainable from the autocorrelogram but not from the power spectrum. However, if it is borne in mind that the power spectral density representing 'white noise' is a constant this, together with the fact that carrier frequencies are represented by 'peaks', provides an indication of the way in which the random content of the profile contributes to the power spectral curve.

In the case of the power spectral density curve representing an electrical signal, an elemental area beneath the curve represents the power associated with that frequency band contained between the limiting ordinates. In the case of the power spectral curve representing a surface profile, such an area represents the variance associated with the heights contained within the frequency band.

Visual inspection of the power spectral curve therefore provides clear indication of the contribution made by carrier frequencies, as represented by pronounced peaks. The contribution to the spectrum made by all other frequencies is represented by areas of greater band width not necessarily associated with well defined peaks. These represent the random content in a form visually descriptive of the surface profile although, admittedly, the correlation length has the advantage of expression by a single number.

Peklenik states that the time required for computation of correlation functions or power spectra by an analogue or digital computer is too long for convenient practical measurement. In the absence of any indication of the time taken to produce the results presented in the paper no comparison with the results of the current investigation is possible although comments on this point will be made at a later stage.

Peklenik also expresses the opinion that interpretation of correlation functions or power spectra requires skill and understanding not necessarily available at shop floor level. However, this problem would appear to be a matter of explanation and training. His proposal to use slope standard deviation as a surface texture parameter additional to arithmetic average value (R_a) or geometric roughness value (R_s) is of interest. The fact that this is a number and not a function although convenient does not necessarily support the statement that the parameter itself will be easily understood at shop floor level.

Finally the fact that power spectral density curves representing different profiles may be compared and related by means of transfer functions appears to considerably enhance their usefulness over auto--correlation functions as a means of surface comparison.

Information obtained from Peklenik's work was interpreted as encouragement to proceed further with the application of power spectra to characterize surfaces involved in the grinding process, bearing in mind the additional possibility of relating the surfaces so represented by means of transfer functions.

The next paper to be considered (26) is devoted to the statistical characterization of grinding wheel profiles. This too was published during 1968 by Stralkowski, Wu and De Vor on the basis of work carried out in the United States. The abstract is as follows.

> The cutting profiles of three common grinding wheels, 32A8-H8, 32A80-L8, and 32A60-J8 were analysed by Box-Jenkins autoregressive-moving average models. The analysis involves three stages, i.e., identification, estimation, and diagnostic checking. It was found that second-order autoregressive models represent the profiles of the three wheels fairly well. An analysis of replicate profiles taken from each wheel indicated that the profiles were ergodic. The models and their parameters were related to the qualitative characteristics of the profiles. The analysis was achieved through the use of many charts developed for engineering applications.

The paper's conclusions summarize the procedure and results as follows:-

> 1. Three grinding wheel profiles were characterized as second-order autoregressive models, AR(2), using the Box-Jenkins

autoregressive-moving average model approach.

2. The two parameters of the AR(2) model were estimated by maximum likelihood principles, and confidence regions for the parameters were constructed, Parameters θ° and C were also estimated and their confidence interval calculated. (Parameter C is a measure of the variation in the observations unaccounted for by the model. $\hat{C}$ = error sum of squares ÷ total sum of squares)

3. The fitted model was diagnostically checked by examination of the residuals. No significant difference was found between replicates of each wheel, confirming the ergodic nature of the cutting space.

4. The distinguishing characteristics of the grinding wheel profiles were interpreted by the parameters of the model: amplitude θ°, modulus r, and variance γ_0.

5. The three-stage procedure of identification, estimation, and diagnostic checking was achieved by using charts developed for engineering applications.

The results of the analysis have some relevance to the present study in providing further confirmation of the ergodicity of grinding wheel surface profiles and the fact that statistical parameters, including autocorrelation functions, are capable of characterizing such surfaces.

Brief reference is made to Peklenik's characterization of grinding wheels using autocorrelation functions (21) and he is credited with having introduced the idea of modelling the grinding process as a linear transfer system.

The only information given about the three grinding wheels examined is contained in the manufacturer's coded specifications and there is nothing to indicate whether the profiles were obtained from surfaces prepared as for a grinding operation. If the surfaces were not subjected to some form of dressing operation they would be unrepresentative of those encountered in actual grinding and doubt would be cast upon the validity of results obtained from them.

Those comments seeking to relate grit size and the amount of bond material on the one hand with statistical paremeters on the other also appear to be based upon some concept of grinding wheel structure neglecting the effects of dressing and wear.

The interest of the paper lies mainly in the application of particular statistical models to abrasive surfaces.

A paper by Shinaishin (27) published in the United States during 1969 deals with stochastic processes in grinding and is summarized as follows.

> The mechanism that links the grinding wheel surface profile to the forces generated during grinding is discussed in the case of surface grinding. A method of describing the profile as a stochastic function in terms of parameters that are pertinent to the grinding operation is also given. The mechanisms by which diamonds in a grinding wheel deteriorate are discussed: these include attrition, fracture, and bond failure. The extent of this deterioration relative to the surface profile, forces, and time parameters is discussed. A relation is suggested betwen the power spectral density, mean square, and number of zero crossings of the profile at any time and their values at an earlier time. This relation includes the forces which

are functions of the profile, and time; it assumes controlled and stable grinding conditions.

Examination of the paper indicated less relevance to the present study than had been assumed from the summary. For this reason it is not proposed to enter into a detailed description but several points arise which call for comment.

The paper discusses at some length the abrasive profile, kinematics of grit-surface interaction, the profile's effect on force generation, the forces generated during grinding, wheel/workpiece stability, abrasive surface wear and the failure mechanisms associated with wear.

The surface profile of the grinding wheel was recorded on polar graphs said to represent waviness, roughness and total profile and also on magnetic tape.

A surface grinding dynamometer was used to measure the low frequency forces during grinding while it appears that accelerometers attached to the workpiece were used to measure high frequency forces.

The results of a correlation analysis to determine the relationship between the cutting forces and the normal forces are described. These results apparently bore no relationship to what was expected on the basis of diamond grit distribution and suggestions are made as possible explanations for this discrepancy.

The results of a frequency analysis of the wheel surface profile are shown in Figure 7.9 It is pointed out that profile A before grinding has it's peak at 6.5 Hz or about 100 cycles per inch which is near the number of diamonds per inch. Profile B shows a shift to 16 Hz or about 256 cycles per inch and it is suggested that this may indicate the exposure of more cutting edges per diamond by reason of some fracture in the abrasive.

Power spectra are also used in attempts to analyse cutting and normal forces in frequency domain but spectra presented are so complex that generalized description is impracticable.

The author admits that the experimental results did not cover all the objectives. This it is said, was due mainly to the difficulty of recording spindle vibration during grinding and also because of the frequency limitations of the accelerometers. However, several conclusions are drawn including the following.

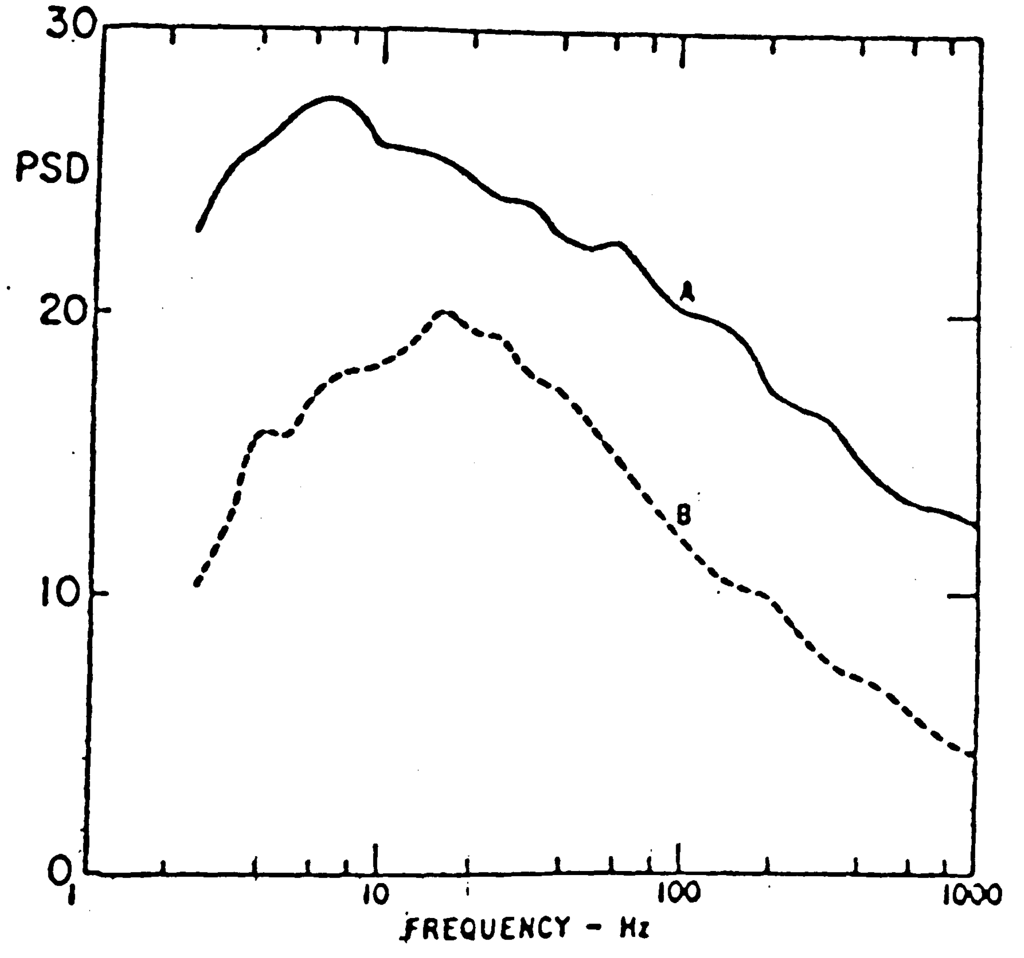

Fig 7.9 Power spectral density of wheel-surface profile

(A) ―――――――― before grinding

(B) - - - - - - - - - - after grinding for 8hr at 1 mil

depth of cut. 1 c.p.s. = 45/π cycles per inch

(diagram and notes after Shinaishin)

Firstly the grinding wheel surface profile changes considerably even while the radius of the wheel has changed 0.5μm or less.

Secondly, as the depth of cut was increased progress--ively from 1μm to 2.5μm a rise in the total energy was demonstrated by the general increase in the power spectral density of the cutting forces.

Next. when grinding began, there was a relatively low energy in the frequency range 700Hz to 8kHz but as grinding progressed, the energy expended in the 2kHz band increased very fast until it reached a value at 2.5μm depth of cut nearly 30 times that at 1μm. This is attributed to the development of six lobes on the surface of the wheel increasing progressively with depth of cut.

Finally a difference in the forces generated after eight hours grinding can be seen, especially at 1.3 and 2.6kHz suggesting that the process of imbalance in the wheel and the development of lobes is self generating due to the grinding process.

Topics dealt with relevant to the present study include some treatment of surface profile and analysis by statistical methods including power spectral density.

However, only surface grinding of tungsten carbide by means of diamond abrasive is considered, there is no information on workpiece surface profile and attention is focussed mainly on the system of forces acting between wheel and workpiece.

The elements in a grinding operation are described in the following terms:

(1) the grinding machine, which is mounted on elastic supports on the floor of the workshop,

(2) a grinding wheel mounted at the end of the grinding machine spindle and

(3) the workpiece, which is mounted on a work table which, in turn, is isolated from the floor by elastic mounts.

The resulting system is said to be represented by the two primary systems coupled by a means for transmitting the forces (Figure 7.10).

It is not clear why elements (1) and (3) in the grinding operation are described as being independently mounted by means of elastic supports on the workshop floor. In typical grinding machine construction the work table is

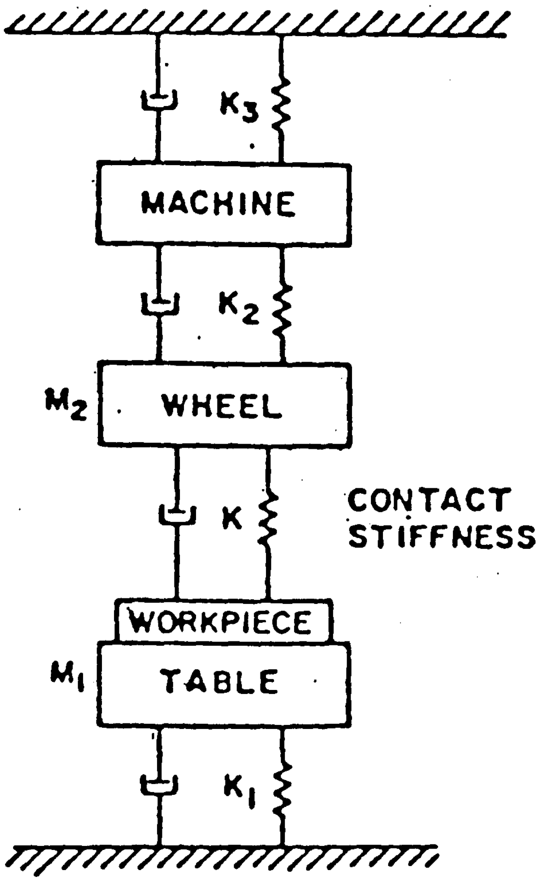

Fig 7.10 Model of grinding operation (after Shinaishin)

mounted on slideways integral with the machine. Therefore in such a machine direct coupling and transmission of forces exists between machine frame and worktable.

The model illustrated in Figure 7.10 appears to be over simplified since it is based upon an unusual description assuming that machine and workpiece are isolated except for transmission of forces through the grinding wheel.

In all power spectra presented in the paper, power spectral density is plotted against a logarithmic frequency scale. All dimensions are in inches with the exception of depth of cut expressed in 'mil' (μm).

To facilitate comparison with material from other sources, the power spectra representing wheel surface profiles in Figure 7.9 have been re-plotted against a natural scale on which frequencies are expressed in cycles per linear unit of surface (Figure 7.11).

Shinaishin's paper deals with a specialized aspect of grinding technology very different from the present study in that it is confined to the grinding of tungsten carbide by means of diamond abrasive. However, grinding wheel surface profiles are represented in terms of power spectra and a suggestion to the effect that wear appeared to produce more cutting edges per

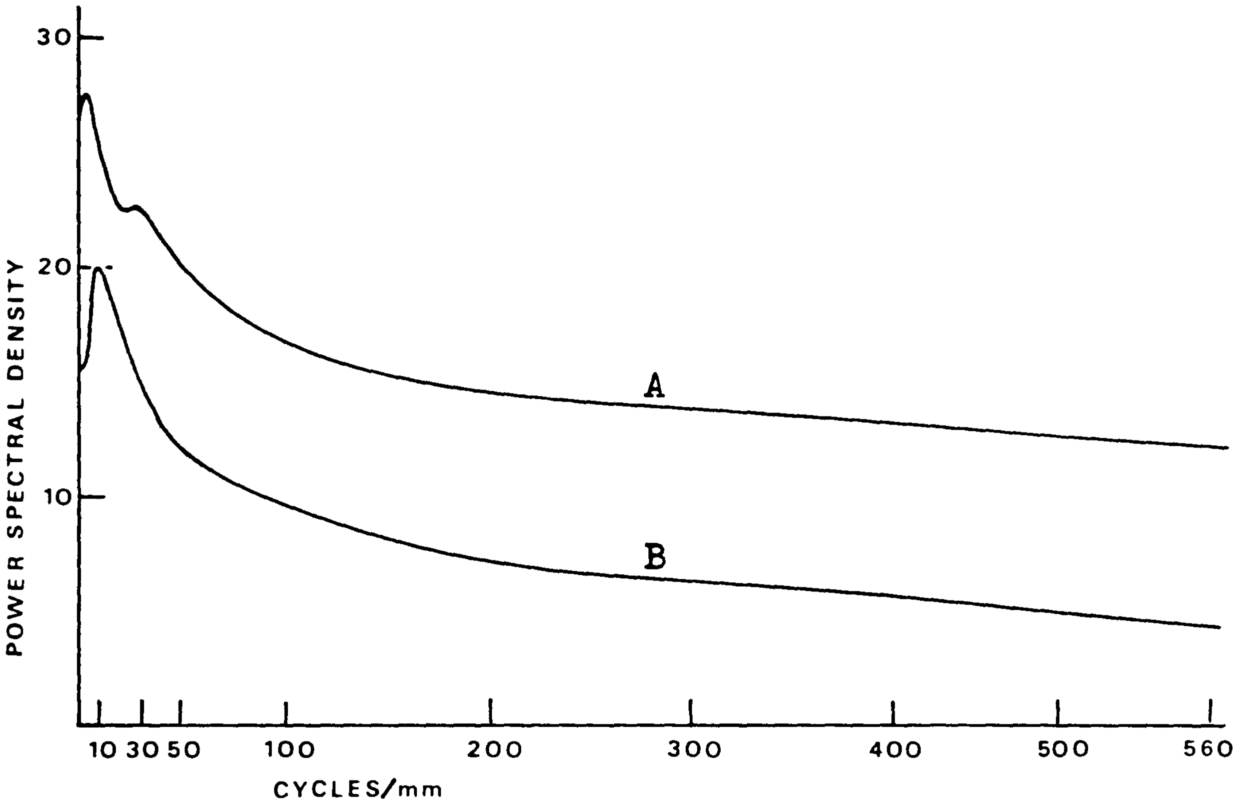

Fig 7.11 Power spectral density of wheel-surface profile

(A) before grinding

(B) after grinding for 8 hours at 1μm depth of cut diamond is consistent with findings elsewhere relating to other abrasives; including the author's in Part 1. Also the presentation of results in terms of power spectral density and the general character of these curves indicated by Figure 7.11 provided further confirmation of the potential usefulness and validity of this parameter.

A paper by Deutsch and Wu (28) published in 1970 deals with the selection of sampling parameters for the study of grinding wheel surface profile and is summarized as follows.

> Autoregressive-moving average models are developed to represent grinding wheel profiles for different combinations of sampling parameters including the sample interval, the number of observations, and the length of record. Using 46 and 120 grinding wheels the effects of the choice of sample interval and number of observations on the appropriate model form are discussed. A new criterion is proposed for the selection of the sample interval, based on observations per grit (OPG), to achieve comparable discrete approximations of the wheels and to maximize discrimination between models of different wheels.

In their introduction the authors point out that statistical techniques used in the analysis of abrasive tools share one common entity - the approximation of a comtinuous record.

> In such situations, the choice of sampling parameters (sample interval, number of observations, length of record) is of paramount importance. The sample interval must be small enough not to miss any appreciable detail in the continuous record. Likewise, for efficiency, it should not be so small that little additional information is gained. The length of record analysed should be chosen to ensure that all representative characteristics of an abrasive tool profile are captured. Furthermore, when a comparison of the statistical results of dissimilar abrasive tools is made, the inherent differences should be elucidated.

In order to select sample interval the average particle size of the aluminium oxide abrasive grains (obtained from a table supplied by the Norton Company) is divided by a number depending on the intended use of the fitted model.

If a true representation of the qualitative characteristics of grinding wheels on an individual and comparative basis is desired, then approximately 6 - 7 OPG should be used. However, if only models to discriminate between grinding wheels are desired, then a large range of OPG can be considered for which the discriminatory power is constant. A reasonable lower bound can be as low as 2 or 3 OPG. When using a smaller level of OPG, the general characteristics of the profile become lost in the approximation since there is a greater chance to miss grits due to the large sample intervals.

Referring to the use of the OPG criterion the following claims are made in the conclusions.

(a) Parameter discrimination is constant for the range of OPG values where good approxim--ations to the continuous profile are obtained.

(b) The efficiency of the models in uniquely representing the different wheels is improved.

(c) The theoretical interpretation of the models appears consistent with the wheel characteristics contained in the continuous profiles.

The following represents the only information on the profile measuring system contained in the paper.

> The abrasive tool profiles are traced by a stylus which oscillates across the surface. The oscillating mechanism permits the reduction of the stylus dimensions, which reduces the distortion in the measured abrasive tools.

Neither the dimensions of the stylus used nor it's mode of oscillation are stated. However there is reference to currently unpublished information which appears to correspond with a paper published about three years later (33).

It is stated that the partial correlations cut off after one lag when using a sample interval of 0.005in. Around a sample interval of 0.005in an autoregressive model of order one can be chosen for reasons of parsimony[1].

Over the range of sample interval from 0.001in to 0.005in an order one model is inadequate and a model

1.Concise Oxford Dictionary. Law of Parsimony: that no more causes or forces should be assumed than are necessary to account for the facts.

of order two should be used to provide an adequate representation of the sampled profiles. In this context reference is made to the use of parsimonious models in an earlier paper (26).

Areas of particular interest and apparent relevance to the present study in Deutsch and Wu's paper were identified as follows.

(a) The discussion of the problems of grinding wheel surface profile sampling.
(b) The application of oscillating stylus profilometry to grinding wheels.
(c) The use of autoregressive models to represent abrasive surface profile.

Considering the foregoing points in reverse order, the use of autoregression provided further indication of some concensus of opinion with other authors relating to the utility of statistical models of this type applied to abrasive profiles.

Claims made for the improved accuracy of the profile record obtained by means of an oscillating stylus were noted but very little information is provided and details were eventually obtained from a subsequent paper (33).

Two ideas emerge in the context of grinding wheel surface profile sampling. One of these relates to the frequency of observations within the sample so as to relate this to the size of individual grits and the amount of detail to be recorded in order to define their profile. The second point is that the use of a small number of observations per grit results in loss of information regarding general profile character--istics because the chance of missing grits is increased. These ideas clearly indicate recognition of discontin--uities as an integral feature of the grinding wheel profile not to be neglected in its analysis.

Information is lacking on the surface condition of the grinding wheels examined. There is no mention of any dressing operation neither is there any indication of whether or not the wheels had been subjected to wear in a grinding operation before profile measurement of their surfaces.

From this it appears that results presented in the paper are intended to discriminate only between grinding wheels of differing grit size and structure. In order to compare grinding wheels differing in surface condition it is suggested that profile samples should contain a larger number of observations per grit but no such comparisons are included in the paper.

The paper serves to draw attention to the significant fact that detailed study of the grinding wheel surface by profilometry requires definition of the profile by ordinates spaced at intervals chosen so as to adequately define the shape of individual grits and also to represent those areas where grits are virtually absent from the profile - namely within the voids.

A more specialized paper published in 1971 by Masashi Harada and Akira Kobayashi (29) deals with the production of mirror-finish ground surfaces making use of an ultrasonic dressing method. The summary is as follows.

> In order to produce evenly sized micro cutting edges of uniform height required for mirror grinding, a flattened head impact at ultrasonic frequency dressing (abbreviation: FL-USD) has been developed, using normally directed impacts from an ultrasonically vibrating dressing tool with a flat-faced Tungsten Carbide S2 (5 × 5 × 3mm) surface on the rotating grinding wheels.

The analysis of cutting edges made by the FL-USD method, as observed under an electron microscope showed that the height of cutting edges made by general dressing (DD) methods was usually about 2μ, whereas the FL-USD heights were found to be 0.2μ, situated between 0.5μ depth and wheel surface. Use of this wheel resulted in obtaining a mirror finish with a surface roughness of H_{max} = 0.05 . A study is made of the cutting edge production process by FL-USD from the crushing load of a single grain, the impact force of the dresser on to the grinding wheel, stock removal and observations on the shapes of cutting edges under the electron microscope.

The paper provides an explicit description of the ultrasonic dressing technique and the surface textures produced using grinding wheels dressed by this method. Comparisons are made between these results and those surface textures produced by grinding wheels dressed by conventional methods with a single diamond. However, there are indications that these comparisons may tend to underrate the potential of diamond dressing.

Neither the nominal diameters of the grinding wheels nor the shape and mode of application of the dressing diamond are specified. Dressing diamond traverse rates of 80mm and 90mm per minute and a surface speed of 30m/s are specified. Assuming the grinding wheel diameter to be 150mm these feed rates are equivalent to 22μm and 25μm per revolution of the grinding wheel which is a fairly high traverse rate when a primary objective of dressing is the production of fine surface texture on the workpiece.

The dressing method described in the paper is very unusual and the results obtained in terms of surface roughness correspondingly exceptional. Results serve to demonstrate the very large extent to which the surface profile of the grinding wheel and the surface texture it produces on the workpiece can be influenced by the method of dressing. Inclusion of the paper in this survey is justified on the basis that it serves to emphasise the importance of wheel dressing as a primary factor affecting surface texture not always fully recognized as such elsewhere in the literature.

The influence of dressing on the quality of ground surfaces together with the effects of grinding wheel wear are the subject of a paper by Bhateja, Chisholm and Pattinson (31) who carried out experiments in which medium carbon steel was ground on a precision surface grinding machine using a vitrified bonded alumina grinding wheel. The wheel was dressed by a single pass of a single point diamond tool at a depth of cut 0.025mm (0.001in) at feeds of 0.025mm/rev and 0.325mm/rev (0.013in/rev) chosen to represent fine and coarse dressing treatments respectively.

The grinding operation was interrupted at intervals corresponding to the removal of one cubic inch of workpiece material. At these intervals the radial wheel wear was measured and profilograms taken of the wheel surface in a direction parallel with it's axis using a specially adapted profilometer. Corresponding profilograms were obtained from workpiece surfaces using a standard profilometer. The stylus used for grinding wheel surfaces had a 90 degree pyramid shape with a tip radius of 0.025mm(0.001in) while that used for workpiece surfaces had a tip radius of 0.0025mm (0.0001in). These profilograms were digitized to provide input data for a computer programme written to evaluate:

(a) the cumulative frequency distributions of the asperity peaks and valleys with increasing depth in the profile,

(b) the bearing area characteristics of the surfaces.

A feature of the paper is that no attempt is made to express surface roughness in terms of any one of the more usual parameters. Instead both grinding wheel surfaces and workpiece surfaces are represented by means of cumulative peak and valley distributions and bearing area curves.

When these distributions were used to compare grinding wheel and workpiece surfaces, they appear to reflect the influence of dressing conditions. Only when wheel wear had progressed to an advanced stage suggesting bond failure was the shape of the distribution ogives significantly affected by this cause.

A coarse dressing feed was found to produce greater bearing area but a rougher surface than a fine feed. In this context it is pointed out that the grinding conditions necessary to produce a good surface finish are not necessarily those which produce a good bearing area. This apparent contradiction may reflect upon the limitations of bearing area curves as a means of representing surface texture rather than the validity of the experimental results.

With regard to the representation of grinding wheel surfaces the validity of a result obtained by means of a stylus and said to represent the distribution of 'valleys' is questionable. Penetration into depressions must always be limited by the finite dimensions of a stylus and particularly so in this case where the stylus used is described as having a 90 degrees included angle.

The methods and parameters used do not appear to have been particularly sensitive to the effects of the considerable amount of wear to which grinding wheels were subjected during the experiments. However, the paper represents a contribution in the same area of study as the current investigation, included as such although the findings are not particularly revealing. Somewhat similar justification applies to the inclusion of a paper by Motoyoshi Hasegawa (32) published in 1974 and described by its title as a statistical analysis of the mechanism resulting in the generation of ground surface roughness. The summary of the paper is as follows.

> This paper discusses a statistical approach for determining the roughness of a ground surface by considering the dressing characteristics of the grinding wheel. The statistical analyses are derived for the distribution curve of the cutting edges and the probability density function for the occurrence of 'peaks' throughout the surface profile of the grinding wheel after

dressing treatment and the root mean square roughness of the workpiece ground by the wheel. The theory shows that when the grinding wheel is repeatedly dressed by a sharp-pointed dresser, the distribution curve of cutting edges is parabolic. The root mean square of the surface ground by the cutting edges may be calculated from wheel speed, wheel diameter, workpiece speed, the apical angle of the dresser, size of sample and the distribution of cuttinge edges on the circumferential direction of the wheel. Good agreement was found between theoretically calculated and experimental results.

A theoretical distribution of 'cutting edges' on the surface of a grinding wheel is derived making use of the three following assumptions.

(1) The vibration of both grinding wheel and dresser is negligible.

(2) The shape of the dresser is conical with an apical angle 2ϕ.

(3) The material of the wheel in contact with the dresser is removed according to the shape of the dresser when this is fed into the grinding wheel.

The second and third of these assumptions together with a related diagram indicate the use of an unorthodox mode of dressing with a conical single point diamond dresser so presented to the wheel as to cut in it's surface a vee groove of included angle corresponding to the apex angle of the diamond.

When dressing with a single point diamond the axis of the tool shank is usually inclined so as to present the flank of the cone (or pyramid) to the surface of the wheel with the axis trailing in relation to the direction of wheel rotation. In this mode an approxim--ately flat surface (or at least a surface which quickly develops a worn, flattened area) is presented to the grinding wheel and there is no possibility of reproducing the apex angle of the diamond on the wheel. Not only does the mode of dressing described by the author represent an unfavourable orientation of the diamond (from the point of view of wear rate and economy in the use of the diamond) but it will tend to produce pronounced grooves in the grinding wheel which may be reproduced on the workpiece in some pattern depending on the kinematics of the process (1).

The author's statement to the effect that repeated dressing under the unusual conditions specified, gives rise to a distribution of cutting edges which is theoretically parabolic, does not appear to be supported by the mathematics. In fact, curves plotted to represent this distribution for m repetitions of the dressing process, show a progressive change from a rectangular distribution when m = 1 to a hyperbolic distribution when m = 5. The relevant equation also appears to support the idea that the proposed model distribution should be described as hyperbolic rather than parabolic.

It is also stated that 'peaks' of the cutting edges follow a Gamma distribution. This conclusion appears to be based upon three diagrams whereon Gamma distribution curves are fitted to histograms representing the experimental probability distribution of 'peaks'. The fit between curve and histogram in all three cases is very approximate and it appears likely that the histograms would be better approximated by a composite distribution taking account of the fact that some parts of the grit profile may be affected by dressing while others are not (30).

Finally the conclusions state that the number of dressing treatments m has a more significant effect than sample size n on the roughness of the ground surface. Sample size n appears to relate to the surface of the grinding wheel but it is not explicitly defined and the meaning of the statement remains obscure.

The paper contains what appear to be rather obvious shortcomings of technique and description, some or all of which may be due to errors and omissions in translation. For this reason it was found impracticable to evaluate its contribution to the subject.

A paper published in 1973 by Deutsch, Wu, and Stralkowski (33) presents what is described as a new non-destructive, on-line irregular surface measuring and data handling system, referred to as the oscillating stylus instrument.

This is almost certainly the paper to which reference is made in an earlier publication by Deutsch and Wu in 1970 (28). The following extracts relate to techniques said to have been previously used for the measurement of abrasive tools.

> Typically, a stylus continually contacting the abrasive tool with a relative motion between the two has been used to measure abrasive tools............................
> This type of system although capable of measuring a fine surface finish has limitations in reproducing the irregular configuration of an abrasive tool.

> In order for the stylus to freely traverse the specimen, a particular stylus geometry is required. Figure 7.12 illustrates a typical grinding wheel cutting space cross section and a stylus. The ability to climb out of the 'valleys' depends upon having a large included angle,α, as well as always having line BC above the highest peak in the profile to prevent the stylus from totally lodging. Any included angle, however, will result in contact of surfaces AC or AB of the stylus and the grains causing the recorder profile to become distorted as shown by dashed lines....................

The following statements are made relating to the oscillating stylus.

> The oscillating stylus, unlike the conventional stylus technique, imposes no dimensional restrictions upon the stylus for functional considerations. It uses a stylus attached directly to the core shaft of a displacement transducer. The stylus is oscillated by a motor driven cam, thereby moving the transducer core to produce a d.c. voltage proportional to the core displacement from electrical centre (Figure 7.13). If this

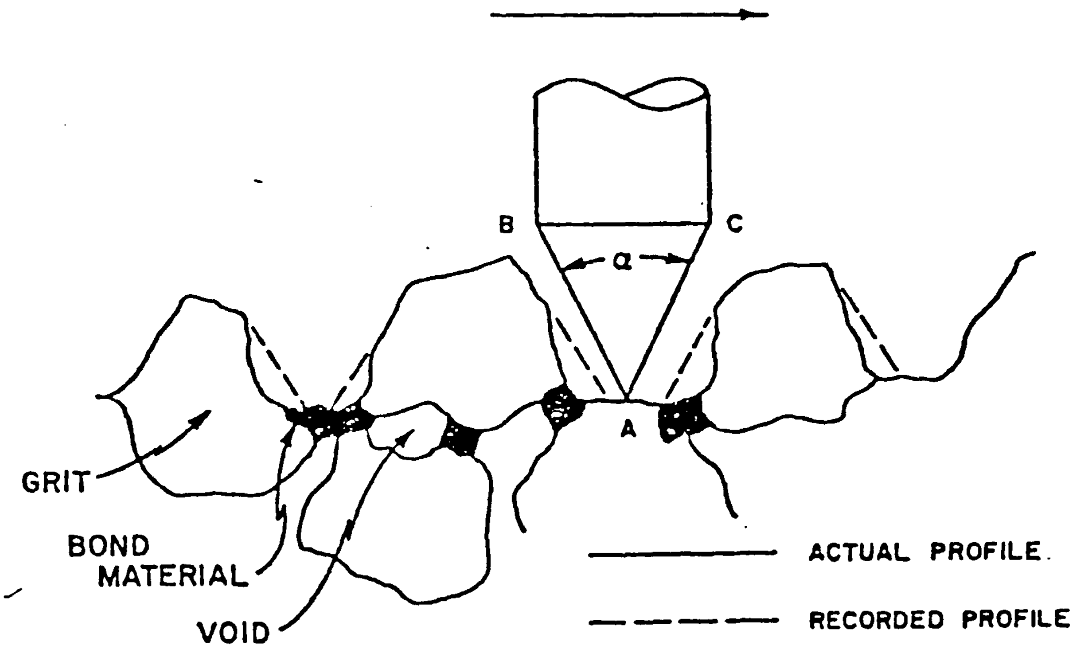

Fig 7.12 Induced distortion produced by the conventional profile measuring technique on grinding wheel cross section (after Deutsch, Wu, and Stralkowski)

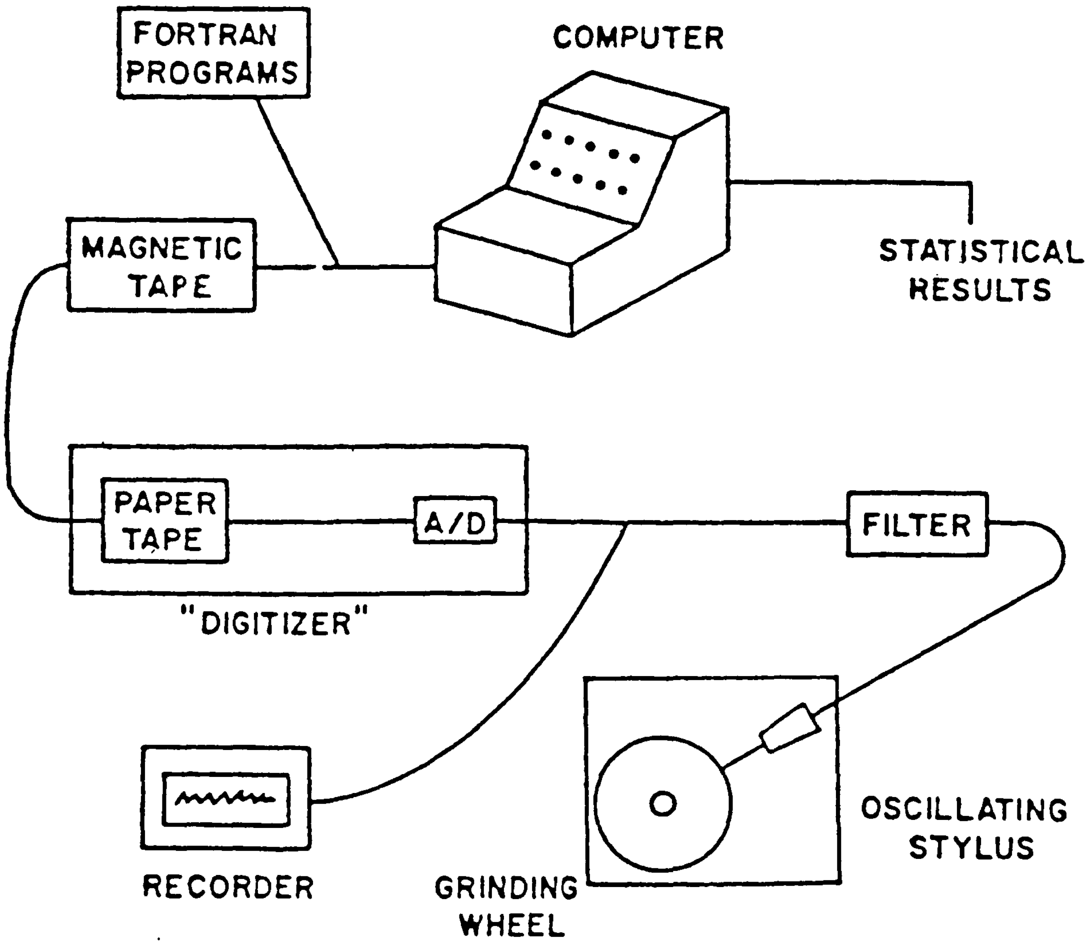

Fig 7.13 Measurement and data handling system
(after Deutsch, Wu, and Stralkowski)

movement is not restricted, the voltage produced by the transducer is sinusoidal with respect to time......................
When this cyclic movement is restricted by a surface, the sinusoidal signal is truncated................................
If there is relative motion between this surface and the stylus, the stylus for each period is dragged over the profile from the first point of contact (A) to the last point of restriction (B), tracing a segment of the surface as illustrated in Figure 7.14

As the frequency of oscillation increases and/or the relative motion between the stylus and the restricting surface decreases, segments for which the stylus traces the restricting object become smaller and approach a single point producing a recorded d.c. signal which elucidates the entire shape of the restricting surface.

The construction, electrical principles and calibration of the apparatus are described in some detail and recorded profiles representing three grinding wheels of different grit size and density are used as examples of this type of application.

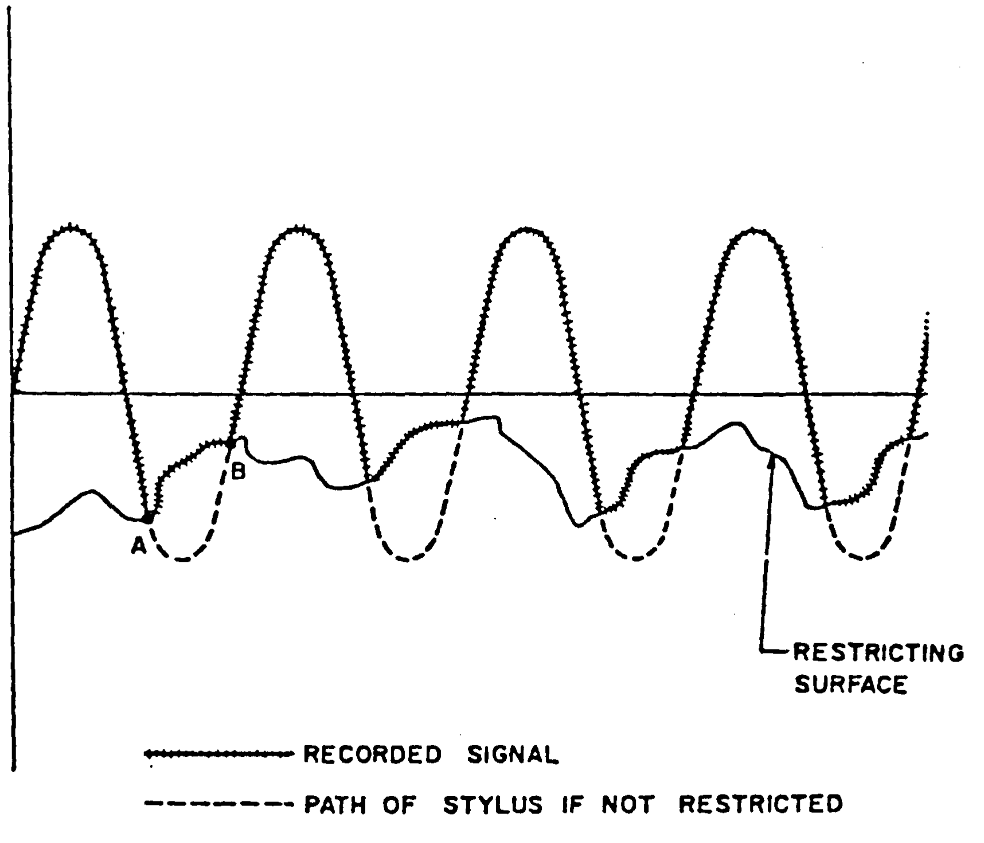

Fig 7.14 Example of surface tracing produced by oscillating stylus mechanism (after Deutsch, Wu, and Stralkowski)

Direct comparisons between the geometry of the oscillating and conventional stylii are shown in Figure 7.15.The accuracy of the oscillating stylus instrument is said to be linear within 0.5 per cent over it's usable range.

The oscillating stylus system was evidently found to be capable of more accurately reproducing the profiles of grinding wheels and craters than methods using a stylus having the relatively large included angle of more conventional systems. However the claim to the effect that the oscillating stylus system imposes no dimensional restrictions upon the stylus for functional considerations is so obviously overstated that comment might be superfluous but for the fact that the description and diagrams on stylus geometry contain no information on tip radius which represents one of the limitations applicable to all stylus methods of surface investigation.

The oversimplified description of grinding wheel surface characteristics represented by the following extract also calls for comment.

> The configuration of a wheel such as the Norton designation 32A46J12VBEP, consists of two dominant characteristics; "localized irregularities" due to closely packed grits

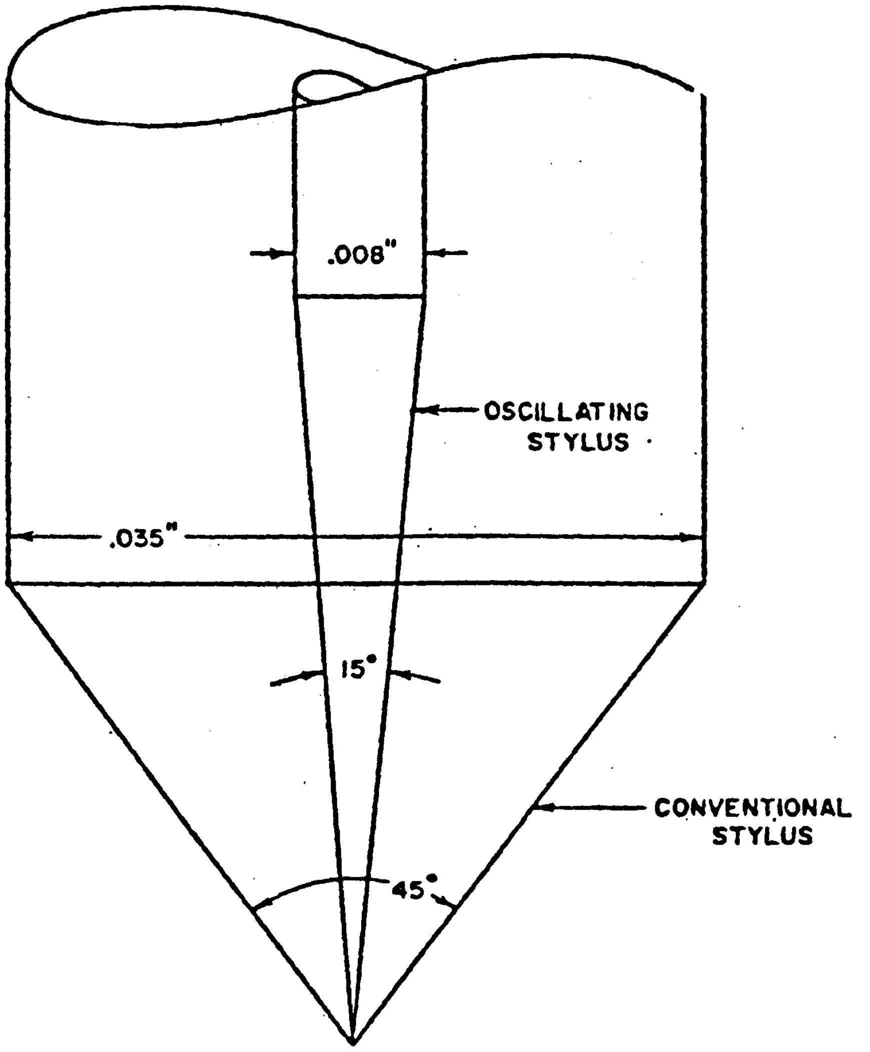

Fig 7.15 Comparison of stylii (after Deutsch, Wu, and Stralkowski)

> and deep "pits", as much as two to four times the peak to valley height of the localized irregularities.

The description of localized irregularities as being due to close packing of grits is incomplete since it neglects the influence of dressing and wear on the surface micro-geometry.

The deep "pits" represent the outermost voids between the bonded grits. These voids in a typical porous structure form a continuous interconnected network throughout the grinding wheel and any attempt to define the depth of surface pits is virtually meaningless.

Difficulties attending stylus measurement are stated as follows.

> These varied characteristics (of grinding wheels) make measurement by conventional stylus techniques physically undesirable. The stylus of appropriate geometry to trace the finer "irregularities" does not have the capability of accurately tracing or freely climbing out of the deep valleys.

Such valleys when represented by the spaces between grits are of virtually unlimited depth, their dimensions and geometry being determined by factors which include the shape and size of grits, the amount and distribution of bond material etc. The accessibility of surfaces enclosed within such voids to stylus examination must inevitably be limited by the dimensions and geometry of any stylus. However, the technique described uses a stylus with an included angle of only 15 degrees the tip of which is therefore capable of tracing much more of the internal surfaces of deep depressions than would be accessible to a more conventional stylus with much larger included angle.

in it's application to grinding wheels the oscillating mode overcomes the problem of stylus withdrawal from deep cavities but since internal surfaces may be vertical or re-entrant, there will be areas which the stylus tip fails to contact with resulting distortions. This limitation probably does not apply to the measurement of craters in cutting tools as described in the paper.

Apart from specifying the 15 degrees included angle the paper gives no information on the geometry or construction of stylii used in the experiments. Neither the material nor the cross section is specified but perhaps the most surprising omissions is the absence of any reference to tip profile.

There is evidence from a number of sources that the active zone of a grinding wheel surface can usefully be reproduced by stylus methods based upon those used for continuous surfaces, typically employing a diamond stylus of small tip radius and large included angle. For the purpose of studying surface texture relationships, a profile representing the cutting space of a grinding wheel obtained by means of such a stylus is comparable with a profile of the ground surface produced with a similar stylus.

It is evident that the oscillating stylus can provide more information about grinding wheel surface profile than more conventional stylus methods. However the additional and more accurate information appears to relate to lower levels within the profile and therefore has little influence on the surface interactions between grinding wheel and workpiece.

Although it contains no information on surface texture, a paper by Thompson and Malkin (34) is included because it deals with grinding wheel topography. Experimental methods and conclusions are explicitly stated in the following abstract.

The topography of grinding wheels of various grain sizes was measured statically by an optical technique and dynamically by studying the scratches left on a smooth steel plate after lightly grinding a single pass. The optical method yielded good results with the coarse grained wheels. At a radial depth into the wheel equal to one grain diameter, the number of grains per unit area was found to approach the theoretical maximum number as calculated from packing considerations. The scratch method provided an effective means for measuring the fine scale topography of the wheel surface. With this method, the number of actual cutting points was found to be relatively insensitive to grain size. This is attributed to large grains each having more cutting points than smaller ones. From the shapes of the scratches left on the steel plate, the undeformed chip was determined to have a trapezoidal cross-section with typically a 120 degree included angle between the sides and a 1 - 2 micron width at the bottom.

Relevant technical data are contained in the following extract.

> The grinding wheels were 8in diameter with 32A aluminium oxide abrasive in grain sizes of 30, 46, 80, and 120. Each wheel was dressed with a single point diamond dressing tool at a crossfeed velocity of 5in/min. After the wheel had been trued, at least one nominal grain diameter was dressed off taking 0.001in during each pass across the wheel. All measurements were taken after 10 passes by plunge grinding of an AISI 1098 hot rolled steel workpiece which was 4in long. Grinding was performed at a wheel velocity $V = 6000$ft/min, work--piece velocity $v = 15$ft/min and depth of cut $a = 0.001$in.

The scratch method used is described as a simplification of one originated by Nakayama and Shaw (14, 30) in which scratches are produced on a steel plate slightly tilted with respect to the wheel surface by grinding with a slow wheel speed and a fast workpiece velocity. The following extract relates to Thompson and Malkin's technique.

> The present method is much simpler (than Nakayama and Shaw's), insofar as there is

no tilt to the plate, and the radial depth of a cutting point is calculated from the length of the scratch it produced. By counting the scratches within a specific area on the plate, measuring their length, and calculating their depth, the number of cutting points per unit area of wheel surface can be determined as a function of the radial distance into the wheel. In addition, the geometry of individual scratches can be studied to determine the shape of the cutting points on the grains.

The experimental results include graphs relating to four grinding wheels of different grain sizes. It is stated that only about the outer 0.0001in of wheel can be examined but that this portion is very important as it has the greatest effect on the topography of the finished workpiece.

Surprise is expressed at the fact that the four curves differ very little, only the curve for the 120 grain size having more cutting points at depths greater than 30 microinches. Results for the 30, 46, and 80 grain sizes are said to be practically identical. Therefore the number of cutting points in the outermost portion of the wheel is about the same regardless of grain size.

Numerous scratches were studied with the object of determining their typical shape and it is stated that the cross-sectional shape of the scratches obtained with all four grain sizes were found to be approximately trapezoidal with side angles typically 60 degrees and a base width of about 40 to 80 microinches (1 - 2 microns).

Thompson and Malkin's paper does not consider roughness of the ground surface but has some relevance to the current study because it deals with the cross sectional profile of the scratches produced by grinding and the distribution of cutting points in the wheel surface.

The fact that the number of cutting points per unit area of wheel surface obtained by the scratch method did not vary much between the 30, 46, 80, and 120 grain size wheels is attributed to larger grains having more cutting points than smaller ones.

Wheel dressing and preliminary grinding wear were both standardized during the experiments described. The rate of cross feed used during dressing and also the depth removed at each pass are fairly typical of normal fine grinding practice. The possibility that variations in dressing conditions and the extent of subsequent wear could affect the number and distribution of cutting points in the wheel surface does not appear to have been considered but the fact that wheels of different grit size were found to have about the same numbers of 'cutting points' supported the view already formulated by the author (30) to the effect that dressing is a more potent factor in determining grinding wheel profile in the active zone than grit size. It is therefore appropriate that the next paper to be considered mentions the influence of dressing on asperity distribution. Bhateja (35) concentrates on the diamond dressing of grinding wheels as stated in the following abstract.

> Recent studies of the diamond dressing of grinding wheels have revealed that, besides influencing the wear behaviour of a wheel, dressing has another fundamental effect, namely, the arrangement of asperities on the wheel's cutting surface. This paper presents a new theory of the diamond dressing process, on the basis of a two stage action of a single diamond tool; the first stage involves a gross fracture of the wheel material and the second is a levelling effect.

The effects of a grinding wheel's inherent compositional properties such as the grade or hardness and the bond type, on the wheel's cutting surface have been invest- -igated experimentally in the light of this proposed theory of diamond dressing. Both wheel grade and bond type have been found to affect significantly the nature of the sharp, newly dressed grinding wheel.

Greater penetration of the dressing influence into the grinding wheel in softer grades of wheels and also for vitrified bonds (as compared with resinoid bonds) has been established.

Experiments were carried out in which four grinding wheels of different specifications were dressed at two feed rates viz. 0.001 in per rev (fine) and 0.010 in per rev (coarse).

Axial profiles of the grinding wheel surfaces were obtained using a 90 degree pyramid-shaped diamond stylus having a tip radius of 0.0005 inch. These profiles were digitized and from the resulting data several surface texture parameters and the cumulative frequency distributions of peaks and valleys were computed. Examples of the results obtained and method of presentation are shown in Figures 7.16 and 7.17

In discussion of these results Figure 7.16(a) is said to confirm the polynomial-shaped cumulative frequency distribution of asperity peaks and somewhat S-shaped pattern of valleys. The plot of the distribution of peaks for the harder wheel Figure 7.16(b) is said to exhibit a much more pronounced polynomial shape of peaks and a similar polynomial shape for the valleys. This was thought to be consistent with a greater and deeper fracture tendency (perhaps complete grit removal) in the softer wheel during the initial gross fracture stage of the diamond dressing process.

The following extracts refer to the influences of wheel grade, bond type, and dressing feed.

> The mean distribution curves of Figures 7.17(a) and (c) for peaks and valleys show that for the vitrified bond, irrespective of the dressing feed, the harder wheel had a stronger polynomial tendency of the distributions than the softer wheel. This is thought to be indicative of the fact that in softer vitrified bonded wheels, the effects of the fracture processes in diamond dressing penetrate deeper than in harder wheels.

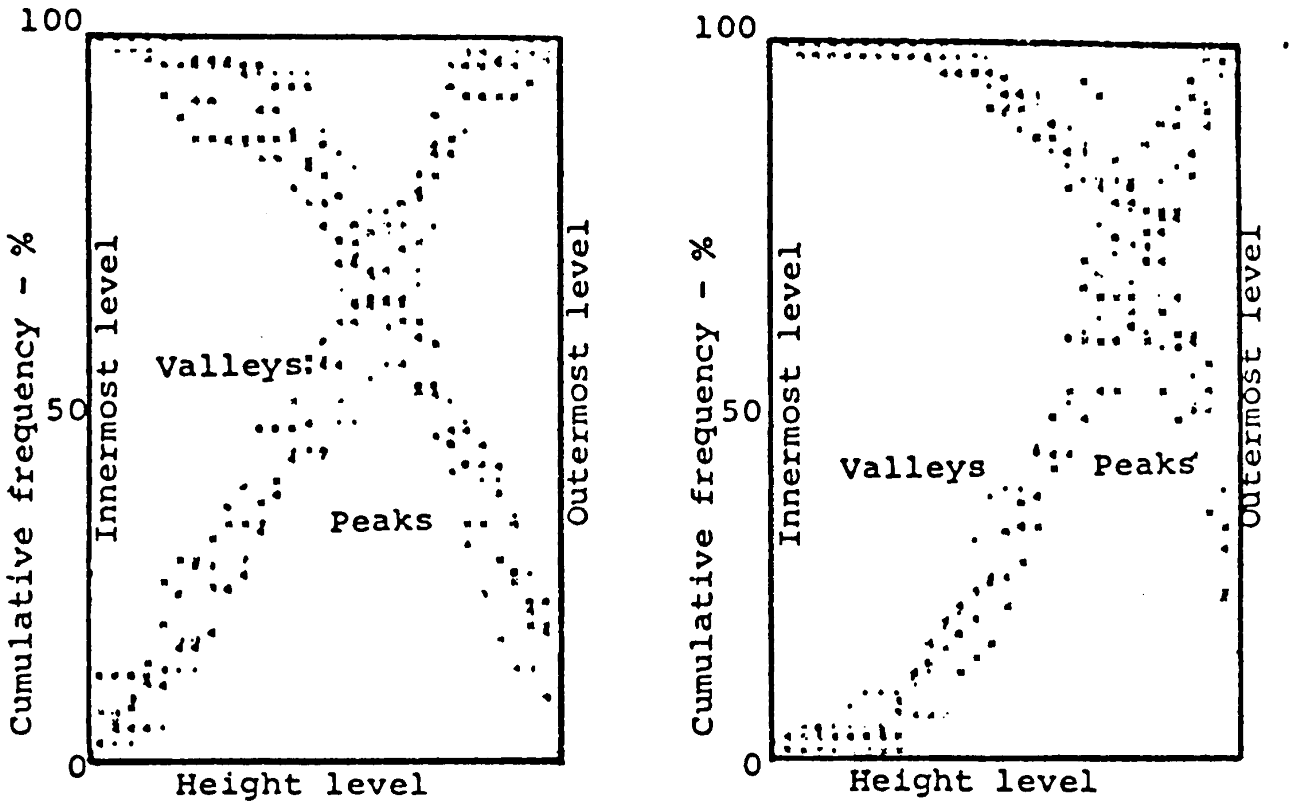

Grinding wheel-WA 46 HV
Dressing feed-0.010in.rev.$^{-1}$
(a)

Grinding wheel-WA 46 MV
Dressing feed-0.001in.rev.$^{-1}$
(b)

EXPERIMENTAL PLOTS OF THE CUMULATIVE FREQUENCY DISTRIBUTIONS OF PEAKS AND VALLEYS ON THE GRINDING WHEEL SURFACE

Fig 7.16 (after Bhateja)

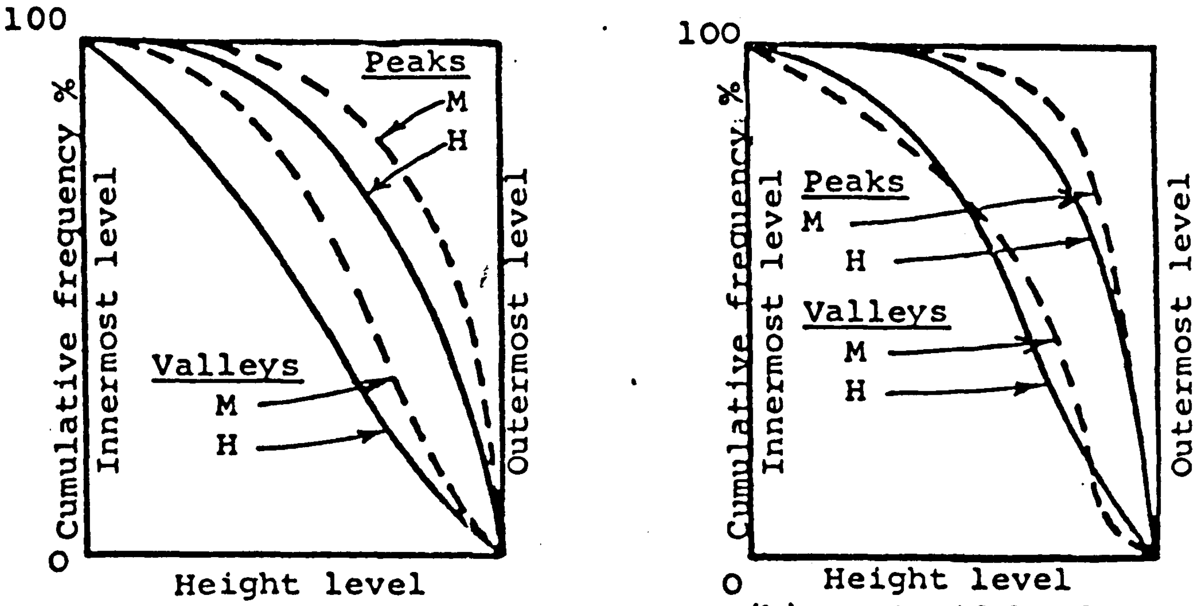

(a) Vitrified bond (b) Resinoid bond

Dressing feed - 0.001 in. per rev.

Grinding wheels - WA 46 HV & MV and WA 46 HB & MB

Note: M and H refer to the wheel grades

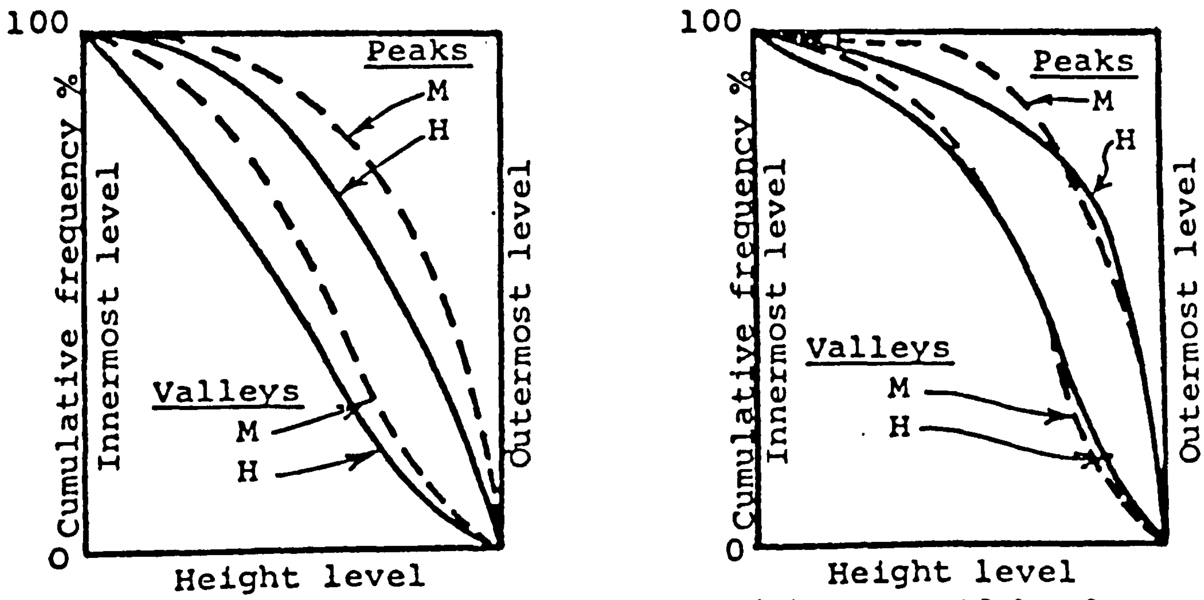

(c) Vitrified bond (d) Resinoid bond

Dressing feed - 0.010 in. per rev.

MEAN CUMULATIVE FREQUENCY DISTRIBUTION CURVES OF PEAKS AND VALLEYS FOR THE GRINDING WHEEL SURFACE SHOWING THE INFLUENCE OF WHEEL GRADE

Fig 7.17 (after Bhateja)

> The mean asperity distributions of Figures 7.17(b) and (d) however do not show any pronounced differences due to wheel hardness. This suggests that owing to it's low friab--ility, the resinoid bond is perhaps some--what insensitive to the fracture process in diamond dressing................the stronger polynomial tendencies associated with the harder wheels, the resinoid bonds and the finer dressing feeds are of significance.

The more obvious functions of dressing are listed as imparting the necessary form to a grinding wheel, removing worn grits, and generating new cutting edges on the wheel surface. More subtle influences of diamond dressing are said to include rearrangement of asperities and imposition of a constraint on the radial location of cutting edges in the wheel surface.

Referring to his earlier work in collaboration with others (31) Bhateja states that diamond dressing always produces a polynomial-type cumulative frequency distribution of asperity peaks. This statement appears to be based upon the shape of the ogives plotted to represent such distributions which have a concentration of asperities in the outer active region of the wheel surface.

The profiles represented by these distributions were obtained using a 90 degree diamond pyramid stylus but no mention is made of the self evident fact that those distributions said to represent valleys will be distorted by reason of the inability of the stylus to follow the contour of surfaces sloping at more than 45 degrees.

In discussing a number of results represented by the distribution curves it is stated that the stronger polynomial tendencies associated with the harder wheels, the resinoid bonds, and the finer dressing feeds have the following significance.

Firstly it is suggested that this would mean larger active grit densities on such grinding wheels and that this could be a factor contributing to the effective hardness of a wheel defined as it's resistance to wear. Furthermore this is said to suggest that the grade of a grinding wheel has a twofold influence on it's hardness, namely, the direct effect, and also an indirect effect the latter influencing the characteristics of the cutting surface.

Secondly the more pronounced polynomial tendency of the cutting asperity distribution for harder wheels and resinoid bonds is said to result in a higher probability of material removal during grinding and finer surface texture on the workpiece.

It is also suggested that a single dressability index for a grinding wheel might be useful in selecting the dressing conditions appropriate to the grinding requirements.

The following extracts and notes serve to outline a paper by Zohdi (36), published in 1974, on the estimation and optimization of surface texture in the grinding process by statistical analysis. The effects of five independent variables on surface texture are considered but these do not include wheel dressing which, in contrast with the two preceding papers, is not even mentioned.

> SUMMARY. A method of identifying the individual as well as the combined effects of the different independent factors on the surface finish in the grinding process is presented. Physical experimentation coupled with subsequent statistical analysis, the factorial experimentation technique, were applied to further the understanding of this process. Mathematical models were developed to estimate the quality of the dependent factor, the surface finish. Optimum conditions that result in the best surface finish with the maximum rate of metal removal are evaluated and discussed.

Five independent variables were selected for the factorial design of experiments as follows.

1. The grain size of the grinding wheel.
2. Coolant - water miscible. Grinding (a) with coolant (b) without coolant.
3. Depth of cut.
4. Table speed.
5. Cross feed.

The dependent variable was the first cut surface finish without sparkout.

In order to limit the size of the study other factors such as material hardness, structure and hardness of the grinding wheel were kept constant. The statistic-ally significant main effects and first order inter-actions considered are listed as follows.

1. Main Effects

   Grinding wheel grain size, A

   Coolant, B

   Depth of cut, C

   Table speed, D

   Cross feed, E

2. First Order Interactions

   Grain size by coolant, AB

   Grain size by depth of cut, AC

   Grain size by table speed, AD

Grain size by cross feed, AE

Coolant by depth of cut, BC

Coolant by table speed, BD

Depth of cut by table speed, CD

Depth of cut by cross feed, CE

Table speed by cross feed, DE

Results are presented in the form of graphs, multiple regression equations for the arithmetic roughness value, and correlation coefficients (r_i) including the following.

For the AA46H8V40 grinding wheel

$$R_a = 4.787 + 11.025X_1 + 0.375X_2 + 61.229X_3 \quad (1a)$$

$$r_i = 0.9298$$

and for the AA60H8V40 grinding wheel

$$R_a = 8.633 + 5.747X_1 + 0.225X_2 + 26.317X_3 \quad (1b)$$

$$r_i = 0.9169$$

where R_a = arithmetic average roughness (μin)

X_1 = depth of cut (0.001in)

X_2 = table speed (ft/min)

X_3 = cross feed (in/stroke)

r_i = correlation coefficient

The F-test was applied to equations (1a) and (1b) and their correlation was found to be significant at the 0.01 level. On the basis of these results and their simple form of expression the equations are said to be adequate for practical applications.

The rate of metal removal (ROMR) was calculated for each case using the following equation

$$ROMR = 0.012X_1X_2X_3 \text{ in}^3/\text{min} \qquad (3)$$

To achieve optimum conditions it is desired to minimize surface roughness represented by the linear equations (1a) and (1b) while maximizing the non-linear equation (3). One way of solving this problem is to plot the values of these equations for each case as in Figure 7.18 The best conditions for a specified rate of metal removal, could be reached by increasing the depth of cut to the maximum allowable level and then consecutively increasing the cross feed and table speed.

In the conclusions grain size is said to have a considerable effect on surface roughness, the ratio

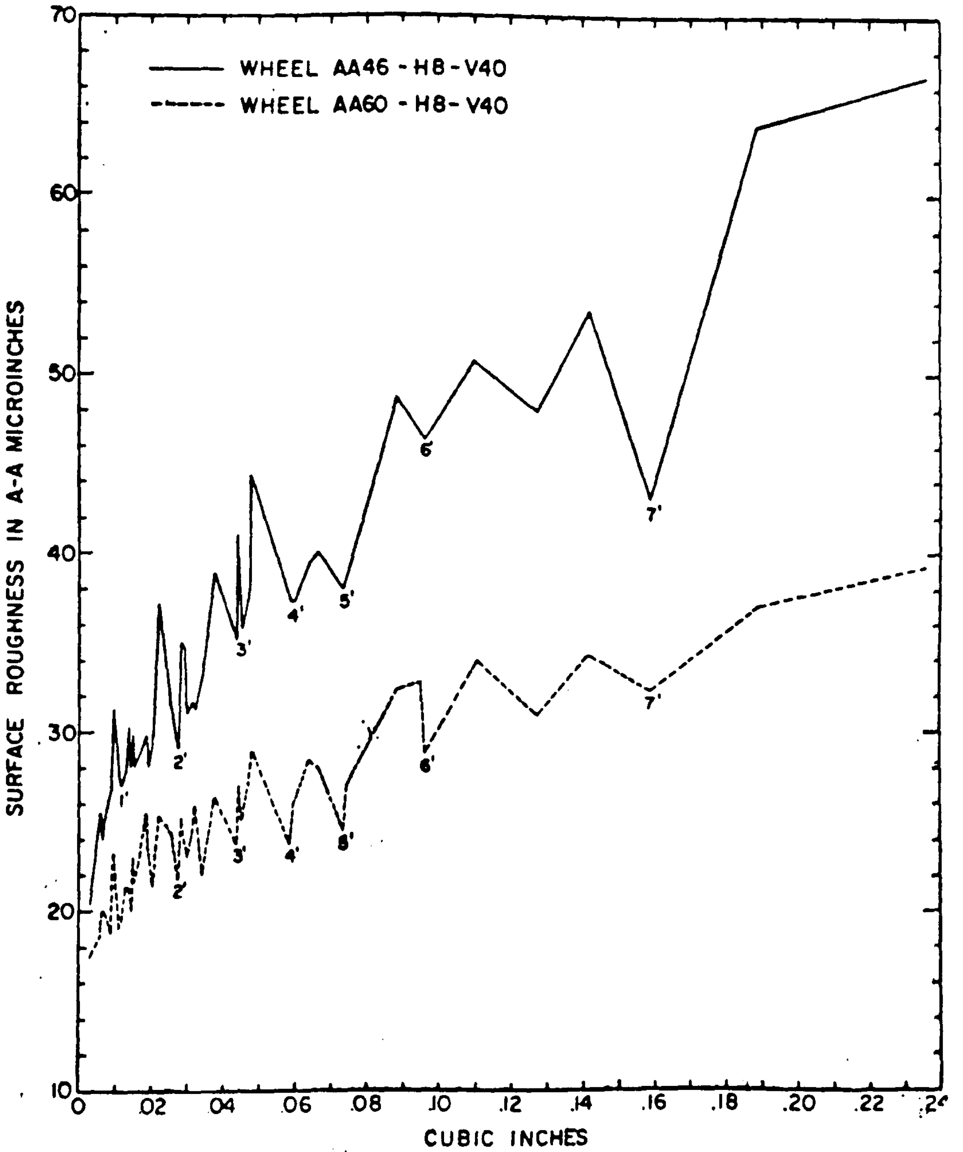

Fig 7.18 Rate of metal removal versus SF (after Zohdi)

of the average roughness values being approximately equal to the inverse ratio of the mesh number of the abrasive grains.

As previously stated the paper deals with the application of factorial experimental design and statistical analysis in an attempt to estimate and optimize surface roughness in relation to metal removal rate. Within the limits of the experiments this object appears to have been achieved, but with little contribution to fundamental understanding of the process.

Dressing conditions and subsequent wear of the grinding wheel surface have been shown by others to have a considerable effect on the surface roughness produced by grinding (29). In view of this it is surprising that Zohdi's paper does not refer to wheel dressing or wear. If these were deliberately excluded as independent variables in order to limit the scope of experiments it is to be expected that dressing conditions would be standardized and specified together with the extent of wear.

However, the paper contains no mention of these factors, an omission which can only be regarded as seriously limiting the potential usefulness of the results as a means of predicting surface texture.

A paper by Friedman, Wu and Suratkar (37) published in 1974, is included in this survey primarily because it contains information on an oscillating stylus profilometer. The paper deals only with the geometric properties of coated abrasive and contains no reference to surface texture. Apart from the following summary only those sections which have some apparent relevance to the present investigation are included.

> The surface topography of a coated abrasive was measured by a specially designed profilometer with an oscillating stylus, revealing very detailed geometric features of the peaks. The criterion for a peak to be a dynamic active cutting edge is analysed and the results are applied for the identif--ication of active cutting edges of the measured profiles. The distributions of some geometric properties of the active cutting edges as heights, distances, rake-angles, and wear lands are evaluated for six grades of coated abrasives.

The specially designed profilometer referred to in the summary is described as a modified version of the "oscillating stylus" device to which reference has already been made (28, 33). It is said to consist basically of a stylus riding over the surface of a coated abrasive which is moving at about 1.5×10^{-3}in/s. The stylus is caused to oscillate by means of a cam (Figure 7.19). The amplitude is a little larger than the amplitude of the measured surface and frequency is about 15Hz. The displacement of the stylus is converted into an electrical signal through an LVDT[1].

The oscillating stylus device is said to permit the use of a very slim probe which is of critical importance in the case of coated abrasive where very steep slopes and sharp corners were found and which would not other--wise be detected by an ordinary stylus method. The radius of the tip is 2.5×10^{-3}in and the included angle is 20°.

The title of a paper by Lal and Shaw (38) refers to the part played by grain tip radius in grinding. An idealized model is proposed for the roughness of a ground surface which relies upon the following three assumptions.

1. LVDT: linear variable differential transformer with reference to a type of transducer.

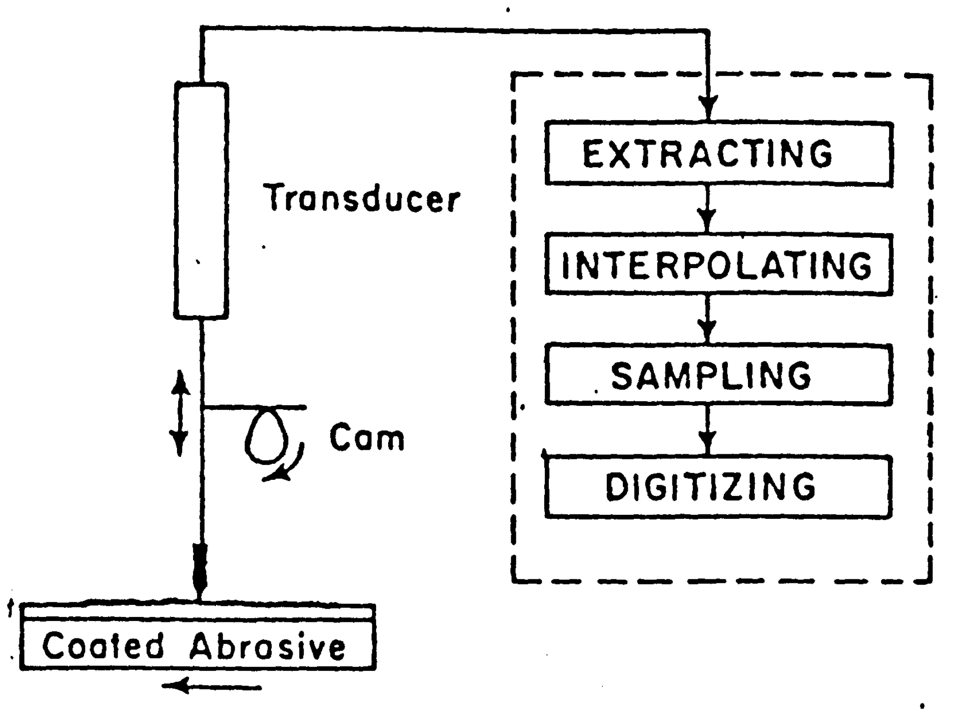

Fig 7.19 Flow diagram for the generating of profile data (after Friedman, Wu, and Suratkar)

(1) that each grit produces a part-circular groove;

(2) "scallops"[2] produced by uniformly spaced grits are the major source of surface roughness;

(3) the tips of all active grits lie at the same level in the wheel surface.

All other sources of surface roughness are neglected.

The wording of the foregoing differs from that used in the paper but it is clear from examination of Figure 7.20 that these represent the assumptions upon which the model is based.

With reference to the experiments it is stated that only "as crushed" grains were used in the tests and the effects of diamond dressing were not investigated.

Scratches produced by grinding with single abrasive grains were examined by stylus profilometry and the results are said to show that the transverse shape of a grain is closely approximated by an arc of a circle.

2. Ornament (edge, material) with scallops. Concise Oxford Dictionary.

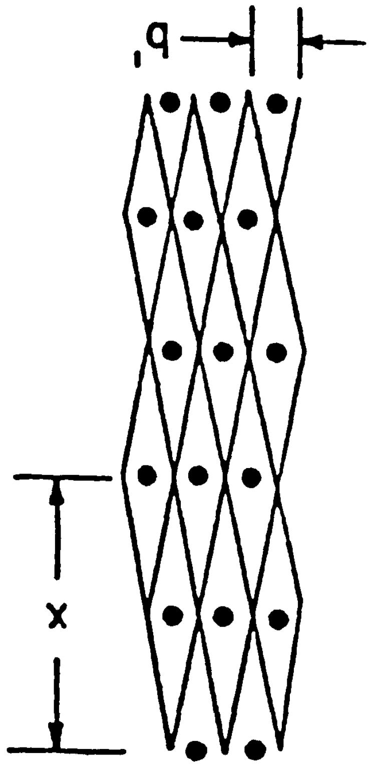

Fig 7.20 Plan view of scratches left on ground surface by wheel having uniformly spaced active grains (after Lal and Shaw)

The idealized model for surface texture to which reference has already been made is formulated on the assumptions that grits in the surface of a grinding wheel are evenly spaced, of uniform height, and will produce scratches of similar shape to those produced by single grits in the experiments.

The experimental results are said to show that the only important variable affecting the grain tip radius is the grain size. However, the reliability of this finding appears to be questionable since the experiments did not include the effects of dressing and grinding wheel wear.

Although not used in the experiments, diamond dressing is dismissed with a cursory statement to the effect that it produces flats at the tips of the grains. This very incomplete description is presented without supporting evidence and there is no mention of the effects of wear on grit surfaces.

In the following equation h is said to represent the idealized mean peak to valley roughness

$$h = \frac{\upsilon}{2VC\sqrt{2\rho D}}$$

and υ = table speed

V = wheel speed

C = number of active cutting points per square inch on the wheel surface

ρ = effective radius of the abrasive grains

D = wheel diameter

This is based upon a geometrical model which assumes "that all active grains extend the same distance from the wheel surface" while the related diagram (Figure 7.20 implies the further assumption that they are evenly spaced.

As a model for surface texture in grinding this is idealized to the point of being unrealistic because a ground surface will inevitably contain scratches of different depth and spacing related to the distribution of active asperities in the wheel surface. In fact the existence of some such distribution is acknowledged by inclusion of a diagram attributed to Nakayama and Shaw corresponding with the curve for the 60H wheel in Figure 1.14 of reference (30).

The treatment of surface texture contained in the paper does not inspire confidence because certain basic assumptions are oversimplified and the experimental methods deviate from normal fine grinding practice. Also none of the experimental results presented relate directly to surface texture.

A noticeable feature of the literature of grinding as it relates to roughness of the ground surface is the diversity of treatment accorded to the grinding wheel surface. Several of the publications already considered including (31), (32) and (35) emphasise the role of wheel dressing in this context, while other including the preceding paper and (36) contain no mention of dressing.

Although it contains no information on roughness of ground surfaces, a paper by König and Lortz (39) appears to have some relevance to the present study in that it deals with the kinematics and dynamics of metal removal by grinding.

The surfaces of grinding wheels of nominal grit sizes 46, 60, and 100 were examined by profilometer measurement over one fifth of their circumference representing a scanning length of 314mm. Signals obtained from the profilometer were processed by computer but, apart from references to statistical algorithms in the summary, no details are given.

An appreciation of the results requires some clarification of terminology as follows.

(1) A "static cutting edge" apparently refers to a peak on the profilogram contained within what appears to be the wheel depth of cut.

(2) The "dynamic distance" between cutting edges appears to represent the distance between "static cutting edges" taking into account the kinematic relationships of the process.

(3) The "dynamic cutting edge number" (C_{dyn}) represents the number of peaks which would make contact with the workpiece under given kinematic conditions i.e. those "static cutting edges" not kinematically screened from workpiece contact.

For the grinding wheels under consideration, graphs are presented showing that the number of dynamic cutting edges is approximately 5 to 12 per cent of the corresponding number of static cutting edges.

These are limiting values reached at a wheel depth of cut of 15 to 25μm depending on grit size.

Chip formation is said to commence at some critical depth of engagement between a grit and the plastically deformed workpiece referred to as the "cutting insertion depth". It is also stated that cutting insertion depth may be determined using a method attributed to Nakayama and Shaw but no details are given.

The suitability of Nakayama and Shaw's technique (14) is not self evident because it involves counting and measuring scratches produced by grinding a lapped steel surface tilted at an accurately predetermined angle of inclination. In this method there is no apparent means of differentiating scratches involving chip removal from those associated with plastic ploughing; neither is there any indication in König and Lortz's text of how this was done.

A diagram (Figure 7.21) is presented from which may be obtained the "effective number of cutting edges" defined, apparently, as those cutting edges which may be expected to result in chip formation. The actual number of cutting edges involved in chip is said to be much less than the number of dynamic

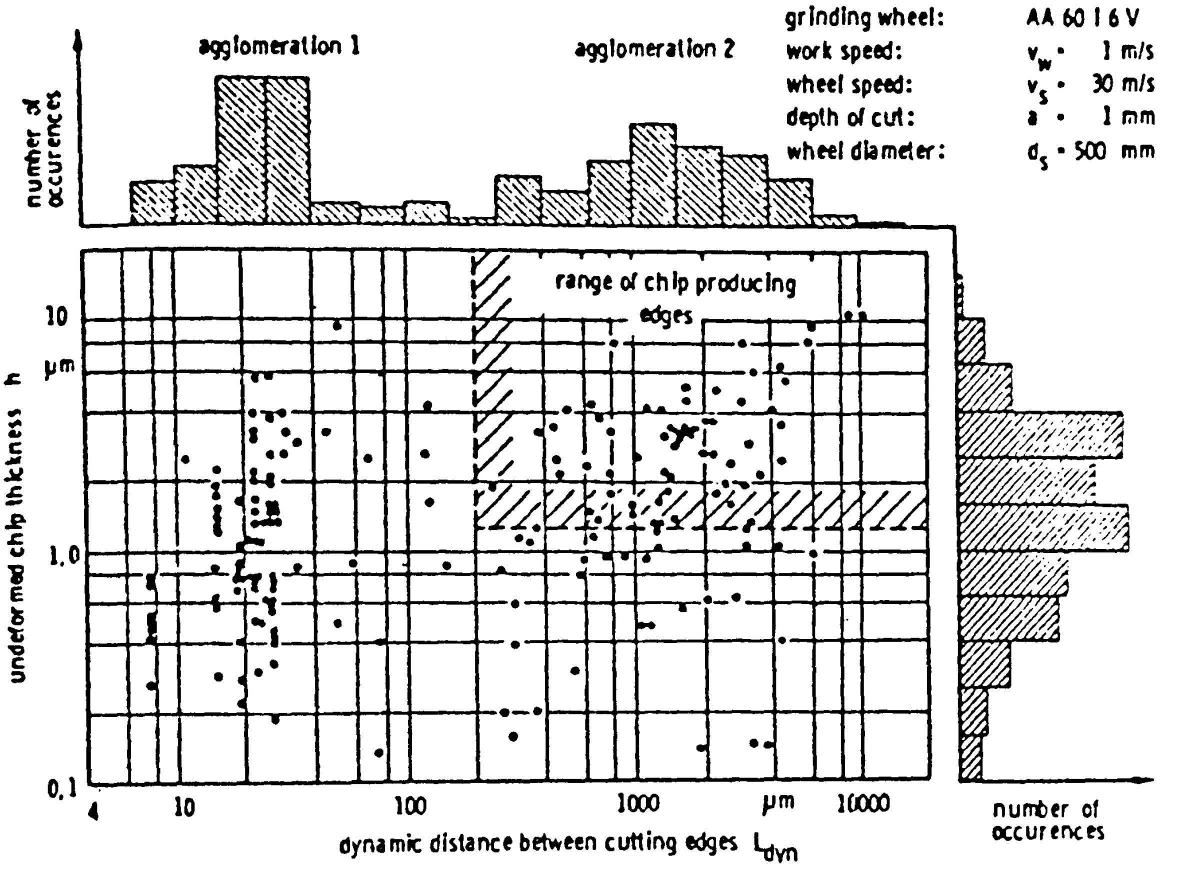

Fig 7.21 Effective cutting edges under consideration of the kinematic and mechanical relationships (after König and Lortz)

cutting edges, for a given combination of grinding wheel and workpiece material.

On the one hand, this reduction is attributed to the fact that not all cutting edges in the cutting engagement depth contribute to chip formation because their maximal depth of cut is less than that of the chip formation range and consequently they only bring about a "displacement process". On the other hand, those cutting edges do not take part in the cutting process whose distance from the preceding cutting edge is less than the average grain diameter.

Finally two scanning electron micrographs are presented. One of these is said to show a grain coated with workpiece material, while the other shows a curled chip contained within a void in the grinding wheel. From this result it is concluded that the coated area can take no part in further chip formation but it is inferred that chip removal by the other cutting edge will continue.

From the preceding statements it seems clear that the authors envisage no effective material removal other than by chip formation notwithstanding earlier work (5, 6) which provides evidence to the effect that plastic ploughing contributes significantly to metal removal.

The paper contributes relatively little information capable of being related to the profile of the ground surface. Certain graphical methods of presenting data relating to the wheel surface are however of interest, for example Figures 7.21 and 7.23.
Figure 7.22 is said to show the influence of dressing on the shape of cutting edges. The "kink" in the upper curve at a depth of 15μm corresponds with the depth of cut used in the dressing operation.

A paper published in 1975 by D. J. Whitehouse (40) points out that during recent years the use of stylus instruments has progressed from mainly engineering applications into research fields. Some practical limitations imposed by the interface between instrument and surface are mentioned in the following extract.

> The stylus type of instrument gives at best a close approximation to the cross-section of a real surface. In limiting cases some features will be missed. Slopes of greater than the stylus semi-angle and re-entrant features cannot be seen. Some integration of the final detail will also be inevitable because of the finite stylus tip size. Because this amounts to only a few per cent it is rarely functionally significant

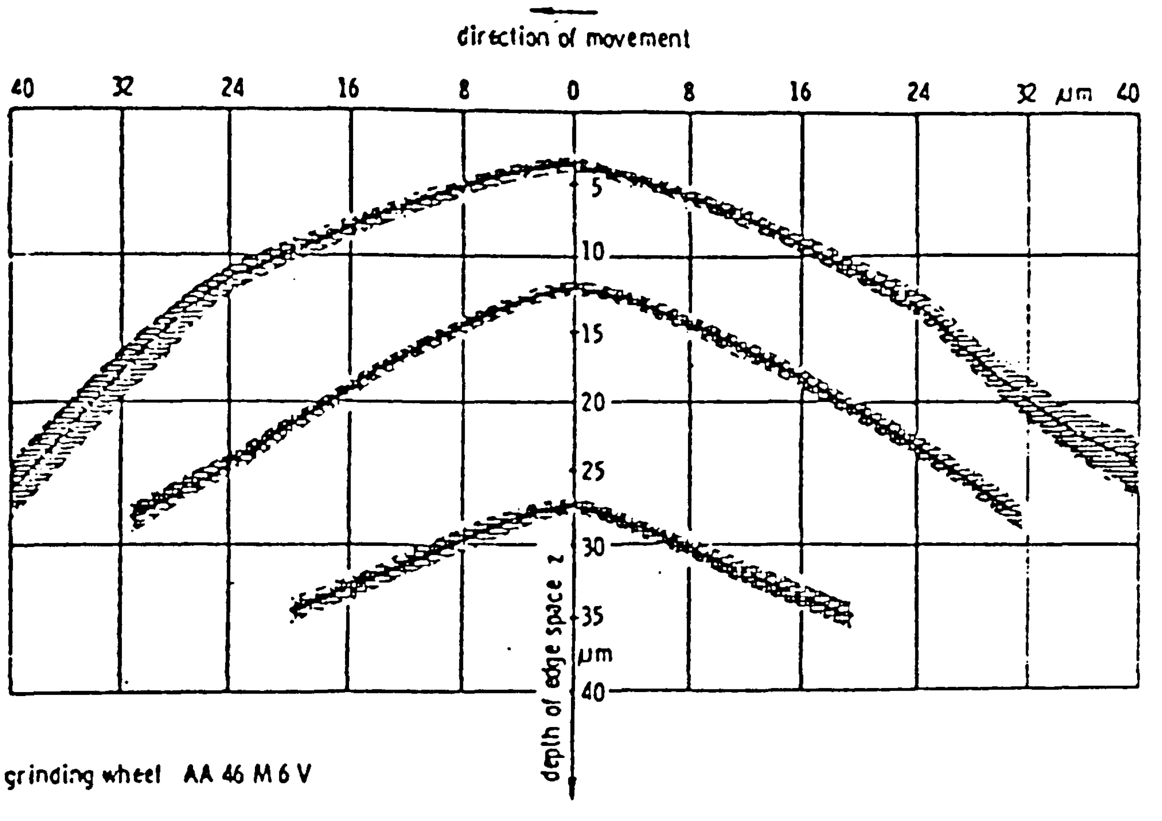

Fig 7.22 Average cutting edge shape with a statistical probability of 97.5 per cent (after König and Lortz)

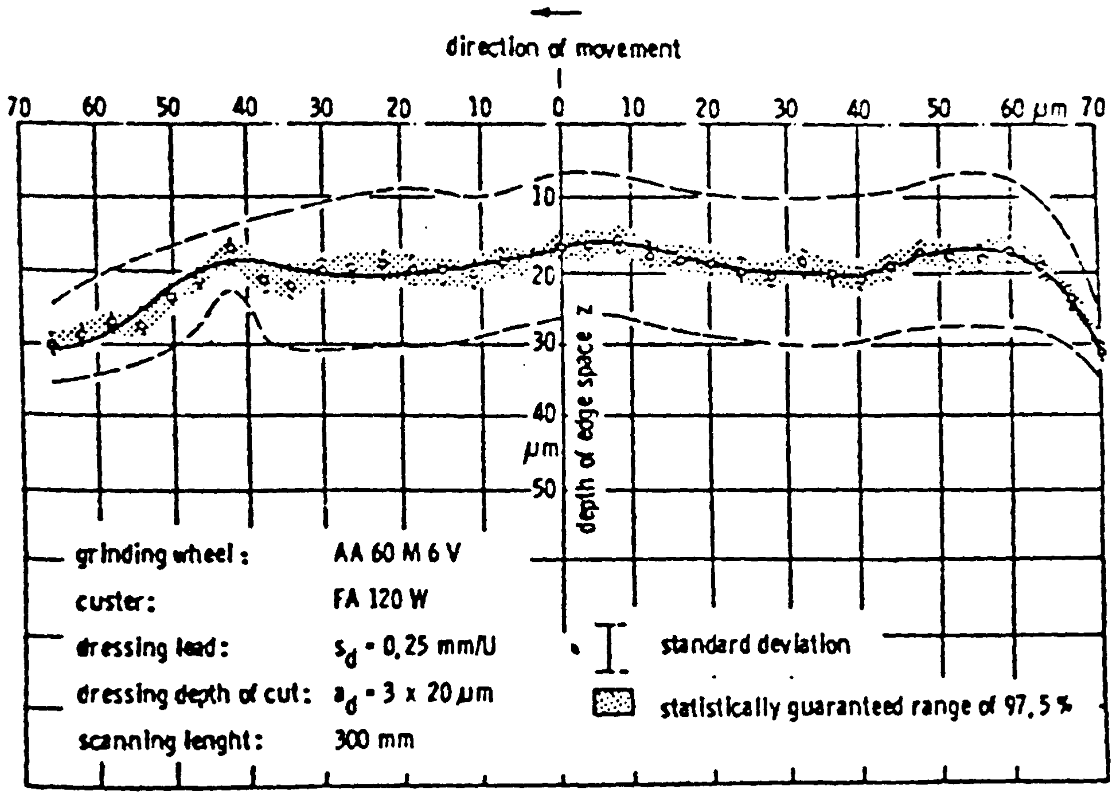

Fig 7.23 Average grain shape with standard deviation and statistically guaranteed range of 97.5 per cent (after König and Lortz)

> except sometimes in the measurement of ultra fine texture. This situation has been recently relieved by the ability to make, measure and use stylii of dimension $\sim 10^4$nm at forces down to 5μN.

The capabilities of stylus methods are summarized in the author's discussion and conclusions from which the following extract is taken.

> The stylus technique has been evolving steadily for 40 years. The foregoing has described some of the limitations in the sub-engineering field. As a technique it continues to improve. It's figure of merit on the limiting resolution criterion of Young is about 100nm which is a factor of 10 better than most methods and there are signs that the technique could be usefully employed to measure some of the mechanical properties of the surface skin.

The stated object of this work is to define some limits of stylus techniques applied to surface measurement. In so doing the paper provides significant information confirming the adequacy of stylus profilometry for examination of the surfaces involved in grinding.

Although it presents no results relating to grinding, a paper by Fugelso and Wu (41) is included, primarily because it describes an oscillating stylus system outlined in the author's abstract as follows.

> An improved oscillating surface profile measuring device has been developed with a large vertical range of measurement combined with a small included angle of the probe which enables very irregular surfaces such as grinding wheels and coated abrasives to be measured with a high degree of accuracy. The digitally controlled mechanism allows the stylus to touch the specimen only at the points of measurement eliminating dragging of the stylus over the specimen.
>
> A complete computerized data processing setup has been built to facilitate the use of the measuring device. The profile height is sampled at constant intervals along the profile with the data presented in digital form. The data can be sent either to a teletype or directly to a computer for mathematical modelling.

Some of the disadvantages of conventional profilometers are stated in the introduction as follows.

> Various commercially available profilometers are being used to measure and characterize the surface profiles. However, for the irregular surfaces such as grinding wheels, coated abrasives, etc these profile measuring devices are found less useful because of their limited vertical range, inability to measure steep slopes due to their 90° measuring points, and the output in the form of continuously varying analog voltage.

An oscillating stylus instrument was first proposed by Stralkowski and reported in reference (33) to measure the irregular surfaces. That instrument had a high degree of accuracy since the distortion of the actual surface was eliminated by providing 15° measuring point. Besides, it had a larger vertical range than the commercial devices (i.e. 30mil oscillating stylus vs 0.2mil commercial devices). However, the stylus slides over the specimen part of the time and results in wear on the stylus and damage to the specimen.

The stated purpose of the paper is to present a digital oscillating stylus device with the following improvements:

(a) the ability to accommodate the large range of surface heights (150μm);

(b) the elimination of bouncing and dragging of the stylus thus avoiding damage to the specimen and reduction of measurement errors;

(c) the collection of digitized data on paper tape so that the data processing procedure is simplified.

A microscope stage is used to carry and position the specimen under the stylus. A stepping motor turning the leadscrew of one axis of the stage moves the specimen. The stepping motor may be programmed so as to adjust the sample interval from 8.8μm to 140μm.

The stylus moves perpendicular to the specimen which is attached to the microscope stage. The stylus is connected to a metal rod held in two sleeve bearings (Figure 7.24). The upper end of the rod is connected to an LVDT[1] armature while the lower end holds the needle that touches the sample being measured. The LVDT output is connected to an A/D (analog/digital) converter.

1. See reference (37).

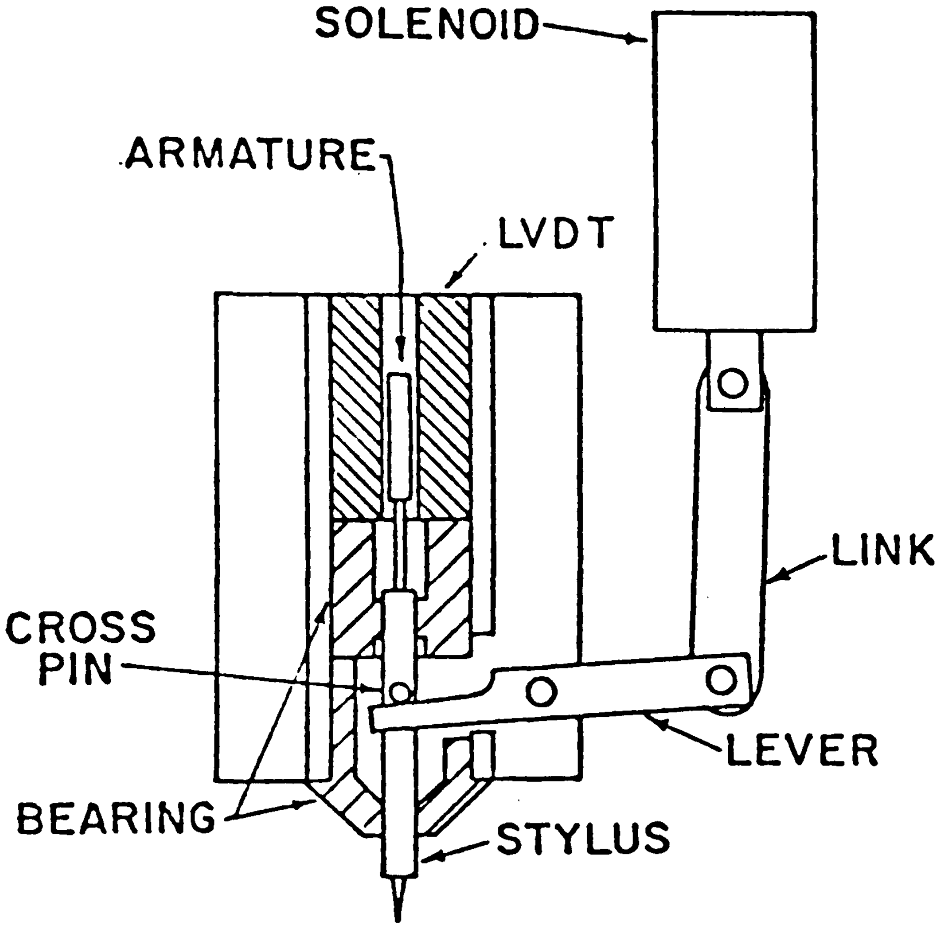

Fig 7.24 Mechanical components of the oscillating stylus (after Fugelso and Wu)

> The stylus is moved up and down by a solenoid. The solenoid is controlled by a solid state relay that in turn is controlled by logic signals from the sequencer. When the solenoid is off, the stylus is in the up position and clear of the specimen enabling the specimen to be moved without damaging the point. Energizing the solenoid lowers the stylus until it contacts the specimen being measured. All the motion is stopped when the height measurement is taken and punched on paper tape. Since all motion is stopped the wear on the point and damage to the specimen is minimized.

Figure 7.25 shows a block diagram of the system in which many of the items shown as blocks are said to be standard components.

One of the features distinguishing the device described in this paper from it's forerunners is actuation of the stylus by a signal controlled solenoid instead of a motor driven cam. The cam operated instrument said to have been proposed by Stralkowski and described in reference (33) was used by Friedman, Wu and Suratkar up to 1974 (37) and the new system appears to incorporate improvements made since that date.

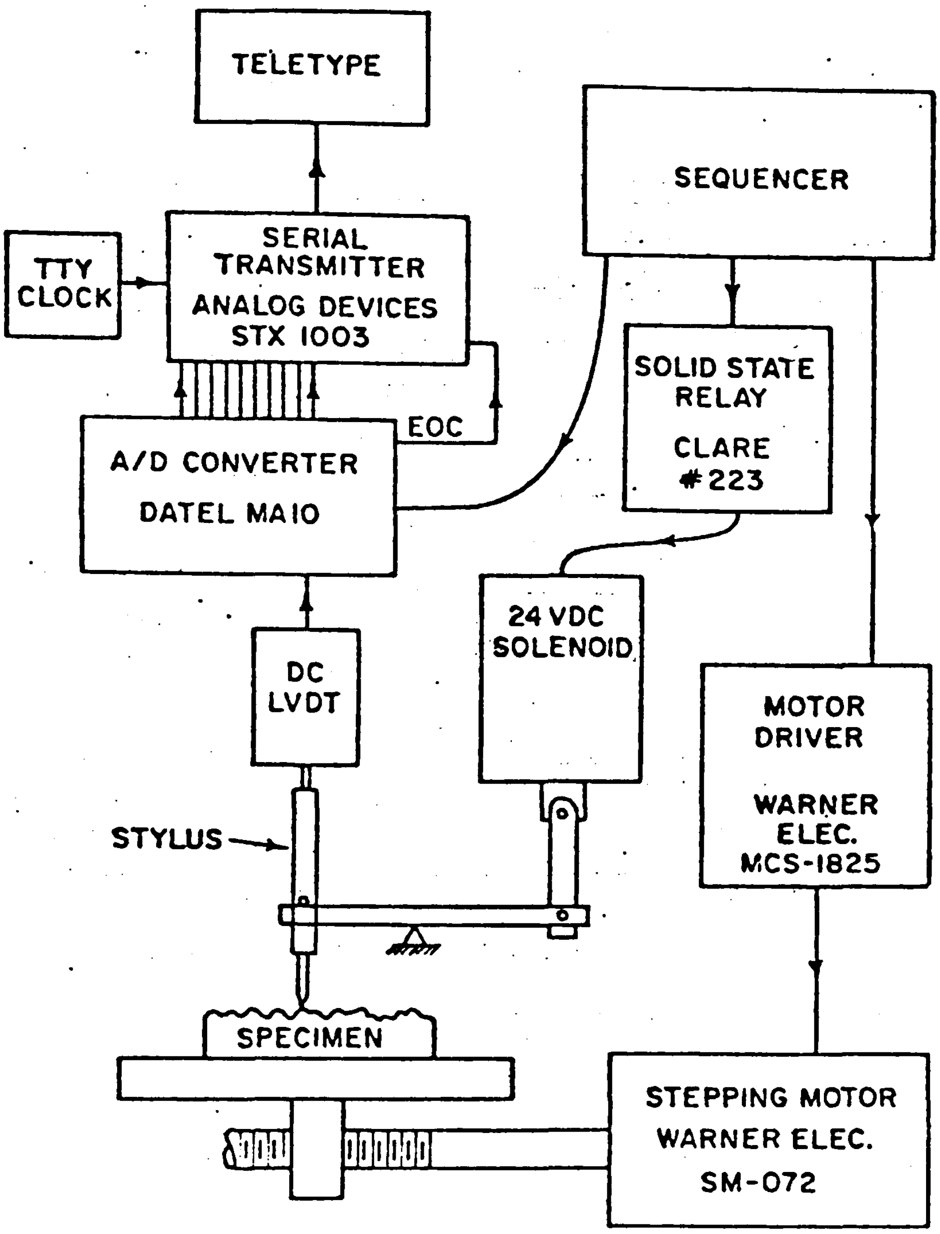

Fig 7.25 Electrical components of the oscillating stylus (after Fugelso and Wu)

It is stated that the earlier (cam driven) and the improved (solenoid actuated) instruments have vertical range of 30µm and 150µm respectively compared with 0.2µm for commercial devices. As a basis of comparison the figure of 0.2µm would appear to be either erroneus or based upon some commercial device having a particularly restricted range. If Talysurf 4 is taken as an example of a profilometer commercially available at the date of this publication it's range (at the lowest magnific--ation) is 100µm.

Referring to the cam operated device (33) it is stated that distortion was eliminated by the use of a 15° measuring point. The included angle of the solenoid operated stylus is specified only to the extent that it is less than 30°.

Figure 7.26 is said to represent two traces taken over the same place on a file. Considering the one tooth profile shown in it's entirety and taking into account the different horizontal and vertical scales it is seen that the apparent inclination of the front of the tooth from the vertical is a little over 7°. Assuming that the profile reproduces the cross section of the tooth, the point of a symmetrical stylus oscillating in the vertical mode could follow this surface only if it's included angle was 14° or less.

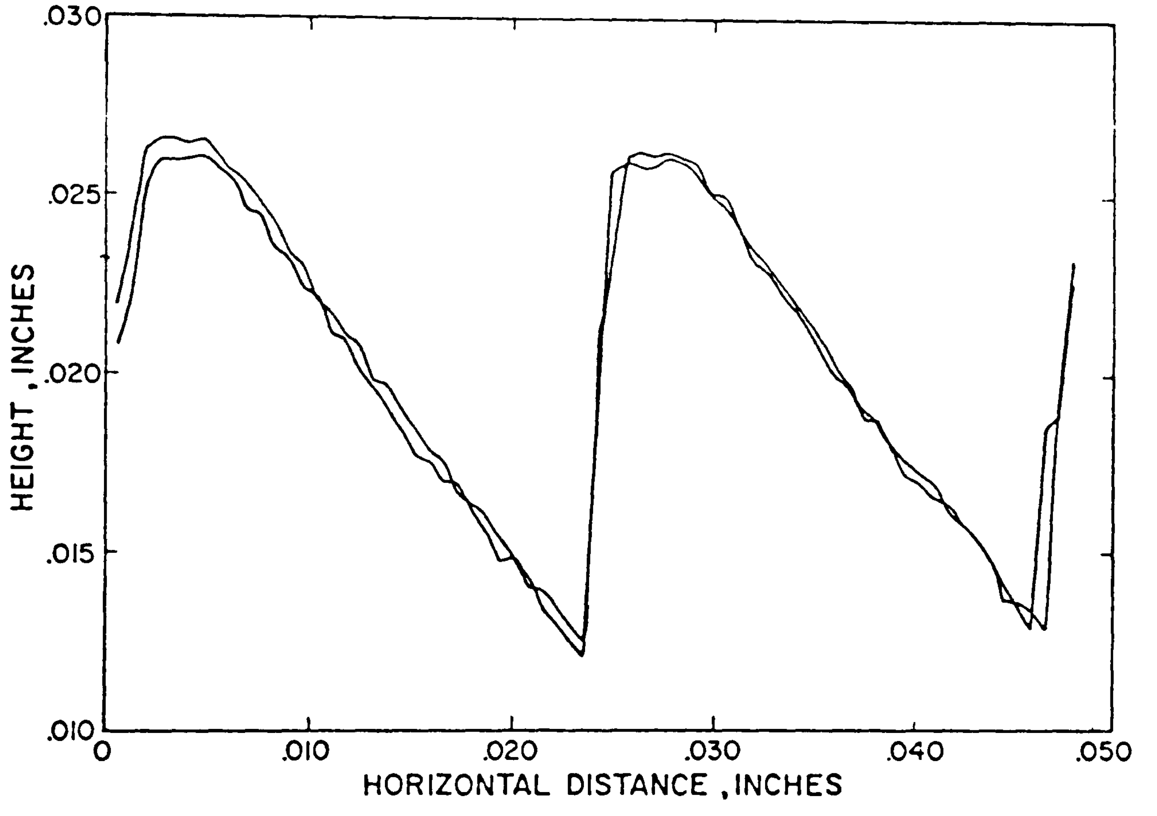

Fig 7.26 Two profiles measured on the same path over a file (after Fugelso and Wu)

The included angle of the stylus appears to have been between 15° and 30° and since slopes exceeding the stylus semi-angle and re-entrant features cannot be seen (40) that part of the profile relating to the front of the tooth cannot be a reproduction of it's shape. A possible explanation is that the tooth face was vertical or overhanging and that this part of the profile derives from successive contacts between the point of the file tooth and the flank of the stylus.

The above comments reflect on presentation rather than performance of the system. Clearly, the use of a measuring stylus with a relatively small included angle reduces distortion arising from stylus shape. Also the repeatability of the profiles appears to substantiate the claim that dragging and bouncing of the stylus have been eliminated with evident advantages for some types of surface examination.

An investigation of grinding wheel topography using oscillating stylus profilometry is the subject of a paper by Nassirpour and Wu (42) published in May 1979 and summarized as follows.

> The grinding wheel topography is character-ized and analyzed as a stochastic isotropic surface. An explicit procedure is given to check the assumption of surface isotropy.

Geometric statistical properties such as the number of active cutting points per unit area, the ratio of real to apparent area of contact, and the mean, root-mean-square rake angle of ten grinding wheels are calculated. Using the characteristic parameters as responses, the relative contribution of the wheel grit size, hardness, and structure of the total wheel topography is quantified by factorial design analysis. The procedure of character--ization is also applicable to other homo--geneous stochastic isotropic surfaces.

Referring to earlier work on the stochastic geometry of coated abrasive surface, it is stated that the conditions for surface isotropy correspond to having the values of height, slope, and curvature character--istics equal for five profiles of the surface in five arbitrary directions.

It is further stated that characterization of an isotropic random surface is complete if any one of the following is known for a single profile: the stochastic differential equation, the autocorrelation function, the power spectrum, or the spectral moments.

On the subject of surface characterization the paper continues as follows.

> However, more important and physically meaningful characteristics of the surface geometry can be obtained if we assume a zero mean normal probability distribution for the surface heights $X(t_1, t_2)$. Figure 7.27 shows the principal geometric properties of an isotropic random surface, which include the asperity, summit, summit curvature, summit contour, rake angle, and wear land area.

The experiments are outlined as follows.

> The topography of ten grinding wheels of different grit sizes (G), hardness (H), and structure (S) was measured. The grain size varied from medium to fine (46-80-120), the structure varied from dense to open (8-12) and the hardness changed over a small range of soft to hard (H-J). The grinding wheels had aluminium oxide grains and were vitrified bonded. All wheels were dressed by a single point diamond with five passes of 5μm at 1mpm with no spark out. Using the Digital Oscillating Stylus

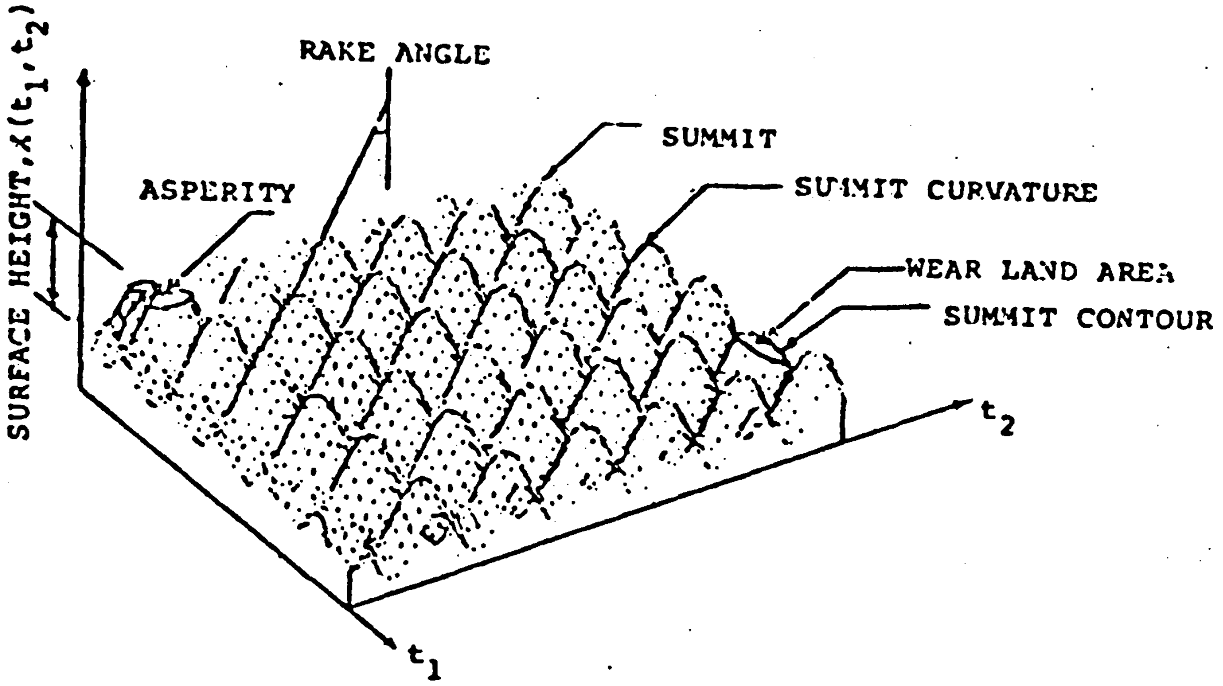

Fig 7.27 Definitions of the geometric properties of the isotropic random surfaces (after Nassirpour and Wu)

> Surface Profilometer, a two dimensional profile along the cross section of each wheel was obtained at a sampling interval of 35.28 m. The profiles were normalized (mean zero, variance one) before plotting. The selection of the wheel characteristics forms a 3×2^2 factorial design (with two missing points) with the grit size, hardness and structure as independent variables.

The fourth order stochastic differential equation said to represent the grinding wheel surface profile is given as follows.

$$\frac{d^4 X(t)}{dt^4} + a_3 \frac{d^3 X(t)}{dt^3} + a_2 \frac{d^2 X(t)}{dt^2} + a_1 \frac{dX(t)}{dt} + a_0 X(t) = Z(t)$$

where Z(t) is the continuous white noise. The parameters of this equation estimated by what is referred to as the Dynamic Data System approach are tabulated. Unlike earlier work the results of this study were said to indicate the need for a fourth order model.

As expected, the grit size was found to be the most important parameter in the study of grinding wheel topography. All three spectral moments increased as nominal grain size decreases (the grain size increases)[1,2]. In other words the variations of height, slope, and curvature are higher for larger grain size. The density of summits on the surface in units of area also follow the same trend, showing that there are more maxima for larger grains. In contrast, the number of asperities per unit area or the number of active cutting edges at a given level of penetration increased for smaller grain size wheels. This illustrates why the surface finish produced by finer grain wheels is smoother.

The experimental results are summarized as follows.

a. The variations of the height, slope, and the curvature are higher for larger grains.

b. The number of active cutting edges per unit area at a given level of penetration is higher for smaller grains.

1. i.e as the grain size number decreases the grain size increases.
2. The profile spectral moments are designated m_0, m_2, m_4. The first of these is the sample variance of the surface profile X(t), while the second and third are related to the first and to parameters of the stochastic differential equation.

c. The absolute mean value of the surface rake angle is smaller for the larger grains.

d. The real area of contact is larger for the smaller grains.

e. The wheel with higher hardness has smaller height variance.

f. As the porosity increases, the height variance, the negative rake angle, the variance of the surface rake angle increase, and the density of summits and the number of active cutting edges decrease.

In this case it is the methods rather than the results which are of particular interest. Information is collected from grinding wheel surfaces by oscillating stylus profilometry and the purpose of analysis is to characterize these surfaces. The paper does not examine surface texture or any other aspect of the ground surface but the number of features described as cutting edges was found to be higher for wheels of smaller grit size and the inference is drawn that such a wheel will produce a smoother surface. The work is included in this survey primarily because it represents an analysis of a number of grinding wheel surface profiles by statistical methods.

LITERATURE SURVEY SUMMARY

The search for information in the literature was undertaken in the knowledge that standardized surface texture parameters were inadequate to describe and compare the surfaces involved in the grinding process. It was therefore necessary to include, not only the relevant literature of grinding, but also papers dealing with surface measurement in related fields which might contain methods and parameters applicable, or capable of being adapted, to the grinding process.

Of the numerous publications examined a total of twenty--two, excluding Part 1 of this Thesis, are included in the foregoing survey. These were selected on the basis of their contributions to knowledge of the grinding process with particular reference to those aspects of the investigation mentioned in the preceding paragraph. Papers on grinding relevant only to the extent of containing conventionally expressed roughness data for ground surfaces were omitted.

Ten of the papers surveyed in the preceding pages deal with the texture and characterization of a variety of surfaces and seven of these relate specifically to ground surfaces. Nine of the papers consider grinding wheel surface profile and four of these also deal with the ground surface.

Twelve papers contain results apparently obtained from actual grinding operations but relatively few of these take account of the effects of dressing and wear of the grinding wheel. However, dressing is considered by Masashi Harada and Akira Kobayashi (29), Motoyoshi Hasegawa (32), Bhateja (35), Nassirpour and Wu (42). Shinaishin (27) deals with wear of diamond grinding wheels while the influence of both grinding wheel wear and dressing on the ground surface is the subject of the paper by Bhateja, Chisholm and Pattinson (31).

Stylus profilometry appears to have been used for some aspect of surface measurement in connection with all except four of the papers, the exceptions being Stralkowski, Wu and De Vor (26), Masashi Harada and Akira Kobayashi (29), Thompson and Malkin (34), and Zohdi (36).

Deutsch, Wu and Stralkowski (33) describe a profilometer in which oscillation of the stylus is produced by means of a motor driven cam. Application of this to grinding wheel surfaces is dealt with by Deutsch and Wu (28). A modified version of this profilometer was used by Friedman, Wu and Suratkar (37) to examine coated abrasive surfaces.

Fugelso and Wu (41) describe an oscillating stylus profilometer system with digital control, applied by Nassirpour and Wu (42) to the measurement of grinding wheel surfaces prepared by diamond dressing.

Statistical parameters have been extensively used for the purpose of characterizing and describing surface profiles, as follows.

Five papers, four of them by Peklenik (21), (22), (24), (25), concentrate on autocorrelation functions and power spectra. Peklenik also makes limited use of transfer functions to relate the power spectrum representing the profile of the ground surface with the spectrum similarly representing the grinding wheel surface.

Five papers also introduce other parameters for surface characterization, some of which are said to be new, as follows.

Myers (20) specifies three profile characteristics including the first and second derivatives of the arithmetical average roughness value. Williamson (23) makes use of surface density, height distribution, and mean radius of curvature of asperities. Peklenik (25) introduces slope variance as a parameter for surface characterization. Stralkowski, Wu and De Vor (26) state that grinding wheel profiles are fairly well represented by second-order autoregressive models. Bhateja, Chisholm, and Pattinson (31) use bearing area curves for the same purpose in addition to cumulative height distributions.

The foregoing analysis indicates the number of contribut--ions found in the literature relating to particular aspects of the current investigation. Very few papers were found dealing with both workpiece and grinding wheel surfaces and their relationship. Next in order of scarcity were works which contained results from actual grinding operations taking account of the effects of dressing and wear of the grinding wheel.

Stylus profilometry applied to the ground surface and that of the grinding wheel features extensively in the literature and it is evident that a concensus of opinion exists with regard to its usefulness and potential. Oscillating stylus profilometry was demonstrated to be superior in its ability to explore areas of the abrasive grit inaccessible to the tip of the stylus of larger included angle used in more conventional profilometers.

Statistical methods were found to be widely used for analysis of surface profiles. Of the statistical parameters, power spectral density was favoured by relatively few authors. However, the only meaningful result found in the literature representing the relationship between the profiles of workpiece and grinding wheel, is a transfer function connecting power spectra derived from two such profiles (21). Despite the evident potential of such transfer functions, the author (Peklenik) does not appear to favour power spectral density for surface characterization and indicates a preference in this and other papers for methods based upon autocorrelation.

The system used by Peklenik to classify autocorrelograms representing surface profiles (24), (25) are somewhat complex but the author clearly states an opinion to the effect that these functions are indispensable. Power spectra are not however abandoned although of these it is stated that computation takes too long and interpret-ation of the resulting curves may present difficulty.

Neither of these objections appear to be fully justified or explained. No details of methods and duration of computation are given and, in the absence of this information, it is not clear why the time taken to compute and plot power spectral density should be excessive compared with that required for autocorrelation coefficients. Using the fast Fourier transform spectral densities can be calculated very rapidly and it is probably now quicker to calculate autocorrelations from spectral densities, rather than to calculate them directly. Also the power spectrum provides estimates of the contribution to surface profile made by various frequencies - a concept which appears easier to interpret than surface profile classification on the basis of correlation length and wavelength of the autocorrelogram.

A few obscurities affect certain of the expressions contained in Peklenik's papers. For example the same notation has been used when referring to the true auto--correlogram and its estimate. Attention has been drawn to minor errors by means of footnotes.

The need to relate the texture of the ground surface with the profile of the grinding wheel in quantitative terms was regarded as being of primary importance when work for Part 1 of this Thesis was undertaken. Reproduction on the workpiece of a pattern related to helical grooves produced on the grinding wheel by relatively coarse single point diamond dressing and depending on the kinamatics of the process formed the subject of a paper by Appun (1). Subsequent work was carried out in the belief that reproduction of such geometric features was not a fundamental aspect of the surface roughness capability of the grinding process. On the other hand, fine dressing producing no detectable grooves, and the effects of grinding wheel wear, were of considerable importance in determining the surface texture of the workpiece. Part 1 experimental results to some extent confirmed this impression and the point is mentioned merely to emphasise that 23 years elapsed between publication of the work by Appun and appearance of one of the most significant contributions exploring this relationship by Peklenik (21).

About half the papers included in this survey contain results obtained from actual grinding operations and half of these consider the effects of dressing and wear of the grinding wheel: a surprisingly small proportion in view of the very considerable influence that surface condition of the grinding wheel has on the surface texture of the workpiece.

The emphasis on stylus profilometry found in the literature and the quality of results obtainable served to indicate that this technique combined with statistical analysis and comparison of profilograms represented promising avenues for further investigation of the grinding wheel/workpiece surface relationship.

Reference has already been made to the capabilities if oscillating stylus profilometry. However, those areas of the abrasive grit interacting with the ground surface were considered to be sufficiently accessible to a stylus of the larger included angle associated with conventional stylus profilometry to satisfy the needs of an investigation of which the primary purpose was to compare, and if possible relate, the active surface of the grinding wheel with that of the workpiece.

The profile of individual grits and the effects of dressing and wear on this profile represent factors to be considered in relation to the surface texture produced. The study of the active surface of an individual grit at different stages of dressing and/or wear during the grinding process requires (a) that it can be identified for examination at different stages, (b) that having been identified it is accessible for measurement and inspection.

Information on single grit grinding was found in papers included in the Literature Survey relating to Part 1 (13), (15), concerned primarily with the mechanisms of metal removal and breakdown of the grit.

Experiments on grinding with a single grit are obviously well adapted to re-examination of the grit. Clearly, for the purpose of studying surface profile relation--ships repeated access to the grits is facilitated by individual mounting. If a number of grits can be individually mounted in a composite grinding wheel this may be more appropriate to a study of surface texture than grinding using, literally, a single grit.

These ideas, originating from some of the earlier literature examined, represent the basis for design and construction of the composite grinding wheel described in Chapter 8.

On the basis of this study of the literature and experience gained from the work of Part 1, the author formed the opinion that considerable effort should be devoted to further experimental work using ordinary bonded grinding wheels in conventional grinding operations. It was also clear that the resulting surface profiles should be reproduced by stylus profilometry and that statistical analysis of these profiles would be necessary. With regard to the statistical methods to be used, there was evidence that power spectra had certain potentialities which appeared to be lacking in alternative statistical parameters. There were also indications that power spectra had not been sufficiently tested in the context of surface profile characterization and comparison.

CHAPTER 8. A COMPOSITE GRINDING WHEEL USING SINGLE CRYSTALS OF NATURAL CORUNDUM

The object of this part of the investigation was to carry out surface grinding operations using single abrasive grits so as to facilitate examination at different stages of their working life. If the abrasive grits are sufficiently large their individual identification during the process presents no difficulty and the possibility can be envisaged of studying the wear process of such grits and the development of the corresponding ground surface during extended periods of grinding.

Design of the composite grinding wheel was influenced by several ideas including the following.

Experiments on grinding with single grits were known to have been previously used as indicated in the Literature Survey. However, for the purpose of studying surface relationships it is clearly expedient to provide an adequate number of grit surfaces for examination and therefore advantageous to grind simultaneously with a number of differently orientated but independently mounted grits rather than with a single grit.

Segmental grinding wheels comprising moulded blocks of bonded abrasive mounted in some form of carrier were known to be used for certain grinding operations where bonded grinding wheels are unsuitable. However, in such wheels the abrasive segments can be bonded to the carrier and in the experiments proposed it was desirable that abrasive grits should be removable from the composite grinding wheel and, if possible, replaceable.

It was also envisaged that the individual grits should preferably be single crystals and that the surfaces of these grits should be examined by stylus profilometry and scanning electron microscopy.

The surface grinding machine to be used was designed to take 7 inch diameter by $\frac{1}{2}$ inch face width bonded grinding wheels mounted on an arbor. Overall dimensions of the proposed composite grinding wheel had therefore to be related to these dimensions.

Profilometry could be applied to the surfaces of grits without removal from a composite wheel of the nominal dimensions indicated but the overall size of the proposed unit greatly exceeded the workstage capacity of the scanning electron microscope. If grits were to be examined by electron microscopy they had to be removable as units of size and shape adapted to the capacity of this workstage.

Details are given of the design, methods, and materials used in attempting to meet the requirements which have been outlined. Some results, mainly in the form of electron micrographs representing grit surfaces are included but these may have been adversely affected by problems encountered in reconciling the secure holding of grits during dressing and grinding with the facility for removal of mounted grits for micrographic examination.

At this stage, work on profilometry of bonded grinding wheels and statistical analysis of the profiles of these and the corresponding ground surfaces had reached a promising stage. This alternative work now appeared likely to provide quantitative results representing grinding wheel surfaces and ground surfaces, possibly throwing some light on the relationships between them. This represented the central purpose of the investigation and therefore work in this area was given priority. Material contained in this chapter is included primarily because, subject to improvements, the composite grinding wheel is believed to represent a potentially useful tool for investigating the behaviour of individual grits, and possibly segments of bonded abrasive in a more general context of the mechanics of grinding.

In view of its widespread use it was decided to concentrate upon aluminium oxide abrasive. Enquiries relating to synthetic aluminium oxide abrasive revealed that the forms of supply widely used for the manufacture of bonded grinding wheels were not particularly suitable for the work proposed. The largest commercially available grit size was No 8 which, to a first approximation, has an average grit diameter rather less than 3 mm. The only alternative form was to be found in manifestly polycrystalline and very porous lumps of material as produced in the electric furnace (Figures 8.1 and 8.2).

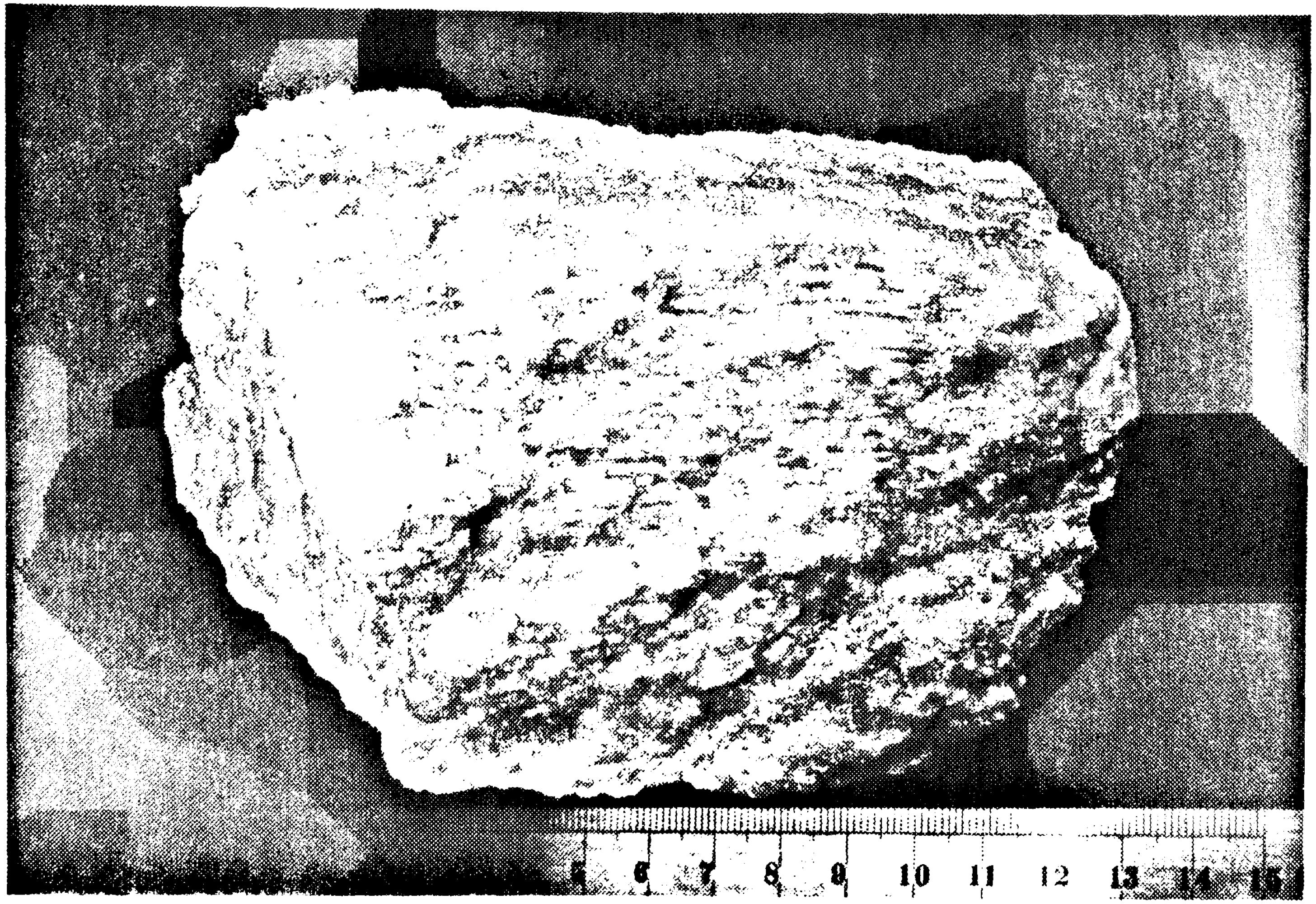

Fig 8.1 White synthetic aluminium oxide abrasive in lump form

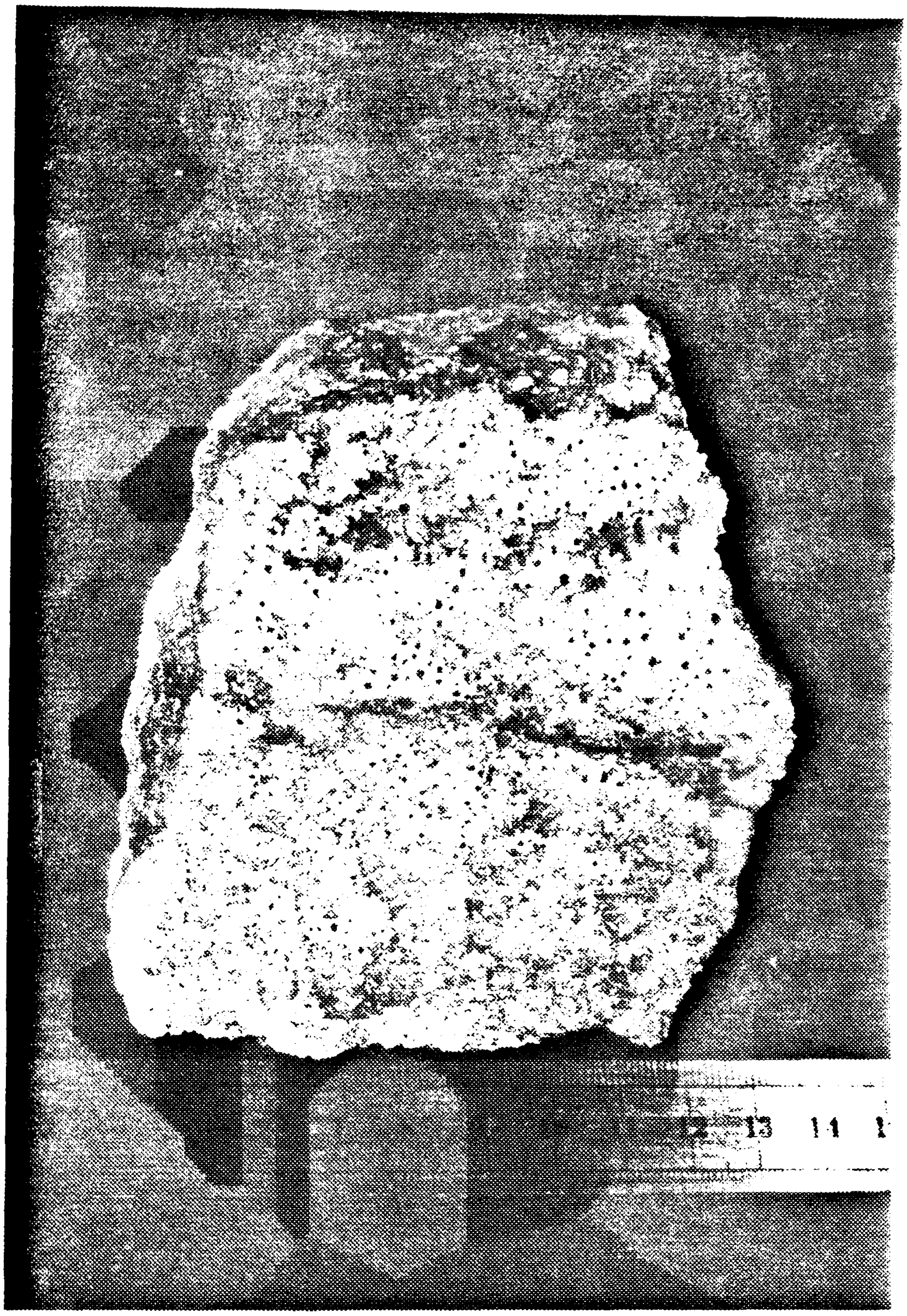

Fig 8.2 White synthetic aluminium abrasive
(another view of the lump shown in Fig 8.1)

The possibility of using some natural form of aluminium oxide was next considered and, with this in mind, samples of fused bauxite were obtained. This material was in the form of irregular pieces of crushed rock having a mean diameter around 25 mm. On the basis of visual examination and some specialized advice it was concluded that the structure contained corundum crystals of about 2 mm diameter in a matrix of feldspar, the latter being a softer and tougher material which would undercut if pieces of this material were used for grinding.

Natural corundum in the form of single crystals was eventually obtained from a specialist supplier of mineralogical specimens. Most of the crystals selected, some of which are shown approximately full size in Fig 8.3, were in the form of steep sided columns of hexagonal cross-section.

With the object of using this material as a grinding abrasive it was decided to cut these crystals into pieces of suitable size and to mount these in a composite grinding wheel. Fig 8.4 shows such a cutting operation using an ISOMET low speed saw in which the cutting blade is a thin diamond-impregnated metal disc. In operation this disc is applied to the workpiece with a very small controlled force and, operating at a speed of approximately 60 rev/min, transverse cutting of each crystal occupied about 15 minutes.

Fig 8.3 Single crystals of natural corundum (approx. $\frac{3}{4}$ natural size)

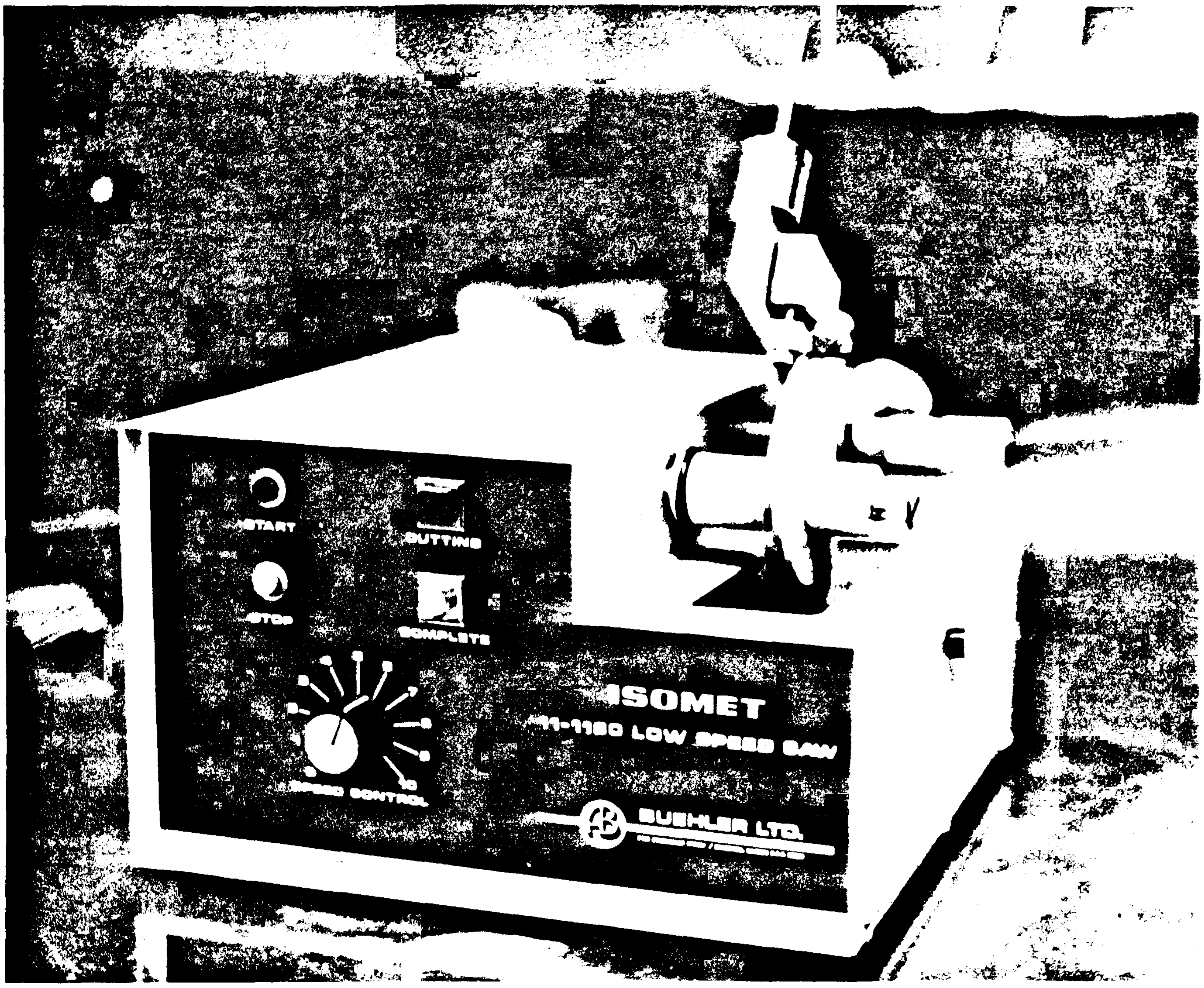

Fig 8.4 Diamond sawing a natural corundum crystal

Fig 8.5 shows the composite grinding wheel assembled and mounted on an arbor of the type normally used with a bonded grinding wheel. This composite wheel comprises two similar components as shown in Fig 8.6 together with a set of steel spacers. This assembly is seen, partly dismantled in Fig 8.7. Fig 8.8 shows a stage in dividing a previously turned steel ring into spacers by means of a milling operation while Fig 8.9 shows a set of spacers nearing completion.

The circular assembly formed by these elements together with the arbor provides a series of recesses of dovetail form at the periphery. Into these recesses pieces of corundum crystal were inserted at selected orientations and the intervening space was filled with a proprietary mixture of polyester resin and filler material. This material, after hardening, secured each grit in a matrix housed in the corresponding recess of the composite grinding wheel from which it was possible to remove them for subsequent examination as shown in Fig 8.10.

Well-developed crystals with a minimum of taper had been selected and cut into pieces of convenient size for insertion into the recesses of the composite wheel.

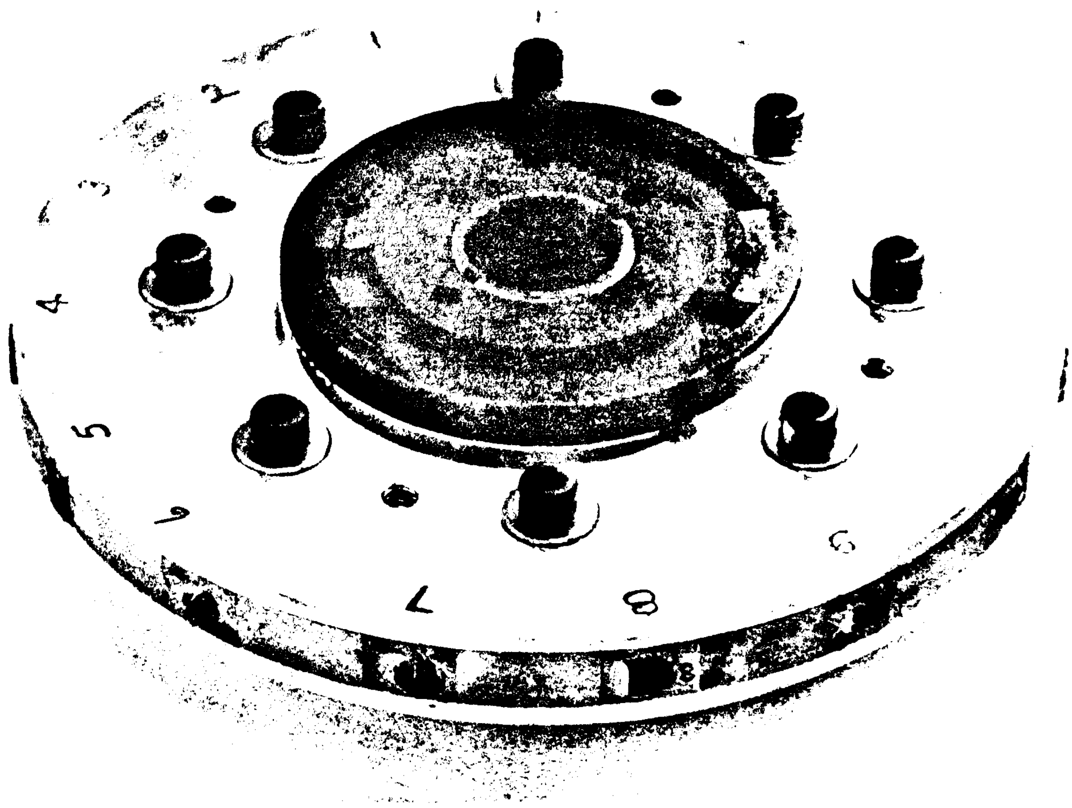

Fig 8.5 The composite grinding wheel and arbor

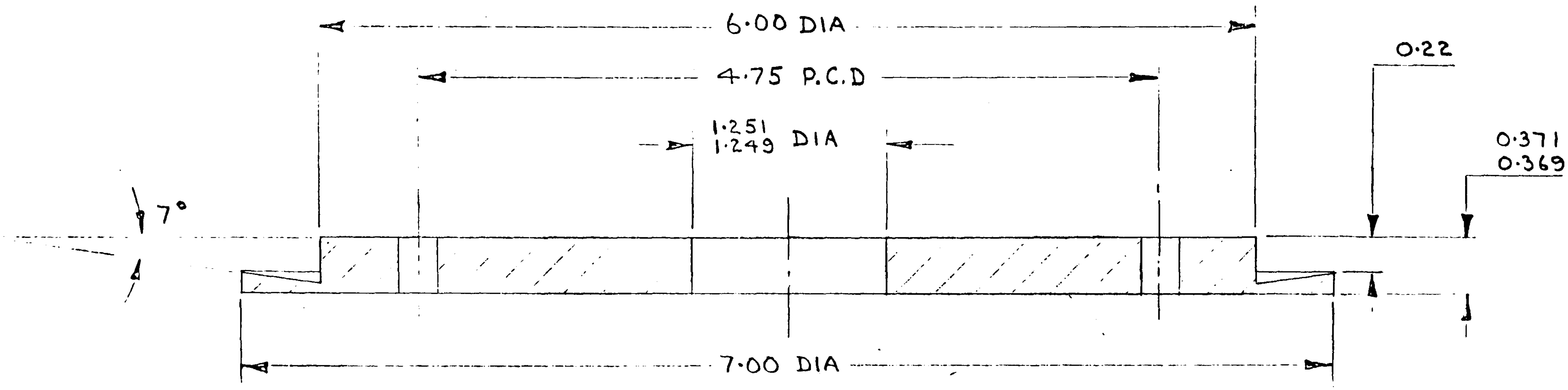

GRINDING DISC COMPONENTS A & B

A - 1 OFF WITH EIGHT $\frac{1}{4}$ DIA HOLES EQUALLY SPACED ON 4·75 P.C.D
B - 1 OFF WITH EIGHT HOLES DRILLED & TAPPED $\frac{1}{4}$ BSW ON 4·75 P.C.D
MATERIAL: $\frac{3}{8}$ FREE-CUTTING ALUMINIUM ALLOY PLATE
DIMENSIONS IN INCHES

Fig 8.6 Working drawing for components of the composite grinding wheel

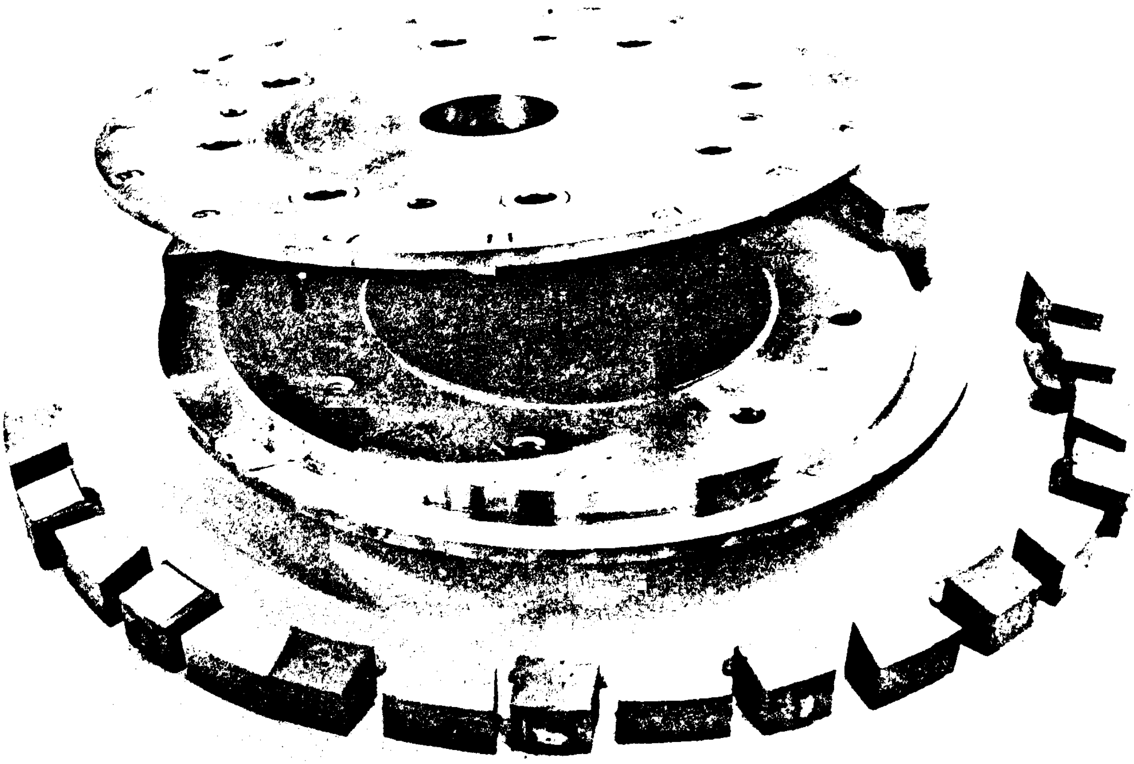

Fig 8.7 Composite grinding wheel dismantled

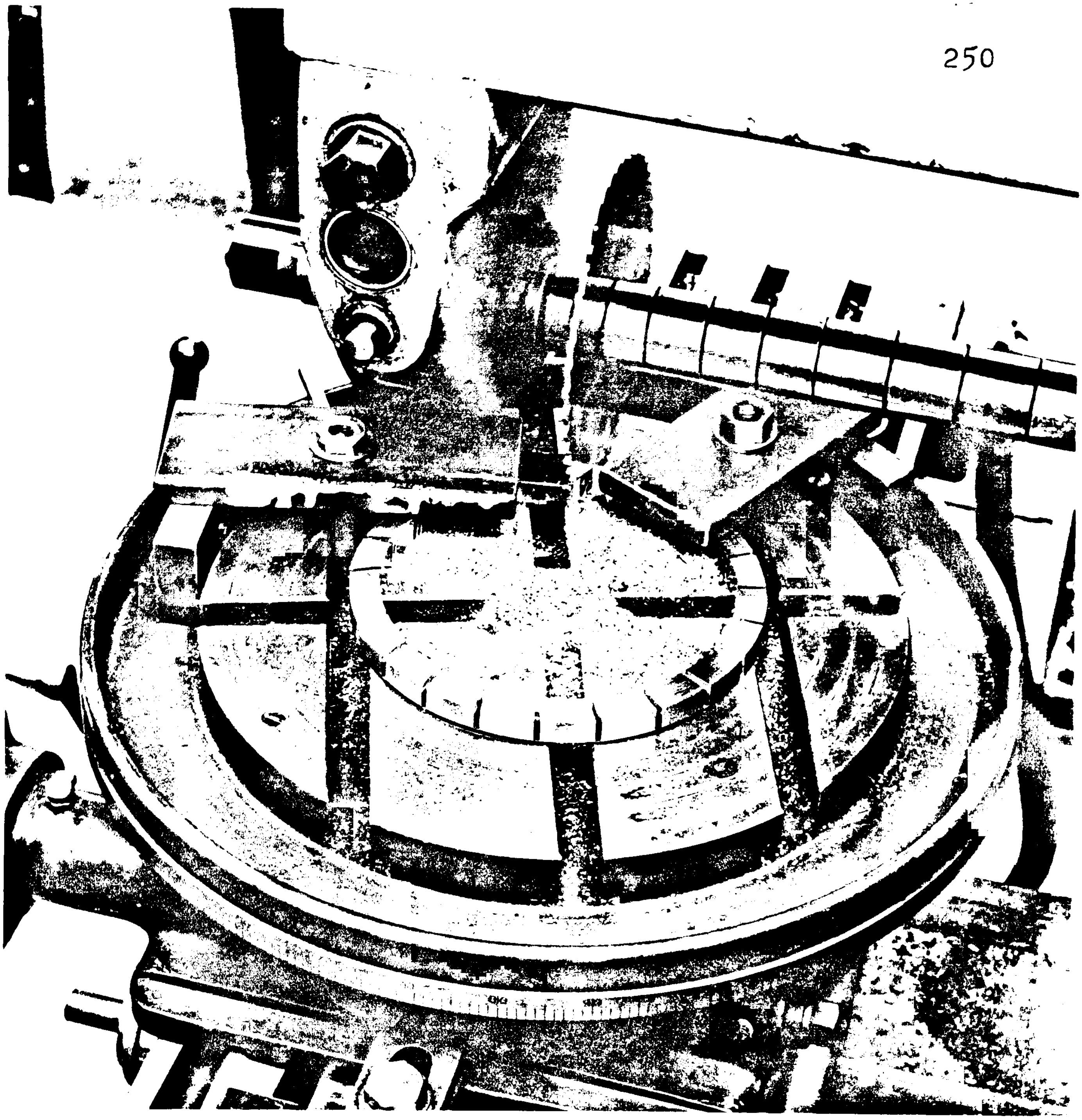

Fig 8.8 A stage in producing mild steel spacers for use in the composite grinding wheel

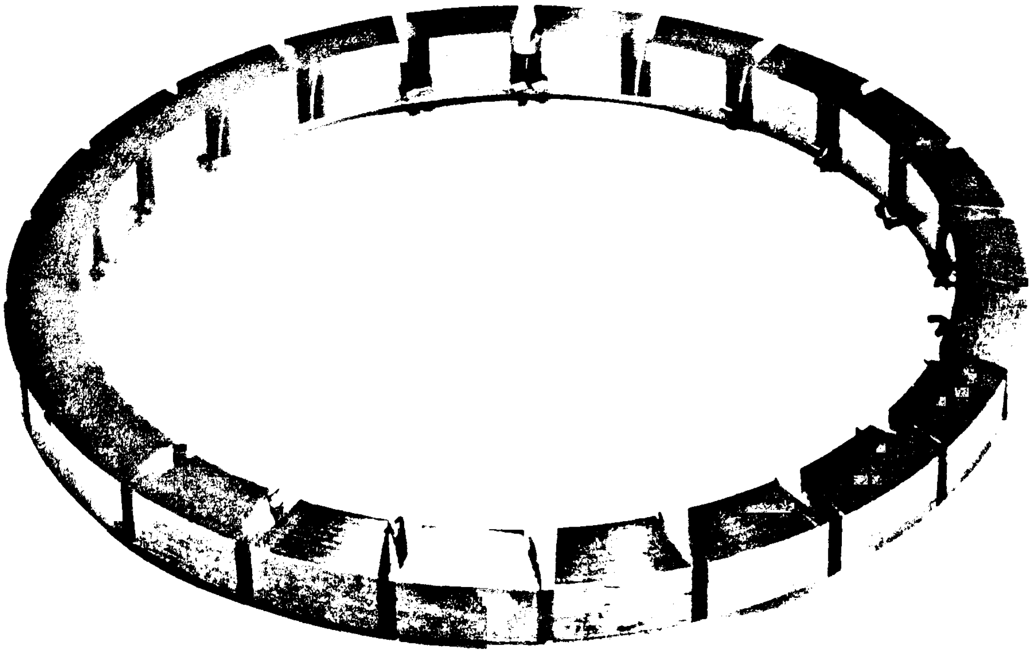

Fig 8.9 Partly completed mild steel spacers for use in the composite grinding wheel

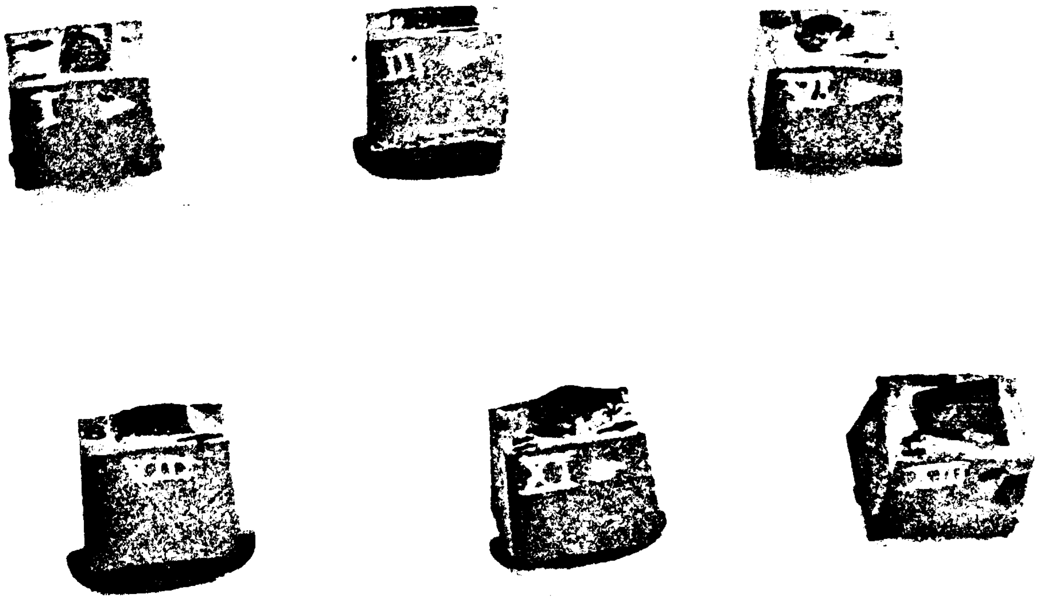

Fig 8.10 Embedded single-crystal corundum grits after removal from the composite grinding wheel

These were embedded in the matrix material in three different orientations. This was done by drawing pencil lines on crystal surfaces in the directions indicated by Fig 8.11 and positioning these lines approximately tangential to the periphery of the composite grinding wheel.

Spacers were arranged in the composite wheel so as to provide a total of fifteen recesses for the reception of individual grits. Each recess was coated with a silicone oil mould release agent and then partly filled with the prepared synthetic resin, filler, and hardener mixture[1]. A piece of corundum crystal, held with forceps, was immediately pressed into the soft material to a depth determined by a simple height gauge so as to protrude above the periphery of the aluminium discs by about 1.5 mm. The embedding medium having set to a gelatinous condition excess material was trimmed away and any voids were filled with additional freshly mixed medium (Fig 8.12).

1. Plastic Padding - hard grade

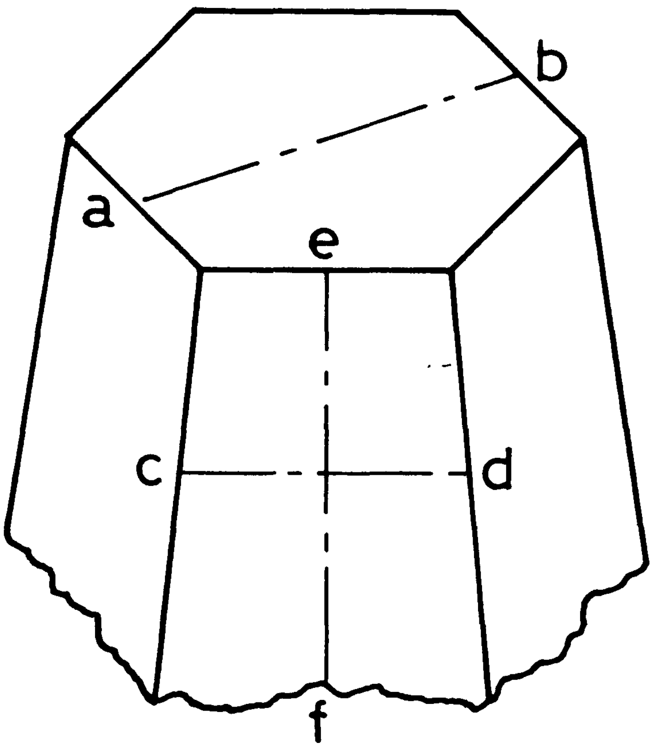

Fig 8.11 Isometric sketch representing part of a natural corundum crystal

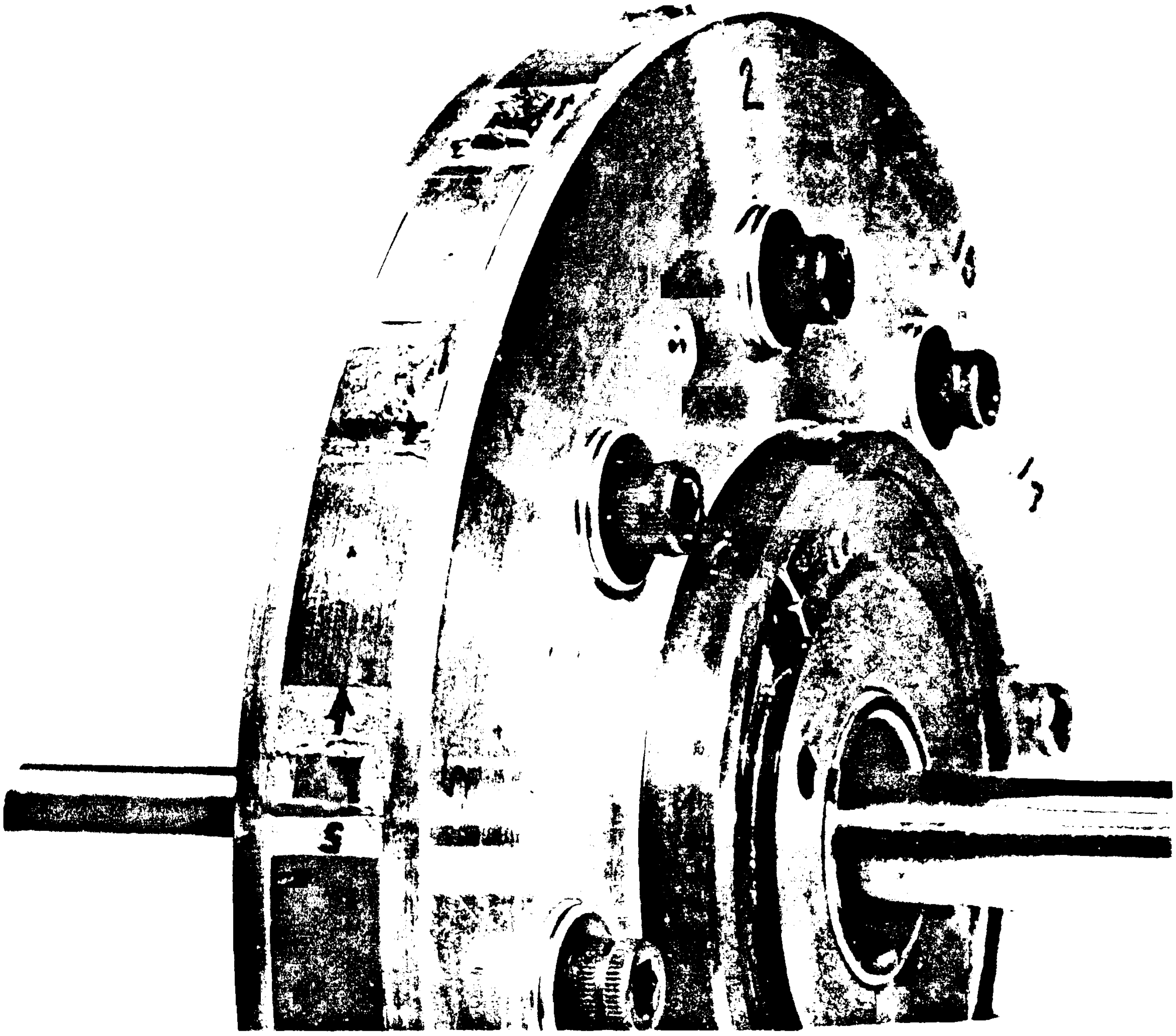

Fig 8.10 Composite grinding wheel assembled with arbor and mounted on balancing mandrel showing the method of labelling single crystal corundum grits

On completion of these operations and curing at room temperature of the embedding medium, the composite grinding wheel was mounted on the spindle of the surface grinder and the grits were dressed using a single-point diamond dresser in exactly the same manner as for a bonded grinding wheel.

Dressing was continued until the minimum of material had been removed from the crystals consistent with producing on each one a dressed surface lying in a common cylindrical envelope (Figs 8.13 and 8.14).

Before this result had been achieved for all fifteen grits it was noticed that two of the embedded grits and their matrices were loose in their recesses and dressing had to be discontinued for this reason. This loosening was attributed to shrinkage of the embedding medium during and/or after curing and by careful measurement of recesses and blocks of matrix material subsequent to their removal from the composite wheel this shrinkage was found to be about eight per cent.

By partial dismantling and the introduction of paper shims it was found practicable to hold the embedded grits firmly enough to permit of satisfactory dressing.

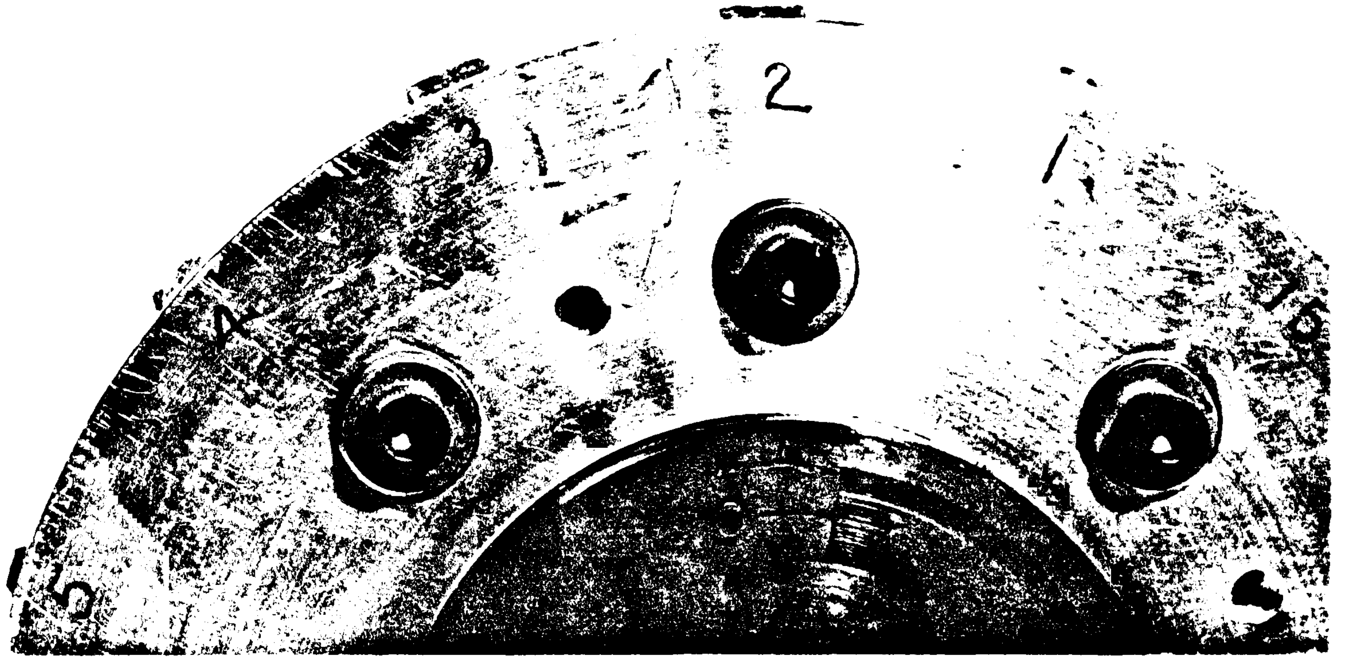

Fig 8.13 Composite grinding wheel and arbor showing single corundum crystals after the dressing and grinding operations

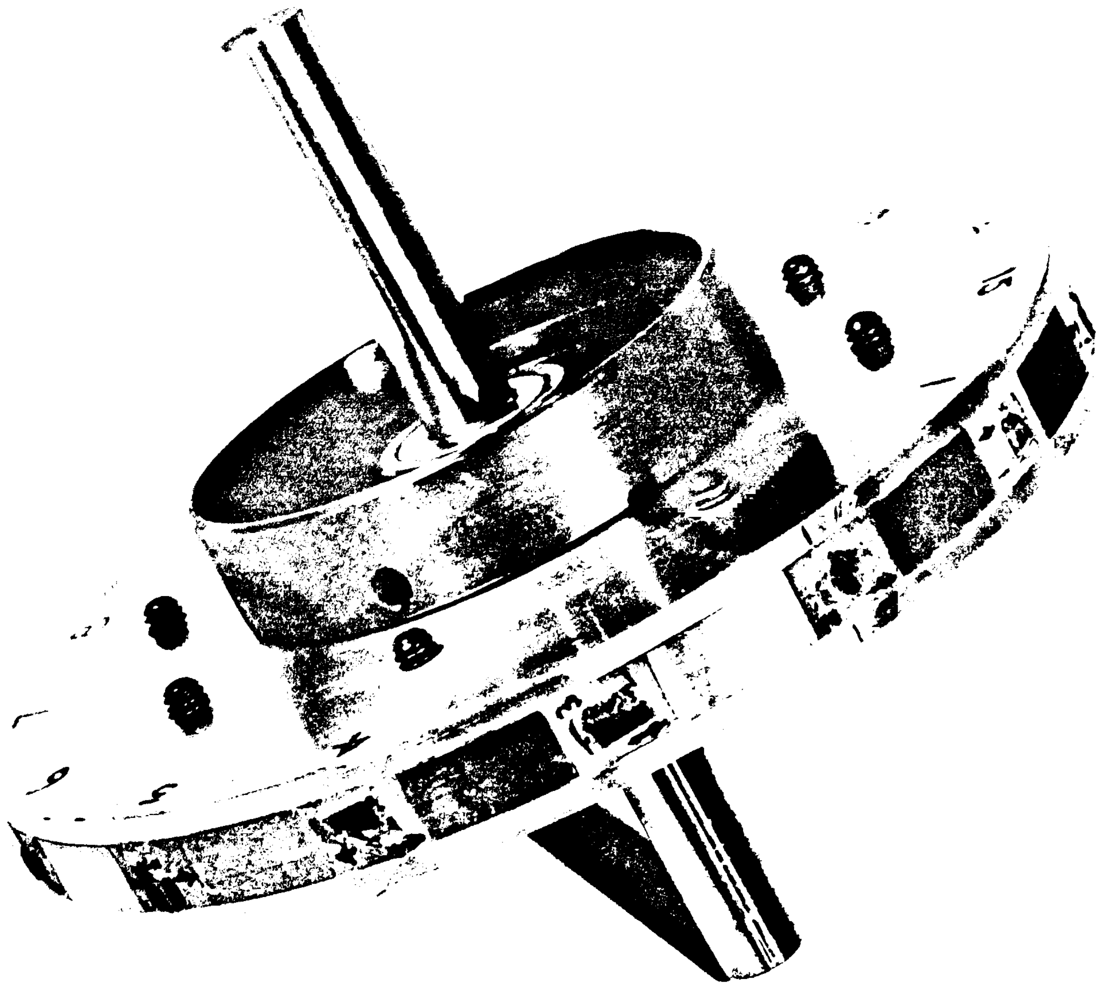

Fig 8.14 Composite grinding wheel assembled with arbor and mounted on balancing mandrel

At a later stage when attempts were made to grind the surface of a steel test specimen with the composite grinding wheel it was found that the larger forces associated with grinding displaced the blocks of matrix material within their recesses and grinding had to be discontinued at a relatively early stage with little workpiece material having been removed.

The design of the composite grinding wheel was intended to provide removable single grinding grits suitably mounted in a matrix of such overall size and shape as to facilitate examination by profilometry and scanning electron microscopy. Profilometry could have been applied to grit surfaces in situ but it was more convenient to remove specimens from the composite wheel for this purpose. The overall dimensions of the composite wheel assembly were far in excess of the workstage capacity of the scanning electron microscope and removal of specimens from the wheel for examination in the microscope was essential.

Removal of some specimens from the wheel was difficult by reason of adhesion between the embedding material and the internal surfaces of recesses. Various types of synthetic resin based media and silicone release agents were tried but neither the problem of shrinkage on the one hand, nor that of selecting and distributing a release agent on the other, were completely overcome. However, by removing specimens at different stages, a total of six representative grit specimens were eventually obtained.

Three of these specimens were in the newly-dressed condition, a total of about 0.4 mm having been removed in increments of about 0.008 mm by dressing, and were representative of the three specified crystal orientations. The other three were also representative of the three orientations but had been used to plunge grind a steel plate for about ten minutes, removing workpiece material to a depth of approximately 0.05 mm in the process.

Profilograms were produced from the surfaces of these specimens and from the ground surface. A series of photographs representing grit surfaces were also obtained using the Stereoscan scanning electron microscope.

Profilograms were conveniently obtained from these large grit surfaces but were not subjected to any form of analysis because it was thought that the profiles of grit and workpiece surfaces may have been affected by movement of matrices within the composite wheel. Some of the scanning electron micrographs are however included as follows.

Fig 8.15 shows the diamond dressed surface of one of the natural corundum grits at a low magnification of ×26. The leading edge of the grit surface occupies the lower part of the print area while the upper part shows the embedding medium. Three sides of the hexagonal crystal are clearly seen in this photograph and the orientation, described as radial, is self evident from this. Fig 8.16 is an oblique view of the same area at much higher magnification (×620) while Fig 8.17 shows the trailing edge at the somewhat lower but still relatively high magnification of ×530.

Figs 8.18 and 8.19 show, respectively, the leading and trailing edges of a grit in axial orientation, which means that the axis of the hexagonal pyramid from which the grit was cut lay parallel with the axis of the grinding wheel.

The single point diamond dressing tool was used in the orientation recommended for dressing a bonded grinding wheel. That is dressing was effected by presenting a

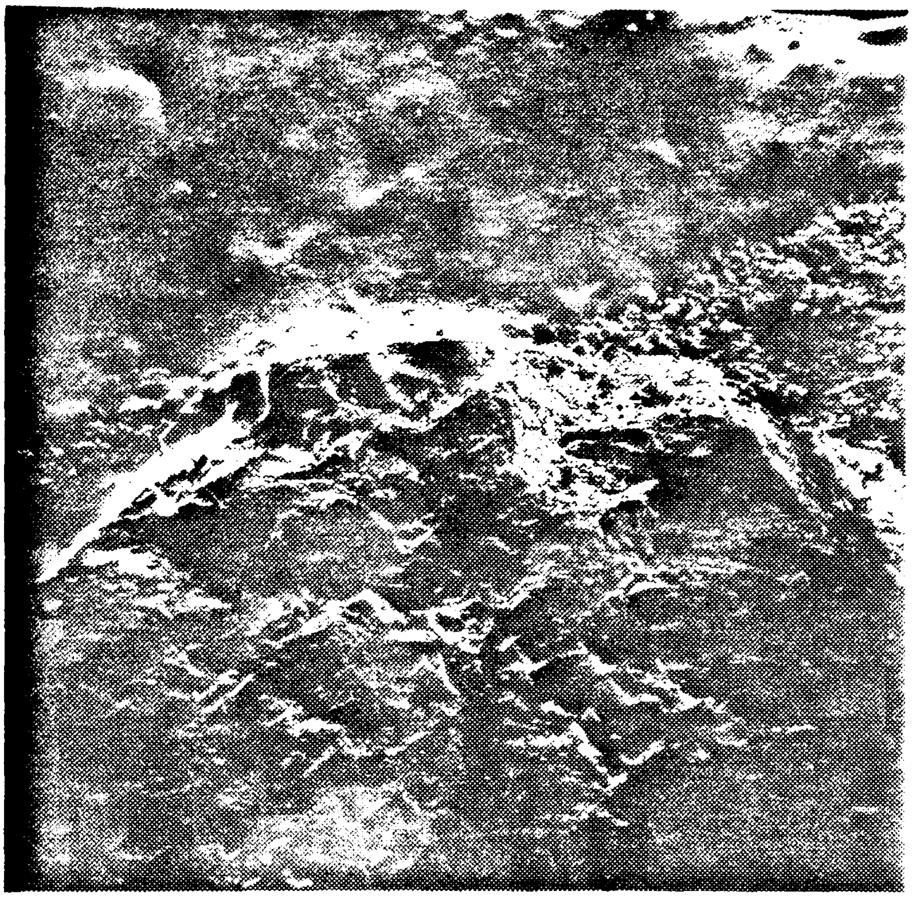

Fig 8.15 Leading edge of a natural corundum single crystal grit after diamond dressing Radial crystal orientation. Magnification ×26

Note. The dressed surface occupies the lower part of the print and the area above represents the mounting medium

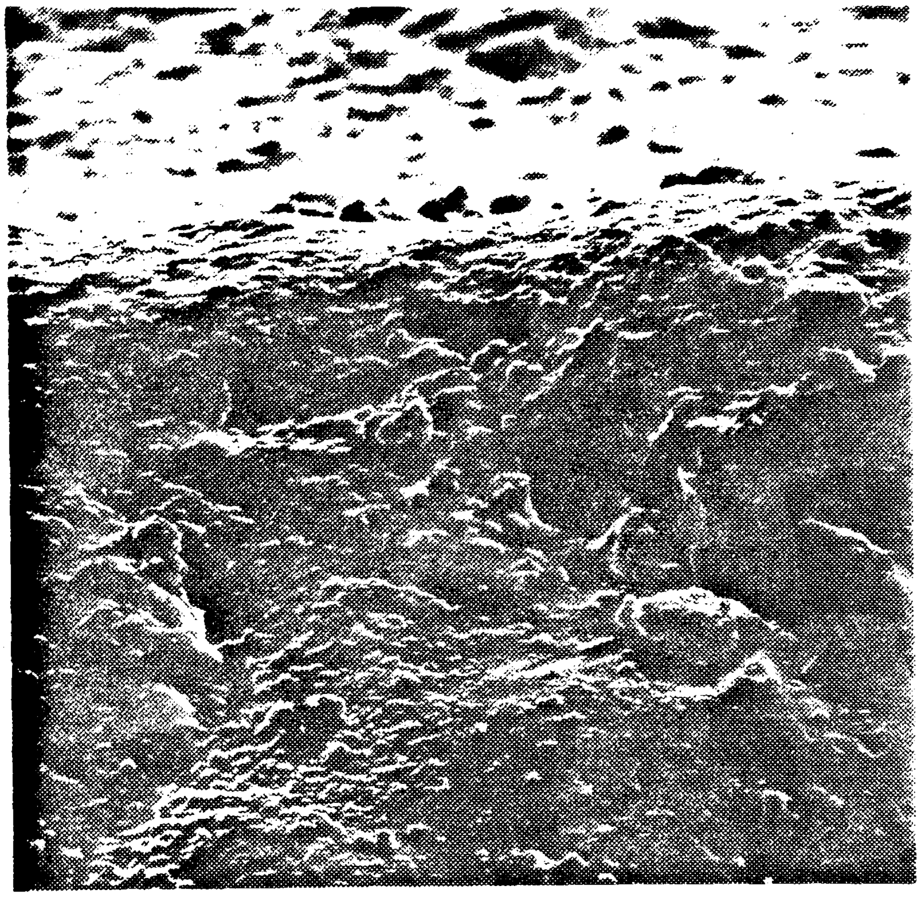

Direction of motion of grit relative to the dressing diamond ⟶

Fig 8.16 Leading edge of a natural corundum single-crystal grinding grit after diamond dressing Radial crystal orientation. Magnification ×620

Direction of motion of the grit relative to the dressing diamond →

Fig 8.17 Trailing edge of a natural corundum single-crystal grinding grit after diamond dressing Radial crystal orientation. Magnification ×530

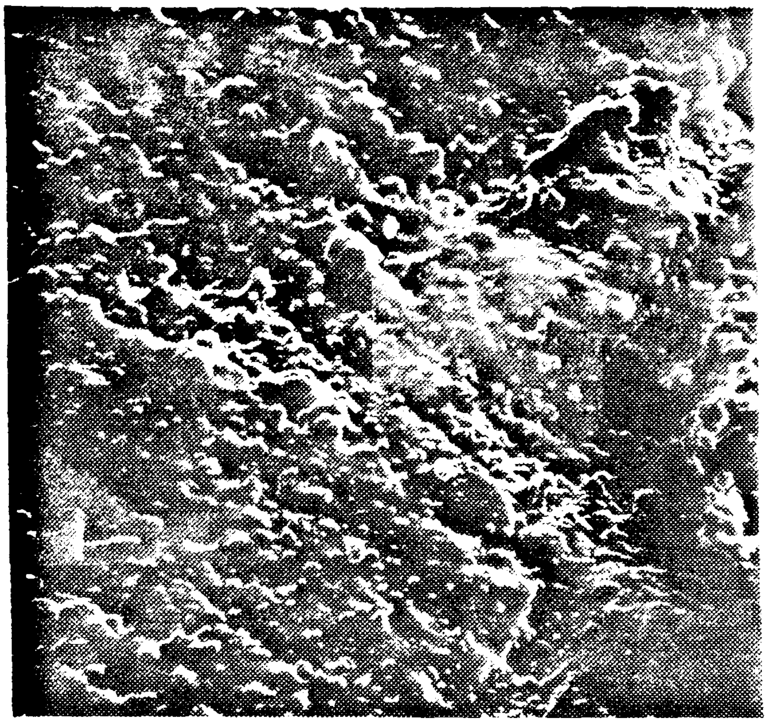

Fig 8.18 Leading edge of a natural corundum single-crystal grinding grit after diamond dressing Axial crystal orientation. Magnification ×550

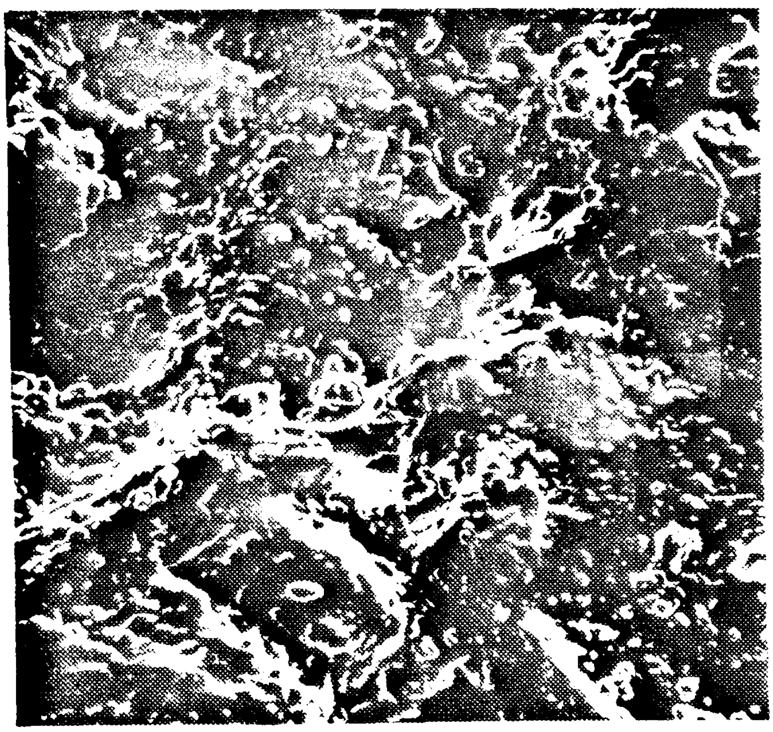

Fig 8.19 Trailing edge of grit as above Magnification ×600

Direction of motion relative to dressing diamond nominally flat surface of the diamond to the abrasive grit surface. The absence of any visible scoring of the grit surfaces by the diamond and the general appearance of these surfaces to some extent confirms that such dressing must, in this case at least, have taken place entirely by the detachment of small chips from the grit surface leaving asperities distributed over the whole area.

Fig 8.20 shows the surface of a grit in radial orientation (x20) subjected to wear by grinding a steel surface and may usefully be compared with Fig 8.15. The general flattening of the surface is clearly apparent and one or two fragments of what appears to be swarf are visible. At higher magnifications (Figs 8.21 and 8.22) this flattened but still fairly rough surface is seen to be confined to the leading edge of the grit.

Figs 8.23, 8.24, and 8.25 represent a comparable set of results to the preceding but obtained from a grit in axial orientation. In these the surface smoothing effect of a similar amount of wear is less apparent than in Figs 8.20, 8.21, and 8.22.

Fig 8.20 Natural corundum single-crystal grinding grit worn by grinding a steel surface
Leading edge. Radial crystal orientation
Magnification ×20

Fig 8.21 Natural corundum single-crystal grinding grit worn by grinding a steel surface. Leading edge. Radial crystal orientation. Magnification ×500

Direction of motion relative to the workpiece or dressing diamond

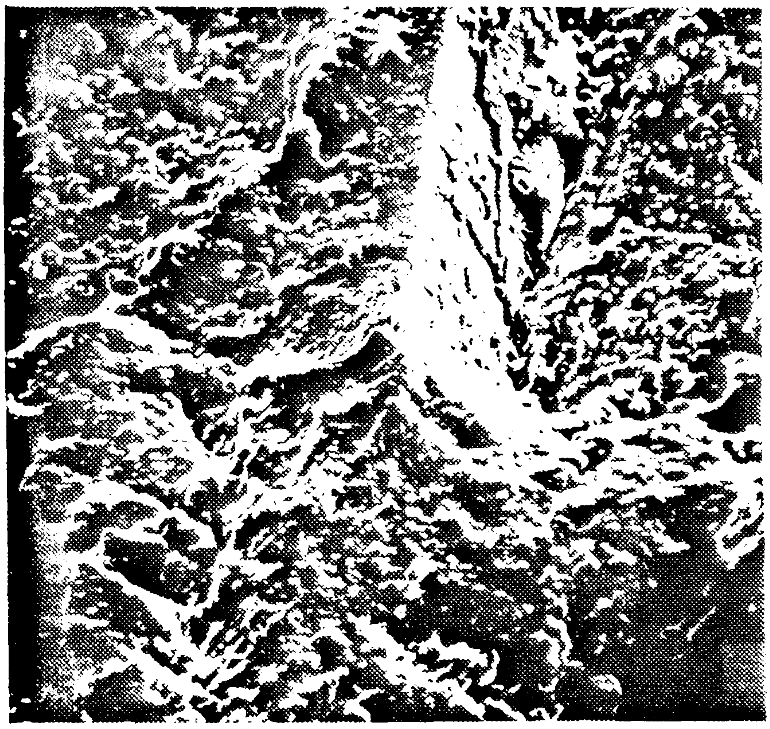

Fig 8.22 Grit as above. Trailing edge Magnification ×640

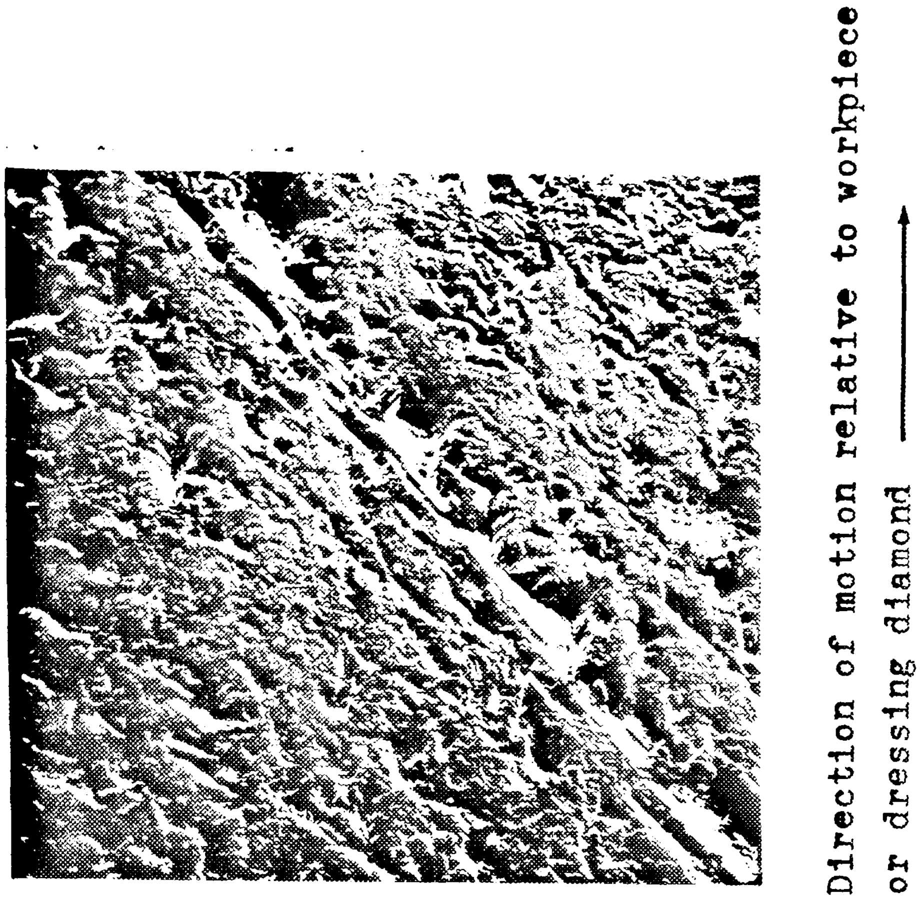

Fig 8.23 Natural corundum single-crystal grinding grit surface worn by grinding steel. Leading edge. Axial crystal orientation. Magnification ×60

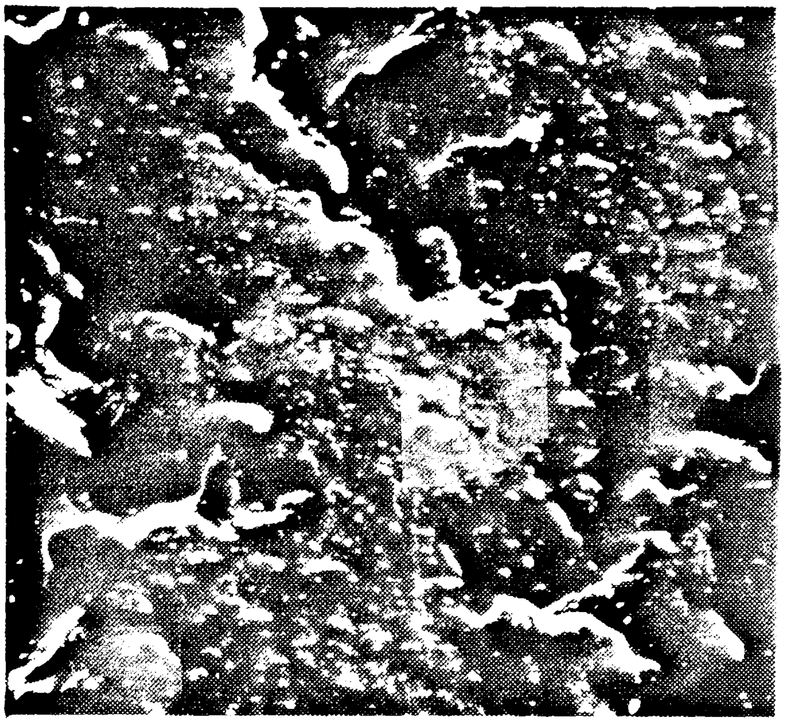

Fig 8.24 Natural corundum single-crystal grinding grit worn by grinding steel. Leading edge. Axial crystal orientation. Magnification ×590

Direction of motion relative to workpiece or dressing diamond →

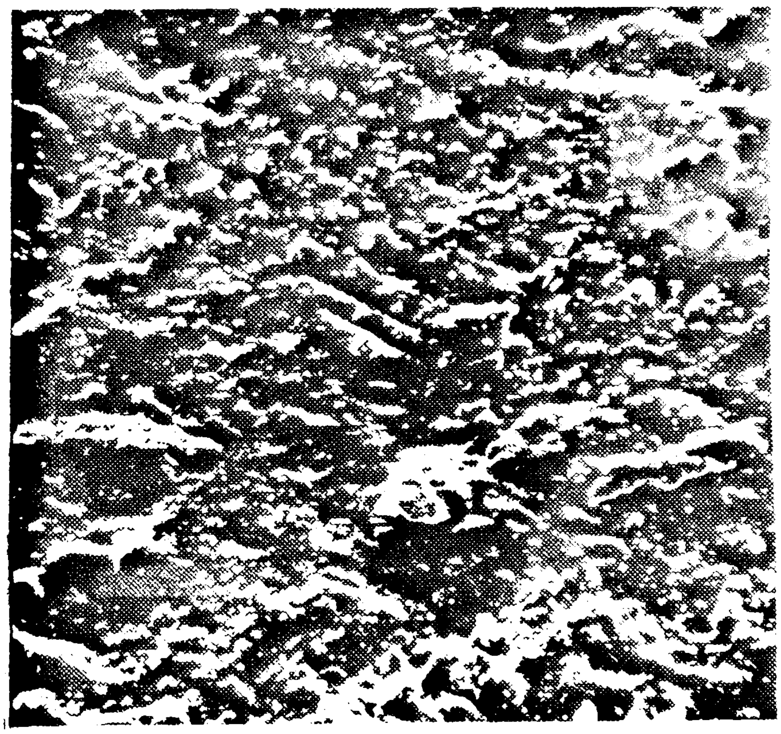

Fig 8.25 Grit surface as above. Trailing edge Magnification ×650

The extent and quality of the results obtained at this stage from work with single crystals of natural corundum were adversely affected by difficulties relating to the secure holding of embedded grits in the composite grinding wheel and subsequent extraction of specimens for examination. While it seemed probably that these difficulties might eventually be overcome, other aspects of the investigation appeared more likely to provide useful quantitative results from bonded grinding wheels and the surfaces ground by such wheels. Work with the composite grinding wheel was therefore discontinued in order to concentrate on profile analysis of bonded grinding wheels and corresponding ground surfaces.

CHAPTER 9. DEVELOPMENT OF SURFACE PROFILE ANALYSIS

Information obtained from the literature provided encouragement to proceed with analysis of surface profiles using statistical parameters including power spectral density. Experience gained in experimental work for Part 1 of this thesis indicated stylus profilometry as an appropriate technique for collecting information from the surfaces of grinding wheels and the corresponding ground surfaces. This view was also supported by the literature.

Work outlined in this chapter includes the acquisition of programs for computation of the statistical parameters and the adaptation of a device last used in connection with profilometry applied to a static grinding wheel in Part 1, to facilitate controlled rotation of a grinding wheel during collection of profile data from its surface. This work proceeded concurrently with other aspects of the investigation some of which are detailed in the preceding chapter.

Chapters 9 and 10 together represent a continuous progression of work on surface profile analysis extending over a considerable period of time and separated into two chapters for convenient presentation. In Chapter 9 profile data were collected by visual inspection of profilograms, which effectively limited profile sample size in terms of the number of ordinates it was feasible to measure and record in this way. A number of power spectra and other statistical parameters were computed and plotted from such samples.

These power spectra were more complex than those found in the literature representing comparable surfaces. Also spectra representing the profiles of virtually identical surfaces differed considerably one from another. Each profile sample contained 100 ordinates and the erratic nature of the results cast doubt on the ability of these samples to represent the surfaces concerned.

Inspection of those samples taken from grinding wheel profiles showed a high proportion of zeros corresponding with voids in the wheel surface and a very small total number of finite numerical values.

Clearly such a sample contained very little information relating to actual grit profiles and was probably quite inadequate to reliably represent the overall surface profile of a grinding wheel. Power spectra representing ground surfaces also provided some indication that samples may have been unrepresentative.

On the assumption that inadequate sample size may have been primarily responsible for the erratic results so far obtained in terms of power spectral density it was evidently necessary to determine the influence of increased sample size.

In order to collect profile samples containing a number of ordinates substantially in excess of 100 it was obviously desirable to devise means for automatic collection and storage of these data. The apparatus and methods used to facilitate this work are detailed in Chapter 10. In the event, sample size was increased in stages until finally samples of 1000 ordinates were regularly used for computation of power spectral density. These samples approached the maximum storage capacity of one of the items of apparatus used, namely the transient recorder.

Results in the form of power spectra presented in Chapter 10 show much improved smoothness and repeat-ability. Also, for the first time in this investigation, transfer functions are plotted with the object of relating spectra representing ground surface and grinding wheel profiles.

Evidence for the isotropy of grinding wheel surfaces after fine dressing and some wear was already available (30) and tracing the circumferential profile had been found the most convenient method for producing profilo-grams sufficiently representative of grinding wheel surfaces. However, these circumferential profiles were obtained using standard Talysurf equipment and accessories. It was possible to set one of these accessories, known as the "2 inch to infinity radius datum element" (30) to match the curve of the grinding wheel surface but the tedious and delicate setting operations rendered this a slow and somewhat unsatis-factory procedure compared with the simplicity of producing a profilogram from the corresponding ground surface.

If profilometry was to be effectively applied to both ground surface and grinding wheel it was clearly necessary to devise improved and simplified methods for application to the latter.

Equipment for supporting a mounted grinding wheel on the Talysurf worktable already existed (Fig 4.5) and preliminary trials in which the pick-up was kept stationary (i.e. not traversed) with the skid resting on the curved surface of the grinding wheel, while the latter was slowly rotated, suggested that profilograms might be produced in this mode by controlled rotation of the grinding wheel.

The possibility of using roundness test equipment for the purpose outlined above was also considered. This had the evident advantage of providing for full circumferential profile measurement of cylindrical workpieces. However the available OMT equipment used sapphire stylii of larger tip radius than those designed for surface texture profilometry, while its capacity in terms of workpiece diameter was restricted to a maximum of six inches.

The practical problems of adapting roundness test equipment to profile measurement of the seven inch diameter grinding wheels then in use did not appear insuperable, but had these been overcome, the grinding wheel profile would have been represented by a polar graph and the ground surface by the usual profilogram in rectangular coordinates. Also surface texture profilometry required specific and different scales of magnification in directions normal to and parallel with the surface; the latter magnification having little relevance to roundness measurement.

Talysurf profilograms of the ground workpiece could be produced at a wide range of magnifications (×500 to ×100000) normal to the surface and at magnifications of ×20 and ×100 parallel with the surface. A range of magnifications normal to the surface up to ×5000 was available on the OMT roundness equipment, but the magnification in the circumferential direction was obviously determined by the ratio between the nominal radii of polar graph and grinding wheel. In this case that ratio was around 1:1 and therefore quite insufficient to resolve fine surface detail; even supposing that the use of a stylus with the necessarily small tip radius had been found practicable. It was therefore decided that profilometry of the grinding wheel surface should be based upon adaptation of surface texture equipment rather than roundness test machines.[1] For this purpose it was decided to construct a device providing for slow controlled rotation of a grinding wheel.

In order to obtain the profilograms used in Part 1 of this thesis each grinding wheel together with an aluminium disc was mounted on the arbor of the surface grinder used in producing the ground surfaces. This sub-assembly was then mounted upon a standard balancing mandrel and the assembly so produced was supported by resting the mandrel in the vees of a fixture designed and made for use with Talysurf 3. The arrangement can be seen in Fig 4.5.

1. At a later stage of the investigation Rotary Talysurf equipment with which surface texture profilograms could be produced using a pick-up traversed by swinging in a long arc about the centre of the workpiece became available. Once again seven inch diameter grinding wheels were beyond the capacity of this machine. Also by this time profilograms had been successfully produced from such wheels using apparatus described in the subsequent text.

This fixture was now converted into a device for slow controlled rotation of the grinding wheel and arbor assembly. The power unit selected for this purpose was a small synchronous clock motor arranged to drive the mandrel so as to rotate the grinding wheel at one revolution per hour. On the basis of this rotational speed, nominal grinding wheel diameter of seven inches, and graph recorder paper speed of twelve inches per minute, profilograms could be produced at a magnification tangential to the grinding wheel surface of $\times 32.74$. The corresponding scale used for ground surface profilograms was $\times 100$ and to facilitate later calculations relating the surfaces of grinding wheel and workpiece 32.74 was eventually taken as one-third of 100, the error introduced by so doing being about 1.6 per cent.

At this stage the device described was transferred from Talysurf 3 to a newly available Talysurf 4, the latter being used for all subsequent work.

For trial purposes a prepared 80 grit grinding wheel and aluminium setting disc were set up on the arbor and mandrel. A profilogram was first produced from the highly finished diamond turned setting disc at a magnification normal to its surface of $\times 20000$.

The recorder pen produced a well centred profilogram from this surface with no evidence of drift or instability.

A profilogram was next produced from the adjacent grinding wheel surface at a normal magnification of ×1000 on which the individual grits were represented as sharply defined peaks with steep sides. Some of these were sharply pointed but a fairly large proportion of flattened tops were recorded in the upper levels, as might be anticipated from the surface of a grinding wheel which had been subjected to a dressing operation and some wear. The general appearance of the profilogram (Fig 9.3) suggested that the use of normal magnification significantly greater than ×1000 would probably be disadvantageous because some lower levels would tend to disappear and the total information contained in a profilogram of given length would be reduced.

On the basis that profilometry would play a significant part in the investigation some thought was given to parameters for use in the analysis and comparison of surface profilograms. Chapter 7 contained clear indications that the most promising methods of analysis were to be found amongst certain statistical parameters.

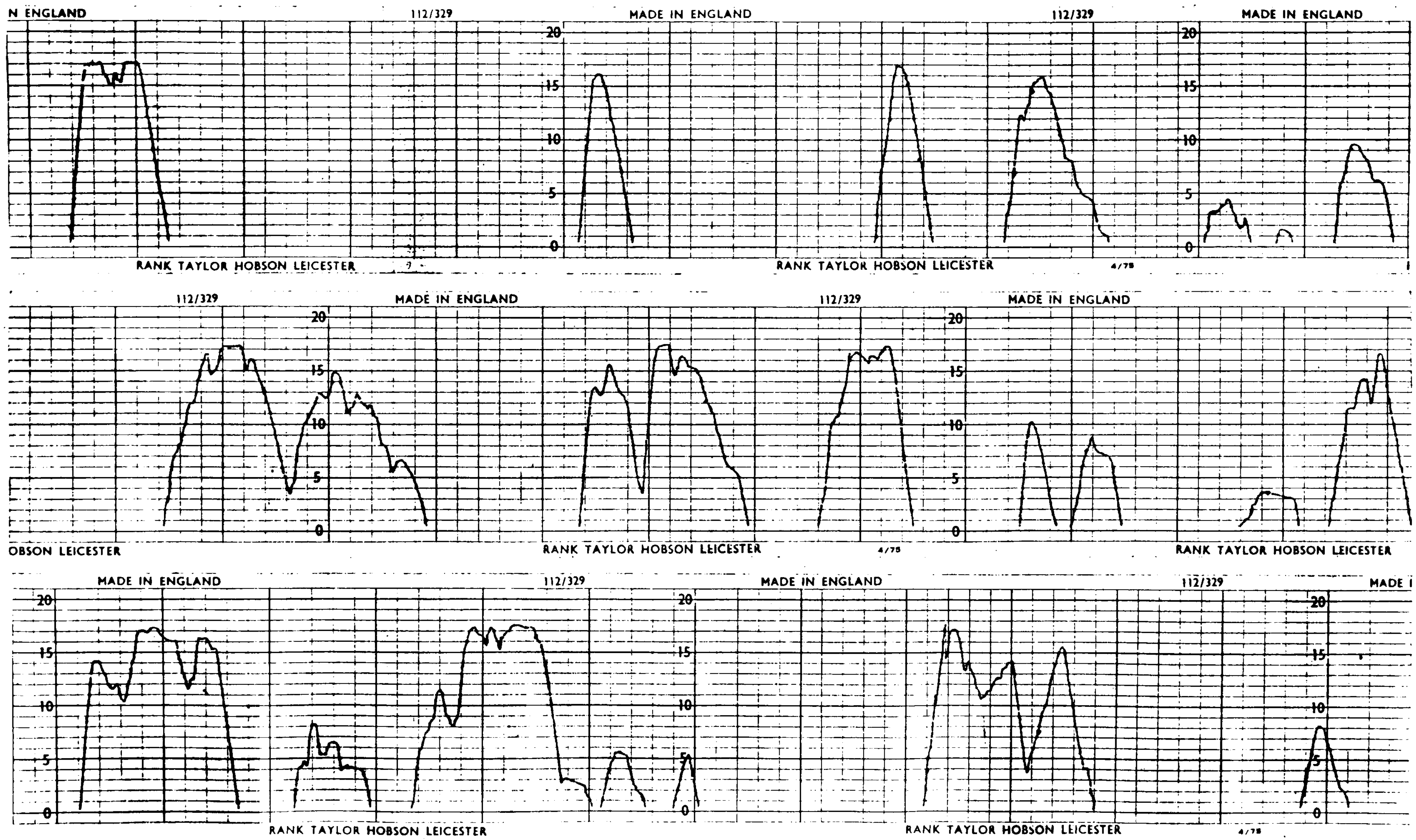

Fig. 9.3 Profilogram representing the surface of an 80 grit grinding wheel

Specialist advice was sought at this stage with the primary purpose of obtaining further information on autocorrelation, power spectra, and possibly other parameters which might be applicable to surface characterization and comparison. Certain basic facts including the following emerged from these discussions.

Autocorrelation refers to the correlation between two sample poimts on a given profile at a specified 'lag' interval. Two points on the same profile close together will always have a high correlation and, if they are coincident, the correlation will be unity. From this it follows that the autocorrelation curve representing any surface profile will always start at unity. If the autocorrelation curve falls rapidly and becomes negative (possibly approaching -1) this indicates strong negative correlation, that is deviation on opposite sides of the mean of similar magnitude.

The power spectrum represents the Fourier transform of the autocorrelation curve and serves clearly to indicate those frequency bands which predominate. If the power spectrum is substantially constant this indicates that all frequencies found in the surface profile are equally represented.

With regard to the application of autocorrelation the following ideas emerged from the discussions.

(i) Some form of aid to calculation would be necessary and the computer programming required in order to produce autocorrelograms would be relatively simple.

(ii) Correlation is not to be expected between separate sections of profilogram - there must be a continuous record. Any attempt to correlate must therefore be confined to the length of strictly continuous profilogram available.

(iii) At least 50 lag intervals should be included in each computation.

The fact that an autocorrelogram must be computed from a continuous record indicated the need for profilograms of considerably greater length than had previously been obtainable. This led to the construction of the device already described by means of which a profilogram of virtually unlimited length can be obtained from the surface of a rotating grinding wheel.

The following expression defines what is called sample autocovariance

$$C_\tau = \frac{1}{N-\tau}\sum_{i=1}^{N-\tau} Y_i Y_{i+\tau}$$

where $Y_i = y_i - \bar{y}$, $Y_{i+\tau} = y_{i+\tau} - \bar{y}$

and y_i is the ordinate of a point on the profile, $y_{i+\tau}$ is another ordinate separated from the first by a number of lag intervals τ and $N - \tau$ is the number of pairs of such values. The above expression facilitates calculation of a series of autocorrelation coefficients for example

$$R_1 = \frac{C_1}{C_0}, \quad R_2 = \frac{C_2}{C_0} \text{ etc.}$$

and these when plotted serve to define the autocorrelogram. This method can be used to obtain the autocorrelogram representing a continuous profile such as that of a ground surface.

The profilogram representing a grinding wheel surface is discontinuous in the sense that there are gaps in the record corresponding to the voids between grits. For the purpose of computing points defining an autocorrel--ogram such a discontinuous profile is open to the objection that it may not represent the record of a stationary process. Certainly the voids influence the computed result because an ordinate within a gap may be taken as zero and will affect the computed result accordingly.

As a means of overcoming this apparent anomaly it was proposed that any pair of values corresponding with a gap in the record should not be used in calculating a correlation coefficient. That is, such sample auto--covariances would be omitted and the denominator adjusted accordingly.[1]

In order to obtain practical experience of the computation of points defining an autocorrelogram, a set of trial calculations were carried out using a manually operated electronic calculator. The data were taken from published work (Theory of Statistics, Yule and Kendall p 640) and a series of eight correlation coefficients were calculated and plotted. Satisfactory agreement with the published results was obtained but the amount

1. This proposal was implemented during programming but its use was abandoned at a later stage.

of work involved in the exercise confirmed that the use of a computer would be essential if any significant use was to be made of autocorrelograms and/or power spectra.

STATMAT programs for autocorrelation

The first step towards making use of computer facilities to obtain autocorrelograms was taken when reference was made to a descriptive program index available at Brunel University Computer Centre. This listed several 'packages' including one called STATMAT which provided for computation of correlation coefficients.

Data were collected by visual inspection of three profilograms each representing the same grinding wheel surface. Table 9.1 shows one such set of data in which a zero entry for 'y' may be taken to represent a gap in the record characteristic of the grinding wheel profile at a point corresponding with a void between grits. Fortran ststament cards were prepared from these data and submitted for running on the London University CDC 7600 Computer via Brunel University Computer Centre.

Table 9.1 Coordinates defining the profile of a worn 80 grit grinding wheel. Sample of 90 ordinates

x	0	1	2	3	4	5	6	7	8
y	12.0	12.5	4.0	16.0	17.5	3.0	0	0	0
x	9	10	11	12	13	14	15	16	17
y	0	0	0	11.0	18.0	4.0	0	0	0
x	18	19	20	21	22	23	24	25	26
y	0	6.0	10.5	12.0	14.0	18.5	8.0	2.0	0
x	27	28	29	30	31	32	33	34	35
y	0	1.5	4.0	10.0	1.0	0	6.0	11.0	12.0
x	36	37	38	39	40	41	42	43	44
y	10.5	8.5	1.0	0	0	0	0	0	0
x	45	46	47	48	49	50	51	52	53
y	0	0	0	0	8.0	4.0	2.0	3.0	8.5
x	54	55	56	57	58	59	60	61	62
y	10.0	9.5	1.0	0	0	0	0	0	0
x	63	64	65	66	67	68	69	70	71
y	0	0	0	0	6.0	10.0	16.0	11.0	0
x	72	73	74	75	76	77	78	79	80
y	3.0	11.0	15.0	0	0	3.5	4.5	1.0	0
x	81	82	83	84	85	86	87	88	89
y	0	0	0	0	0.5	1.0	1.0	0	0
x	90								
y	0								

y in units of 0.0001 inch

x intervals 0.00207 inch

Preparation and submission of data on the lines indicated was repeated several times over a period of about one month during which the only responses obtained from the computer having relevance to the computation related to editing. On completion of editing a response was received to the effect that files had been 'corrupted' and this statement was interpreted as indicating that results were unlikely to be obtained from the package currently in use.

A considerable amount of time had been devoted to collection of data and preparation of Fortran cards leading to no positive results. Suggestions were obtained regarding the availability of alternative statistical program packages on the same computer but the slow and tedious data preparation coupled with the difficulty previously experienced in interpreting information fed back from the computer served to discourage further work on these lines and no progress in statistical investigation was made for about one year. However, work was eventually resumed on somewhat different lines as follows.

MACJO Programs

The availability of a Prime 300 Computer at Willesden College of Technology led to discussions with colleagues which resulted in a series of seven programs being written in Basic language. These were identified by the combined initials of two of the participants (see acknowledgements) as follows.

Program	Statistical Parameter
MACJ01	Autocorrelation (1)
MACJ02	Autocorrelation (2)
MACJ04	Power Spectral Density
MCJ04H	Power Spectral Density
MACJ05	Cross Correlation
MACJ06	Cross Spectral Density
MACJ07	Cross Coherency Spectra

Those programs relating to autocorrelation and power spectra were written with their known potential for surface profile characterization in mind. MACJ01 and MACJ04 included in the computation the effect of gaps in the input data: that is, zero ordinates on the profilogram corresponding with voids in a grinding wheel surface. MACJ02 and MCJ04H were designed to eliminate the effect of such gaps by the methods previously indicated.

The remaining programs were written in the belief that they might be useful for comparing surfaces as, for example, the profiles of grinding wheel and workpiece.

The validity of programs was tested by using them to process data leading some predictable result. An example of a set of test data is given in Table 9.2 Appendix 9 which contains 100 values of Sin θ at angular intervals of $\frac{\pi}{2}$ arranged in 12 columns and 9 lines with line address codes. These data were used in the knowledge that the autocorrelation function of a sine wave is a periodic function of amplitude 2 (upper and lower limits +1 and -1) having the same frequency as the input signal.

Such tests applied to the autocorrelation programs MACJ01 and MACJ02 yielded the anticipated results. Programs MACJ04 and MCJ04H for power spectral density representing the Fourier transforms of the autocorrelation programs may be regarded as indirectly subject to the same tests. Similar remarks apply to cross correlation (MACJ05) and cross spectral density (MACJ06) respectively.

Sets of matched data intended for comparison of the surfaces of grit and workpiece were collected. Each of these sets comprised two arrays of 100 ordinates obtained by visual inspection of profilograms. An example of such real data is reproduced in Table 9.3 Appendix 9. Lines 1000 to 1160 contain ordinates representing the input surface and lines 1500 to 1660 the output. Input and output in this context refer to surfaces it was hoped to compare: typically those of grinding wheel and ground workpiece respectively. The format of these tables was designed to suit the data filing layout adopted for Programs MACJ01 to MACJ07. This tabulation of ordinates into six columns was consistently used for all subsequent work with the specified programs.

The next step was transfer of tabulated data to punched paper tape by manual operation of a Teletype machine. Rather more than 30 tapes representing individual surfaces and combinations of two surfaces were produced in this way and, during a period of several months, a total approaching 100 computer outputs representing real surfaces were obtained.

Each output consisted of a graph defining the function three of which are reproduced in Appendix 9 as Figs 9.31 9.32 and 9.33.

These graphs served to indicate the general shape of functions but were of little use for purposes of comparison having been plotted at a scale such that the maximum ordinate is represented by five inches in every case: the maximum available paper width.

In order to facilitate comparisons it was necessary to re-plot the tabulated values at suitable and consistent scales. Tables 9.4, 9.5, and 9.6 Appendix 9 were compiled to facilitate re-plotting the spectral density curves. Each column in the tables refers to a particular spectrum with which it is identifiable by the notation used.

Re-plotting and the considerable amount of re-tabulation needed for this occupied several months and the result was a total of 64 graphs (54 spectral curves, 5 cross spectral density, and 5 cross coherency).

Although programs had been written to cover five statistical parameters, attention at this stage was confined almost entirely to spectral curves obtained by plotting power spectral density against abscissae obtained by converting the angular frequencies to wavelength in mm. Marking the frequency scale in terms of wavelength or period was done in order to facilitate interpretation of results in relation to the spacing of surface profile features. Power spectral density was plotted at a consistent scale but no attempt was made at this stage to define the units of measurement.

The primary reasons for this concentration on power spectral density were to be found in the accumulation of evidence suggesting that meaningful interpretation and comparison of power spectra representing surface profiles was almost certainly practicable. Interpret--ation of autocorrelation functions, on the other hand, appeared to depend on classification into different types which appeared less likely to distinguish between surface profiles as closely similar as those produced under different grinding conditions. Also comparisons would probably have to be made in terms of cross-correlation, which presented problems of interpretation and classification similar to those of autocorrelation.

Cross-spectral density was also rejected as a means of comparing surface profiles because it is expressed in the form of complex numbers. This additional obstacle was avoidable by comparison of power spectra in terms of transfer functions; for which some precedent existed (21), Cross-coherency was also neglected mainly by reason of lack of information as to its potential.

Fig 9.4 represents the spectral density curve obtained from the profile of a finely dressed grinding wheel subjected to minimal wear (30 seconds grinding). More than half the area beneath the curve lies between infinity and 1 mm on the wavelength scale but a further well-defined peak occurs at about 0.4 mm.

Sharply defined peaks in a power spectrum represent narrow-band random noise and broader peaks represent a wide-band random signal. The profile of Fig 9.4 may therefore be said to represent a random signal in three bands of medium width, one being associated with very low frequencies.

Figs 9.5 and 9.6 are both representative of the surface of a grinding wheel subjected to five minutes wear. The ordinates from which Fig 9.5 was computed were taken from a profilogram produced at a magnification normal to the surface of the grinding wheel of 1000 while the corresponding magnification for the profilogram relating to Fig 9.6 was 2000. The most conspicuous difference is that Fig 9.6 is representative of narrow-band random noise while Fig 9.5 suggests wide-band random noise. Both curves differ greatly from Fig 9.4 in that the highest points are at a wavelength around 1 mm and the ordinates near infinity wavelength are relatively small.

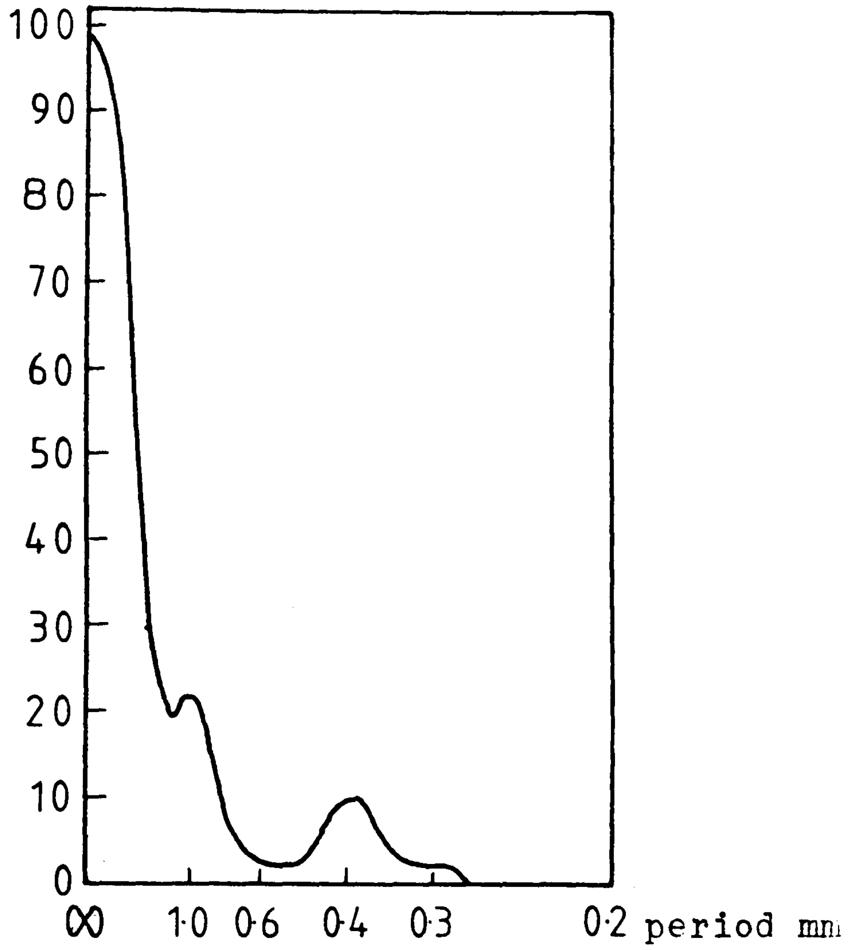

Fig. 9.4 Sample Power Spectral Density Function for an 80 grit grinding wheel after 30 seconds wear.

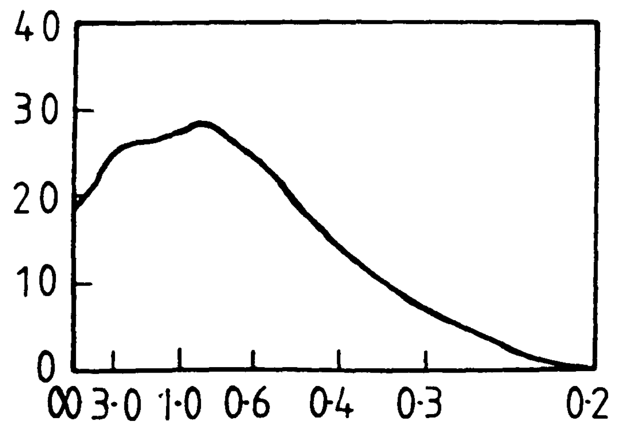

Fig. 9.5 Sample Power Spectral Density Function for an 80 grit grinding wheel after 5 minutes wear.

Fig 9.7 represents the surface of a grinding wheel after 10 minutes wear, the normal magnification of the profilogram from which the spectrum is computed being the same as for Figs 9.4 and 9.5, from both of which the spectrum differs considerably, the peak representing narrow-band random noise having its highest point at about 2 mm wavelength.

Fig 9.8 also represents the surface of a grinding wheel after 10 minutes wear and relates to Fig 9.7 in the same way that Fig 9.6 relates to Fig 9.5, that is, the spectrum is based upon a profilogram produced at a higher normal magnification (2000 as compared with 1000). Again the differences are considerable.

Figs 9.9, 9.10, and 9.11 represent ground surfaces corresponding to grinding wheel wear of 30 seconds, 5 minutes, and 30 seconds respectively and all were produced at a normal magnification of ×20000.

The profilogram relating to Fig 9.11 was produced using a curved datum element set to match the slight transverse curvature of the plunge ground track on the workpiece. This was not done in the case of the profilogram relating to Fig 9.9 and the absence of compensation for curvature may account for the occurrence of the peak at 10 mm wavelength.

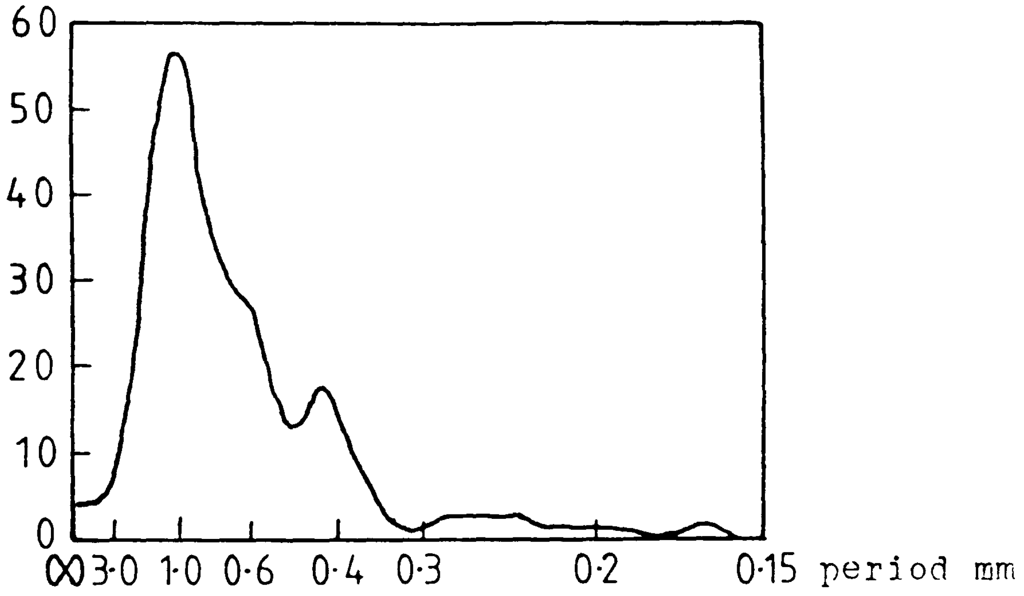

Fig. 9.6 Sample Power Spectral Density Function for an 80 grit grinding wheel after 5 minutes wear.

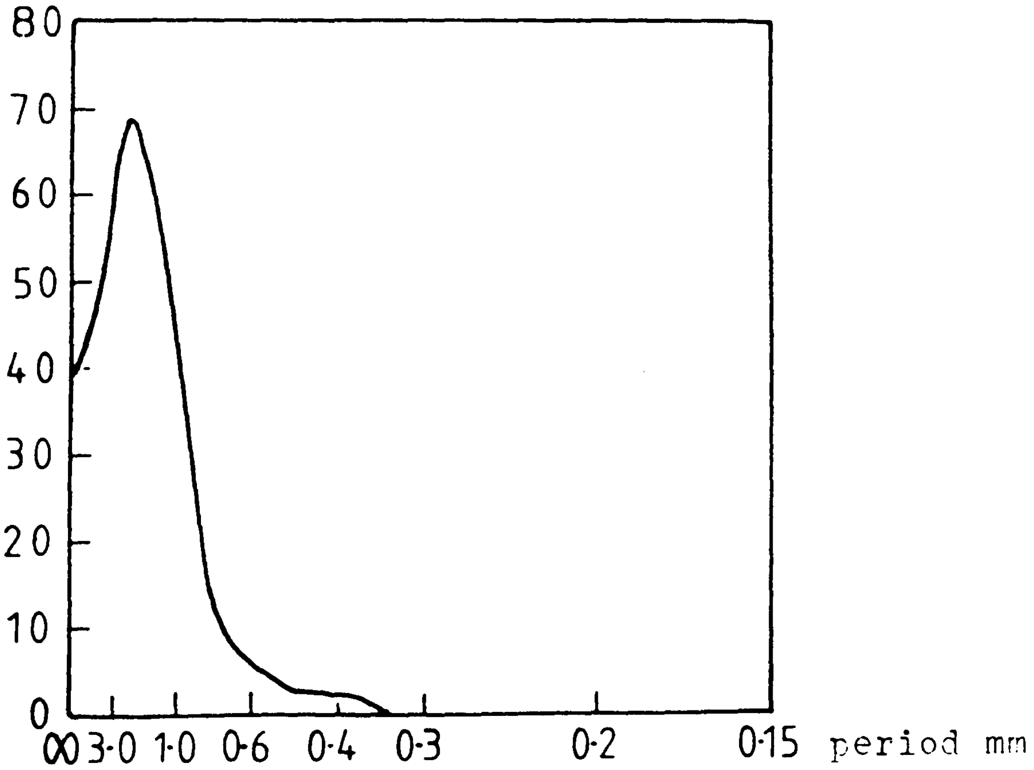

Fig. 9.7 Sample Power Spectral Density Function for an 80 grit grinding wheel after 10 minutes wear.

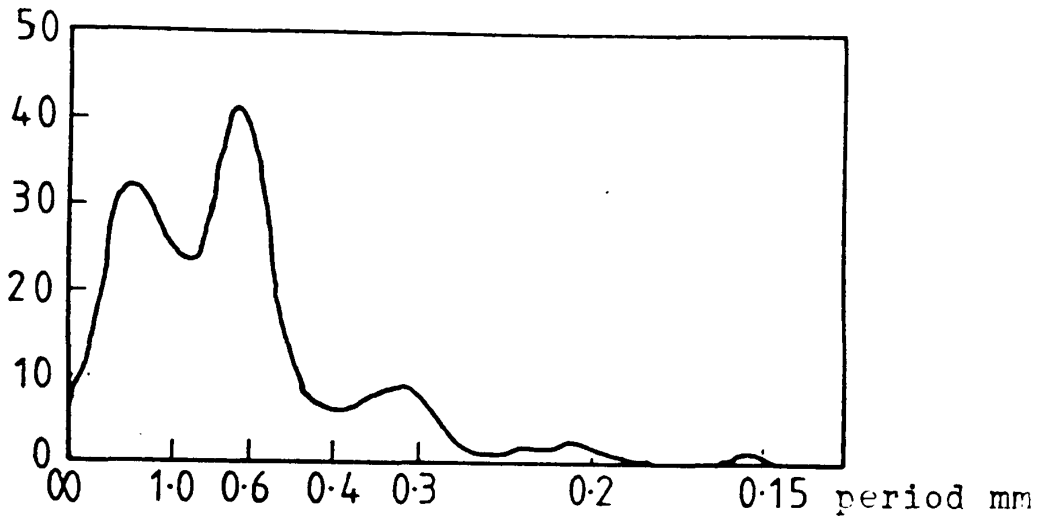

Fig. 9.8 Sample Power Spectral Density Function for an 80 grit grinding wheel after 10 minutes wear.

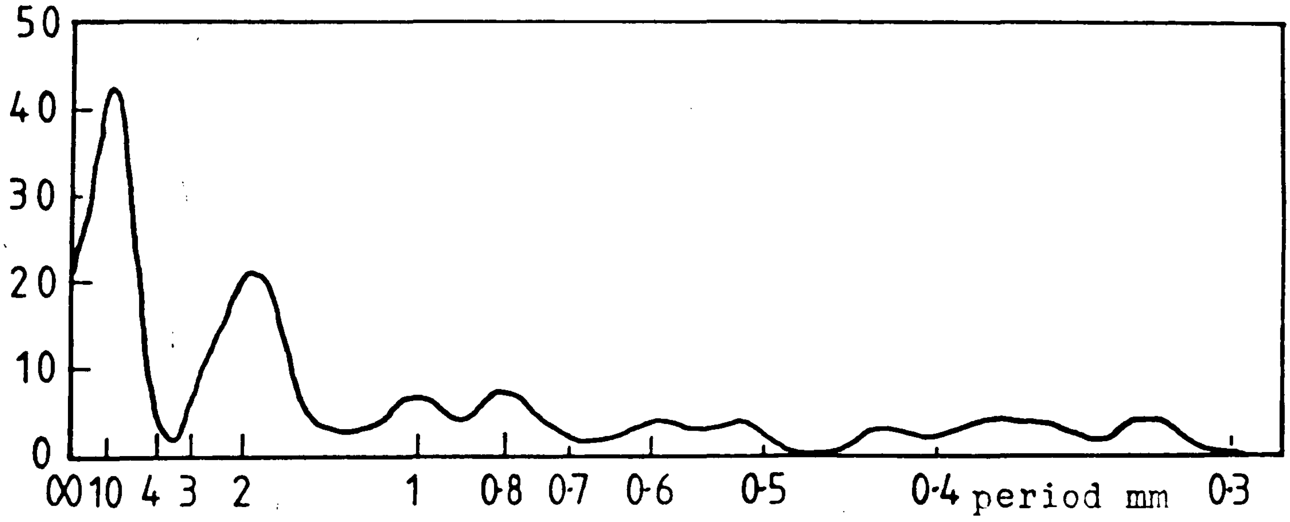

Fig. 9.9 Sample Power Spectral Density Function for a surface ground by an 80 grit grinding wheel for 30s.

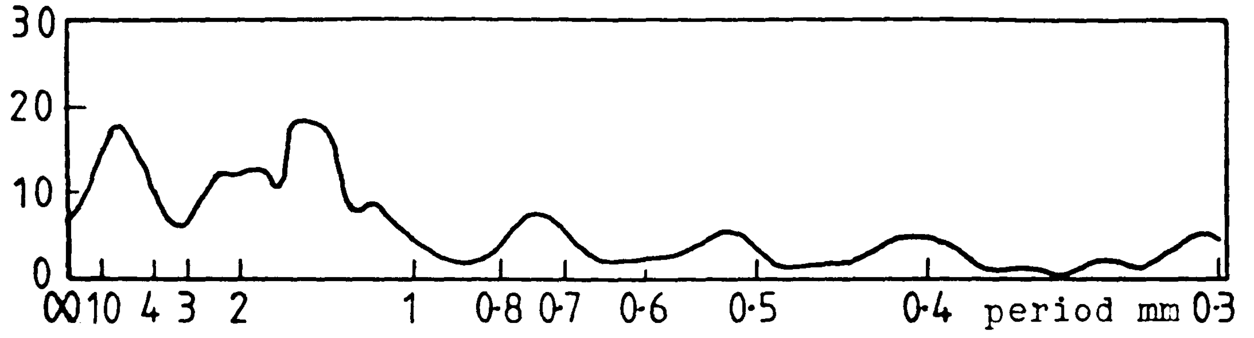

Fig. 9.10 Sample Power Spectral Density Function for a surface ground by an 80 grit grinding wheel for 5 min.

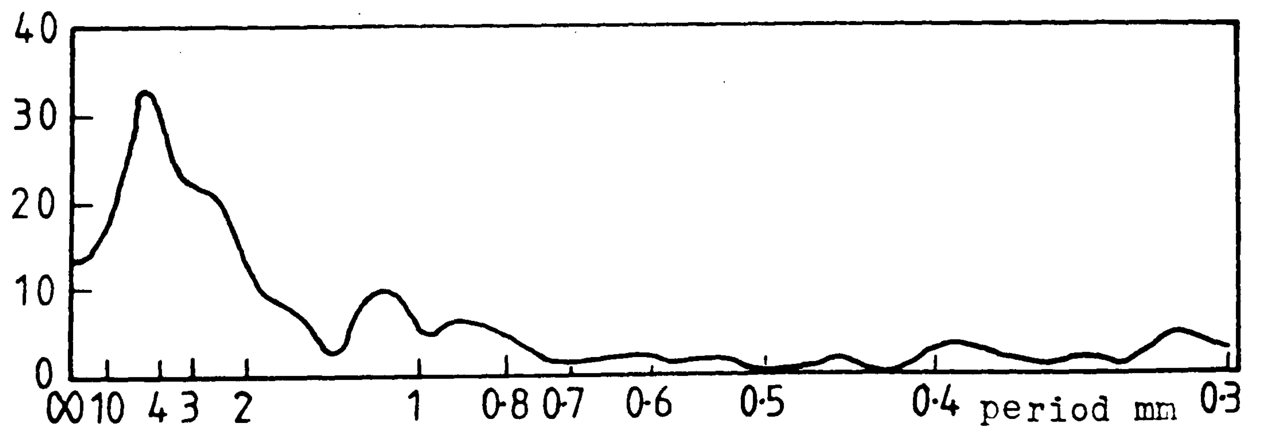

Fig. 9.11 Sample Power Spectral Density Function for a surface ground by an 80 grit grinding wheel for 30s.

The eight spectral density curves represented by Figs 9.4 to 9.11 were selected from a total of over fifty spectra produced using the same techniques with some minor variation of computer operational instructions and sampling methods in an effort to secure optimum results.

Some attempt has been made to use these curves to explain the interpretation of power spectra but this does not imply confidence in them as experimental results. At an early stage it was realised that the complexity and variability of these curves was such as to cast doubt on their validity for surface character--ization. In their complexity they differ from results for machined and abrasive surfaces published elsewhere. Secondly, when two or more spectra representing the same surface profile were compared, the differences between them were seen to be considerable even for virtually identical conditions of sampling and computation. These impressions were confirmed on the basis of a large number of comparisons not by any means confined to the eight spectra illustrated which were selected as typical examples.

Detailed examination of the spectral curves and data from which they were computed led to attention being focussed on inadequate sample size as being a probable key factor in the apparent unreliability of these results. For example, the data associated with Fig 9.32 Appendix 9, and Fig 9.5 contain a group of only eight numerical values representing ordinates defining points on the profile of abrasive grits, the remaining 92 ordinates in the sample being zero, corresponding with voids between grits in the wheel surface.

A relatively large proportion of zero levels is obviously to be expected in a profilogram representing the surface of a grinding wheel but in the case of the example quoted the sample appears so unbalanced and lacking in information relating to grit surfaces as to undermine any confidence in the corresponding power spectrum.

If meaningful power spectra were to be obtained the inference was obvious. In order to obtain enough information relating to grit surfaces for a grinding wheel such as that of Fig 9.32 it would be necessary to take a sample representing a much greater length of surface profile.

From time to time the validity of including in the computation voids represented by zero values in the data had been considered and at this stage it was clear that voids could feature extensively in the profilogram of a grinding wheel surface.

In discussion objection had been raised to the inclusion of zero values in computation for the following reasons. Autocorrelation represented a stage in the computation of power spectral density and where zero coincided with zero there would be complete correlation represented by unity. This correlation of zeros would lead to the voids they represent influencing the shape of the spectral density curve.

One possibility was to include in the computer program instructions which would lead to the zero values being ignored. This was said to overcome the objection outlined above, which has been stated elsewhere in terms to the effect that a discontinuous profile represents non-stationary, and therefore unsuitable, data.

To ignore the existence of spaces between grits in the grinding wheel surface is unrealistic. These represent features of the wheel surface structure which must play a part in production of the ground surface. If meaningful representation and comparison of grinding wheel and ground surface was to be achieved these voids must be considered.

For practical purposes the voids were of virtually infinite depth. Taking the lowest level recorded on the profilogram as zero, ordinates coinciding with a void could be recorded as such or alternatively by some relatively large and arbitrary negative value. In either case the effects on the autocorrelogram and power spectrum would be comparable.

These considerations led to a decision to continue with the investigation of grinding wheel surfaces and ground surfaces by means of power spectra computed from larger samples of the profile. With regard to grinding wheel surfaces, gaps in the record representing voids would be taken as zero for the purpose of computation.

The samples of 100 profile ordinates so far used in computation were obtained by visual inspection and measurement of profilograms with manual transfer of these data to punched paper tape. The need for larger and possibly very much larger samples was now apparent and these laborious methods should be replaced by some form of automatic data collection and storage.

CHAPTER 10. SEMI-AUTOMATIC PROFILE DATA PROCESSING AND ANALYSIS

Planning for partially automatic collection and processing of data derived from surface profiles was commenced during the later stages of the work discussed in Chapter 9. These preparations included identifying suitable items of equipment and investigating the problems of linking these into a set of apparatus capable of performing as many of the required functions as possible.

The overall requirements were to digitize the analogue signal from the profilometer and to record this information on punched paper tape, preferably in a format such that the data could be input directly to the computer with a minimum of keyboard operation. Profile data were to be stored on punched tape because equipment for collecting, digitizing and recording data was located at Brunel University while the programs it was proposed to use were written for and stored in the memory of the Prime 300 Computer at Willesden College of Technology.

The apparatus selected and used for collection of data from ground surfaces are listed below, the order being that in which they appear from left to right in Fig 10.1

Rectilinear Recorder for use with Talysurf 4
Talysurf 4 fitted with Curved Datum Element
Talysurf 4 Average Meter and Control Unit
Coordinate Plotter
Transient Recorder DATALAB DL 901 (A/D Converter)
Cathod Ray Oscilloscope TELEQUIPMENT Type D 43 R
High Speed Tape Punch

For the purpose of recording information from grinding wheel surfaces, the device for controlled rotation described in Chapter 9 was set up on the worktable of Talysurf 4 using the standard pick-up with its skid resting on the wheel surface as shown in Fig 10.2.

Specific information was supplied by Messrs Rank Taylor Hobson regarding the procedure to be followed in connecting the profile signal of the Talysurf 4 to the digitizer (Transient Recorder). This advice included methods of connection and test and also the maximum permissible external load. The signal voltage was stated to be one volt per inch of recorder

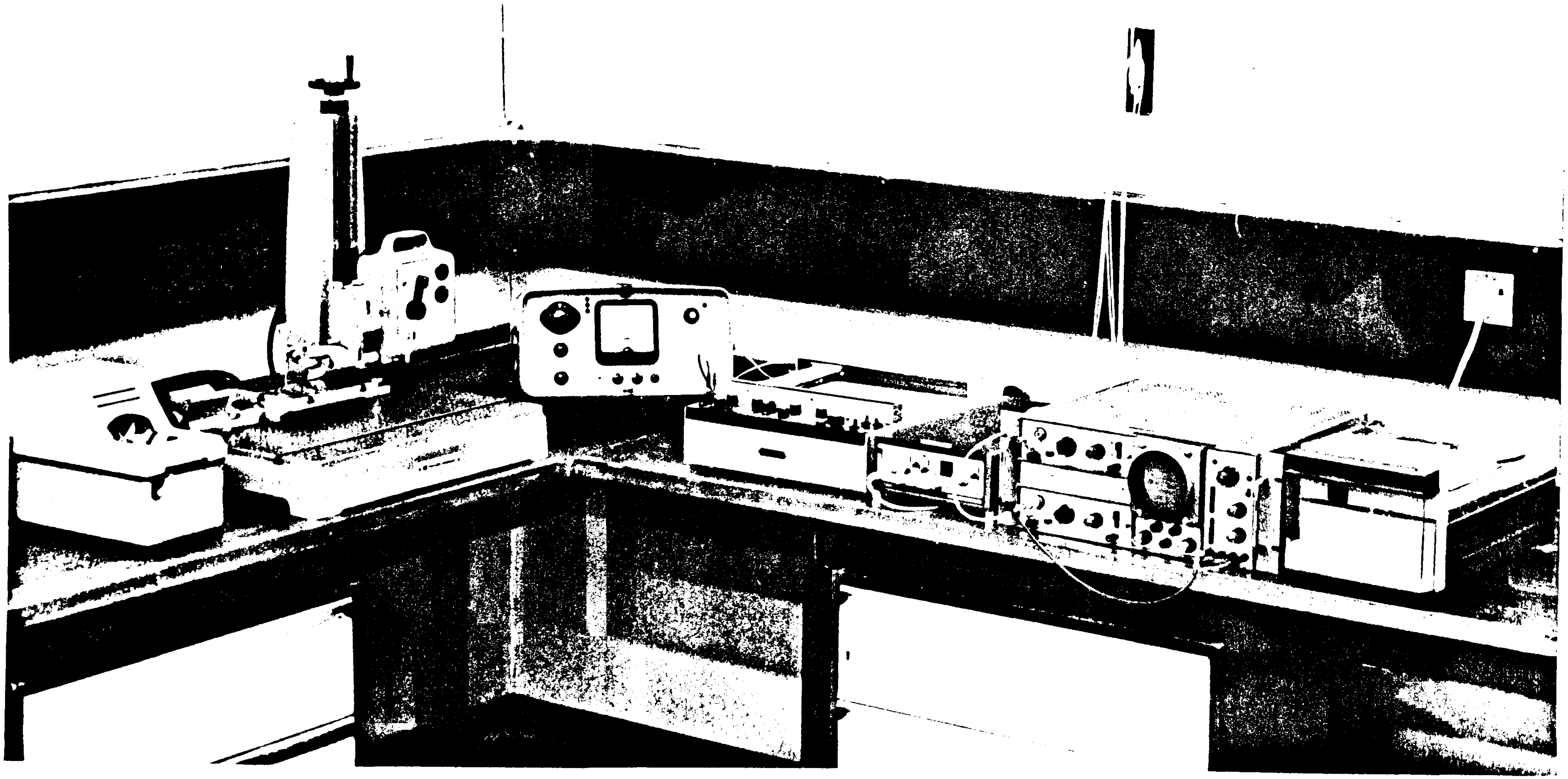

Fig 10.1 Left to right. Talysurf 4 graph recorder, Talysurf 4 with curved datum elements, Talysurf 4 average meter, coordinate plotter, transient recorder (A/D converter), cathode ray oscilloscope, rapid tape punch

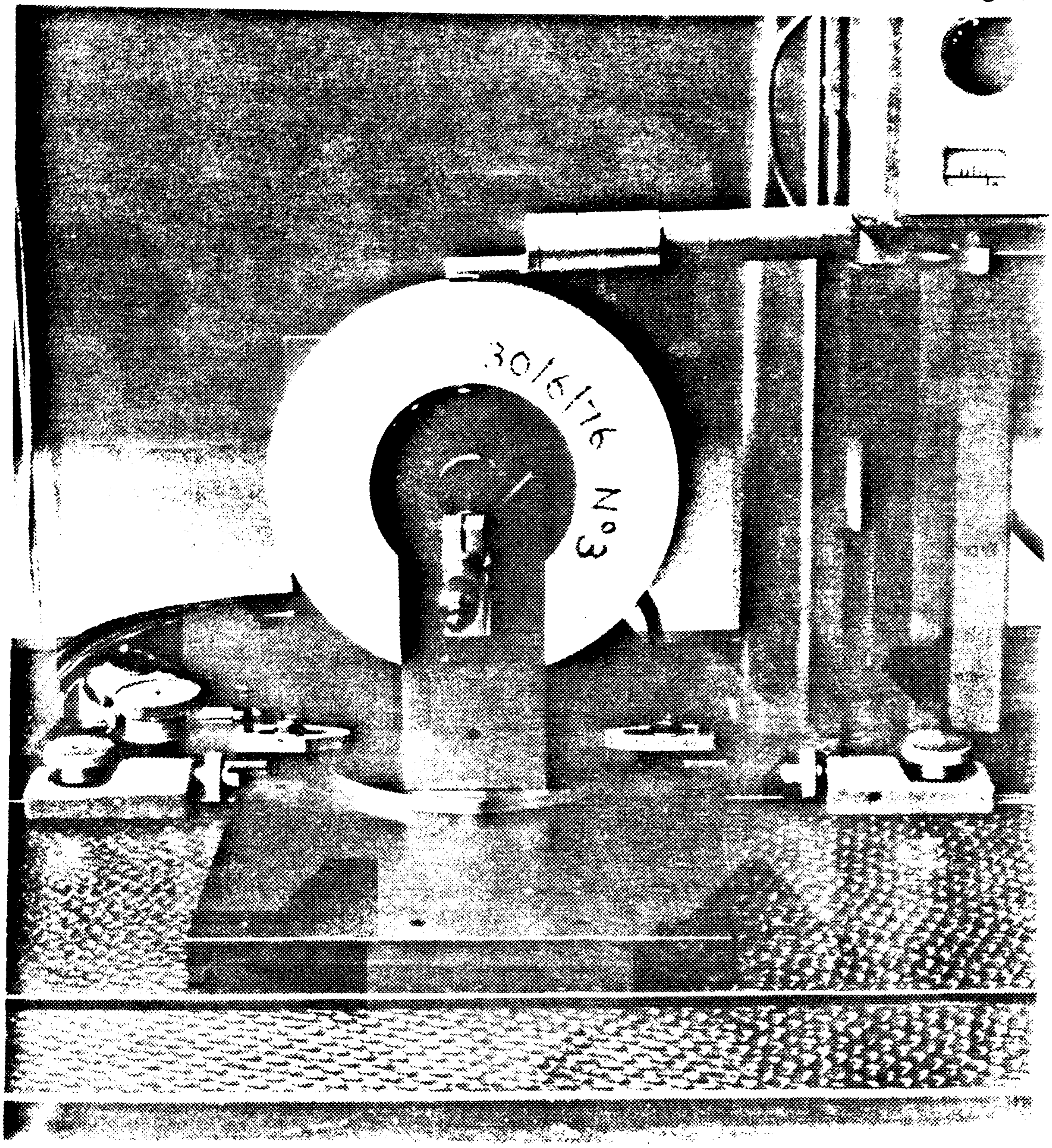

Fig 10.2 Method of obtaining a profilogram from the surface of a grinding wheel usimg Talysurf 4 in conjunction with a device providing slow controlled rotation of the grinding wheel

deflection and using the recommended arrangement the recorder would continue to operate. The wiring diagram supplied was unsuitable for reproduction.

The coordinate plotter and cathode ray oscilloscope were introduced in order to provide means of displaying and testing the digitized data for possible distortion and attenuation of the analogue signal generated by Talysurf 4. Testing was effected by examining the known profile of a machined surface having well-defined periodic features and comparing the profilogram obtained from the rectilinear recorder with the profile drawn by the coordinate plotter from the digitized signal. The profile corresponding with the latter was also displayed by the CRO.

Profilograms obtained from the rectilinear recorder and from the coordinate plotter were compared by measurement and found to be closely similar. Fig 10.3 shows the CRO in use for test purposes and Fig 10.4 surface profiles from the rectilinear recorder and coordinate plotter at (a) and (b) respectively.

The DATALAB Transient Recorder was designed to store a total of 1024 (2^{10}) digitized values during selected

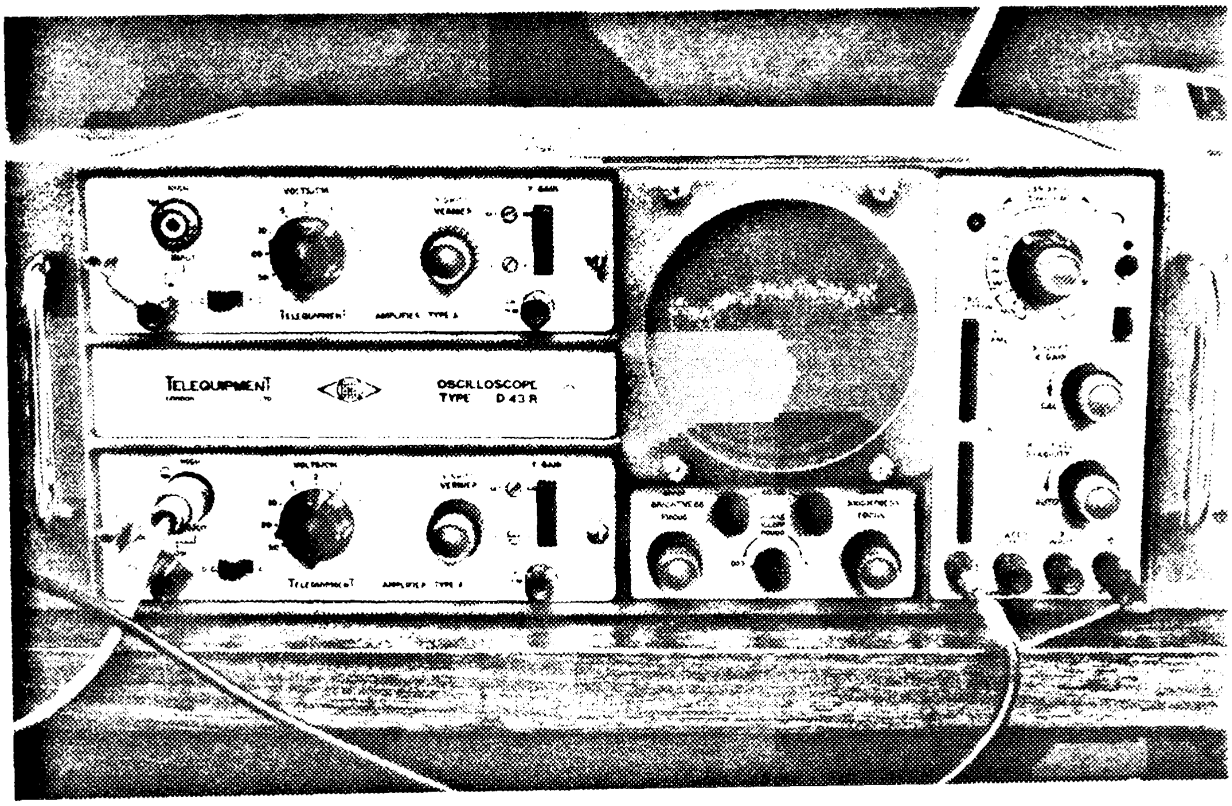

Fig 10.3 Oscilloscope displaying the profile of a surface derived from Talysurf signals

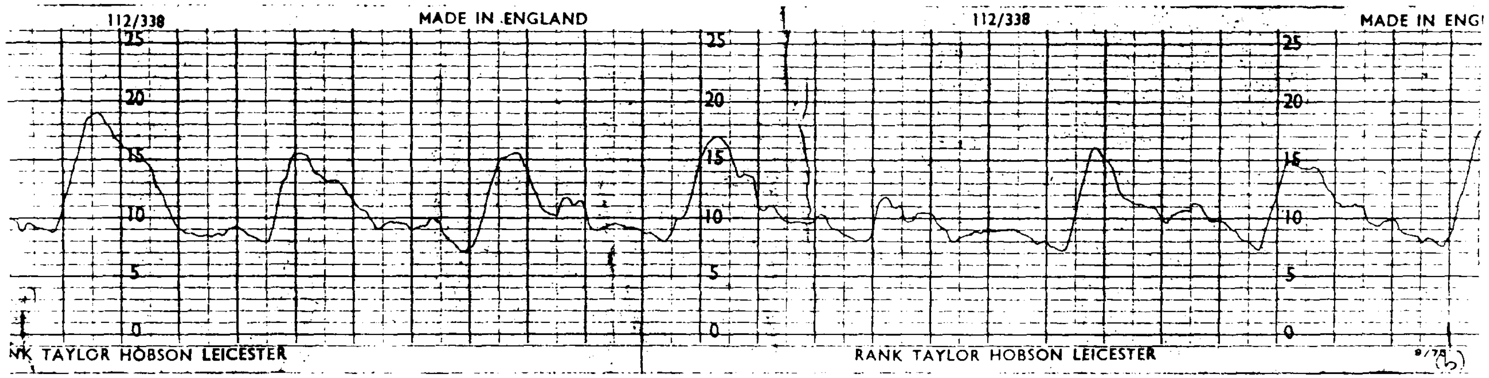

(a) Graph produced by Rectilinear Recorder

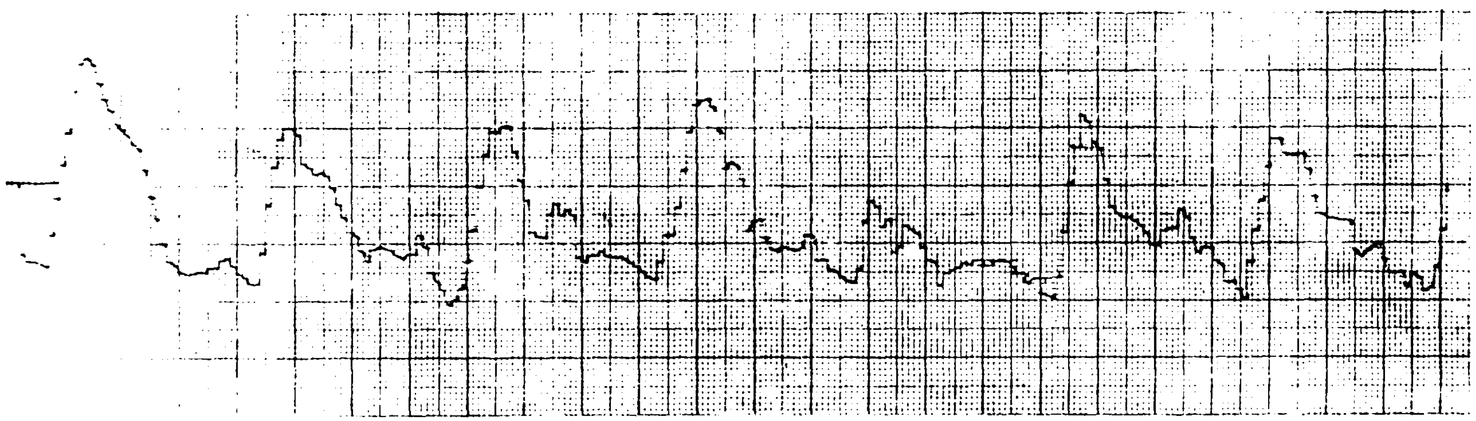

(b) Graph produced by Coordinate Plotter

Fig. 10.4 Profile of a machined surface

time intervals ranging from 5 milliseconds to 200 seconds. The Talysurf Rectilinear Recorder graph paper speed of 12 inches per minute corresponds with 40 inches of profilogram per 200 seconds. If 1024 ordinates are recorded during this interval their linear spacing on the profilogram will be 40/1024 = 0.3906 in. Corresponding intervals between ordinates on actual surfaces will be given by the latter value divided by the appropriate magnification. For example, at ×100 the interval will be approximately 0.00039 in (about 10 μm) or at ×20 approximately 0.002 in (50 μm).

It was decided that a sample of 1024 ordinates distributed over lengths from 0.4 to 2 inches (depending on the magnification used) should be adequately representative of any ground surface . Similar remarks apply to samples of the grinding wheel surface for which the corresponding magnification using the rotary device was intermediate between the two standard Talysurf magnifications.

All subsequent work using spectral density curves and transfer function relates to six surfaces which may be specified as follows.

Three 80 grit white aluminium oxide vitreous bonded grinding wheels of seven inches nominal diameter were used (Universal Abrasives Ltd designation WA80HV).

Each of the above wheels was mounted on its own separate arbor on which it remained throughout the balancing, dressing, grinding and profile measurement procedures.

Dressing and grinding were carried out on a Model 540 Surface Grinder manufactured by Jones & Shipman Ltd.

The wheel and arbor assemblies were balanced and the wheels roughly dressed with a single point diamond. Re-balancing was then carried out and the wheels dressed once again using the flat face of a pyramidal diamond dressing tool as follows: five passes with 0.0005 inches in feed, two passes with 0.0002 inches in feed and three passes with no further in feed. All dressing passes were made at very slow and uniform cross feed to minimize the possibility of grooving the wheel surfaces.

Each of the grinding wheels was numbered for identification and surface grinding operations were carried out as follows on carbon steel work--pieces.

Wheel No.	Duration of grinding	Depth of material removed	Conditions
1	30 seconds	0.0005 in	plunge
2	5 minutes	0.004 in	plunge
3	8 minutes		traverse
	2 minutes	0.0003 in	plunge

Profilograms produced at right angles to the lay at magnifications respectively perpendicular and parallel to the ground surface of ×20000 and ×100 are reproduced in Fig 10.5.

The combined apparatus that has been described and illustrated in Fig 10.1 was next used to produce a total of twelve punched paper tapes each containing 1024 ordinates obtained under various conditions from the six different surfaces. The object was to obtain a stock of information from which samples could be taken for subsequent computation of power spectra. The index compiled for identification of the surfaces with the conditions under which they were produced appears as Table 10.1 Appendix 10. Relevant entries in this table refer to six tapes representing grinding wheel surfaces and six representing the corresponding ground surfaces.

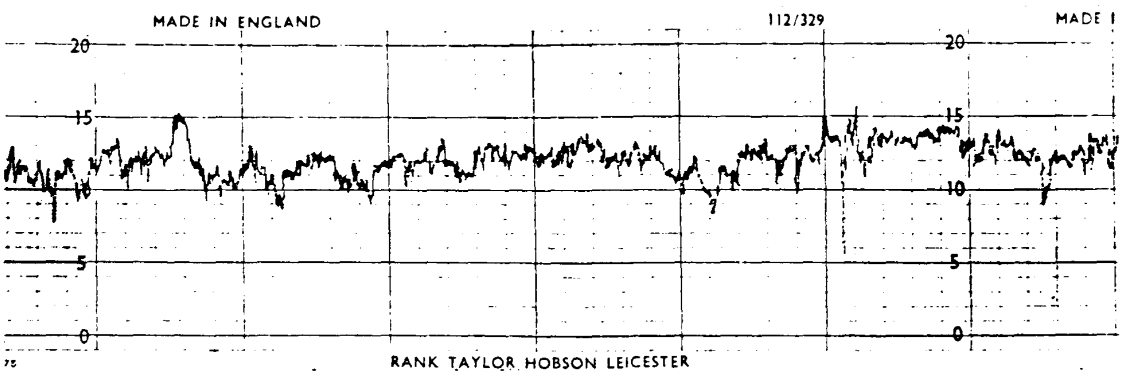

(i) 30 seconds

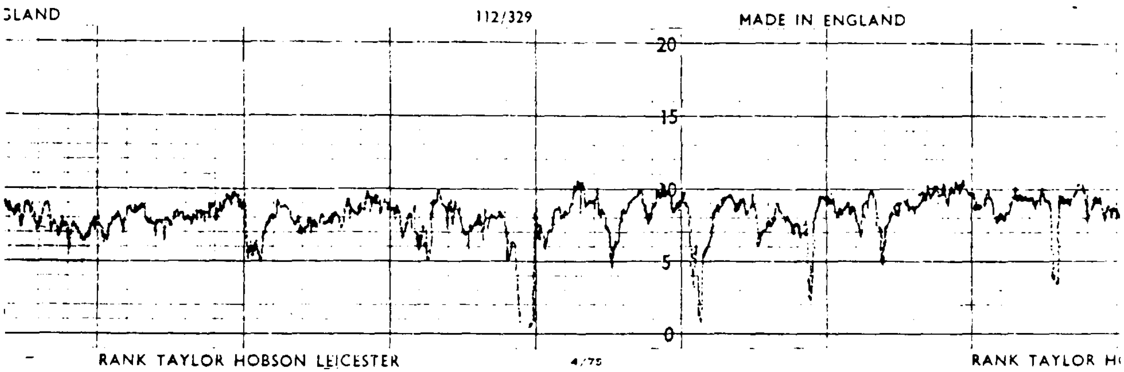

(ii) 5 minutes

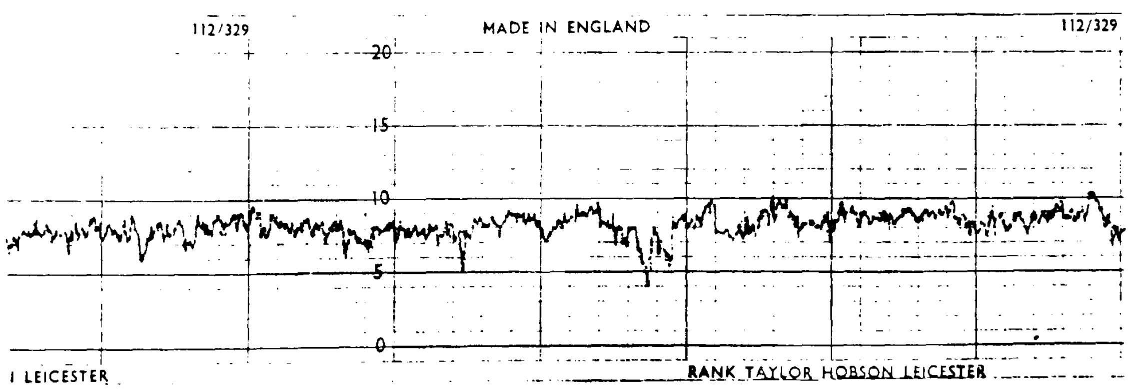

(iii) 10 minutes

Fig 10.5 Profilograms representing ground surfaces produced by grinding wheels subjected to wear for the duration indicated. Vertical magnification × 20 000, horizontal magnification × 100

Information on these tapes was not in a form immediately suitable for power spectral computation. Reasons for this were as follows.

1. Ordinates were recorded on these tapes as coded numerical values not arranged in the tabular format required by the available statistical programs.

2. 1024 ordinates were recorded on each tape and it was desired to take samples from these representing selected groups of ordinates.

To overcome these problems a program was written the purpose of which was to process information recorded on the existing tapes and to output new punched tapes representing profile ordinate samples in the required format. This program designated GJEDIT (see Appendix 10) was to be run on the MINIC Computer (Microcomputers Ltd, Woking, Surrey) at Brunel University and was written in machine code with provision for instructions to be given regarding the number of ordinates in the samples, their spacing and location within the sequence of 1024 ordinates on the input tape.

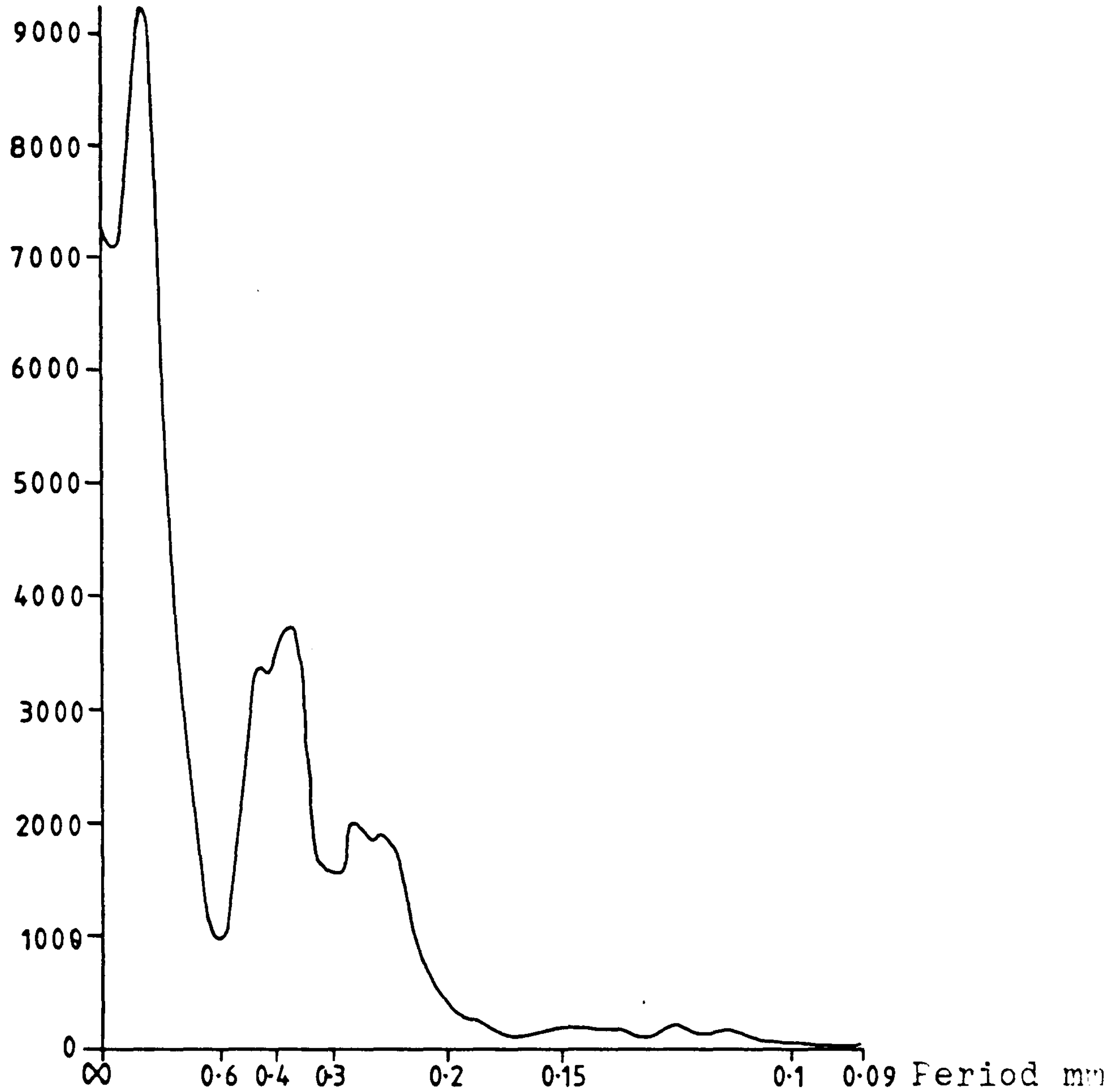

Fig 10.6 Spectrum representing the surface of an 80 grit grinding wheel after 5 minutes grinding computed from a sample of 300 ordinates. Voids between grits included in the computation.

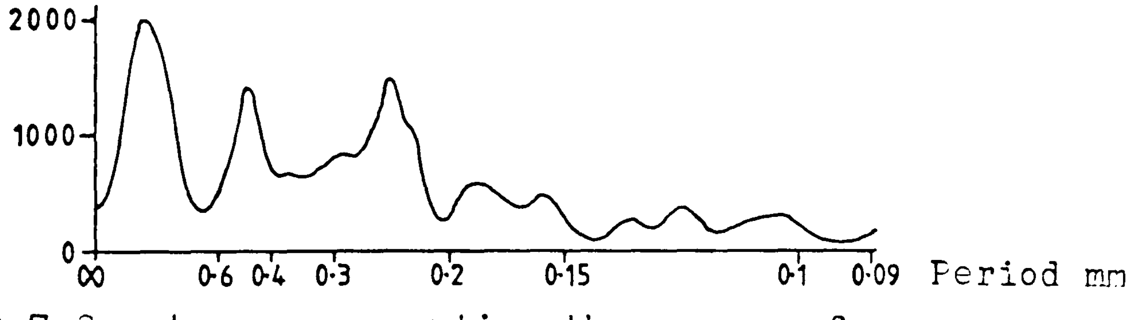

Fig 10.7 Spectrum representing the same surface as in Fig 10.6 The effect of voids between grits eliminated from the computation but sample and operating conditions otherwise identical

A total of 61 tapes representing samples of 300, 500 and 1000 ordinates were produced by means of this program and identified as MJ1IA to MJ61IA in Table 10.2 Appendix 10.

As a first step in computing power spectra from profile samples containing more than 100 ordinates it was decided to make further comparisons between the results obtainable from grinding wheel surfaces (i) when voids are included in the computation (Program MACJ04) and (ii) when the effects of voids are eliminated (Program MCJ04H).

Typical results are illustrated by Figs 10.6 and 10.7 respectively which, in terms of smoothness, represent an improvement over spectra previously computed from samples of 100 ordinates. Between wavelengths of 0.3 mm and 0.09 mm the two curves are fairly closely similar. These results were typical of comparisons between spectra produced by the two programs from samples of the same grinding wheel surface.

The conclusion drawn from such comparisons was that the main effect of eliminating the influence of grinding wheel voids from the computation was to produce a spectrum with much less emphasis on the longer wavelengths. The value of such a spectrum was not discounted but the view taken at this stage was that a spectrum neglecting voids was incomplete and possibly misleading. The resulting decision was to use programs including the effects of voids for all subsequent work involving spectral density applied to both grinding wheel and workpiece surfaces.

Sample size having been increased with some apparent measure of improvement it was decided to attempt computation of power spectra based upon still larger samples. Necessary small amendments having been made to the relevant programs, the number of ordinates sampled was increased to 500 and subsequently to 1000 with progressively encouraging results.

The time required to input the data had been increased by nearly a factor of ten but editing and computing times were not greatly increased. Overall it was found possible to produce a power spectrum in tabular form from a sample of 1000 ordinates in about forty minutes or less depending upon current computer loading.

Some experience of power spectral computation having been gained together with a considerable accumulation of recorded data representing a limited number of related surfaces, re-appraisal of this line of investigation appeared to be timely.

Once again discussion took place regarding power spectra during which it was emphasised that spectral density curves computed from finite samples represent estimates of true power spectra for infinitely large samples. Also the inclusion in a computation of too large a number of lag intervals in relation to sample size was said to increase sampling errors.

In the earlier computations as many as 67 lag intervals had been included when using samples of 100 ordinates. Given the possibility of samples of 1000 profile ordinates it was now suggested that computation for as few as 34 lag intervals might be appropriate.

A program for computing spectral density includes what is known as a smoothing window which influences the extent to which areas of apparent high power associated with particular frequency bands are attributable to contamination by neighbouring frequencies.

The smoothing window so far used in the spectral density programs MACJO4 and MCJO4H is represented by the following expression and the operation as Hanning after its originator.

$$\omega_\tau = \frac{1}{2}\left(1 + \cos\frac{\pi\tau}{M}\right)$$

An alternative called Hamming[1] may give more smoothing and the corresponding expression is as follows.

$$\omega_\tau = \left(0{\cdot}54 + 0{\cdot}46\cos\frac{\pi\tau}{M}\right)$$

In both expressions ω_τ is the angular frequency, τ is the lag and M the number of lags computed.

While there appeared no reason to doubt that power spectra could be used to meaningfully describe surface profiles it was also evident that spectral density was influenced by several factors related to the methods of computation. Given suitable conditions the spectrum would apparently provide a good estimate of some ideal model of surface profile.

1. Hamming was tried but no improvement was detected and the Hanning window was retained in the programs.

While accurate characterization of the surfaces of grinding wheel and workpiece were obviously desirable, perhaps even more important was the possibility of establishing some relationship between the grinding wheel surface and that of the corresponding ground surface. Provided that power spectra were produced under satisfactory standardized conditions there might be a prospect of throwing light on such a relationship even though the spectra fell short of the optimum for individual surface characterization.

One measure of the success of investigation into surface relationships would be the ability to differentiate between and effectively compare closely similar surfaces. Data obtained from such surfaces were available and it was decided to concentrate upon these at the expense of broadening the investigation to include a greater diversity of surfaces. This decision was take in the anticipation that more exhaustive examination was most likely to result in significant progress in the application of both spectral density curves and transfer functions to these problems.

Results from Samples containing 1000 Profile Ordinates

Nine tapes each representing a sample of 1000 ordinates were selected for further processing. Tables 10.4, 10.5, 10.6, 10.7, 10.8, 10.9, 10.10, 10.11, and 10.12 Appendix 10 each contain one such set of data in the prescribed format and these are indexed in Table 10.13.

Power spectra were computed from these data and the plotted graphs together with tables containing the 67 ordinates defining each spectrum appear in Appendix 10 as Figs 10.8, 10.9, 10.10, 10.11, 10.12, 10.13, 10.14, 10.15, 10.16, 10.17, 10.18, and 10.19.

Power spectra produced from these much larger samples were smoother and appeared more consistent when preliminary comparisons were made between these and spectra representing similar profiles computed from smaller samples. The extent to which they were capable of characterizing and distinguishing between surface profiles was not immediately evident from visual inspection for the following reasons.

Spectral density ordinates having the largest values were in all cases located near the low frequency end of the spectrum. With increasing frequency, power

Table 10.13. Index of Tables 10.4 to 10.12 each representing data in the form of 1000 ordinates defining a profilogram

Grinding Wheels Table	Ground Surfaces Table	Duration of Grinding
10.4	10.5	30 seconds
	10.6	30 seconds
10.7	10.9	5 minutes
10.8		5 minutes
10.10	10.12	10 minutes
10.11		10 minutes

spectral density fell steeply in all cases to a very low value relative to the maximum ordinate and then continued indefinitely at a low level with a small downward trend.

When two such spectra representing the surfaces of grinding wheel and workpiece are superimposed for comparison the curves are usually well separated at the lowest frequencies but appear to merge at the higher frequencies (Figs 10.20, 10.22 and 10.24).

Examination of the numerical values of the spectral density ordinates (Table 10.14) shows that the apparent merging of curves is misleading and results from the use of a common natural scale at which all ordinates within the spectrum can be plotted.

The ratios between ordinates representing a pair of corresponding profiles (treating the profile of the ground workpiece as output and that of the grinding wheel as input) have minimal values near the low end of the frequency scale increasing progressively with frequency. Such ratios are plotted to obtain the transfer functions represented by Figs 10.21, 10.23, and 10.25.

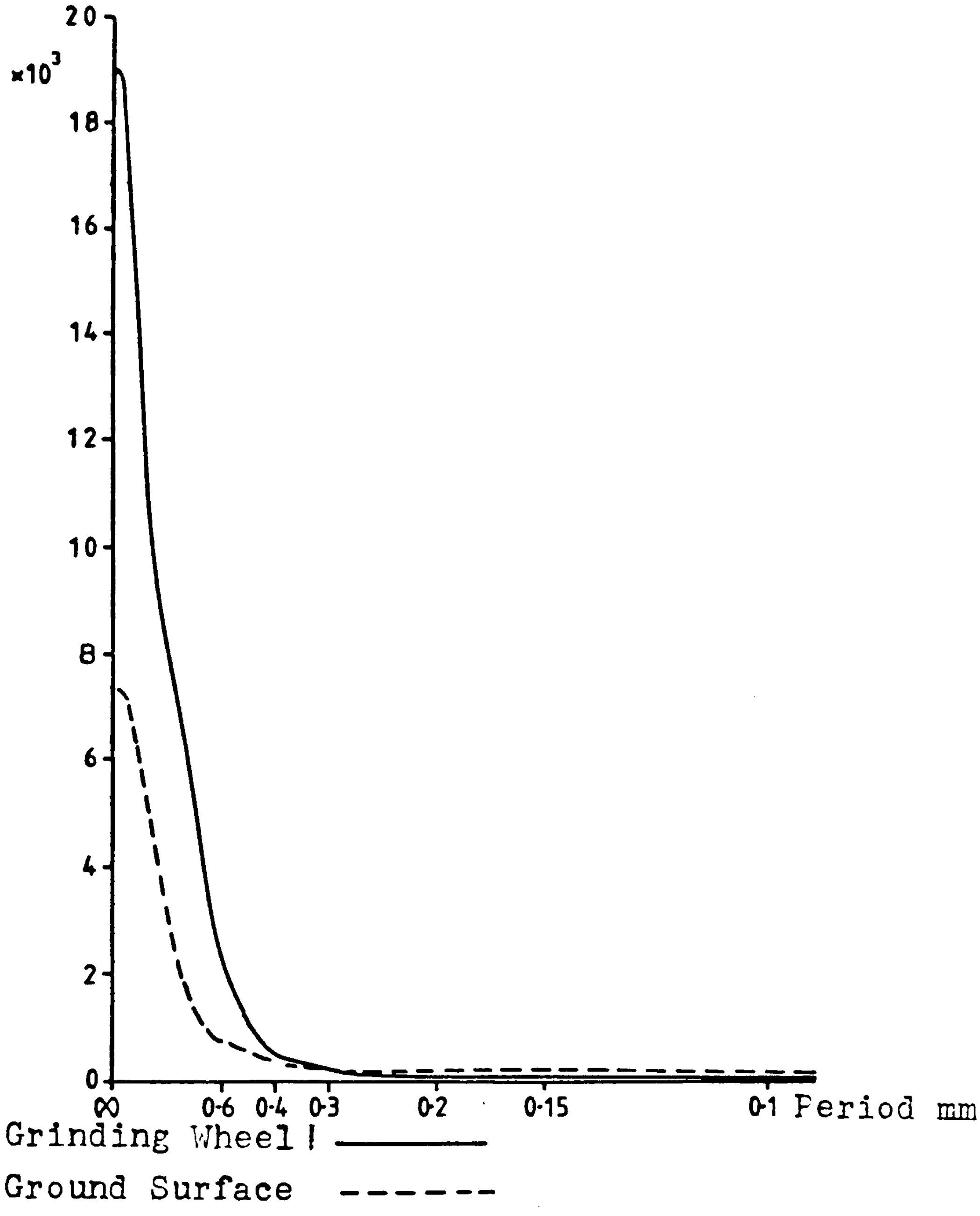

Fig 10.20 Power Spectral Density Curves

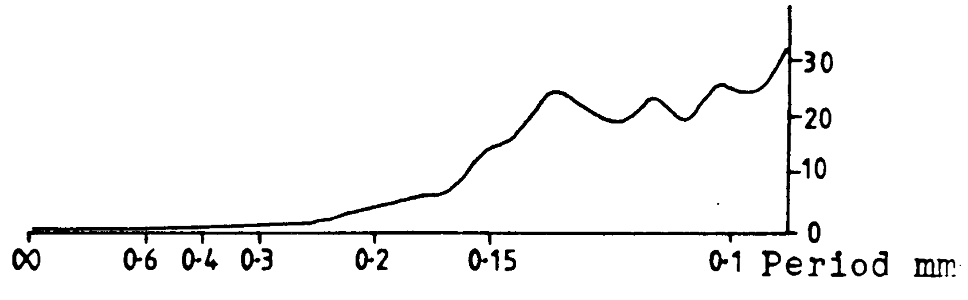

Fig 10.21 Transfer Function $\frac{\text{Ground Surface Spectrum}}{\text{Grinding Wheel Spectrum}}$

Surfaces of 80 Grit Grinding Wheel and corresponding Ground Surface after 30 seconds Grinding

Each of the spectra and transfer functions derived from them are defined by 23 ordinates. The explanation of this relates to the different magnifications at which profilograms were produced from the grinding wheel and workpiece. The tangential magnification used for grinding wheels approximates closely to one third of that used for the ground surface therefore in order to compare spectra in terms of transfer functions it was necessary to calculate the ratio between every third ordinate in the grinding wheel spectrum (i.e. 23 out of 68 ordinates) and the first 23 ordinates in the ground surface spectrum (Table 10.15).

Figs 10.20 and 10.21 on the one hand with Figs 10.22 and 10.23 on the other, represent the relationship between surfaces associated with 30 seconds grinding. In Fig 10.22 the surface profile of the ground track was partly corrected for transverse curvature. In Fig 10.20 this correction was omitted and the apparent result is an increase in ordinates defining the low frequency region of the relevant spectrum. The two sets of results are otherwise similar.

The characteristic waviness of the right hand part of the transfer function curves may be produced by

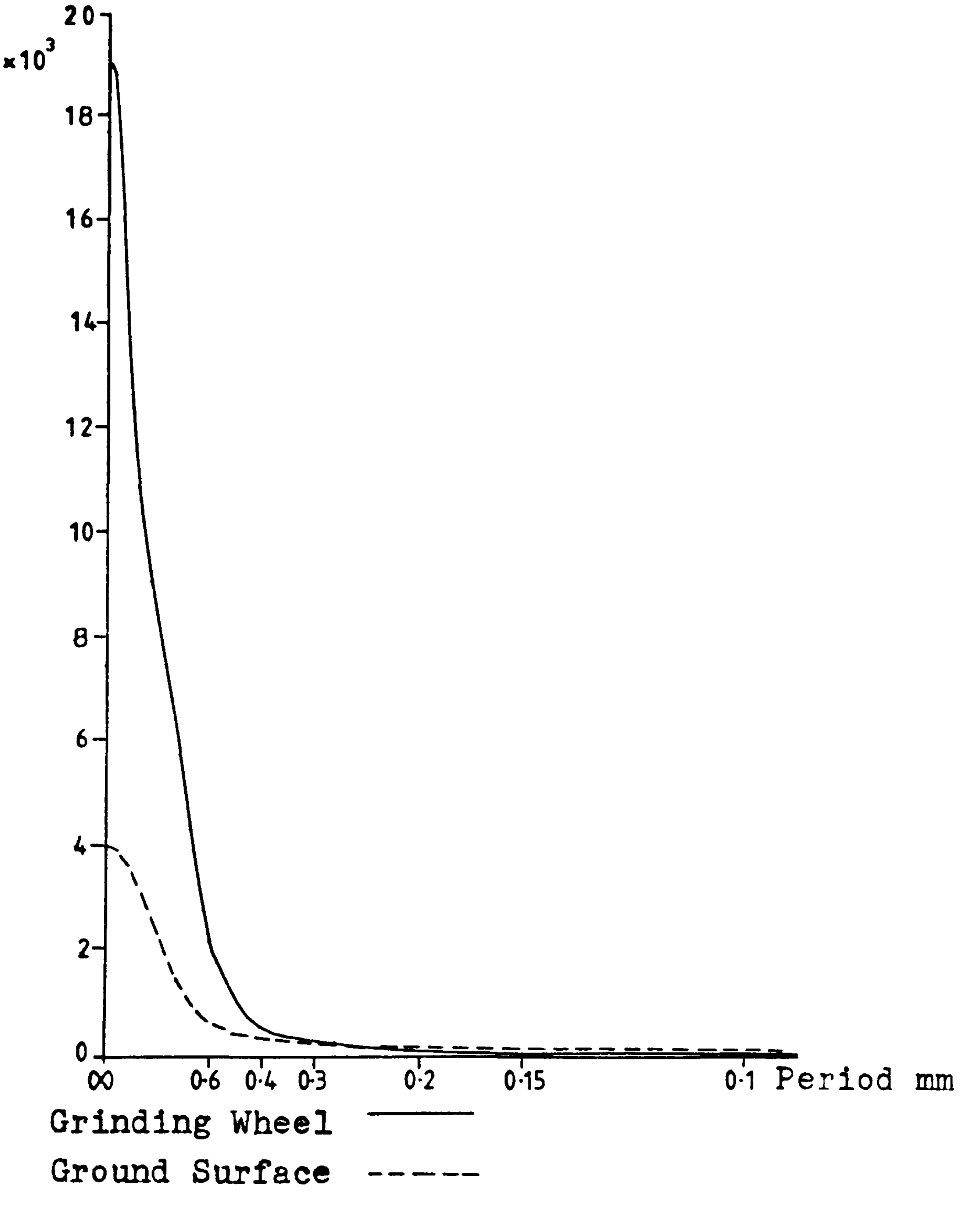

Fig 10.22 Power Spectral Density Curves

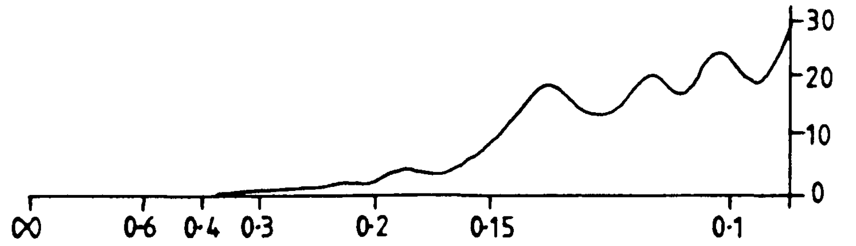

Fig 10.23 Transfer Function $\frac{\text{Ground Surface Spectrum}}{\text{Grinding Wheel Spectrum}}$

Surfaces of an 80 grit grinding wheel and corresponding workpiece after 30 seconds grinding deviations in terms of smoothness between the ideal theoretical spectrum and that which was computed. The extent of this waviness appeared to depend, in some measure, on the number of lags included in the computation, the optimum being considerably less than the number of spectral density ordinates. For these spectra 68 ordinates were computed and inclusion of 22 lags appeared to give the most satisfactory results of the alternatives tried. Smoothness of the spectral curve was found to deteriorate noticeably when this number approached the number of ordinates computed.

Figs 10.24 and 10.25 represent the relationship between the same type of grinding wheel and the corresponding ground surface after 10 minutes grinding. The two power spectral curves differ markedly from Figs 10.20 and 10.21 while the transfer function has lower values the the frequency band around 0.13 mm wavelength and larger values above 0.10 mm wavelength.

Figs 10.26 and 10.27 represent attempts to relate the development of a ground surface during 9½ minutes grinding with the corresponding change in the grinding wheel surface. Wear of the grinding wheel is represented by the transfer function in Fig 10.26 while the corresponding change in the ground surface is similarly shonw in Fig 10.27

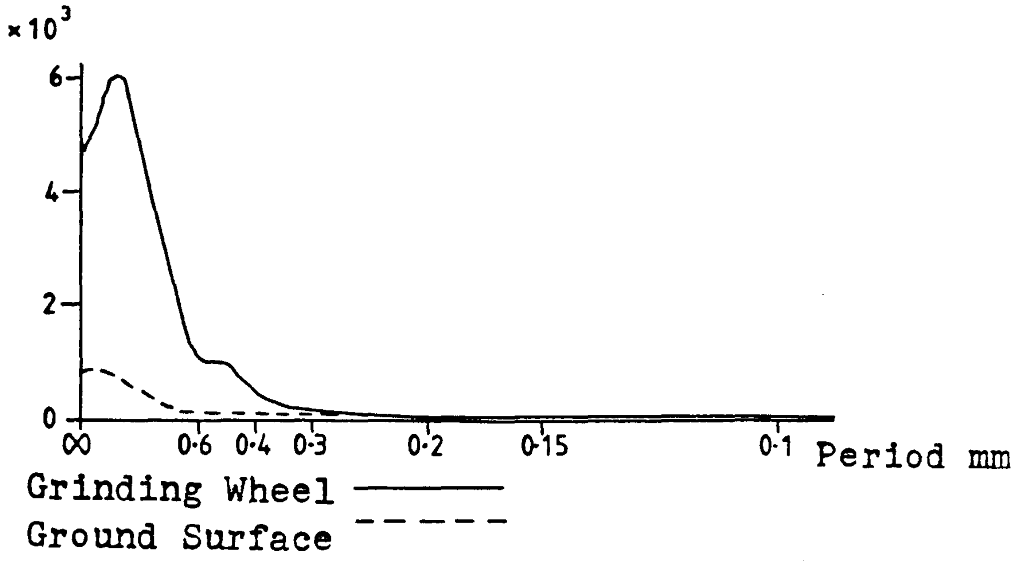

Fig 10.24 Power Spectral Density Curves

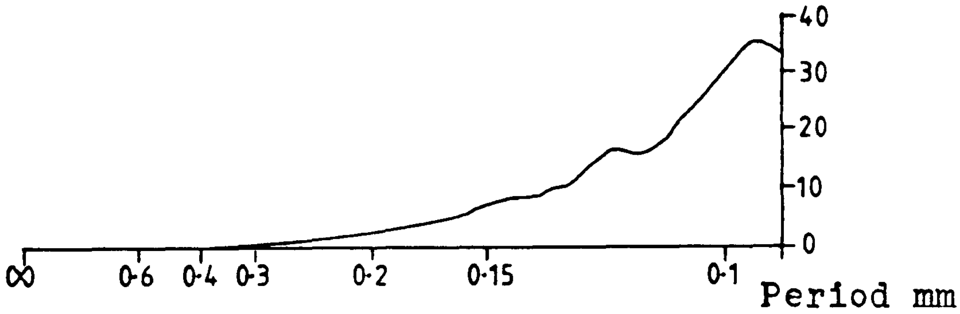

Fig 10.25 Transfer Function $\frac{\text{Ground Surface Spectrum}}{\text{Grinding Wheel Spectrum}}$

Surfaces of an 80 grit grinding wheel and corresponding workpiece after 10 minutes grinding

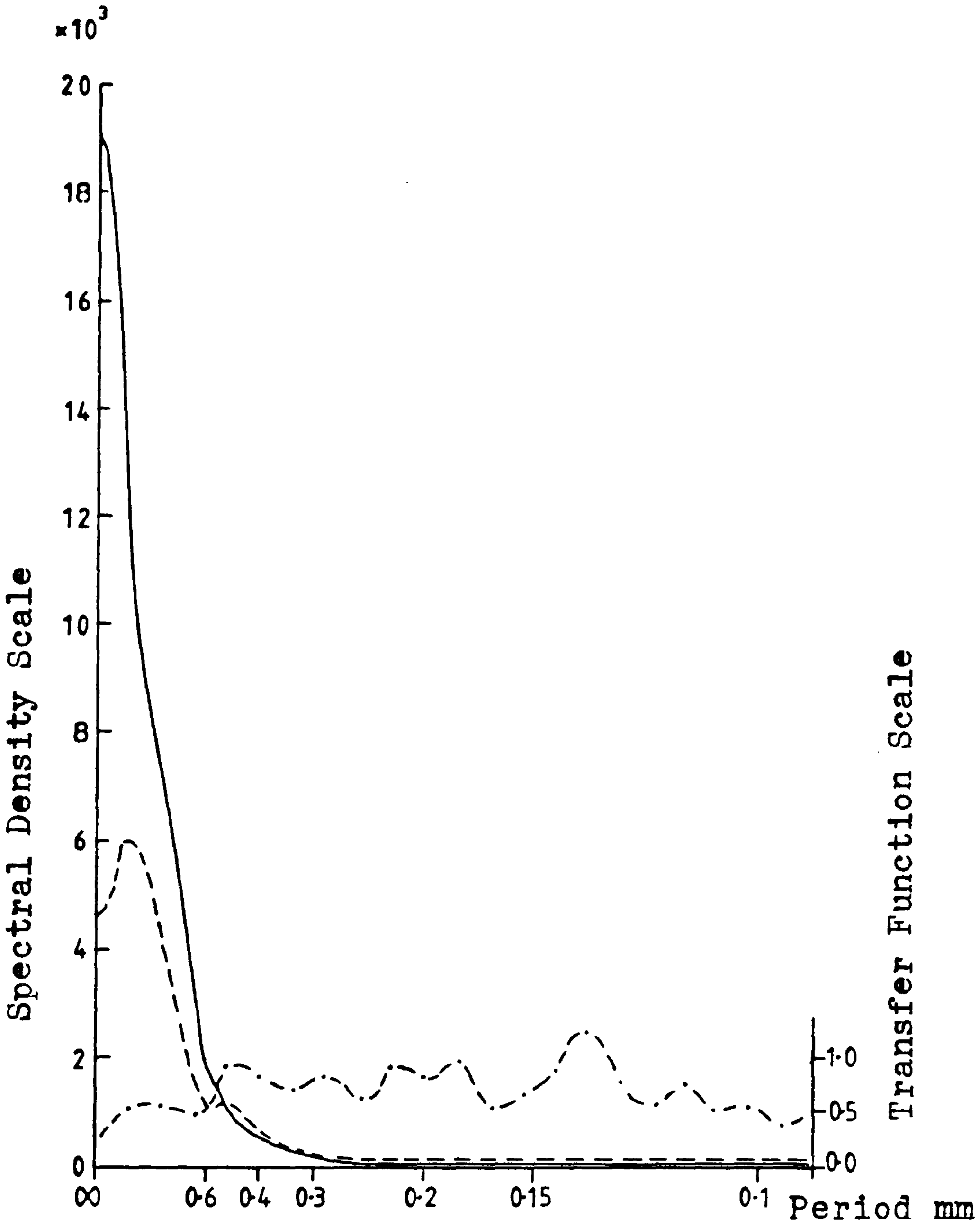

Grinding Wheel at 30 Seconds ————

Grinding Wheel at 10 Minutes - - - - -

Transfer Function _._._.

Fig 10.26 Wear of a grinding wheel during $9\frac{1}{2}$ minutes represented by spectral density curves and transfer function

$$\text{Transfer Function} = \frac{\text{Grinding Wheel Spectrum at 10 min}}{\text{Grinding Wheel Spectrum at 30 sec}}$$

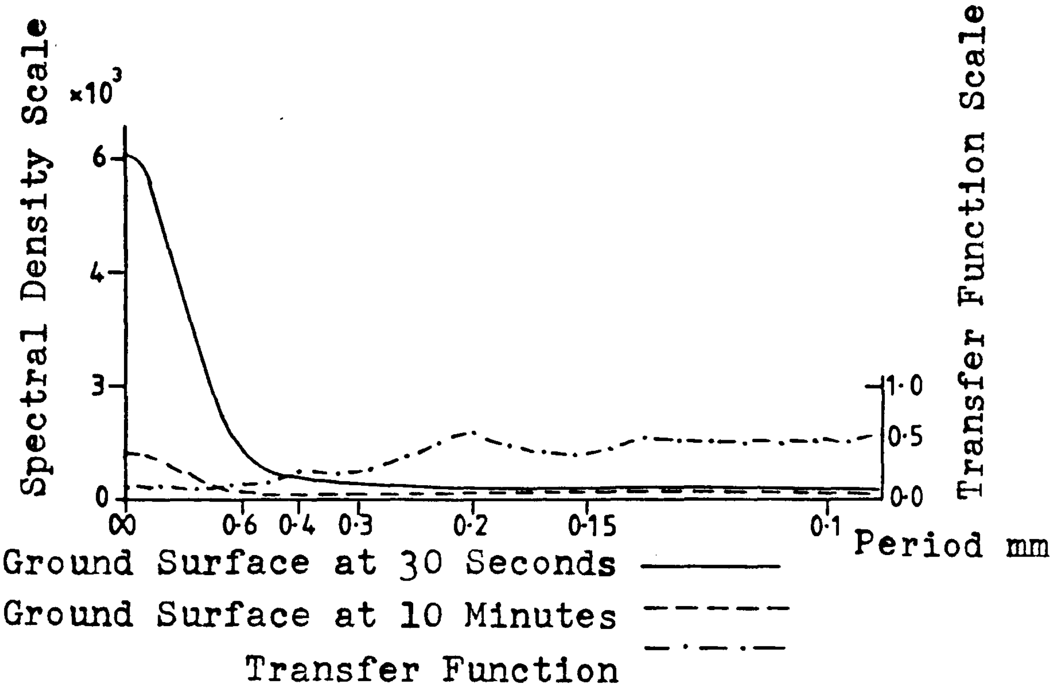

Fig 10.27 Development of a ground surface during $9\frac{1}{2}$ minutes grinding represented by spectral density curves and transfer function

$$\text{Transfer Function} = \frac{\text{10 Minutes Surface Spectrum}}{\text{30 Seconds Surface Spectrum}}$$

Some similarities between the two transfer functions are self evident but Fig 10.26 shows a lack of smoothness in the transfer function which appears to refelect somewhat adversely on the quality of the grinding wheel spectra compared with those derived from the ground surfaces.

In Figs 10.28 and 10.29 power spectral density and transfer coefficients are plotted on logarithmic scales against a natural frequency scale. Fig 10.28 corresponds with Figs 10.20 and 10.21 while Fig 10.29 corresponds with Figs 10.24 and 10.25. Some of the more obvious effects of plotting logarithms are as follows.

The general form of the two spectral density curves in each diagram is such that they are conveniently plotted on the same pair of axes while retaining separate identities. Also the point of intersection between spectra, at which the value of the transfer function is unity, is more clearly seen.

Some points of similarity are more clearly seen from Figs 10.28 and 10.29 than from their counterparts plotted on natural scales. For example the point of intersection between the two power spectra in both

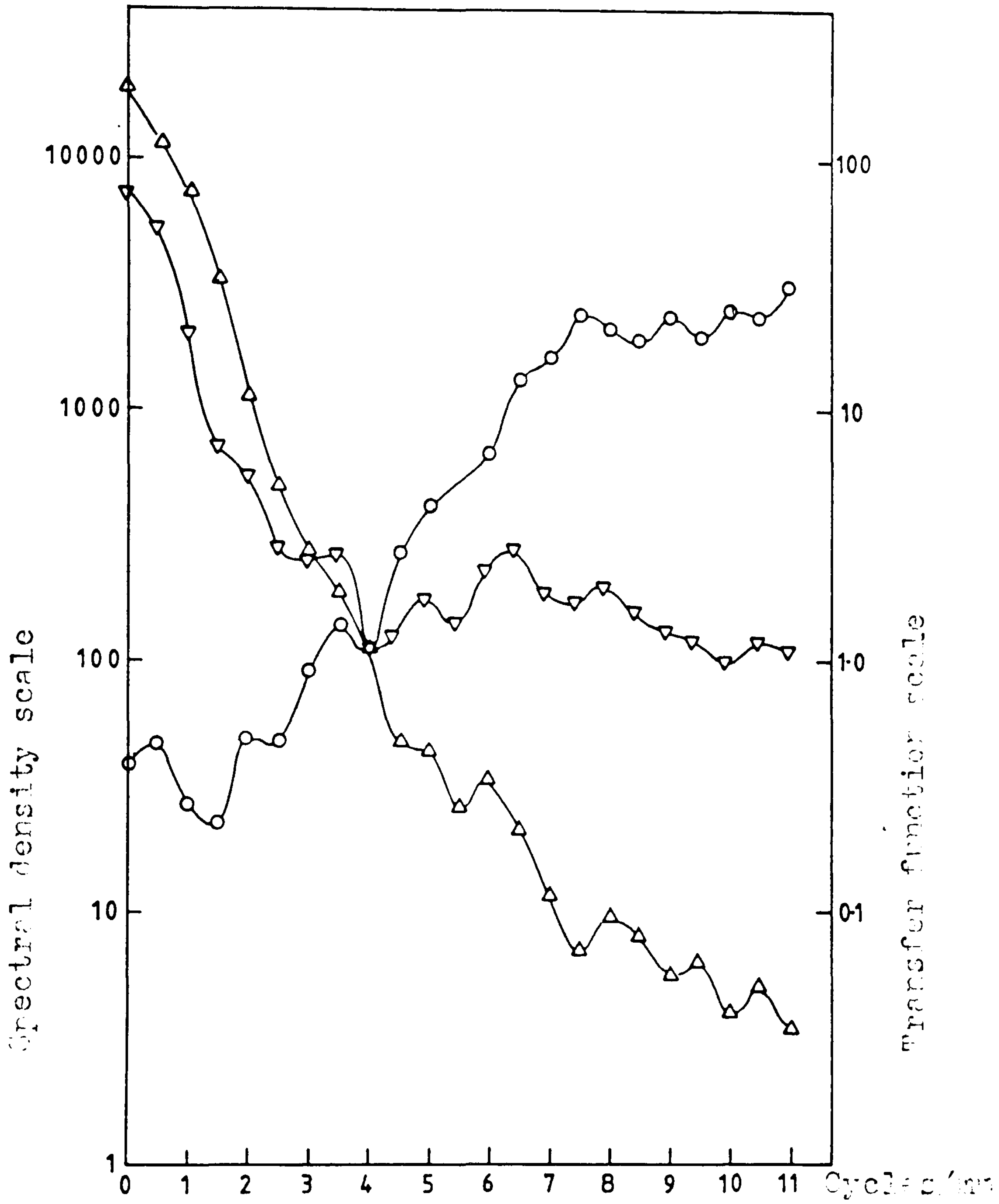

Fig 10.28 Comparison of surfaces representing 30 seconds grinding

Grinding wheel spectrum △

Ground surface spectrum ▽

Transfer function ○

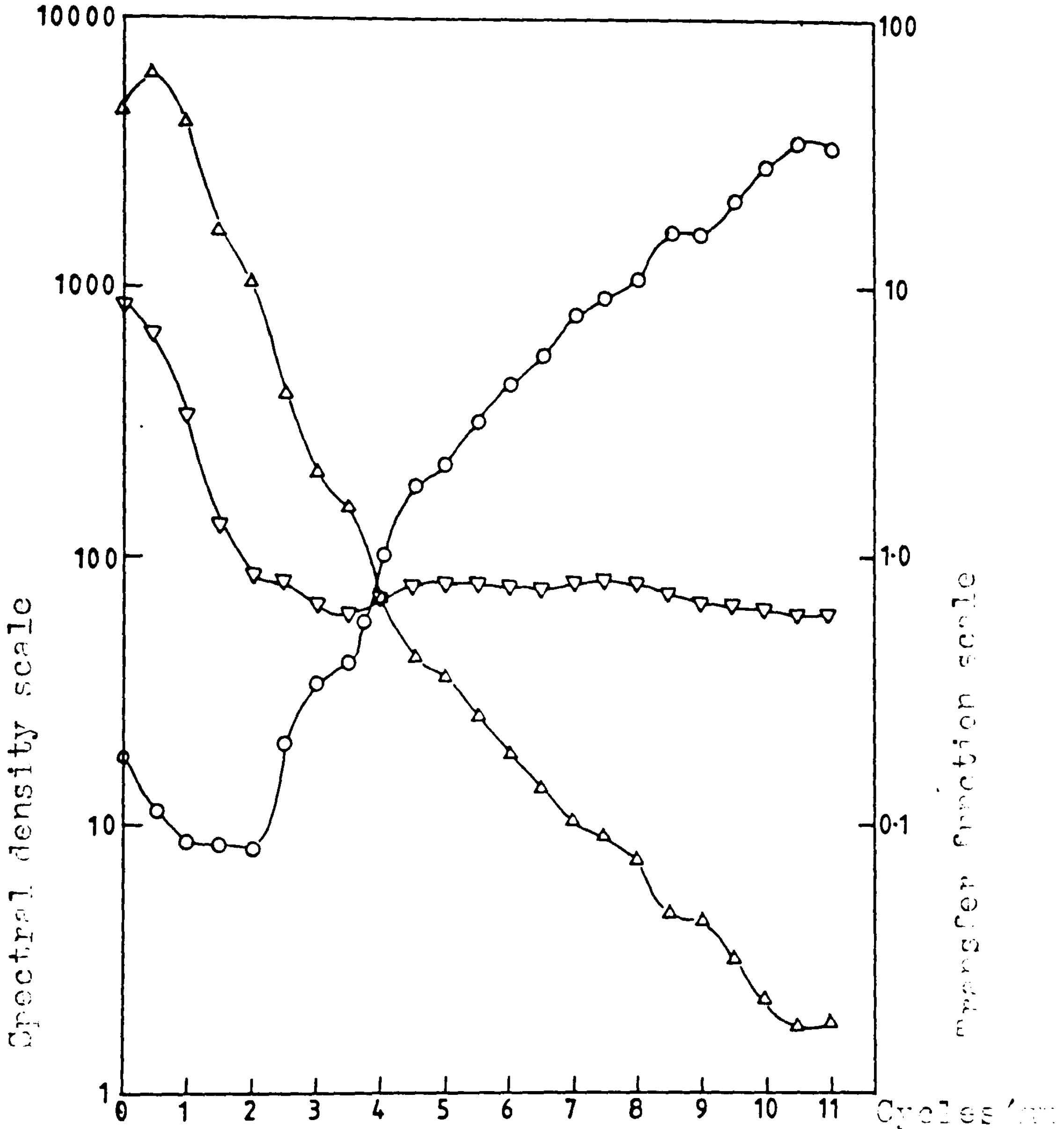

Fig 10.29 Comparison of surfaces representing 10 minutes grinding

Grinding wheel spectrum △

Ground surface spectrum ▽

Transfer function ○

Figs 10.28 and 10.29 approximates to the coordinates (4, 100) on the frequency and spectral density axes respectively.

On the assumption that the transfer function curves of Figs 10.28 and 10.29 might be represented by straight lines, linear regression was applied to the points defining the transfer function of Fig 10.28. The result obtained is shown in Fig 10.30 together with 95 per cent confidence limits.[1]

Graphs obtained by plotting log. spectral density served to distinguish much more clearly between power spectra throughout the frequency range considered. Also the corresponding transfer functions, of which Fig 10.30 is typical, were of fairly constant shape implying that a relationship might be established between such power spectra but did little to suggest the form this might take. Alternative methods of representing spectral density curves were therefore explored in the hope that some relationship might be apparent.

1. Strictly, these should called 2 standard deviation limits.

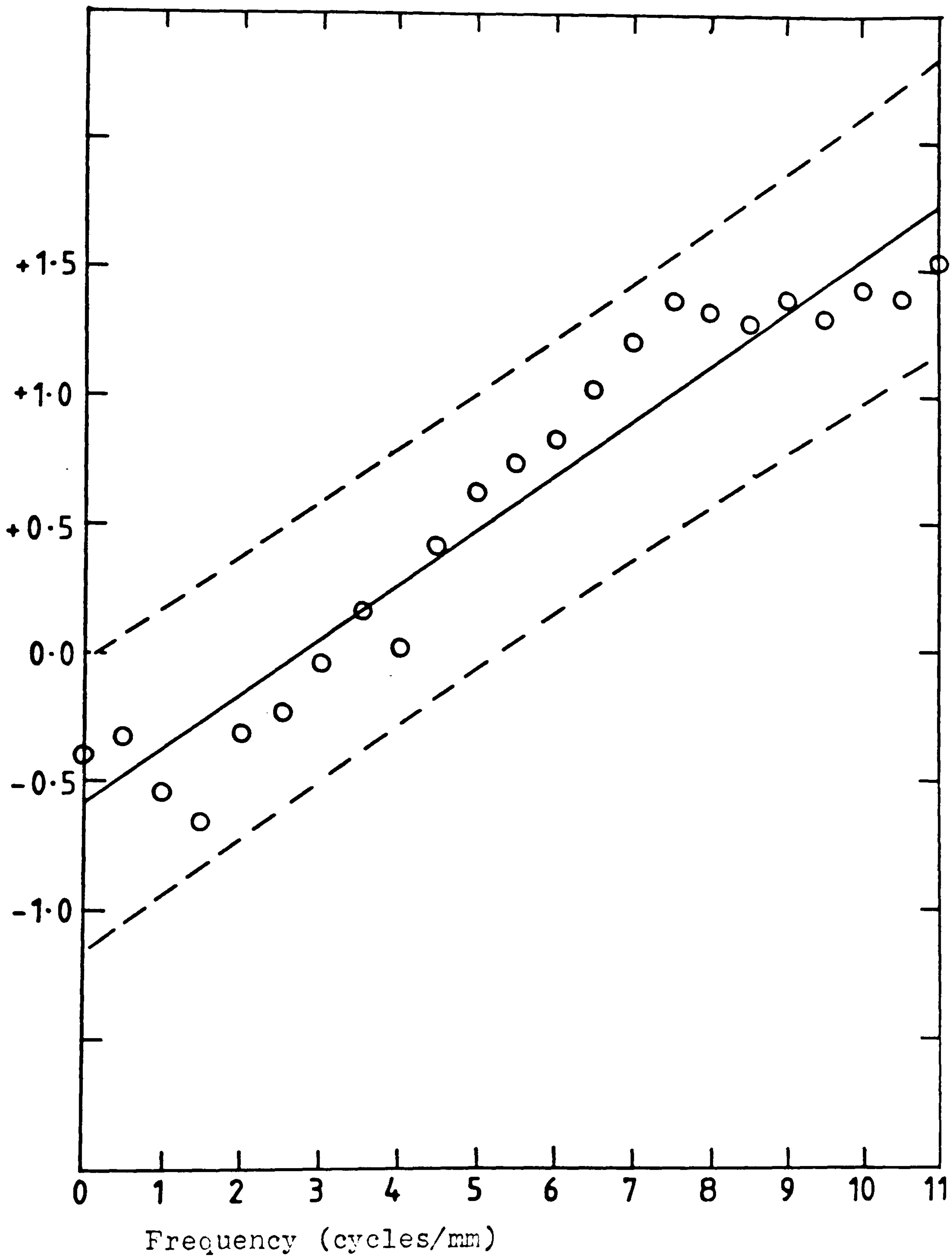

Fig 10.30 Comparison of surfaces representing 30 seconds grinding

Regression line representing transfer function ————

95 per cent confidence limits — — — — —

Table 10.14 Power Spectral Density

J	L	T	W
19023.5	6138.85	3969.08	7462.12
11501.0	5044.52	3207.71	5382.87
7300.77	2803.45	1703.62	2037.86
3324.84	1141.33	691.719	735.527
1131.02	528.826	395.8	554.212
490.33	388.636	317.415	278.863
275.474	300.975	208.436	251.2
188.214	235.488	135.815	269.899
111.81	193.032	115.411	113.102
47.0472	155.8	105.77	126.378
44.1186	147.053	107.572	180.351
26.0999	169.755	121.542	139.882
34.4567	194.066	131.861	225.074
21.0643	198.247	135.916	279.869
11.5396	181.279	138.319	184.516
7.21762	163.674	139.114	170.943
9.57556	162.376	135.723	198.91
8.12763	163.015	126.105	151.687
5.58208	149.738	113.978	130.508
6.2243	134.065	104.461	120.674
3.92929	126.652	97.6757	99.0421
5.03001	119.339	95.922	119.627
3.47297	108.005	102.126	111.913
(Figs 10.20 & 10.22)		(Fig 10.22)	(Fig 10.20)

Table 10.15 Transfer Coefficients.

Freq. mm^{-1}	$\frac{L}{J}$	$\frac{T}{J}$	$\frac{W}{J}$
0.0	0.323	0.209	0.392
0.5	0.439	0.279	0.468
1.0	0.384	0.233	0.279
1.5	0.343	0.208	0.221
2.0	0.468	0.350	0.490
2.5	0.793	0.647	0.569
3.0	1.093	0.757	0.912
3.5	1.251	0.722	1.434
4.0	1.726	1.032	1.012
4.5	3.312	2.248	2.686
5.0	3.333	2.438	4.088
5.5	3.848	4.657	5.359
6.0	5.688	3.827	6.532
6.5	9.412	6.452	13.286
7.0	15.709	11.987	15.989
7.5	22.677	19.274	23.684
8.0	16.957	14.174	20.773
8.5	20.056	15.516	18.663
9.0	26.825	20.419	23.379
9.5	21.539	16.783	19.388
10.0	32.233	24.858	25.206
10.5	23.725	19.070	23.783
11.0	31.099	29.406	32.224

(Fig 10.22)
(Fig 10.20)

CHAPTER 11. ALTERNATIVE PRESENTATION OF SPECTRAL DENSITY CURVES

The desirability of plotting spectral curves in some alternative form which might facilitate comparisons was now clearly apparent and trials in which the square root of spectral density was plotted against frequency provided encouragement to proceed along some such lines.

For some time it had been found more convenient to scale the horizontal axes of spectral curves in terms of frequency rather than wavlength. This method of scaling which has the advantage of linearity, is used on all subsequent diagrams of this type.

Spectral density in all preceding work is plotted in the form of consistent but arbitrary numerical values. The curves had been thought of as providing means by which the relative frequency contributions to the spectrum might be compared, and given consistency of units, one spectrum might be compared with another. Furthermore the quantitative significance of power spectral density in the context of surface profile measurement was by no means obvious and therefore little consideration had been given to the units in which it might be expressed.

With the object of obtaining a better understanding of power spectra in the present context, spectral density ordinates were expressed to scale in appropriate units. Results so obtained are collected in Table 11.1 each column representing a spectrum being identified by a capital letter with numerical suffix.

Consideration was also given to the units and designation of the parameter usually described as a power spectrum in which the use of the word 'power' has no apparent relevance to the description of a surface profile. The total area enclosed beneath a spectral density curve used for this purpose equals the dispersion or variance of the stationary surface profile it describes (25) and variance must obviously be measured in units consistent with those in which the profile is measured. Therefore if ordinates of points on the profile are measured in mm their variance will be in mm^2. Abscissae of points on the profile having also been measured in mm, frequency can be expressed in cycles per mm for which the units will be mm^{-1}.

Units of area beneath the spectral curve are given by the product of the units of spectral density and frequency. If this area represents variance in mm^2 and frequency is expressed in mm^{-1} then spectral density will be in mm^3.

Table 11.1

Frequency (mm^{-1})		Spectral Density of Variance at Frequency X ($\mu m^2 mm = 10^3 \mu m^3$)					
X	X^2	A_1	F_1	G_1	K_1	M_2	Q_1
0.0	0.00	3039.58	20.61	2.72	1005.82	5.37	3230.00
0.5	0.25	2381.08	19.40	2.57	925.23	5.20	2441.52
1.0	1.00	1358.72	16.14	2.14	709.09	4.72	1368.42
1.5	2.25	693.40	11.81	1.59	439.70	4.06	702.70
2.0	4.00	268.18	7.52	1.05	222.36	3.36	212.62
2.5	6.25	107.25	4.18	0.65	104.21	2.74	92.68
3.0	9.00	58.39	2.12	0.42	54.59	2.27	67.71
3.5	12.25	35.51	1.20	0.35	30.00	1.96	33.80
4.0	16.00	20.97	0.98	0.36	16.09	1.76	16.47
4.5	20.25	11.66	1.02	0.40	10.27	1.63	11.16
5.0	25.00	7.45	1.05	0.42	7.20	1.52	8.39
5.5	30.25	6.13	1.01	0.43	4.79	1.40	6.59
6.0	36.00	5.63	0.95	0.42	3.64	1.27	3.90
6.5	42.25	4.27	0.91	0.42	2.84	1.12	3.12
7.0	49.00	2.30	0.92	0.42	2.01	0.97	2.43
7.5	56.25	1.66	0.93	0.42	1.67	0.83	1.92
8.0	64.00	1.61	0.91	0.41	1.41	0.73	1.48
8.5	72.25	1.52	0.86	0.40	0.98	0.66	1.26
9.0	81.00	1.20	0.79	0.38	0.77	0.63	0.83
9.5	90.25	1.08	0.72	0.36	0.64	0.62	0.81
10.0	100.00	0.87	0.68	0.35	0.44	0.63	0.70
10.5	110.25	0.84	0.66	0.36	0.37	0.63	0.61
11.0	121.00	0.74	0.64	0.36	0.39	0.61	0.45
11.5	132.25	0.71	0.64	0.37	0.39	0.59	0.41
12.0	144.00	0.74	0.65	0.37	0.41	0.57	0.37
12.5	156.25	0.75	0.68	0.36	0.43	0.56	0.43
13.0	169.00	0.59	0.72	0.34	0.37	0.54	0.36
13.5	182.25	0.41	0.76	0.31	0.33	0.54	0.40
14.0	196.00	0.35	0.77	0.28	0.31	0.53	0.35
14.5	210.25	0.38	0.76	0.25	0.27	0.51	0.28
15.0	225.00	0.40	0.71	0.24	0.25	0.50	0.25
15.5	240.25	0.39	0.65	0.22	0.23	0.47	0.29
16.0	256.00	0.37	0.57	0.22	0.20	0.44	0.31
16.5	272.25	0.40	0.51	0.21	0.19	0.41	0.29

$\Sigma X = 280.5 \quad \Sigma X^2 = 3132.25 \quad \bar{X} = 8.25$

With regard to designation, it appears more logical in the context of surface profile measurement, to describe the parameter as a 'variance spectrum' or 'dispersion spectrum' rather than 'power spectrum' provided that the common statistical derivation remains clearly apparent.

At this stage further small modifications were made to computer program MACJO4 making it possible to compute a spectrum defined by 100 ordinates instead of 68. This was done to extend the scope of investigation into lower frequencies. The same sets of data were used as those represented by Tables 10.4 to 10.12 in Appendix 10. The computer outputs obtained under the new conditions are designated as Figs 11.1, 11.2, 11.3, 11.4, 11.5, 11.6, 11.7, 11.8, and 11.9.

In Fig 11.10 three of the spectra representing grinding wheel profiles are plotted on a common pair of axes, ordinates at frequencies greater than about 5 cycles per mm being also plotted at an alternative scale. Spectral representative of 30 seconds and 5 minutes are so closely superimposed as to be indistinguishable at the smaller vertical scale. At the alternative scale used on the right of the diagram the 10 minute spectrum is fairly well differentiated from the other two.

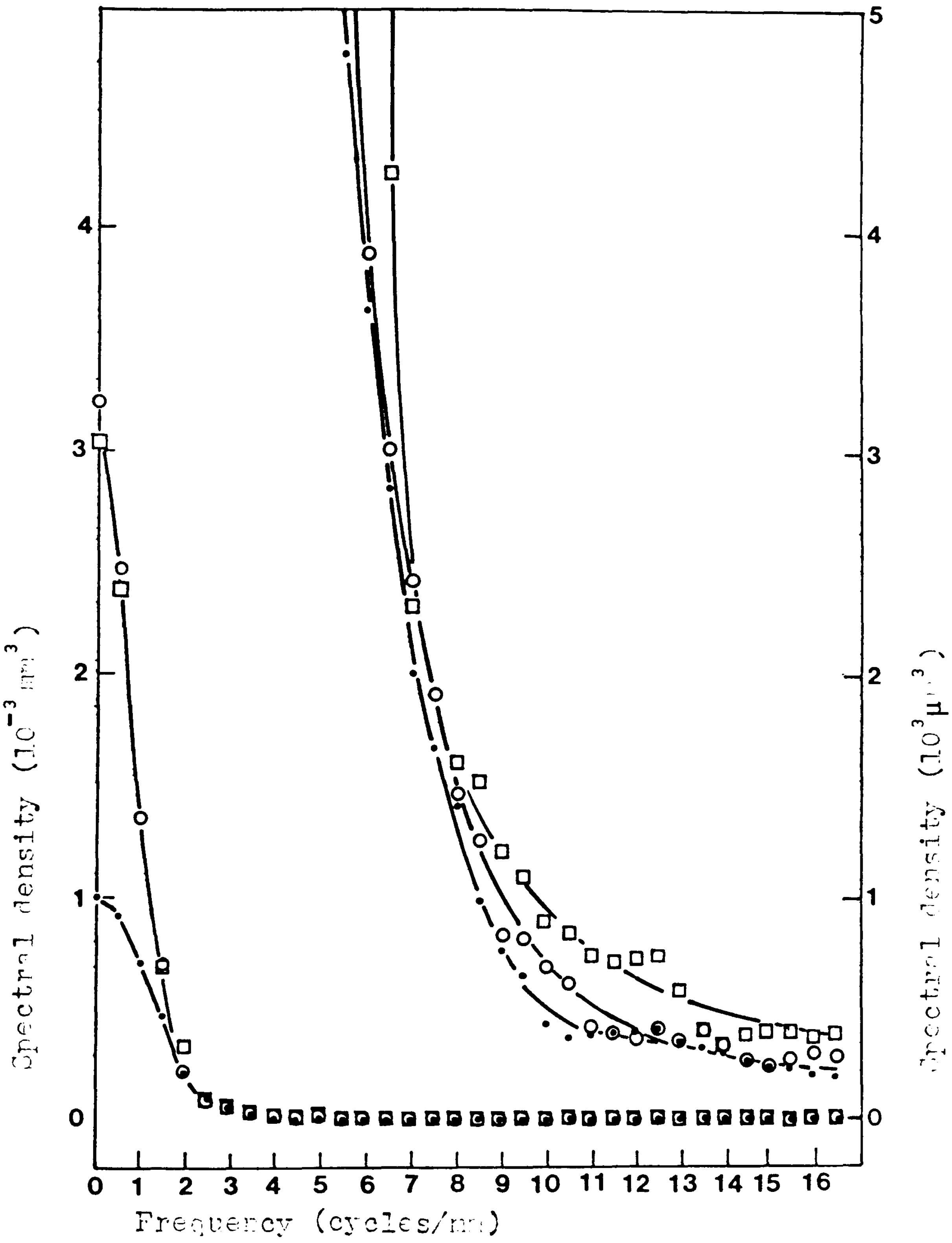

Fig 11.10 Variance Spectra representing Grinding Wheel Surfaces at different stages of wear

30 seconds wear □

5 minutes wear ○

10 minutes wear •

Fig 11.11 represents the three ground surfaces corresponding to the stages of grinding wheel wear. The vertical scale chosen for reasonable separation of the curves is such as to exclude the low frequency region of two of the curves.

Table 11.2 contains the square roots of the spectral density ordinates in Table 11.1 and in Fig 11.12 (i) two spectral curves based upon these are plotted representing a comparison between two grinding wheel surfaces at different stages of wear. Fig 11.13 (i) represents the comparison between the corresponding ground surfaces expressed in the same way.

As a result of taking the square root of spectral density, numerical values of ordinates associated with lower frequencies are depressed and those at higher frequencies elevated. The resulting range of ordinates was more conveniently plotted on a natural scale than spectral density.

Transfer functions based upon these modified curves were plotted (Figs 11.12 (ii) and 11.13 (ii)) using information recorded in Table 11.4 Appendix 11.

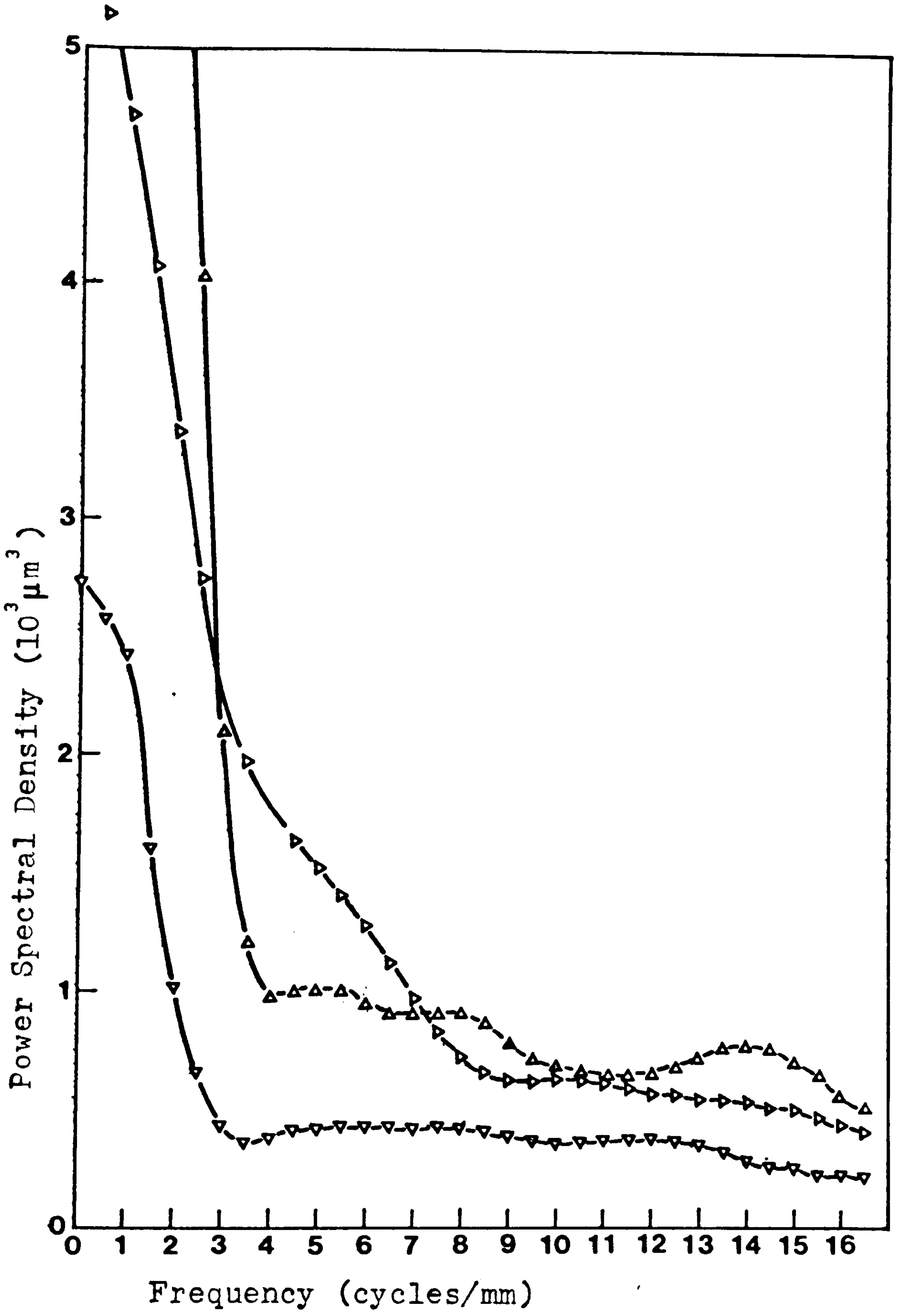

Fig 11.11 Variance Spectra representing ground surfaces corresponding with stages of grinding wheel wear

Duration of grinding:

30 seconds △ 5 minutes ▷ 10 minutes ▽

Table 11.2 $\sqrt{\text{Spectral Density}}$

X	$\sqrt{A_1}$	$\sqrt{F_1}$	$\sqrt{G_1}$	$\sqrt{K_1}$	$\sqrt{M_2}$	$\sqrt{Q_1}$
0.0	55.13	4.54	1.65	31.71	2.32	56.84
0.5	48.80	4.40	1.60	30.42	2.28	49.41
1.0	36.86	4.02	1.46	26.63	2.17	36.99
1.5	26.33	3.44	1.26	20.97	2.02	26.51
2.0	16.38	2.74	1.02	14.91	1.83	14.58
2.5	10.36	2.04	0.80	10.21	1.66	9.63
3.0	7.64	1.46	0.65	7.39	1.51	8.23
3.5	5.96	1.10	0.59	5.48	1.40	5.81
4.0	4.58	0.99	0.60	4.01	1.33	4.06
4.5	3.41	1.01	0.63	3.20	1.27	3.34
5.0	2.73	1.03	0.65	2.68	1.23	2.90
5.5	2.47	1.00	0.65	2.19	1.18	2.57
6.0	2.37	0.97	0.65	1.91	1.13	1.97
6.5	2.07	0.96	0.65	1.69	1.06	1.77
7.0	1.52	0.96	0.65	1.42	0.99	1.56
7.5	1.29	0.97	0.65	1.29	0.91	1.39
8.0	1.27	0.96	0.64	1.19	0.85	1.22
8.5	1.23	0.93	0.63	0.99	0.81	1.12
9.0	1.09	0.89	0.61	0.87	0.79	0.91
9.5	1.04	0.85	0.60	0.80	0.79	0.90
10.0	0.93	0.83	0.59	0.66	0.79	0.84
10.5	0.92	0.81	0.60	0.61	0.79	0.78
11.0	0.86	0.80	0.60	0.63	0.78	0.67
11.5	0.84	0.80	0.61	0.62	0.77	0.64
12.0	0.86	0.81	0.61	0.64	0.76	0.61
12.5	0.86	0.82	0.60	0.66	0.75	0.65
13.0	0.77	0.85	0.59	0.61	0.74	0.60
13.5	0.64	0.87	0.56	0.58	0.73	0.63
14.0	0.59	0.88	0.53	0.56	0.73	0.59
14.5	0.61	0.87	0.50	0.52	0.72	0.53
15.0	0.63	0.84	0.48	0.50	0.70	0.50
15.5	0.63	0.80	0.47	0.48	0.69	0.54
16.0	0.61	0.76	0.47	0.45	0.66	0.55
16.5	0.63	0.71	0.46	0.44	0.64	0.54

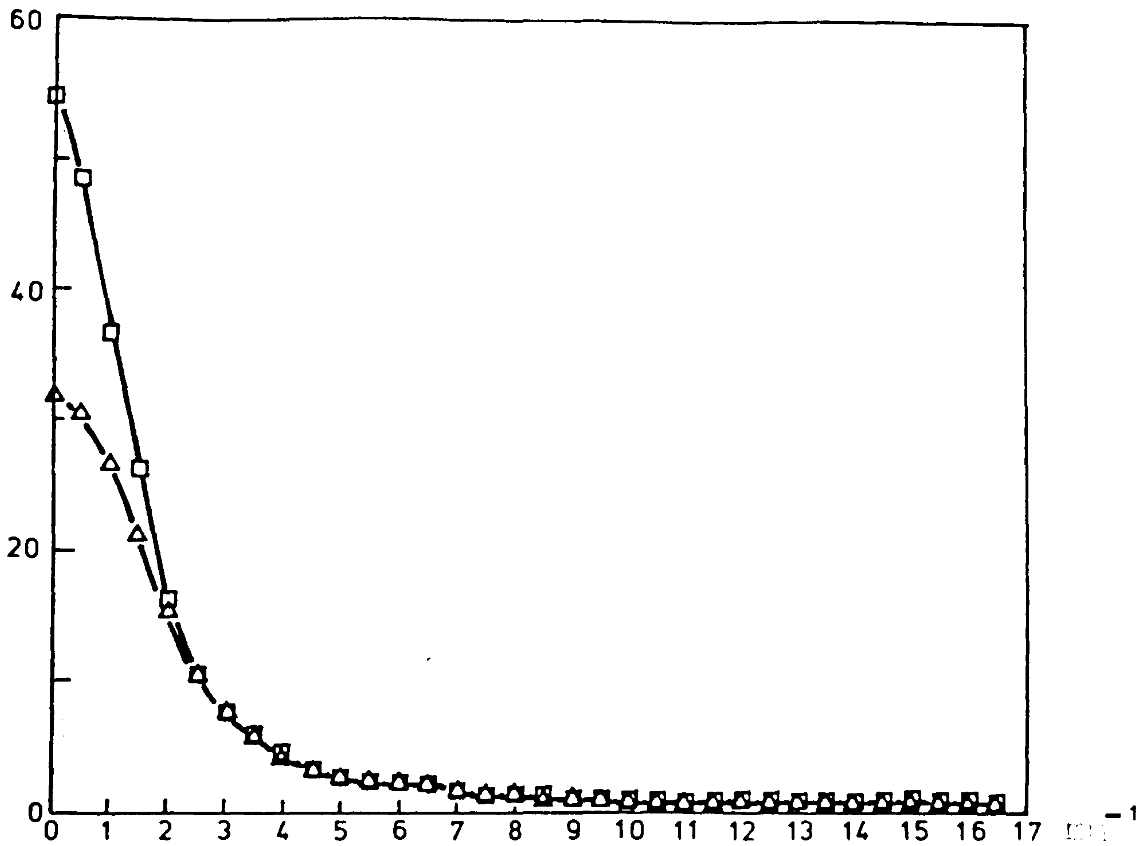

(i) Spectral curves representing grinding wheel surfaces after 30 seconds wear □ ($\sqrt{A_1}$) and after 10 minutes wear △ ($\sqrt{K_1}$)

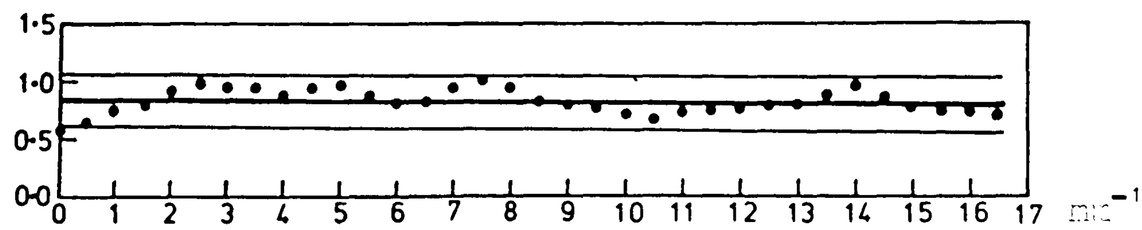

(ii) Transfer function with regression line and 95 per cent confidence limits obtained from the spectra in (i)

Fig **11.12** Comparison of grinding wheel surfaces

In (i) $\sqrt{\text{spectral density}}$ is plotted v. frequency. Ratios of corresponding pairs of ordinates are plotted v. frequency in (ii) i.e. $(\sqrt{K_1/A_1})$.
A_1 and K_1 identify the surfaces, samples, and operating conditions used in computing spectral density.

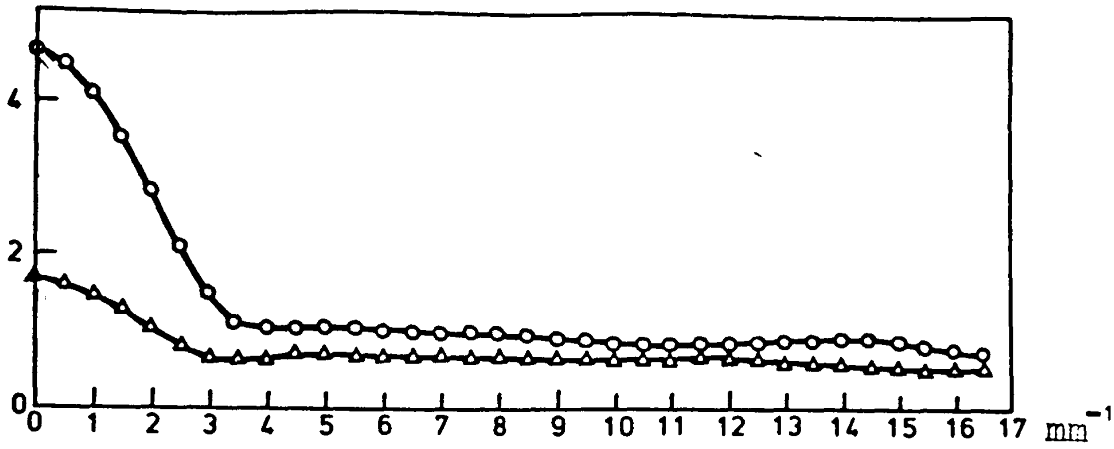

(i) Spectral curves representing ground surfaces after grinding for the periods indicated 30 seconds o ($\sqrt{F_1}$), 10 minutes △ ($\sqrt{G_1}$)

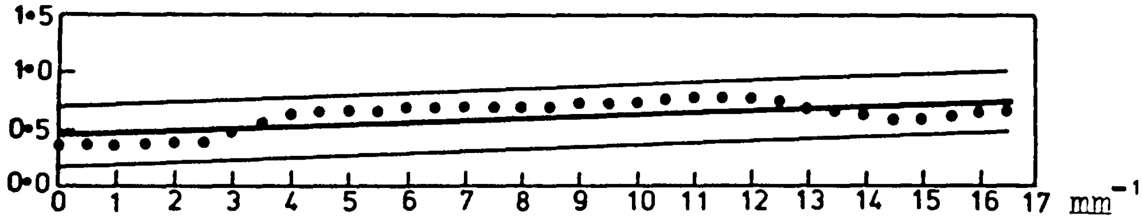

(ii) Transfer function with regression line and 95 per cent confidence limits obtained from the spectra in (i)

Fig 11.13 Comparison of ground surfaces

In (i) $\sqrt{\text{spectral density}}$ is plotted v. frequency. Ratios of corresponding pairs of ordinates so obtained are plotted v. frequency in (ii) i.e. $\sqrt{G_1/F_1}$. F_1 and G_1 identify the surfaces, samples, and operating conditions used in computing spectral density.

Treating these transfer functions as approximations to straight lines, regression lines and corresponding 95 per cent confidence limits have been added. Relevant information and calculations appear in Tables 11.3, 11.5, 11.6, 11.7, and 11.8 Appendix 11. Other transfer functions plotted from the data of Table 11.2 showed a similar approximation to linearity.

The potential usefulness of a linear transfer function relating spectral curves is self evident. However, only two such sets of results each representing a comparison between closely similar surfaces are illustrated here. This limited treatment calls for some explanation as follows.

Plotting the square root of spectral density was one of the expedients adopted with the primary object of representing spectral ordinates at a more convenient scale. This having been done, with the results indicated, attention was given to the units in which the spectrum is expressed.

'Variance spectrum' or 'dispersion spectrum' have already been proposed as more appropriate descriptive titles than 'power spectrum' in the context of surface profile characterization. It is also shown that spectral density is expressed as the third power, and the area beneath the curve (variance) as the second power of the linear units in which the profile is measured.

Ordinates obtained by taking the square root of spectral density will therefore be in $mm^{\frac{3}{2}}$. These plotted against frequency in mm^{-1} lead to a situation wherein the units of area enclosed by the resulting curve will be $mm^{\frac{1}{2}}$.

Consideration of the units in which variance and standard deviation are expressed led to formulation of the alternative spectrum outlined in the following chapter.

CHAPTER 12. AN ALTERNATIVE SPECTRUM FOR DESCRIBING THE SURFACES OF GRINDING WHEELS AND GROUND SURFACES

The preceding chapter discusses the units in which power spectral density is expressed when computed from data in the form of an array of ordinates defining a surface profile. It was shown that if this array is dimensioned in mm, power spectral density will be in mm^3 and the spectral curve is defined by plotting this on a frequency scale dimensioned in mm^{-1}.

The area under a curve defined in this way will be in mm^2 and will represent variance, while the shape of the curve will represent an estimate of the distribution of this parameter with respect to frequency. This being so the ordinates defining the curve represent the spectral density of variance with respect to frequency and the curve itself may be described as a variance spectrum rather than a power spectrum.

Variance (or power) spectral density was computed from surface profile data obtained from grinding wheels and ground surfaces. Results from these data when plotted on a natural scale were not well adapted for visual comparison. This was because the range of variance density values representing each profile is so wide that the smaller values associated with the higher frequencies appear to be virtually zero when plotted: particularly so in the case of spectra representing grinding wheel profiles.

Spectral curves more suitable for visual comparison were obtained by plotting the square root of variance density versus frequency. The resulting curves including those representing surface profiles as closely similar as those of the same grinding wheel at different stages of wear are quite well different-iated for visual comparison. Additionally it was found that transfer functions plotted in order to show the comparison between any pair of surfaces were well approximated by straight lines of differing slope and intercept.

If surface data are expressed in mm the area beneath a spectral curve defined by plotting the square root of variance density will be in units of $mm^{\frac{1}{2}}$. These units are dimensionally inconsistent with a statement of area and also with any standard parameter representing variability.

These inconsistencies led to reconsideration with the object of formulating a more generally satisfactory alternative to the variance density spectrum than the one described in the preceding chapter. This was achieved as follows.

Standard deviation is the square root of variance and is expressed in the same units as the variate while variance itself is expressed as the second power of these units. From this it follows that a spectrum derived from a variance spectrum such that the area beneath the derived curve is in linear units will represent the distribution of standard deviation with respect to frequency. This standard deviation spectrum is shown to have similar attributes, when applied to the surface profiles considered here as the dimensionally inconsistent type discussed in Chapter 11.

If variance spectral density is in mm^3, ordinates calculated as (spectral density)$^{\frac{2}{3}}$ will be expressed in mm^2. These plotted against frequency in mm^{-1} define a spectrum in which the units of area beneath the curve are mm. Given that the area under the power spectral density curve represents variance in mm^2 it follows that the area beneath this modified curve represents standard deviation in mm.

Calculation of ordinates by raising spectral density to the power $\frac{2}{3}$ has the effect of reducing the range of numerical values to be plotted to a lesser extent than the reduction obtained by taking the square root. Also if a power spectral density curve represents profile ordinate variance density distribution with respect to frequency, the new curve defines the corresponding distribution of standard deviation density.

Table 12.1 contains ordinates calculated as described above from the spectral density values in Table 11.1. The spectra so defined are plotted as Figs 12.2, 12.3, 12.4, 12.5, 12.6, and 12.7.

Table 12.1

Frequency (mm^{-1})	Spectral Density of Standard Deviation at Frequency X ($10^2 \mu m^2$)					
X	$A_1^{\frac{2}{3}}$	$F_1^{\frac{2}{3}}$	$G_1^{\frac{2}{3}}$	$K_1^{\frac{2}{3}}$	$M_2^{\frac{2}{3}}$	$Q_1^{\frac{2}{3}}$
0.0	209.83	7.52	1.95	100.39	3.07	218.51
0.5	178.31	7.22	1.88	94.95	3.00	181.32
1.0	122.67	6.39	1.66	79.52	2.81	123.26
1.5	78.34	5.19	1.36	57.82	2.54	79.04
2.0	41.59	3.84	1.03	36.70	2.24	35.62
2.5	22.57	2.59	0.75	22.14	1.96	20.48
3.0	15.05	1.65	0.56	14.39	1.73	16.61
3.5	10.80	1.13	0.50	9.65	1.57	10.45
4.0	7.60	0.99	0.51	6.37	1.46	6.47
4.5	5.14	1.01	0.54	4.72	1.39	4.99
5.0	3.81	1.03	0.56	3.73	1.32	4.13
5.5	3.35	1.01	0.57	2.84	1.25	3.51
6.0	3.16	0.97	0.56	2.37	1.17	2.48
6.5	2.63	0.94	0.56	2.01	1.08	2.14
7.0	1.74	0.95	0.56	1.59	0.98	1.81
7.5	1.40	0.95	0.56	1.41	0.88	1.54
8.0	1.37	0.94	0.55	1.26	0.81	1.30
8.5	1.32	0.90	0.54	0.99	0.76	1.67
9.0	1.13	0.85	0.52	0.84	0.73	0.88
9.5	1.05	0.80	0.51	0.74	0.73	0.87
10.0	0.91	0.77	0.50	0.58	0.73	0.79
10.5	0.89	0.76	0.51	0.52	0.73	0.72
11.0	0.82	0.74	0.51	0.53	0.72	0.59
11.5	0.80	0.74	0.52	0.53	0.70	0.55
12.0	0.82	0.75	0.52	0.55	0.69	0.52
12.5	0.83	0.77	0.51	0.57	0.68	0.57
13.0	0.70	0.80	0.49	0.52	0.66	0.51
13.5	0.55	0.83	0.46	0.48	0.66	0.54
14.0	0.50	0.84	0.43	0.46	0.65	0.50
14.5	0.52	0.83	0.40	0.42	0.64	0.43
15.0	0.54	0.80	0.39	0.40	0.63	0.40
15.5	0.53	0.75	0.36	0.38	0.60	0.44
16.0	0.52	0.69	0.36	0.34	0.58	0.46
16.5	0.54	0.64	0.35	0.33	0.55	0.44

Table 12.2

Frequency (mm^{-1}) X	Transfer Coefficients Relating Surfaces Represented by Standard Deviation Spectra Y_{FA}	Y_{MQ}	Y_{GK}	Y_{GF}	Y_{KA}
0.0	0.036	0.016	0.021	0.259	0.478
0.5	0.040	0.016	0.021	0.259	0.533
1.0	0.052	0.021	0.021	0.261	0.648
1.5	0.066	0.033	0.025	0.263	0.738
2.0	0.092	0.063	0.029	0.270	0.882
2.5	0.115	0.097	0.033	0.290	0.981
3.0	0.109	0.105	0.040	0.340	0.956
3.5	0.105	0.150	0.052	0.440	0.894
4.0	0.130	0.225	0.079	0.513	0.838
4.5	0.196	0.277	0.115	0.536	0.919
5.0	0.271	0.320	0.150	0.543	0.977
5.5	0.301	0.355	0.201	0.566	0.848
6.0	0.306	0.474	0.236	0.580	0.748
6.5	0.357	0.505	0.280	0.598	0.762
7.0	0.543	0.542	0.351	0.593	0.914
7.5	0.679	0.571	0.398	0.589	1.004
8.0	0.683	0.624	0.439	0.588	0.916
8.5	0.683	0.650	0.550	0.600	0.746
9.0	0.757	0.832	0.625	0.614	0.744
9.5	0.763	0.836	0.682	0.630	0.706
10.0	0.981	0.932	0.858	0.642	0.635
10.5	0.852	1.022	0.982	0.667	0.578
11.0	0.908	1.225	0.948	0.682	0.652
11.5	0.933	1.275	0.966	0.694	0.670
12.0	0.917	1.334	0.934	0.687	0.675
12.5	0.937	1.192	0.888	0.654	0.690
13.0	1.142	1.310	0.945	0.606	0.733
13.5	1.509	1.221	0.959	0.550	0.865
14.0	1.692	1.319	0.934	0.510	0.922
14.5	1.587	1.491	0.950	0.476	0.797
15.0	1.466	1.587	0.973	0.485	0.731
15.5	1.406	1.379	0.971	0.485	0.703
16.0	1.334	1.263	1.066	0.530	0.664
16.5	1.176	1.260	1.069	0.554	0.609
ΣY =	23.124	24.522	17.791	17.554	26.156
$\bar{Y}$ =	0.680	0.721	0.523	0.516	0.769

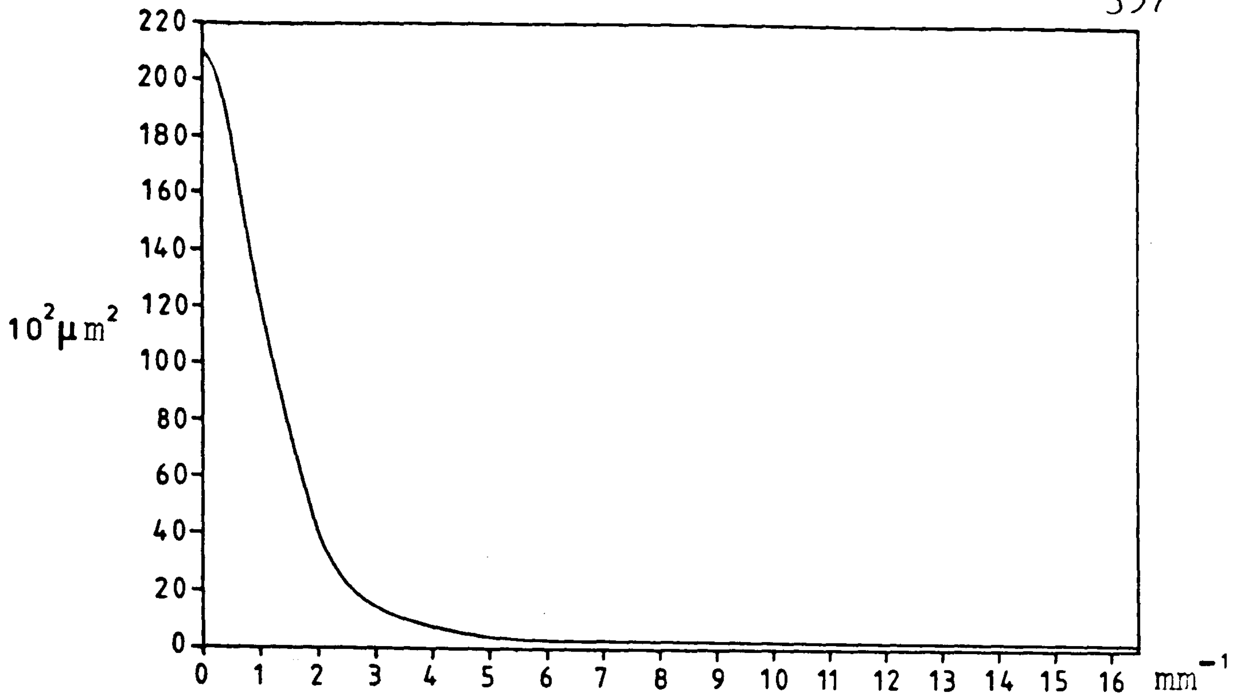

Fig 12.2 Standard deviation spectrum for the surface of an 80 grit grinding wheel after 30 seconds wear (A_1)

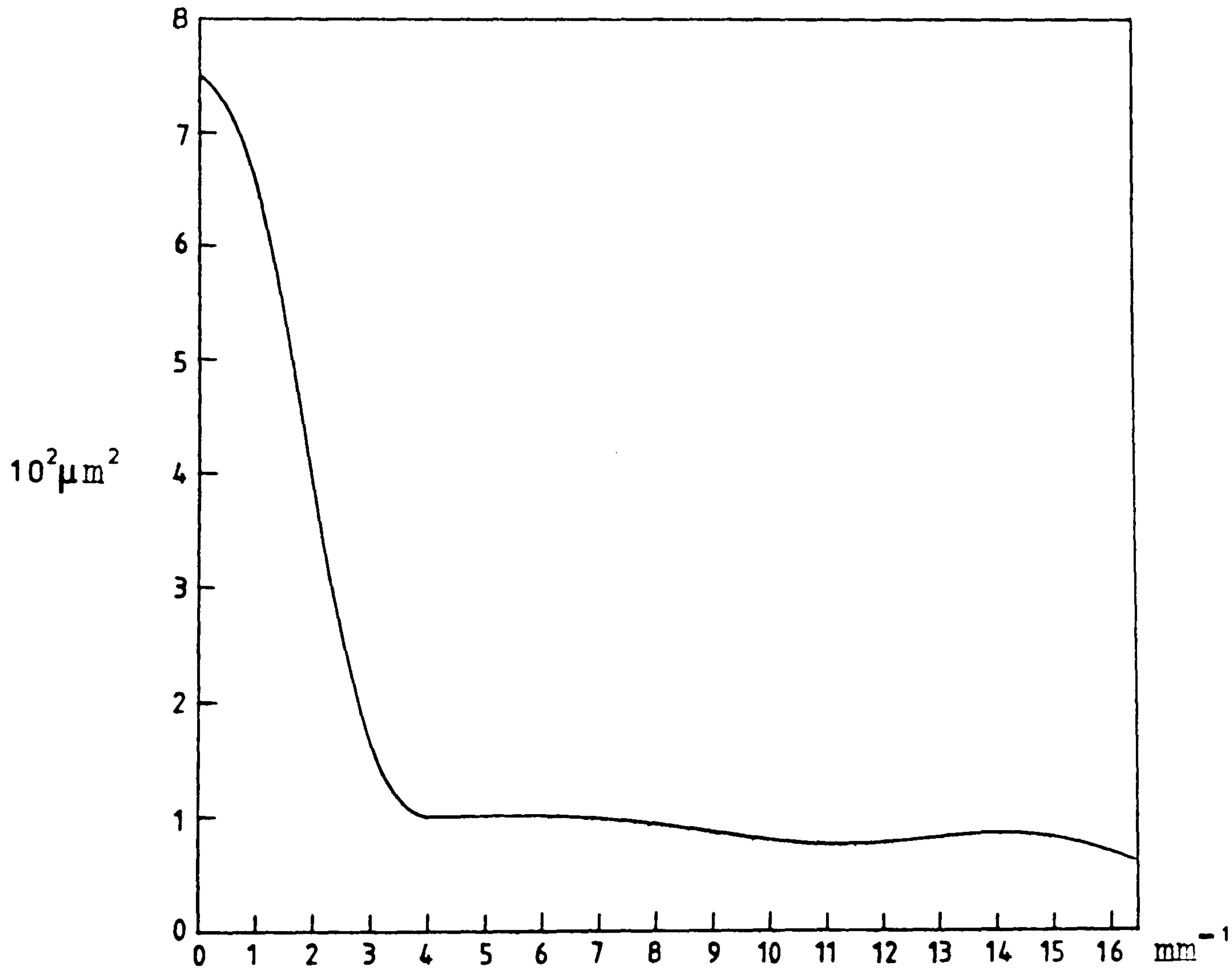

Fig 12.3 Standard deviation spectrum for a ground surface corresponding with 30 seconds wheel wear (F_1)

In the above diagrams, density of standard deviation is plotted against frequency. A_1 and F_1 identify the surface samples, computing conditions etc.

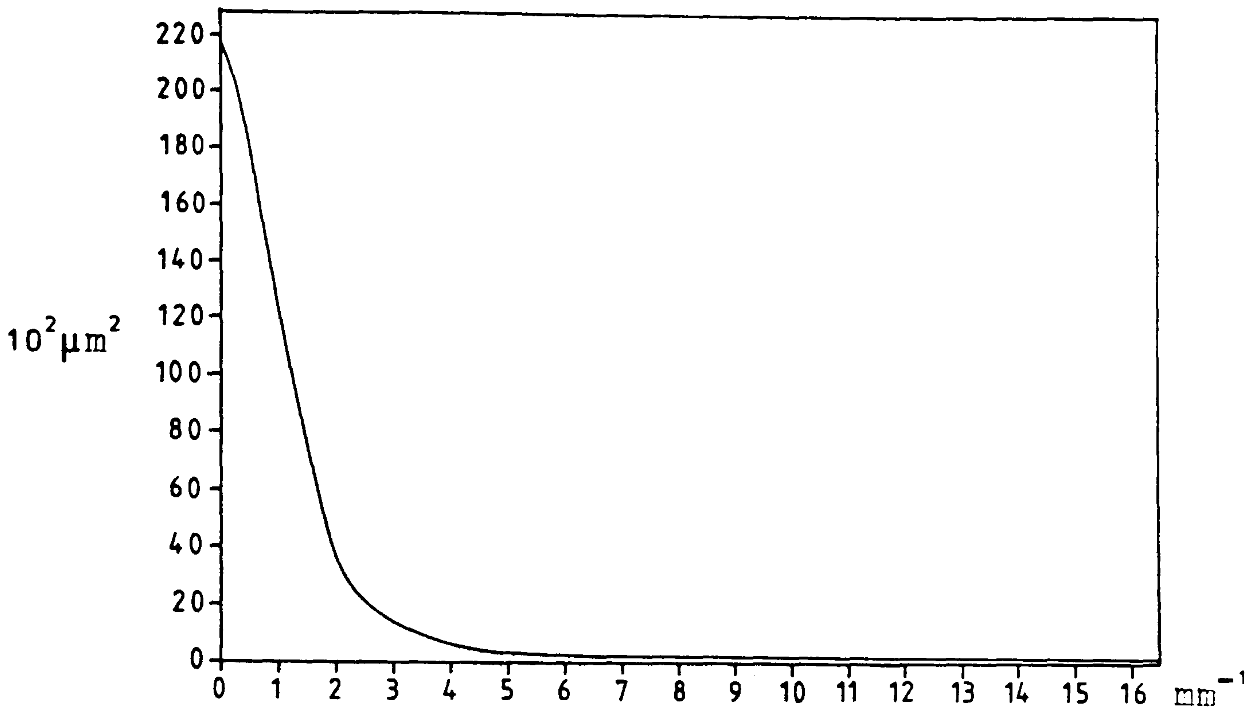

Fig 12.4 Standard deviation spectrum for the surface of an 80 grit grinding wheel after 5 minutes wear (Q_1)

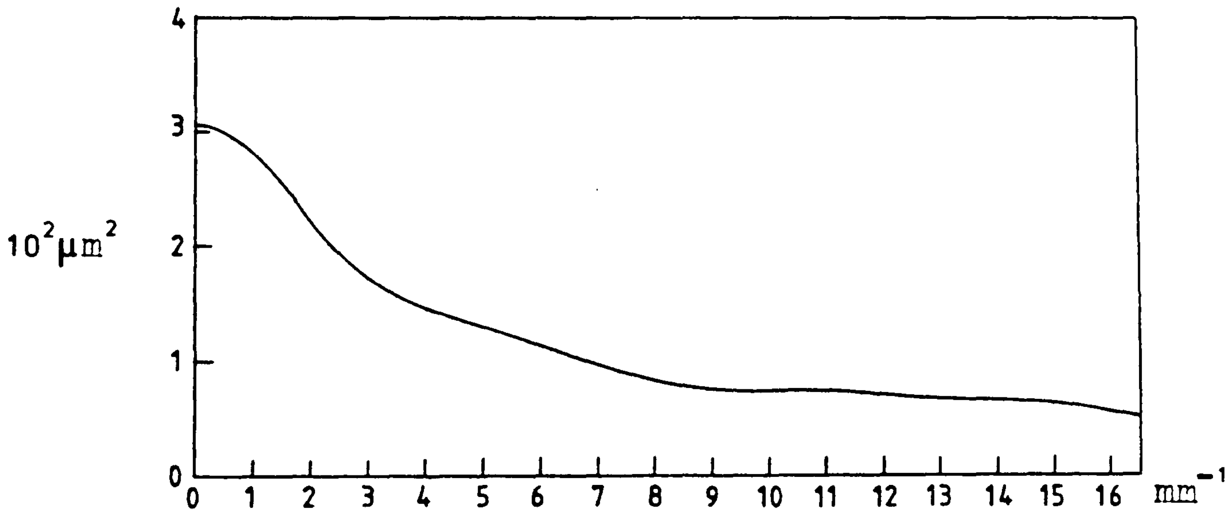

Fig 12.5 Standard deviation spectrum for a ground surface corresponding with 5 minutes wheel wear (M_2)

In the above diagrams, density of standard deviation is plotted against frequency. Q_1 and M_2 identify the surface samples, computing conditions etc.

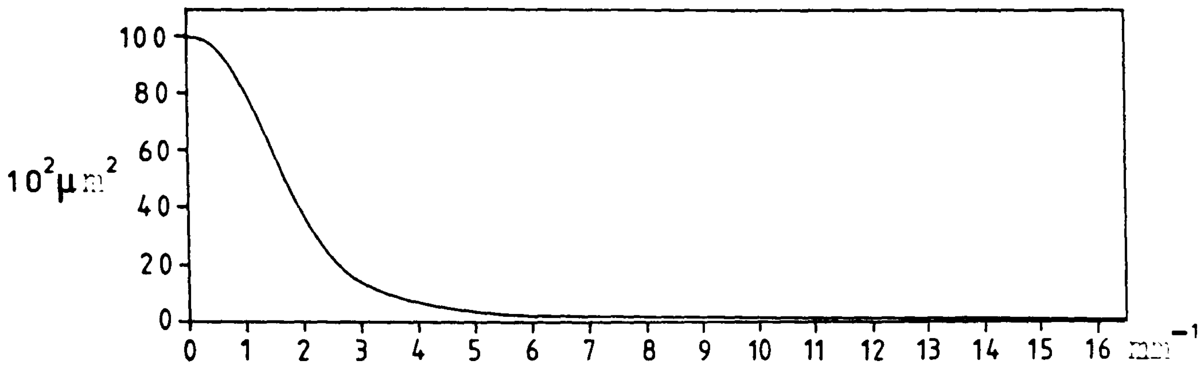

Fig **12.6** Standard deviation spectrum for the surface of an 80 grit grinding wheel after 10 minutes wear (K_1)

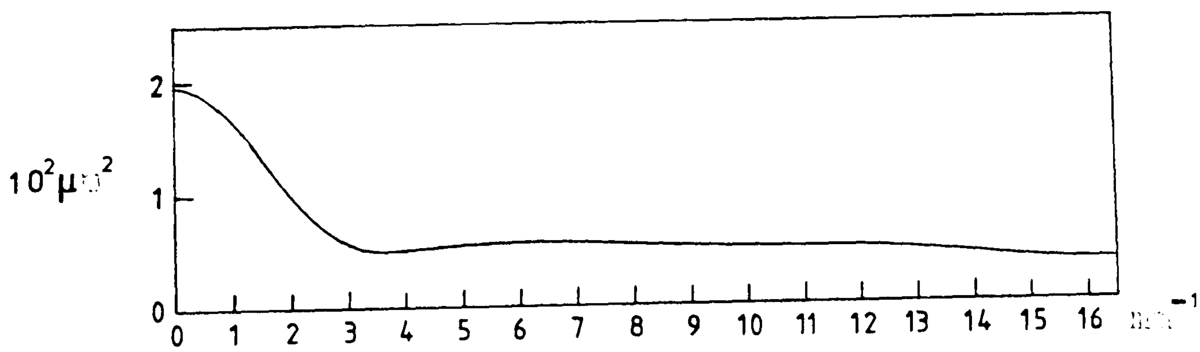

Fig **12.7** Standard deviation spectrum for a ground surface corresponding with 10 minutes wheel wear (G_1)

In the above diagrams, density of standard deviation is plotted against frequency. K_1 and G_1 identify the surface samples, computing conditions etc.

For purposes of comparison, transfer coefficients were calculated and these listed in Table 12.2 are plotted as follows.

Fig 12.8 shows the transfer function relating to the surface of a grinding wheel subjected to 30 seconds wear while Figs 12.9 and 12.10 are similarly representative of 5 minutes and 10 minutes wear respectively. Linear regression was applied to the plotted points and the resulting lines added to the diagrams together with 95 per cent confidence limits.

Fig 12.11 represents the development of the ground surface in $9\frac{1}{2}$ minutes grinding and Fig 12.12 the corresponding change in the grinding wheel surface by reason of wear.

The procedure followed in calculating regression lines and confidence intervals is set out in Tables 12.3, 12.4, 12.5, 12.6, 12.7, and 12.8 Appendix 12.

In Fig 12.13 the five regression lines are plotted on a single pair of axes to facilitate comparison. On all six transfer function diagrams a line is drawn corresponding with unity transfer coefficient, since transfer functions represented by straight lines may conveniently be compared in terms of their slope and intercept relative to this line.

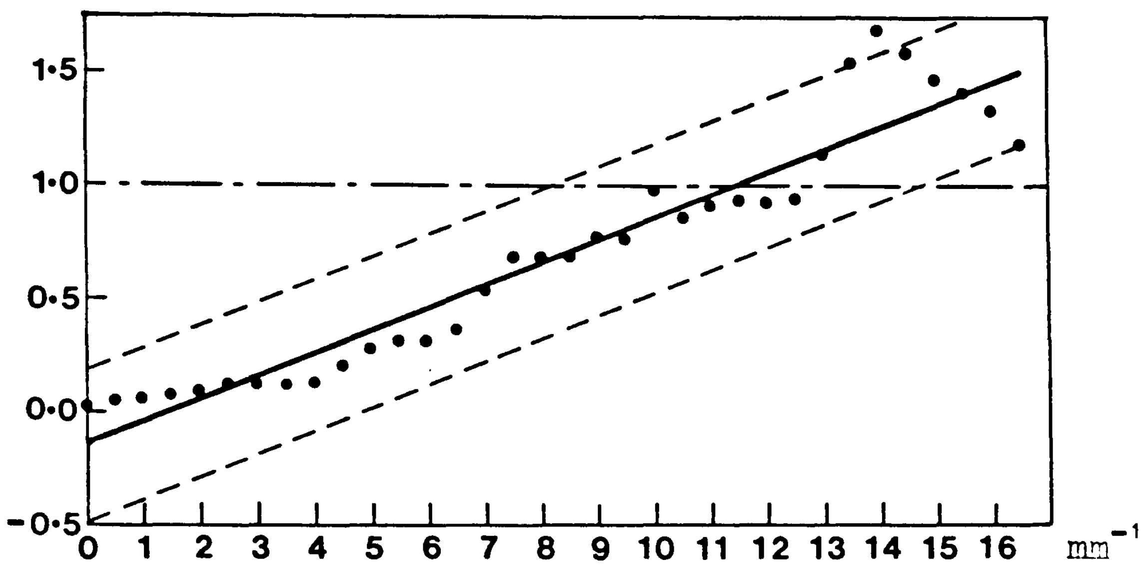

Fig 12.8 Transfer function at 30 seconds (Y_{FA})

Figs 12.8, 12.9, and 12.10 Transfer functions with regression line and 95 per cent confidence interval relating standard deviation spectra representing the ground surface and corresponding grinding wheel surface for the duration of wear indicated. The ratios of corresponding pairs of standard deviation density ordinates are plotted v. frequency, the ground surface being treated as output. Y_{FA} ,Y_{MQ} , and Y_{GK} identify relevant columns in Table 12.2

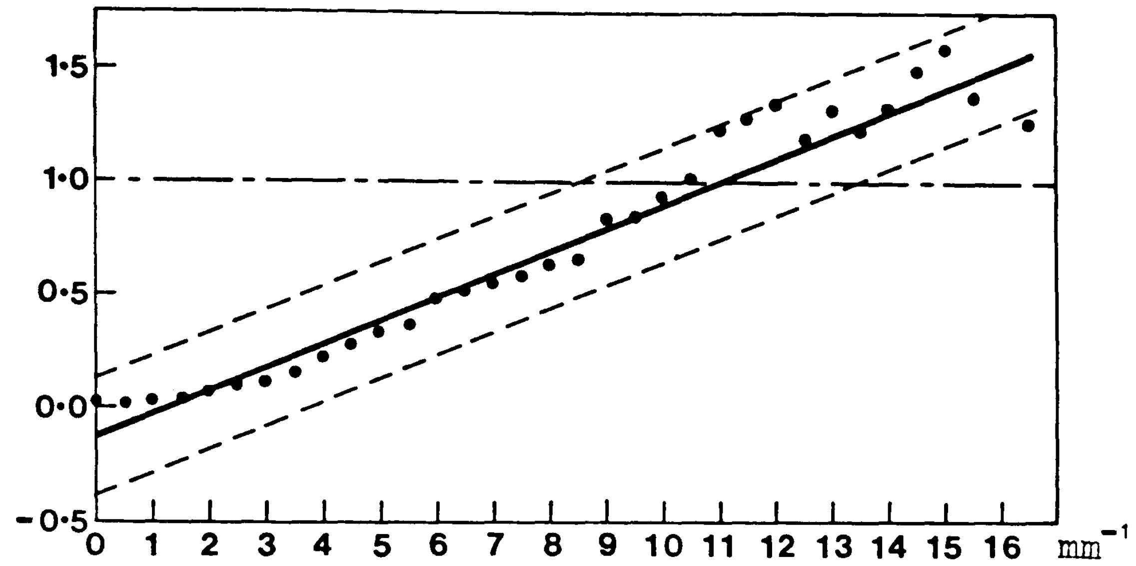

Fig 12.9 Transfer function at 5 minutes (Y_{MQ})

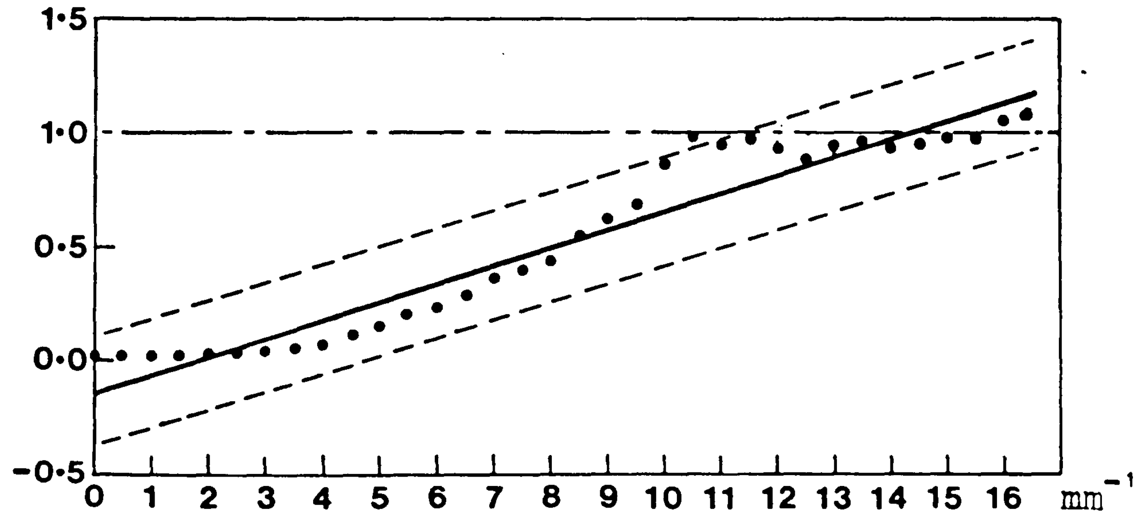

Fig 12.10 Transfer function at 10 minutes (Y_{GK})

See notes accompanying Fig 12.8

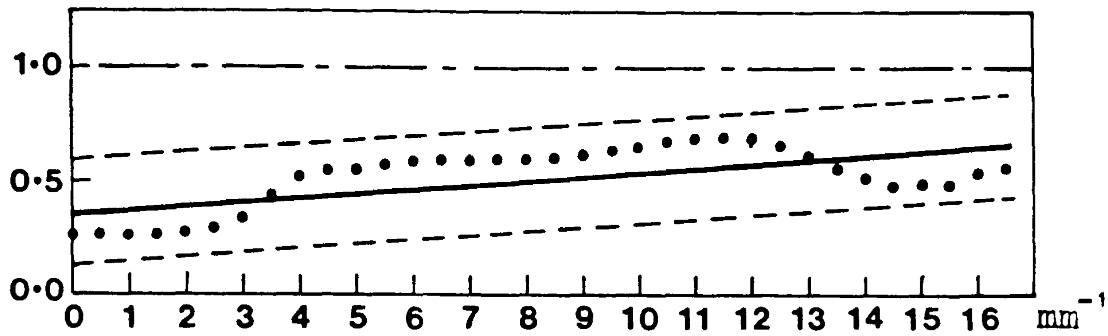

Fig 12.11 Transfer function representing development of a ground surface corresponding with 9½ minutes grinding wheel wear (Y_{GF})

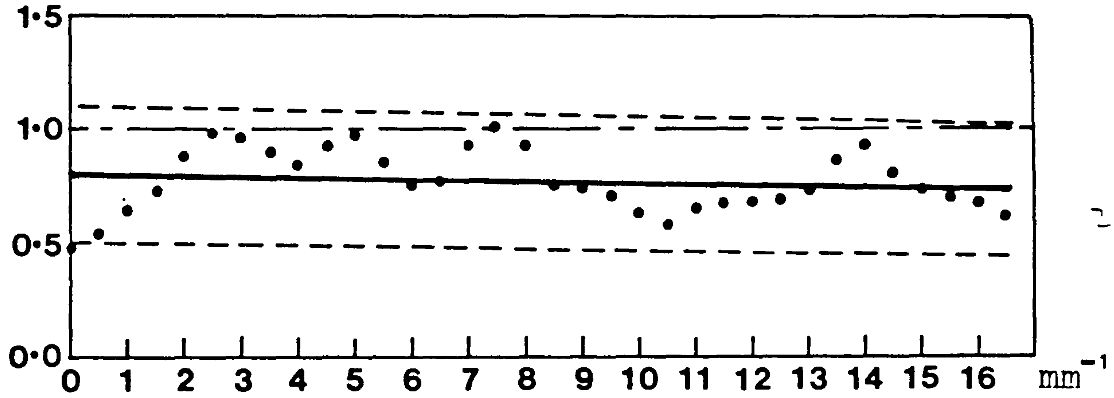

Fig 12.12 Transfer function representing 9½ minutes wear of a grinding wheel surface (Y_{KA})

Figs 12.11 and 12.12 Transfer functions obtained by plotting the ratios of corresponding pairs of standard deviation density ordinates v. frequency. Y_{GF} and Y_{KA} identify relevant columns in Table 12.2

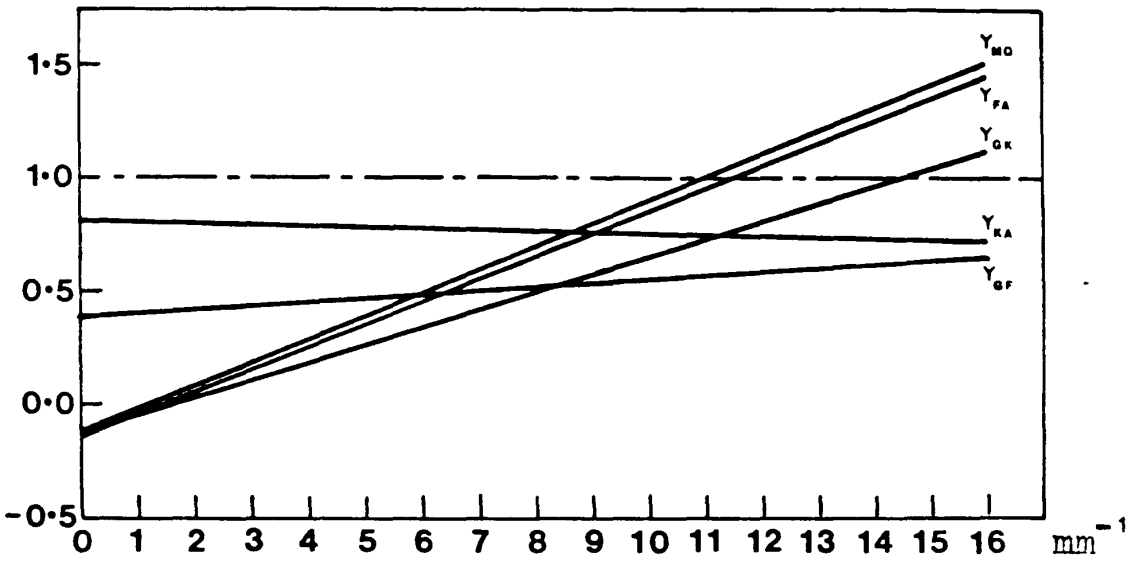

Fig 12.13 Transfer function regression lines representing relationships between surfaces as follows.

Y_{FA} workpiece and wheel after 30 seconds grinding

Y_{MQ} workpiece and wheel after 5 minutes grinding

Y_{GK} workpiece and wheel after 10 minutes grinding

Y_{GF} workpiece before and after $9\frac{1}{2}$ minutes grinding

Y_{KA} grinding wheel before and after $9\frac{1}{2}$ minutes grinding

The above are re-plotted from Figs 12.8, 12.9, 12.10, 12.11, and 12.12,to facilitate comparison

The width of the 95 per cent confidence zones indicates significant uncertainty in slope and position of the regression lines. However, if it is borne in mind that the transfer function representing the comparison between two identical spectra will be a horizontal straight line at unit level, it is clear that all regression lines plotted, with the possible exception of the one representing $9\frac{1}{2}$ minutes grinding wheel wear, differ very considerably from this situation. The regression lines differ from one another in terms of both slope and intercept to an extent much greater than that which could be accounted for by variations within the confidence limits. Exceptions to this are the lines representing the comparison between grinding wheel and workpiece after 30 seconds and 5 minutes grinding. These are very similar but differ significantly from all the others.

If it is accepted that a power spectrum, in the context of surface profile investigation, is conveniently described as a variance spectrum , then it is clearly appropriate to describe the modification presented here as a standard deviation spectrum. Apart from the fact that density of standard deviation is more conveniently plotted on a natural scale than density of variance, there is the added advantage that for the range of data used in these experiments, transfer functions relating standard deviation spectra may justifiably be represented by straight lines, which is clearly not the case for the variance spectra.

CONCLUSIONS 13. CONCLUSIONS

The following notes are intended to show the contribution made by this work in relation to deductions based upon the literature survey.

Information from the literature which proved to be most relevant to this investigation can be considered in three categories. The first of these relates to methods of characterizing surfaces involved in the grinding process, the second to means of comparing or relating these surfaces, and the third to the collection of information from the surfaces with a view to measurement and comparison.

Characterization by statistical methods was clearly essential because of the predominantly random nature of grinding wheel and ground surface profiles. Of the various methods dealt with in the literature, autocorrelation and power spectral density appeared to be the most promising parameters for effective measurement and comparison. Information on these was not plentiful and came from relatively few sources.

Prediction of output surface profile from input surface profile for a given set of conditions was envisaged as a future possibility. In this context the input and output represented by the profiles of grinding wheel and ground surface respectively were of primary interest.

The possibility of output surface prediction pre--supposes the establishment of some curve or equation connecting the parameter or parameters representing the two surface profiles. Relevant information was particularly scarce and the only significant contribut--ion was found in the work of one author. This refers to the transfer function curves relating pairs of power spectra published by Peklenik (21).

Information on stylus profilometry applied to abrasive surfaces including grinding wheels was plentiful and served to confirm this as the most appropriate method of data collection from surface profiles for the purpose of computing statistical parameters.

The main theme of the present work relates to measure--ment of dressed and worn surfaces of grinding wheels by stylus profilometry, analysis of these profiles in terms of spectral density, and comparison of spectra by means of transfer functions. This, of course, implies the application of similar methods to surfaces produced by the grinding wheels. Concentration on spectral density for surface profile analysis may well be an unique feature of this investigation although this statement cannot be made with confidence because of the extended time scale of the part time research.

Initially, power spectral density was used for surface characterization and comparison. At a somewhat later stage this parameter, appropriately dimensioned, is referred to as spectral density of variance, and the curve itself as a variance spectrum. This was done in order to clarify the meaning of such a spectrum as it relates to surface profile.

Some measure of dissatisfaction with variance (or power) spectra for surface profile characterization led finally to formulation of an alternative spectrum capable of better representation of the surface profiles involved in grinding. A further advantage of the new parameter, described as a standard deviation spectrum, is the strong linear correlation with frequency, characteristic of transfer functions relating these spectra.

Interpretation of variance spectra and standard deviation spectra is basically similar, since they represent the distribution with respect to frequency of profile ordinate variability; in terms of variance and standard deviation respectively.

Standard deviation densities representing a given profile are contained within a considerably smaller range of values than the corresponding densities of variance. As a result of this, surface profiles typical of the grinding process are shown to be more clearly represented and compared in graphical terms, by means of standard deviation spectra rather than by variance spectra.

Linearity is obviously not essential for interpretation and use of a transfer function. Here there is some evidence for its existence and, if close correlation was established between density of standard deviation and frequency, this would represent a particularly convenient relationship between surface profiles.

At this point it seems appropriate to compare rsults with some of those contained in Part 1 of this thesis.

In the Conclusions to Part 1 (p 78) it was noted that the compression of asperities into a zone of reduced depth as a result of grinding wheel wear could be expressed in terms of a diminution in the corresponding standard deviation as represented by differences in the slope of distribution curves. Here in Part 2 similar comments can be applied to the transfer functions representing grinding wheel wear and the corresponding development of a ground surface shown in Figures 12.12 and 12.11 respectively.

Regression lines in both diagrams are below unity which means that the area beneath the spectral curve representing the output is less than that for the input. The simplest interpretation is that the standard deviation of surface profile heights is reduced by grinding wheel wear: a virtually identical conclusion to that formulated in Part 1.

Results presented here in the form of standard deviation spectra contain significantly more information than the above Part 1 result because the spectrum provides not only an estimate of standard deviation for the profile but also the distribution of this parameter with respect to frequency.

Spectral curves appear to provide the best combination of readily interpreted surface profile characteristics to be had in a single parameter. Using standard deviation spectra it is possible to estimate the relative contributions to surface profile content of a given frequency band. Also the easily obtainable transfer functions facilitate quantitative comparison between profiles in terms of standard deviation.

Although the transfer functions derived from standard deviation spectra show a strong linear correlation, individual transfer coefficients deviate appreciably from the regression lines. Direct comparison between regression lines (Figure 12.13) shows these to be clearly differentiated in terms of slope and intercept but the position is seen to be less satisfactory when these differences are considered in relation to the width of the 95 per cent confidence bands.

If it is accepted that these deviations represent random errors relative to a straight line several possible and perhaps interrelated causes can be suggested.

Errors will arise at various stages of data collection and computation. Firstly in connection with digitizing measured surface profile ordinates and secondly in connection with the actual computation which will inevitably be affected by rounding errors. Any spectral curve represents an estimate of some ideal spectrum and smoothing is necessary in order to approach this optimum. Over smoothing will result in suppression of real surface profile characteristics and little or no guidance appears to be available regarding the extent of smoothing necessary other than by visual inspection of trial spectra.

Inspection of the tables of ordinates defining the various spectra shows apparently random deviations from a smooth curve particularly evident in the case of the smaller ordinates associated with the higher frequencies. These deviations will obviously affect the transfer coefficient ratios between corresponding pairs of ordinates.

There is also a possibility that spectra may have been adversely affected by the method of dealing with gaps in the profile caused by voids in the grinding wheel, which are recorded as zero ordinates. However, comparison between tables of spectral density ordinates representing grinding wheel surfaces with those representing ground surfaces does not reveal the former to be inferior. Furthermore inclusion of data to represent voids in some way is clearly essential because the extent and distribution of these defines the spacing of abrasive grit surfaces within the profile.

Samples of 100 profile ordinates have been shown to be quite inadequate for spectral density computation and increasing this to 1000 ordinates, a limit imposed by the equipment, produced a striking improvement.

Samples of intermediate sizes produced somewhat inferior results suggesting that samples of 1000 were by no means too large.

In order to provide clear visual differentiation between spectra various methods of plotting have been used. In Chapter 10, variance spectral density is plotted on a logarithmic scale versus frequency (Fig. 10.28). In Chapter 11 the square root of variance spectral density has been plotted while in Chapter 12, ordinates were obtained by raising spectral density to the power $\frac{2}{3}$. Each of these methods has been shown to facilitate visual comparison between surface profiles so represented.

An objection to the 'standard deviation spectra' of Chapter 12 is that standard deviation (unlike variance) is not additive. bearing in mind this objection the idea of a standard deviation spectrum can be avoided as follows.

The transfer function from the input profile to the output profile (i.e. from the grinding wheel to the ground surface) is

$$H(\omega) = \frac{f_o(\omega)}{f_i(\omega)}$$

where $f_i(\omega)$ and $f_o(\omega)$ are the variance spectral density functions of the input and output profiles respectively. Then the transfer function is characterised by finding a power of a such that

$$[H(\omega)]^a = \text{a linear function of } \omega .$$

In effect, the transfer function of Chapters 11 and 12 were characterised by taking a as $\frac{1}{2}$ and $\frac{2}{3}$ respectively. Of these the first is seen to provide the closer approx--imation to linearity.

The extent of the work involved in computing and presenting spectral curves and related information in this thesis may not be altogether apparent from the text. To convey this adequately would involve tediously dwelling upon difficulties with hardware and software and upon details of the methods and expedients adopted to overcome them. Nevertheless it is evident that much more remains to be done with considerable emphasis on the equipment and methods of spectral computation. However, it is believed that sufficient evidence has been presented to justify continuation of work on these lines and that the concept of spectral density applied to standard deviation provides a convenient and appropriate parameter for use in future work.

Work relating to the composite grinding wheel has not so far been mentioned in these conclusions. This was commenced at a stage when further statistical investigation of the profiles of bonded grinding wheels appeared to present insuperable difficulty.

Further developments brought about a partial reversal of this situation and it was decided to concentrate upon the latter, which now appeared to offer prospects of significant progress towards an understanding of surface texture problems in grinding. No conclusions are presented relating to results obtained with the composite grinding wheel because of a lack of confidence in the results available when work was discontinued. However, subject to improvements, the device itself is believed to represent a potentially useful tool for investigation into the grinding process where study of surface texture may not be the primary objective.

(20) Myers, N. O. Characterization of Surface Roughness. Wear, 5 (1962) 182-189

(21) Peklenik, J. Contribution to the Correlation Theory for the Grinding Process. A.S.M.E. Trans., J. of Eng. for Industry, May 1964, 85-94

(22) Peklenik, J. Grundlagen zur Korrelationstheorie technischer Oberflachen (Principles of the Correlation Theory for Commercial Surfaces). Industrie-Anzeiger, Essen, 1965, 456-462

(23) Williamson, J.B.P. Microtopography of Surfaces. Proc Instn Mech Engrs 1967-68 Vol 182 Pt 3K, 21-30

(24) Peklenik, J. Investigation of the Surface Typology. Annals of the C.I.R.P. Vol. XV, 1967, 381-384

(25) Peklenik, J. New Developments in Surface Characterization and Measurements by means of Random Process Analysis. Proc Instn Mech Engrs 1967-68 Vol 182 Pt 3K, 108-125

(26) Stralkowski, C.M. Wu, S.M. DeVor, R.E. Characterization of Grinding Wheel Profiles by Autoregressive-Moving Average Models. Int J Mach Tool Des Res Vol 9, 145-163, 1969

(27) Shinaishin, O.A. Stochastic Processes in Grinding. Stochastic Processes in Dynamical Problems 1969. Los Angeles, Nov 1969, Symposium at ASME Winter Annual Meeting. 75-93.

(28) Deutsch, S.J. Wu, S.M. Selection of Sampling Parameters for Modeling Grinding Wheels. ASME Trans J of Eng for Industry August 1970, 667-676.

(29) Masashi Harada — Akira Kobayashi — Producing a Mirror Surface Ground by Ultrasonic-dressed Wheels. Annals of the C.I.R.P. Vol XVIV, 1971, 361-367

(30) Gordon J. Jones — A Study of the Surface Finish Produced by Grinding. Research Thesis for the Degree of M. Tech. Brunel University 1972.

(31) Bhateja, C. P. — Chisholm, A. W. J. — Pattinson, E. J. — The Influence of Grinding Wheel Wear and Dressing on the Quality of Ground Surfaces. New New Developments in Grinding. Proc. of Int. Grinding Conf. April 18-20, 1972, Carnegie Press, Pittsburgh.

(32) Motoyoshi Hasegawa — Statistical Analysis for the Generating Mechanism of Ground Surface Roughness. Wear Vol 29 No 1 (1974), 31-39.

(33) Deutsch, S.J. A New Irregular Surface Measuring
Wu, S.M. System. Int. J. Mach. Tool Des. Res.
Stralkowski, C.M. Vol 13, 1973, 29-42.

(34) Thompson, D.L. Grinding Wheel Topography and
Malkin, S. Undeformed Chip Shape.
Proc Int Conf Prod Engng
Tokyo, Japan, 1974 (Part 1)
727-732

(35) Bhateja, C.P. On the Mechanism of the Diamond
Dressing of Grinding Wheels.
Proc Int Conf Prod Engng.
Tokyo, Japan, 1974 (Part 1)
733-739

(36) Zohdi, M.E. — Statistical Analysis, Estimation, and Optimization of Surface Finish in the Grinding Process. ASME Trans J of Engng for Industry Feb 1974, 117-123.

(37) Friedman, M.Y., Wu, S.M., Suratkar, P.T. — Determination of Geometric Properties of Coated Abrasive Cutting Edges. ASME Trans., J of Engng for Industry, Nov 1974, 1239-1244.

(38) Lal, G.K., Shaw, M.C. — The Role of Grain Tip Radius in Fine Grinding. ASME Trans, J of Engng for Industry, Aug 1975, 1119- 1125.

(39) König, W.
Lortz, W.

Properties of cutting edges related to chip formation in grinding.
Annals of the CIRP Vol 24/1/1975
231-235.

(40) Whitehouse, D.J.

Some ultimate limits on the measurement of surfaces using stylus techniques.
Measurement and Control, Vol 8, Apr 1975, 147- 151.

(41) Fugelso, M.
Wu, S.M.

Digital oscillating stylus profile measuring device.
Int. J. Mach. Tool Des. Res., Vol 17, 1977, 191-195.

(42) Nassirpour, F. Wu, S.M. Characterization and Analysis of Grinding Wheel Topography as a Stochastic Isotropic Surface. ASME Trans, J of Engng for Industry, May 1979, Vol 101, 165-170

APPENDIX 9

Table 9.2 Test Data

(100 values of Sinθ at intervals of $\frac{\pi}{2}$)

```
1000 DATA 0,1,0,-1,0,1,0,-1,0,1,0,-1
1010 DATA 0,1,0,-1,0,1,0,-1,0,1,0,-1
1020 DATA 0,1,0,-1,0,1,0,-1,0,1,0,-1
1030 DATA 0,1,0,-1,0,1,0,-1,0,1,0,-1
1040 DATA 0,1,0,-1,0,1,0,-1,0,1,0,-1
1050 DATA 0,1,0,-1,0,1,0,-1,0,1,0,-1
1060 DATA 0,1,0,-1,0,1,0,-1,0,1,0,-1
1070 DATA 0,1,0,-1,0,1,0,-1,0,1,0,-1
1080 DATA 0,1,0,-1
```

Table 9.3 Input and Output Data obtained from Profilograms of a Grinding Wheel and Ground Surface

1000	DATA	0	0	0	0	16.0	17.8
1010	DATA	6	0	0	0	0	0
1020	DATA	0	0	7.5	17.8	16.8	18.0
1030	DATA	17.6	17.0	5.0	0	0	0
1040	DATA	0	0	0	0	0	0
1050	DATA	0	0	0	4.0	4.6	5.0
1060	DATA	4.3	6.0	3.0	2.3	2.0	2.0
1070	DATA	2.8	0	0	0	0	0
1080	DATA	0	0	0	0	2.0	4.7
1090	DATA	1.5	0	0	0	0	0
1100	DATA	0	0	0	0	0	0
1110	DATA	0	0	0	0	7.0	16.0
1120	DATA	13.5	4.0	0	0	0	0
1130	DATA	0	0	0	0	0	0
1140	DATA	0	10.0	16.5	17.9	17.8	12.5
1150	DATA	5.0	0	0	0	0	0
1160	DATA	10.0	10.0	8.0	5.0		
1500	DATA	11.0	10.8	9.2	10.4	10.4	10.0
1510	DATA	9.7	10.1	11.0	10.5	11.0	10.5
1520	DATA	9.4	9.6	9.2	9.6	9.0	7.0
1530	DATA	9.2	9.3	8.4	8.8	9.7	10.1
1540	DATA	9.4	9.4	9.2	10.7	11.0	11.0
1550	DATA	11.0	11.0	11.2	12.0	12.3	12.1
1560	DATA	11.0	10.7	11.9	12.8	13.3	12.2
1570	DATA	12.0	11.4	11.7	11.9	11.8	11.0
1580	DATA	10.8	11.5	11.0	11.8	9.4	11.0
1590	DATA	12.0	13.0	12.5	12.3	11.2	12.2
1600	DATA	10.0	13.2	10.5	10.9	9.2	10.9
1610	DATA	11.5	10.3	9.7	10.0	10.4	11.2
1620	DATA	9.5	10.0	9.3	9.6	9.8	9.7
1630	DATA	8.0	8.5	10.6	9.8	10.7	10.5
1640	DATA	10.4	10.8	9.9	10.8	10.1	10.5
1650	DATA	9.3	9.3	9.3	9.4	9.0	9.2
1660	DATA	7.0	9.0	9.8	9.5		

(Values tabulated are ordinates measured at intervals of 0.1 inch)

Table 9.4

TABLE C FOR SAMPLE POWER SPECTRA [illegible]

ORDINATE (INCHES)	237.917 MJ41I	328.397 MJ41Z	100.796 MJ43I	70.664 MJ44I	57.737 MJ46I	51.1577 MJ47I	116.237 MJ48I	285.816 MJ49I	54.5714 MJ50I	181.727 MJ51I	22.3729 MJ52I	94.8631 MJ53I	15.1114 MJ54I	6.44421 MJ58I	11.6706 MJ59I	24.2529 MT60T	14.4967 MT6[illegible]
0.1	1.5	2.0	0.5	0.5	0.5	0.0	1.0	2.0	0.5	1.0	0.0	0.5	0.0	0.0	0.0	0.0	
0.2	3.0	4.5	1.5	1.0	1.0	"	1.5	4.0	0.5	2.5	0.5	1.5	0.2	0.0	0.0	0.5	
0.3	5.0	6.5	2.0	1.5	1.0	"	2.5	5.5	1.0	3.5	0.5	2.0	0.2	0.0	0.0	0.5	
0.4	6.5	9.0	2.5	2.0	1.5	"	3.0	7.5	1.5	5.0	0.5	2.5	0.4	0.0	0.5	0.5	
0.5	8.0	11.0	3.5	2.5	2.0	"	4.0	9.5	2.0	6.0	0.5	3.0	0.4	0.2	0.5	1.0	
0.6	9.5	13.0	4.0	3.0	2.5	0.2	4.5	11.5	2.0	7.5	1.0	4.0	0.6	0.2	0.5	1.0	
0.7	11.0	15.5	4.5	4.0	2.5	"	5.5	13.5	2.5	8.5	1.0	4.5	0.6	0.2	0.5	1.0	
0.8	12.5	17.5	5.5	4.5	3.0	"	6.0	15.0	3.0	9.5	1.0	5.0	0.8	0.2	0.5	1.5	
0.9	14.5	20.0	6.0	5.0	3.5	0.3	7.0	17.0	3.5	11.0	1.5	5.5	0.8	0.2	0.5	1.5	
1.0	16.0	22.0	6.5	5.5	4.0	"	7.5	19.0	3.5	12.0	1.5	6.5	1.0	0.4	1.0	1.5	
1.1	17.5	24.0	7.5	6.0	4.0	"	8.5	21.0	4.0	13.5	1.5	7.0	1.0	0.4	1.0	2.0	
1.2	19.0	26.5	8.0	6.5	4.5	0.4	9.5	23.0	4.5	14.5	2.0	7.5	1.2	0.4	1.0	2.0	
1.3	20.5	28.5	8.5	7.0	5.0	"	10.0	25.0	4.5	15.5	2.0	8.0	1.4	0.4	1.0	2.0	
1.4	22.0	30.5	9.5	7.5	5.5	"	11.0	26.5	5.0	17.0	2.0	9.0	1.4	0.6	1.0	2.5	
1.5	24.0	33.0	10.0	8.0	5.5	0.5	11.5	28.5	5.5	18.0	2.0	9.5	1.6	0.6	1.0	2.5	
1.6	25.5	35.0	11.0	8.5	6.0	"	12.5	30.5	6.0	19.5	2.5	10.0	1.6	0.6	1.0	2.5	
1.7	27.0	37.0	11.5	9.0	6.5	"	13.0	32.5	6.0	20.5	2.5	11.0	1.8	0.6	1.5	2.5	
1.8	28.5	39.5	12.0	9.5	7.0	0.6	14.0	34.5	6.5	22.0	2.5	11.5	1.8	0.6	1.5	3.0	
1.9	30.0	41.5	13.0	10.0	7.5	"	14.5	36.0	7.0	23.0	3.0	12.0	2.0	0.8	1.5	3.0	
2.0	31.5	44.0	13.5	11.0	7.5	0.7	15.5	38.0	7.5	24.0	3.0	12.5	2.0	0.8	1.5	3.0	
2.1	33.5	46.0	14.0	11.5	8.0	"	16.5	40.0	7.5	25.5	3.0	13.5	2.2	0.8	1.5	3.5	
2.2	35.0	48.0	15.0	12.0	8.5	"	17.0	42.0	8.0	26.5	3.5	14.0	2.2	0.8	1.5	3.5	
2.3	36.5	50.5	15.5	12.5	9.0	"	18.0	44.0	8.5	28.0	3.5	14.5	2.4	0.8	2.0	3.5	
2.4	38.0	52.5	16.0	13.0	9.0	0.8	18.5	45.5	8.5	29.0	3.5	15.0	2.6	1.0	2.0	4.0	
2.5	39.5	54.5	17.0	13.5	9.5	"	19.5	47.5	9.0	30.5	3.5	16.0	2.6	1.0	2.0	4.0	
2.6	41.0	57.0	17.5	14.0	10.0	"	20.0	49.5	9.5	31.5	4.0	16.5	2.8	1.0	2.0	4.0	
2.7	43.0	59.0	18.0	14.5	10.5	0.9	21.0	51.5	10.0	32.5	4.0	17.0	2.8	1.0	2.0	4.5	
2.8	44.5	61.5	19.0	15.0	10.5	-	21.5	53.5	10.0	34.0	4.0	17.5	3.0	1.2	2.0	4.5	
2.9	46.0	63.5	19.5	15.5	11.0	-	22.5	55.5	10.5	35.0	4.5	18.5	3.0	1.2	2.5	4.5	
3.0	47.5	65.5	20.0	16.0	11.5	1.0	23.0	57.0	11.0	36.5	4.5	19.0	3.2	1.2	2.5	5.0	
3.1	49.0	68.0	21.0	16.5	12.0	"	24.0	59.0	11.5	37.5	4.5	19.5	3.2	1.2	2.5	5.0	
3.2	51.0	70.0	21.5	17.0	12.0	"	25.0	61.0	11.5	39.0	5.0	20.0	3.4	1.2	2.5	5.0	
3.3	52.5	72.0	22.0	18.0	12.5	1.1	25.5	63.0	12.0	40.0	5.0	21.0	3.4	1.4	2.5	5.5	
3.4	54.0	74.5	23.0	18.5	13.0	"	26.5	65.0	12.5	41.0	5.0	21.5	3.6	1.4	2.5	5.5	
3.5	55.5	76.5	23.5	19.0	13.5	"	27.0	66.5	12.5	42.5	5.0	22.0	3.6	1.4	2.5	5.5	
3.6	57.0	79.0	24.0	19.5	14.0	1.2	28.0	68.5	13.0	43.5	5.5	23.0	3.8	1.4	3.0	6.0	
3.7	58.5	81.0	25.0	20.0	14.0	"	28.5	70.5	13.5	45.0	5.5	23.5	3.8	1.4	3.0	6.0	
3.8	60.5	83.0	25.5	20.5	14.5	"	29.5	72.5	14.0	46.0	5.5	24.0	4.0	1.6	3.0	6.0	
3.9	62.0	85.5	26.0	21.0	15.0	"	30.0	74.5	14.0	47.0	6.0	24.5	4.0	1.6	3.0	6.5	
4.0	63.5	87.5	27.0	21.5	15.5	1.4	31.0	76.0	14.5	48.5	6.0	25.5	4.2	1.6	3.0	6.5	
4.1	65.0	90.0	27.5	22.0	15.5	"	32.0	78.0	15.0	49.5	6.0	26.0	[illegible]	1.6	3.0	6.5	
4.2	66.5	92.0	28.0	22.5	16.0	"	32.5	80.0	15.5	51.0	6.5	26.5	4.4	1.8	3.5	7.0	
4.3	68.0	94.0	29.0	23.0	16.5	-	33.5	82.0	15.5	52.0	6.5	27.0	4.6	1.8	3.5	7.0	
4.4	70.0	96.5	29.5	23.5	17.0	1.5	34.0	84.0	16.0	53.5	6.5	28.0	4.6	1.8	3.5	7.0	
4.5	71.5	98.5	30.0	24.0	17.0	-	35.0	86.0	16.5	54.5	6.5	28.5	4.8	1.8	3.5	7.5	
4.6	73.0	101.0	31.0	24.5	17.5	"	35.5	87.5	16.5	55.5	7.0	29.0	4.8	1.8	3.5	7.5	
4.7	74.5	103.0	31.5	25.5	18.0	"	36.5	89.5	17.0	57.0	7.0	29.5	5.0	2.0	3.5	7.5	
4.8	76.0	105.0	32.5	26.0	18.5	"	37.0	91.5	17.5	58.0	7.0	30.5	5.0	2.0	3.5	8.0	
4.9	77.5	107.5	33.0	26.5	18.5	"	38.0	93.5	18.0	59.5	7.5	31.0	5.2	2.0	4.0	8.0	
5.0	79.5	109.5	33.5	27.0	19.0	1.5	38.5	95.5	18.0	60.5	7.5	31.5	5.4	2.0	4.0	8.0	5.0

SEE ORDINATE COLUMN

Highest ordinate value of the series MJ41Z & MT70T = 328.393 [illegible] values in table are calculated from scale factor × 100/328.393 × ordinate [illegible] values = 15 × 0.0006 [illegible] / 15
The results are plotted in mm

Table 9.5

TABLE B. FOR NORMALIZED POWER SPECTRA 6/12/72

Ordinate (inches)	0.069	0.042605	0.016302	0.012618	0.012634	0.0198578	0.0176266	0.0392452	0.0125216	0.0470312	0.0089772	0.0290865	0.00714662	0.0132202	0.0201517	0.0281765	0.0140451
0.1	2.0	1.2	0.5	0.5	OMIT	0.5	0.5	1.0	OMIT [illegible]	1.5	0.5	1.0	0.0	0.5	0.5	OMIT [illegible]	0.5
0.2	3.9	2.4	1.0	0.5		1.0	1.0	2.0		2.5	0.5	1.5	0.5	1.0	1.0		1.0
0.3	5.9	3.7	1.5	1.0		1.5	1.5	3.5		4.0	1.0	2.5	0.5	1.0	1.5		1.5
0.4	7.9	4.9	2.0	1.5		2.5	2.0	4.5		5.5	1.0	3.5	1.0	1.5	2.5		1.5
0.5	9.9	6.1	2.5	2.0		3.0	2.5	5.5		6.5	1.0	4.0	1.0	2.0	3.0		2.0
0.6	11.8	7.3	3.0	2.0		3.5	3.0	6.5		8.0	1.5	5.0	1.0	2.5	3.5		2.5
0.7	13.8	8.5	3.5	2.5		4.0	3.5	8.0		9.5	2.0	6.0	1.5	2.5	4.0		3.0
0.8	15.8	9.7	3.5	3.0		4.5	4.0	9.0		10.5	2.0	6.5	1.5	3.0	4.5		3.5
0.9	17.7	11.0	4.0	3.0		5.0	4.5	10.0		12.0	2.5	7.5	2.0	3.5	5.0		4.0
1.0	19.7	12.2	4.5	3.5		5.5	5.0	11.0		13.5	2.5	8.5	2.0	4.0	6.0		4.0
1.1	21.7	13.4	5.0	4.0		6.0	5.5	12.5		15.0	3.0	9.0	2.0	4.0	6.5		4.5
1.2	23.7	14.6	5.5	4.5		7.0	6.0	13.5		16.0	3.0	10.0	2.5	4.5	7.0		5.0
1.3	25.6	15.8	6.0	4.5		7.4	6.5	14.5		17.5	3.5	11.0	2.5	5.0	7.5		5.5
1.4	27.6	17.0	6.5	5.0		8.0	7.0	15.5		19.0	3.5	11.5	3.0	5.5	8.0		6.0
1.5	29.6	18.3	7.0	5.5		8.5	7.5	17.0		20.0	4.0	12.5	3.0	5.5	8.5		6.5
1.6	31.5	19.5	7.5	6.0		9.0	8.0	18.0		21.5	4.0	13.5	3.5	6.0	9.0		7.0
1.7	33.5	20.7	8.0	6.0		9.5	8.5	19.0		23.0	4.5	14.0	3.5	6.5	10.0		7.0
1.8	35.5	21.9	8.5	6.5		10.2	9.0	20.0		24.0	4.5	15.0	3.5	7.0	10.5		7.5
1.9	37.5	23.1	9.0	7.0		11.0	9.5	21.5		25.5	5.0	16.0	4.0	7.0	11.0		8.0
2.0	39.4	24.3	9.5	7.0		11.5	10.0	22.5		27.0	5.0	17.0	4.0	7.5	11.5		8.5
2.1	41.4	25.6	9.5	7.5		12.0	10.5	23.5		28.0	5.5	17.5	4.5	8.0	12.0		9.0
2.2	43.4	26.8	10.0	8.0		12.5	11.0	24.5		29.5	5.5	18.5	4.5	8.5	12.5		9.5
2.3	45.3	28.0	10.5	8.5		13.0	11.5	26.0		31.0	6.0	19.0	4.5	8.5	13.0		10.0
2.4	47.3	29.2	11.0	8.5		14.0	12.0	27.0		32.0	6.0	20.0	5.0	9.0	14.0		10.0
2.5	49.3	30.4	11.5	9.0		14.0	12.5	28.0		33.5	6.5	21.0	5.0	9.5	14.5		10.5
2.6	51.3	31.6	12.0	9.5		15.0	13.0	29.0		35.0	6.5	22.0	5.5	10.0	15.0		11.0
2.7	53.2	32.9	12.5	9.5		15.5	13.5	30.5		36.5	7.0	22.5	5.5	10.0	15.5		11.5
2.8	55.2	34.1	13.0	10.0		16.0	14.0	31.5		37.5	7.0	23.5	5.5	10.5	16.0		12.0
2.9	57.2	35.3	13.5	10.5		16.5	14.5	32.5		39.0	7.5	24.0	6.0	11.0	16.5		12.5
3.0	59.1	36.5	14.0	11.0		17.0	15.0	33.5		40.5	7.5	25.0	6.0	11.5	17.0		12.5
3.1	61.1	37.7	14.5	11.0		17.5	15.5	35.0		41.5	8.0	26.0	6.5	11.5	18.0		13.0
3.2	63.1	38.9	15.0	11.5		18.0	16.0	36.0		43.0	8.0	26.5	6.5	12.0	18.5		13.5
3.3	65.1	40.2	15.5	12.0		18.5	16.5	37.0		44.5	8.5	27.5	6.5	12.5	19.0		14.0
3.4	67.0	41.4	16.0	12.5		19.5	17.0	38.0		45.5	8.5	28.5	7.0	13.0	19.5		14.5
3.5	69.0	42.6	16.5	12.5		20.0	17.5	39.0		47.0	9.0	29.0	7.0	13.0	20.0		15.0
3.6	71.0	43.8	17.0	13.0		20.5	18.0	40.5		48.5	9.0	30.0	7.5	13.5	21.0		15.0
3.7	72.9	45.0	17.0	13.5		21.0	18.5	41.5		49.5	9.5	31.0	7.5	14.0	21.5		15.5
3.8	74.9	46.3	17.5	13.5		21.5	19.0	42.5		51.0	9.5	31.5	8.0	14.5	22.0		16.0
3.9	76.9	47.5	18.0	14.0		22.0	19.5	43.5		52.5	10.0	32.5	8.0	14.5	22.5		16.5
4.0	78.9	48.7	18.5	14.5		22.5	20.0	45.0		53.5	10.0	33.0	8.0	15.0	23.0		17.0
4.1	80.8	49.9	19.0	15.0		23.5	20.5	46.0		55.0	10.5	34.0	8.5	15.5	23.5		17.5
4.2	82.8	51.1	19.5	15.0		24.0	21.0	47.0		56.5	10.5	35.0	8.5	16.0	24.0		18.0
4.3	84.8	52.3	20.0	15.5		24.5	21.5	48.0		58.0	11.0	35.5	9.0	16.0	25.0		18.0
4.4	86.7	53.6	20.5	16.0		25.0	22.0	49.5		59.0	11.0	36.5	9.0	16.5	25.5		18.5
4.5	88.7	54.8	21.0	16.0		25.5	22.5	50.5		60.5	11.5	37.5	9.0	17.0	26.0		19.0
4.6	90.7	56.0	21.5	16.5		26.0	23.0	51.5		62.0	11.5	38.0	9.5	17.5	26.5		19.5
4.7	92.7	57.2	22.0	17.0		26.5	23.5	52.5		63.0	12.0	39.0	9.5	18.0	27.0		20.0
4.8	94.6	58.4	22.5	17.5		27.0	24.0	54.0		64.5	12.0	40.0	10.0	18.0	27.5		20.5
4.9	96.6	59.6	23.0	17.5		28.0	24.5	55.0		66.0	12.5	41.0	10.0	18.5	28.0		21.0
5.0	98.6	60.9	23.0	18.0	18.0	28.5	25.2	56.1	17.9	67.2	12.5	41.6	10.0	19.0	29.0	41.0	21.0
	1	2	3	4	5	6	7	8	9	10	11	12	13	14	15	16	17

Values in Column 3, 6, 17 are rounded to 0.5 [illegible]

Values in table are given by scale factor × $\frac{100}{0.07 \times 5}$ × ordinate in inches
= scale factor × $\frac{20}{0.07}$ × ordinate in inches.

0.07 = [illegible] for the first [illegible] longest ordinate in table

Table 9.6

TABLE B (CONTINUED) 3/1/78. FOR NORMALIZED POWER SPECTRA

Ordinate (inches)	0.0576584 (MJ62I)	0.0554021 (MJ63I)	0.0613807 (MJ64I)	0.0190052 (MJ65I)	0.0121187 (MJ66I)	0.0639844 (MJ67I)	0.0227217 (MJ68I)	0.0115416 (MJ69I)	0.0241184 MJ70I
0.1	1.5	1.5	2.0	0.5		2.0	0.5	0.5	0.5
0.2	3.5	3.0	3.5	1.0		3.5	1.5	0.5	1.5
0.3	5.0	4.5	5.5	1.5	ONLY SEE COLUMNS 4,5	5.5	2.0	1.0	2.0
0.4	6.5	6.5	7.5	2.0		7.5	2.5	1.5	3.0
0.5	8.0	8.0	9.5	2.5		9.0	3.0	1.5	3.5
0.6	10.0	9.5	11.0	3.5		11.0	4.0	2.0	4.0
0.7	11.5	11.0	13.0	4.0		13.0	4.5	2.5	5.0
0.8	13.0	12.5	15.0	4.5		14.5	5.0	2.5	5.5
0.9	15.0	14.0	17.0	5.0		16.5	6.0	3.0	6.0
1.0	16.5	16.0	18.5	5.5		18.0	6.5	3.5	7.0
1.1	18.0	17.5	20.5	6.0		20.0	7.0	3.5	7.5
1.2	20.0	19.0	22.5	6.5		22.0	8.0	4.0	8.5
1.3	22.0	20.5	24.5	7.0		24.0	8.5	4.0	9.0
1.4	23.5	22.0	26.0	7.5		25.5	9.0	4.5	9.5
1.5	25.0	23.5	28.0	8.0		27.5	9.5	5.0	10.5
1.6	27.0	25.5	30.0	8.5		29.0	10.5	5.5	11.0
1.7	28.5	27.0	32.0	9.0		31.0	11.0	6.0	11.5
1.8	30.0	28.5	33.5	10.0		33.0	11.5	6.0	12.5
1.9	32.0	30.0	35.5	10.5		34.5	12.5	6.5	13.0
2.0	33.5	31.5	37.5	11.0		36.5	13.0	7.0	14.0
2.1	35.0	33.0	39.5	11.5		38.5	13.5	7.0	14.5
2.2	37.0	35.0	41.0	12.0		40.0	13.5	7.5	15.0
2.3	38.5	36.5	43.0	12.5		42.0	15.0	8.0	16.0
2.4	40.5	38.0	45.0	13.0		44.0	15.5	8.0	16.5
2.5	42.0	39.5	47.0	13.5		45.5	16.0	8.5	17.5
2.6	43.5	41.0	48.5	14.0		47.5	17.0	9.0	18.0
2.7	45.5	42.5	50.5	14.5		49.5	17.5	9.0	18.5
2.8	47.0	44.5	52.5	15.0		51.0	18.0	9.5	19.5
2.9	48.5	46.0	54.5	15.5		53.0	19.0	10.0	20.0
3.0	50.5	47.5	56.0	16.5		54.5	19.5	10.0	20.5
3.1	52.0	49.0	58.0	17.0		56.5	20.0	10.5	21.5
3.2	53.5	50.5	60.0	17.5		58.5	21.0	11.0	22.0
3.3	55.5	52.0	62.0	18.0		60.0	21.5	11.0	23.0
3.4	57.0	54.0	63.5	18.5		62.0	22.0	11.5	23.5
3.5	58.5	55.5	65.5	19.0		64.0	22.5	12.0	24.0
3.6	60.5	57.0	67.5	19.5		65.5	23.5	12.0	25.0
3.7	62.0	58.5	69.5	20.0		67.5	24.0	12.5	25.5
3.8	63.5	60.0	71.0	20.5		69.5	24.5	13.0	26.5
3.9	65.5	61.5	73.0	21.0		71.0	25.5	13.0	27.0
4.0	67.0	63.5	75.0	21.5		73.0	26.0	13.5	27.5
4.1	69.0	65.0	77.0	22.5		75.0	26.5	14.0	28.5
4.2	70.5	66.5	79.0	23.0		76.5	27.0	14.0	29.0
4.3	72.0	68.0	80.5	23.5		78.5	28.0	14.5	29.5
4.4	74.0	69.5	82.5	24.0		80.5	28.5	15.0	30.5
4.5	75.5	71.0	84.5	24.5		82.0	29.0	15.0	31.0
4.6	77.0	73.0	86.0	25.0		84.0	30.0	15.5	32.0
4.7	79.0	74.5	88.0	25.5		85.5	30.5	16.0	32.5
4.8	80.5	76.0	90.0	26.0		87.5	31.0	16.0	33.0
4.9	82.0	77.5	92.0	26.5		89.5	32.0	16.5	34.0
5.0	84.0	79.0	93.5	27.0		91.0	32.5	17.0	34.5

```
?ED
>1000 DATA 152,152,152,152,152,152
>FILE 'MJ411'
>NEW
>LOAD  'MACJ04'
>LOAD'MJ411'
>RUN
SAMPLE POWER SPECTRAL DENSITY FUNCTION F(W)
(22)N(SAMPLE SIZE)= 100
(1220) LAG NO. M= 67
(1225)F(ANG.FREQ.INTERVAL:PI/(10*F))= 10
(4130)E(VERTICAL SCALE FACTOR:RANGE 50*F)= 237.933
MAX.F(W)= 11396.7 MIN.F(W)= 0
```

```
OK, ED
GO
INPUT
1000 DATA 152,152,152,152,152,152
1010 DATA 152,152,152,152,152,152
1020 DATA 152,152,152,152,152,152
1030 DATA 152,152,152,152,152,152
1040 DATA 152,152,152,152,152,152
1050 DATA 152,152,151,151,151,151
1060 DATA 150,150,149,149,149,149
1070 DATA 149,149,148,148,148,148
1080 DATA 147,147,146,145,143,141
1090 DATA 133,103,072,037,009,015
1100 DATA 017,062,098,125,134,143
1110 DATA 143,121,095,071,047,047
1120 DATA 075,087,110,117,113,109
1130 DATA 105,097,081,070,052,031
1140 DATA 010,000,000,000,000,000
1150 DATA 000,000,000,000,000,000
1160 DATA 000,000,000,000

EDIT
FILE MJ411

OK, LBASIC
GO
>LOAD 'MJ411'
```

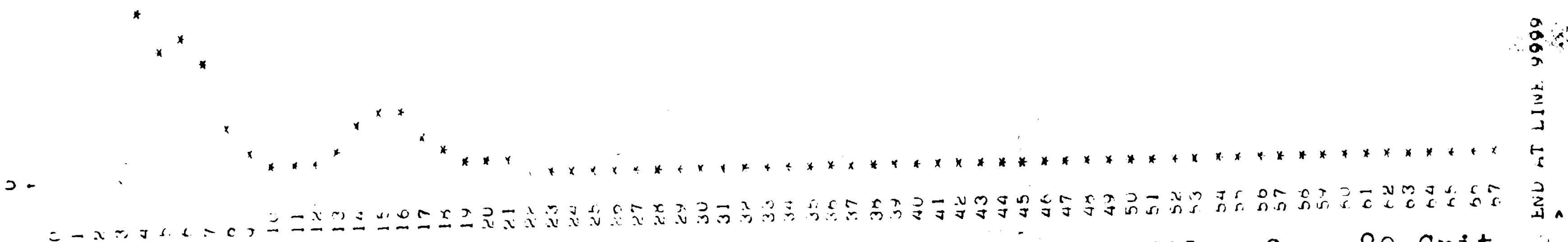

Fig.9.31 Sample Power Spectral Density Function for the Profile of an 80 Grit Grinding Wheel after 30 seconds Grinding. Normal Profilogram Magnification 1000

```
>FILE 'MJ47I'
>LOAD 'MACJO4'
>LOAD 'MJ47I'
>RUN
SAMPLE POWER SPECTRAL DENSITY FUNCTION F(W)
(22)N(SAMPLE SIZE)= 100
(1220) LAG NO. M= 67
(1225)F(AVG.FREQ.INTERVAL:PI/(10*F))= 10
(4130)E(VERTICAL SCALE FACTOR:RANGE 50*E)= 5.11573
MAX.F(W)= 255.787 MIN.F(W)= 0
```

```
OK, ED
GO
INPUT
1000 DATA 000,000,000,000,000,000
1010 DATA 000,000,000,000,000,021
1020 DATA 054,063,079,078,073,049
1030 DATA 016,000,000,000,000,000
1040 DATA 000,000,000,000,000,000
1050 DATA 000,000,000,000,000,000
1060 DATA 000,000,000,000,000,000
1070 DATA 000,000,000,000,000,000
1080 DATA 000,000,000,000,000,000
1090 DATA 000,000,000,000,000,000
1100 DATA 000,000,000,000,000,000
1110 DATA 000,000,000,000,000,000
1120 DATA 000,000,000,000,000,000
1130 DATA 000,000,000,000,000,000
1140 DATA 000,000,000,000,000,000
1150 DATA 000,000,000,000,000,000
1160 DATA 000,000,000,000

EDIT
FILE MJ47I

OK, LBASIC
GO
>LOAD 'MJ47I'
```

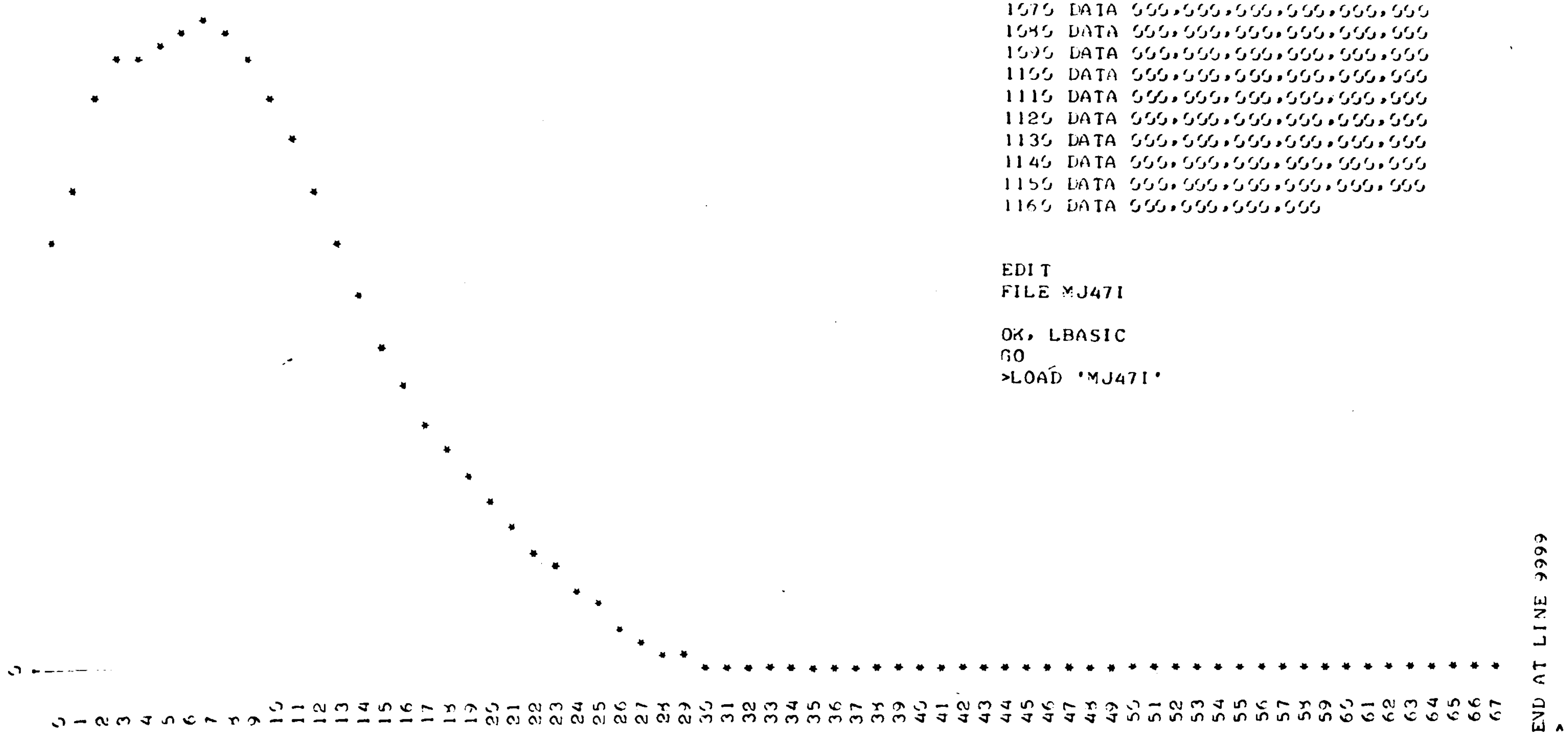

Fig. 9.32 Sample Power Spectral Density Function for the Profile of an 80 Grit Grinding Wheel after 5 minutes wear. Normal Profilogram Magnification 1000

```
>FILE'MJ49I'
>LOAD 'MACJ04'
>LOAD 'MJ49I'
>RUN
SAMPLE POWER SPECTRAL DENSITY FUNCTION F(W)
(22)N(SAMPLE SIZE)= 100
(1220) LAG NO. M= 67
(1225)F(ANG.FREQ.INTERVAL:PI/(10*F))= 10
(4130)E(VERTICAL SCALE FACTOR:RANGE 50*E)= 235.836
MAX.F(W)= 14291.3 MIN.F(W)= 0
```

```
OK, ED
GO
INPUT
1000 DATA 000,000,101,172,160,119
1010 DATA 087,079,064,023,000,000
1020 DATA 000,000,000,000,000,061
1030 DATA 185,224,232,198,223,232
1040 DATA 233,233,211,183,127,101
1050 DATA 102,102,093,053,020,001
1060 DATA 000,000,000,000,000,000
1070 DATA 000,000,000,000,000,000
1080 DATA 000,000,000,000,000,000
1090 DATA 000,000,031,141,139,130
1100 DATA 151,210,233,235,222,183
1110 DATA 116,068,030,004,000,000
1120 DATA 000,000,000,000,000,000
1130 DATA 000,000,000,000,000,000
1140 DATA 000,000,019,124,212,238
1150 DATA 223,157,098,031,000,000
1160 DATA 000,000,000,000

EDIT
FILE MJ49I

OK, LBASIC
GO
>LOAD 'MJ49I'
```

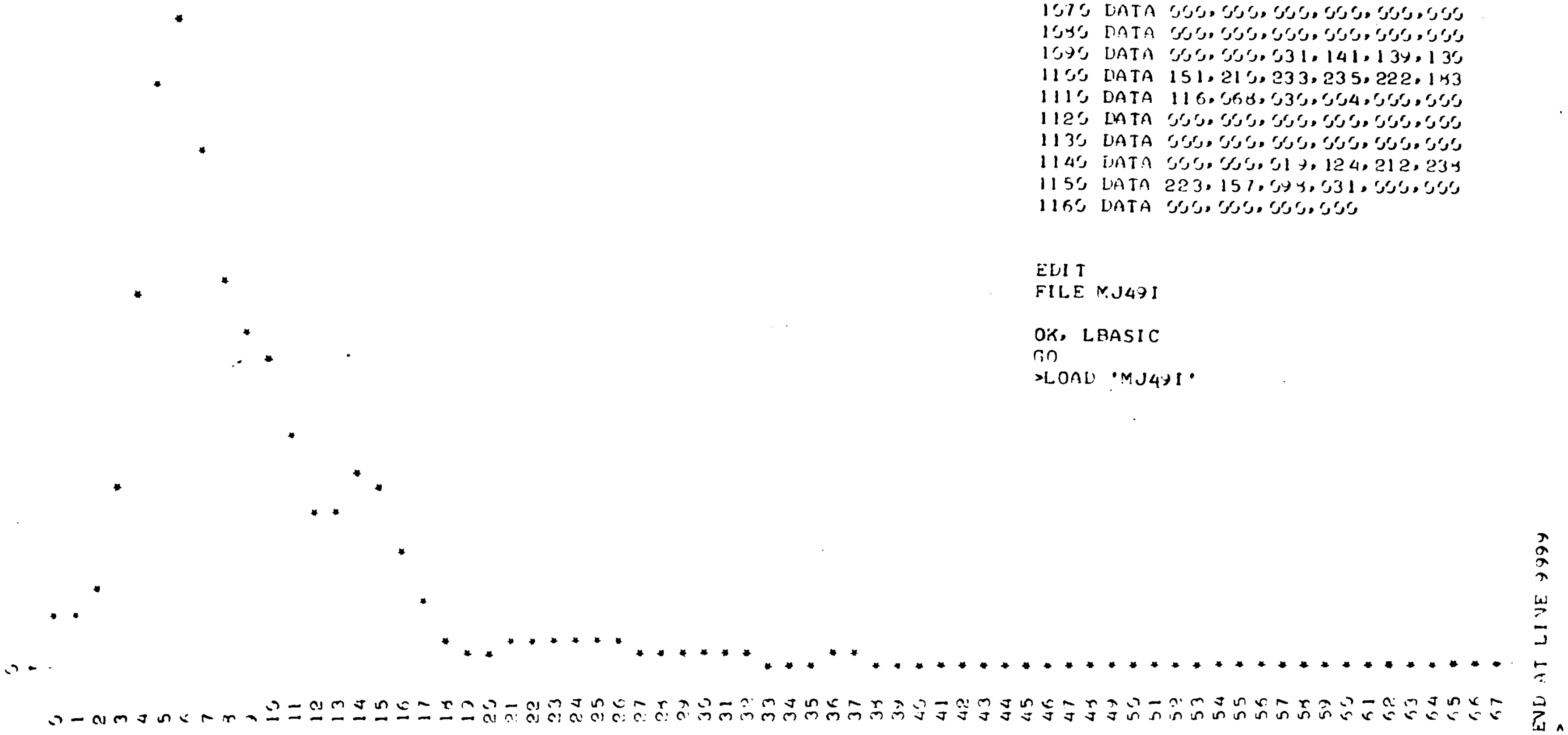

Fig. 9.33 Sample Power Spectral Density Function for the Profile of an 80 Grit Grinding Wheel after 5 minutes wear. Normal Profilogram Magnification 2000.

APPENDIX 10

Program MACJ04 with data representing 1000 grinding wheel surface profile ordinates

```
LOGIN STHUMP
STHUMP (4) LOGGED IN AT  11'04 06170
WELCOME STHUMP

OK, LBASIC
GO
>LOAD 'MACJ04'
>9026 PRINT 'GIVE LAG NO M'
>9027 INPUT M
>9028 PRINT 'GIVE VALUE FOR L'
>9029 INPUT L
>FILE 'MACJ04'
>LIST
   5  PRINT 'SAMPLE POWER SPECTRAL DENSITY FUNCTION F(w)'
  10  DIM X(1000)
  12  DIM C(1000)
  14  DIM w(1000)
  16  DIM S(100)
  18  DIM F(100)
  20  LET P=4*ATN(1)
  22  N=1000
  23  PRINT '(22)N(SAMPLE SIZE)=':N
  30  GOSUB 500
  32  GOSUB 7500
  33  GOSUB 9000
  34  GOSUB 100
  35  GOSUB 3000
  50  GOSUB 1500
  52  GOSUB 800
  57  GOSUB 4000
  58  GOSUB 7000
  59  GOSUB 6000
  60  GOSUB 3030
  70  GOTO 9999
 100  REM CALCULATE C(T)
 105  LET T=0
 110  LET K=1
 120  LET S(T)=0
 130  LET S(T)=S(T)+X(K)*X(K+T)
 140  IF K=N-T THEN 200
 150  LET K=K+1
 160  GOTO 130
 200  C(T)=S(T)/N
 210  LET T=T+1
 220  IF T=L+1 THEN 240
 230  GOTO 110
 240  FOR T=L+1 TO N
 250  C(T)=0
 260  NEXT T
 270  RETURN
 500  REM READ X
 510  FOR I=1 TO N
 520  READ X(I)
 530  NEXT I
 540  RETURN
 800  REM CALCULATE F(w)
 810  LET w=0
 820  LET T=1
 830  LET S=0
 840  LET S=w(T)*C(T)*COS(w*P*T/(10*F))+S
 850  IF T=M THEN 880
 860  LET T=T+1
 870  GOTO 840
 880  LET F(w)=(C(0)+2*S)/(2*P)
 890  LET w=w+1
 900  IF w=L+1 THEN 920
 910  GOTO 820
 920  RETURN
```

```
1000  DATA 152,152,152,152,152,152
1001  DATA 152,152,152,152,152,152
1002  DATA 152,152,152,152,152,152
1003  DATA 152,152,152,152,152,152
1004  DATA 152,152,152,152,152,152
1005  DATA 152,152,151,151,151,151
1006  DATA 150,150,149,149,149,149
1007  DATA 149,149,148,148,148,148
1008  DATA 147,147,146,145,143,141
1009  DATA 133,103,72,37,9,15
1010  DATA 17,62,98,125,134,143
1011  DATA 143,121,95,71,47,47
1012  DATA 70,87,110,117,113,109
1013  DATA 105,97,81,70,52,31
1014  DATA 10,0,0,0,0,0
1015  DATA 0,0,0,0,0,0
1016  DATA 0,0,0,0,0,0
1017  DATA 0,0,0,0,0,0
1018  DATA 0,34,35,71,122,143
1019  DATA 170,205,208,212,215,195
1020  DATA 163,141,137,127,100,58
1021  DATA 28,23,15,11,0,3
1022  DATA 1,0,0,0,0,0
1023  DATA 0,0,0,0,0,61
1024  DATA 125,171,167,153,126,101
1025  DATA 85,58,31,10,0,0
1026  DATA 0,0,0,0,0,0
1027  DATA 0,0,0,0,0,0
1028  DATA 0,0,0,0,0,0
1029  DATA 0,0,0,0,0,0
1030  DATA 0,0,0,0,0,0
1031  DATA 0,0,0,0,0,0
1032  DATA 0,0,0,0,0,0
1033  DATA 0,0,0,0,0,0
1034  DATA 0,0,0,0,0,0
1035  DATA 0,0,0,0,0,0
1036  DATA 0,0,0,0,0,0
1037  DATA 0,0,0,0,0,0
1038  DATA 0,0,0,0,0,0
1039  DATA 0,0,0,0,0,0
1040  DATA 0,0,0,0,0,0
1041  DATA 0,0,0,32,95,145
1042  DATA 177,184,213,185,162,138
1043  DATA 102,66,69,69,87,102
1044  DATA 117,140,153,160,169,193
1045  DATA 210,200,153,160,163,154
1046  DATA 143,129,169,189,210,221
1047  DATA 222,200,193,200,204,194
1048  DATA 167,138,152,103,55,17
1049  DATA 0,0,0,0,0,0
1050  DATA 42,103,173,199,208,215
1051  DATA 216,216,216,216,222,219
1052  DATA 220,186,145,102,55,9
1053  DATA 0,0,0,0,0,0
1054  DATA 0,0,0,0,0,0
1055  DATA 0,0,0,0,0,0
1056  DATA 0,0,0,0,0,0
1057  DATA 0,0,0,0,0,0
1058  DATA 0,0,0,0,0,0
1059  DATA 0,0,0,0,0,0
1060  DATA 0,0,0,0,0,0
1061  DATA 0,0,0,0,0,0
1062  DATA 0,0,0,0,0,0
1063  DATA 0,0,0,0,0,0
1064  DATA 0,0,0,0,0,11
1065  DATA 33,57,94,78,57,89
1066  DATA 113,123,149,151,147,139
1067  DATA 127,119,75,34,0,0
1068  DATA 0,0,0,0,0,0
1069  DATA 0,0,0,0,0,0
1070  DATA 0,0,0,56,103,147
1071  DATA 189,220,208,197,194,195
1072  DATA 194,187,181,180,165,145
1073  DATA 119,92,69,37,15,0
1074  DATA 0,0,0,0,0,0
1075  DATA 0,0,0,0,0,0
1076  DATA 0,0,0,0,16,37
1077  DATA 46,42,38,35,11,0
1078  DATA 0,0,0,0,0,0
1079  DATA 0,0,0,0,0,0
1080  DATA 0,0,0,0,0,0
1081  DATA 0,0,0,0,0,0
1082  DATA 0,0,0,0,0,0
```

```
1083  DATA 0,0,0,0,0,0
1084  DATA 0,0,0,0,0,0
1085  DATA 0,0,0,0,0,0
1086  DATA 0,0,0,0,0,0
1087  DATA 0,0,15,75,134,193
1088  DATA 216,228,229,229,222,209
1089  DATA 228,227,223,202,176,150
1090  DATA 121,105,81,101,125,127
1091  DATA 127,127,127,157,171,175
1092  DATA 194,225,196,168,140,115
1093  DATA 92,60,35,19,5,0
1094  DATA 0,0,0,0,0,0
1095  DATA 0,0,0,37,76,102
1096  DATA 112,145,159,159,156,155
1097  DATA 176,194,232,233,224,234
1098  DATA 235,242,241,233,229,218
1099  DATA 233,233,226,226,227,219
1100  DATA 193,171,147,125,102,63
1101  DATA 40,22,0,0,0,1
1102  DATA 25,41,57,63,69,76
1103  DATA 85,97,114,127,143,160
1104  DATA 177,189,191,188,199,199
1105  DATA 189,162,121,77,35,0
1106  DATA 0,0,0,0,0,0
1107  DATA 0,0,35,56,66,61
1108  DATA 47,47,37,7,0,0
1109  DATA 0,9,37,41,60,81
1110  DATA 110,130,156,183,203,203
1111  DATA 220,217,185,159,135,133
1112  DATA 129,118,91,52,8,0
1113  DATA 0,0,0,0,0,0
1114  DATA 0,0,0,0,0,0
1115  DATA 0,0,0,0,0,1
1116  DATA 4,16,44,84,123,129
1117  DATA 129,129,129,116,108,90
1118  DATA 74,57,49,27,0,0
1119  DATA 0,0,0,0,35,95
1120  DATA 159,191,201,217,228,229
1121  DATA 226,210,189,182,169,173
1122  DATA 172,127,86,45,2,0
1123  DATA 0,0,0,0,0,0
1124  DATA 0,0,21,63,106,107
1125  DATA 115,123,123,124,115,55
1126  DATA 43,13,0,0,0,0
1127  DATA 0,0,0,0,0,0
1128  DATA 0,0,0,0,0,0
1129  DATA 0,0,0,0,0,0
1130  DATA 0,0,0,0,0,0
1131  DATA 0,0,0,0,0,0
1132  DATA 0,0,0,0,0,0
1133  DATA 0,0,0,0,0,0
1134  DATA 0,0,0,0,0,0
1135  DATA 0,0,0,0,0,0
1136  DATA 0,0,26,75,101,132
1137  DATA 134,162,187,221,232,231
1138  DATA 225,232,218,198,190,205
1139  DATA 208,209,205,222,223,230
1140  DATA 226,209,177,148,187,199
1141  DATA 202,221,228,227,225,215
1142  DATA 230,229,220,218,207,151
1143  DATA 174,156,132,109,78,50
1144  DATA 15,0,0,0,0,0
1145  DATA 0,0,0,0,0,0
1146  DATA 0,0,0,0,0,0
1147  DATA 0,0,0,0,27,41
1148  DATA 50,50,52,85,108,89
1149  DATA 129,167,181,220,227,223
1150  DATA 183,143,140,125,109,84
1151  DATA 50,82,109,109,86,57
1152  DATA 15,0,0,0,0,0
1153  DATA 0,0,0,0,0,0
1154  DATA 0,0,0,0,0,0
1155  DATA 0,0,0,0,0,0
1156  DATA 0,0,0,0,0,0
1157  DATA 0,0,0,0,0,0
1158  DATA 0,0,0,0,0,0
1159  DATA 0,0,0,0,0,0
1160  DATA 0,0,0,0,0,0
1161  DATA 20,40,66,93,127,179
1162  DATA 213,197,136,161,118,95
1163  DATA 66,44,23,0,0,0
1164  DATA 0,0,0,0,0,0
1165  DATA 0,0,0,0,0,0
1166  DATA 0,0,0,0
```

```
1500  REM CALCULATE W(I)
1510  FOR I=0 TO M
1520  W(I)=(1+COS(P*I/M))/2
1530  NEXT I
1540  FOR I=M+1 TO N
1550  W(I)=0
1560  NEXT I
1570  RETURN
3000  REM PRINT DATA
3024  PRINT '(1220) LAG NO. M=':M
3028  PRINT '(1225)F(ANG.FREQ.INTERVAL:PI/(10*F))=':F
3029  RETURN
3030  REM PRINT F(W)
3031  PRINT 'VALUES OF F(W)'
3040  FOR I=0,(L+1)/4-1
3050  PRINT TAB(1):I:
3060  PRINT TAB(5):F(I):
3070  PRINT TAB(14):I+(L+1)/4:
3080  PRINT TAB(18):F(I+(L+1)/4):
3090  PRINT TAB(27):I+(L+1)/2:
3100  PRINT TAB(31):F(I+(L+1)/2):
3110  PRINT TAB(40):I+3*(L+1)/4:
3120  PRINT TAB(44):F(I+3*(L+1)/4)
3130  NEXT I
3150  RETURN
4000  REM VERTICAL AXIS SCALE:POWER SPECTRAL DENSITY FN
4010  LET W=0
4020  LET M1=0
4030  LET M2=0
4040  IF F(W)<=M1 THEN 4090
4050  IF F(W)>=M2 THEN 4110
4060  LET W=W+1
4070  IF W=L+1 THEN 4130
4080  GOTO 4040
4090  LET M1=F(W)
4100  GOTO 4060
4110  LET M2=F(W)
4120  GOTO 4060
4130  LET E=(M2-M1)/50
4131  PRINT '(4130)E(VERTICAL SCALE FACTOR:RANGE 50*E)=':E
4132  PRINT 'MAX.F(W)=':M2:
4133  PRINT 'MIN.F(W)=':M1
4140  IF M1<0 THEN 4170
4150  LET V=0
4160  GOTO 4190
4170  LET V=INT(0-M1/E)
4190  RETURN
6000  REM PLOT F(W)
6010  FOR I=0,L
6020  LET W=INT(F(I)/E)
6030  PRINT TAB(1):I:
6040  PRINT TAB(W+V+6):'*'
6050  NEXT I
6060  RETURN
7000  REM VERTICAL AXIC SCALE
7010  PRINT
7012  PRINT TAB(V+6):'0'
7013  PRINT TAB(V+6):'↑'
7070  RETURN
7500  REM CONVERT X TO X LESS MEAN X
7510  LET S=0
7520  LET J=1
7530  LET S=S+X(J)
7540  IF J=N THEN 7640
7550  LET J=J+1
7600  GOTO 7530
7640  LET K=1
7650  LET X(K)=X(K)-S/N
7660  IF K=N THEN 7690
7670  LET K=K+1
7680  GOTO 7650
7690  RETURN
9000  REM DATA
9020  M=67
9022  L=100
9025  F=10
9026  PRINT 'GIVE LAG NO M'
9027  INPUT M
9028  PRINT 'GIVE VALUE FOR L'
9029  INPUT L
9040  RETURN
9999  END
```

```
GGGGGGGGGGGGGGGGGGGGGGGGGGGGGGGGGGGGGGGGGGGGGGGGGGGGGGGGGGGGGGGGGGGGGGC
GGGGGGGGGGGGGGGGGGGGGGGGGGGGGGGGGGGGGGGGGGGGGGGGGGGGGGGGGGGGGGGGGGGGGGC
GGGGGGGGGGGGGGGGGGGGGGGGGGGGGGGGGGGGGGGGGGGGGGGGGGGGGGGGGGGGGGGGGGGGGGC
GGGGGGGGGGGG                                                  GGGGGGGGC
GGGGGGGGGGGG                                                  GGGGGGGGC
GGGGGGGGGGGG          REQUESTED BY R DUGGAN        SPOOL      GGGGGGGGC
GGGGGGGGGGGG          JOB NO : 1      CONSOLE NO : 0          GGGGGGGGC
GGGGGGGGGGGG          DATE:  9-MAY-78    TIME: 14.27          GGGGGGGGC
GGGGGGGGGGGG                                                  GGGGGGGGC
GGGGGGGGGGGGGGGGGGGGGGGGGGGGGGGGGGGGGGGGGGGGGGGGGGGGGGGGGGGGGGGGGGGGGGC
GGGGGGGGGGGGGGGGGGGGGGGGGGGGGGGGGGGGGGGGGGGGGGGGGGGGGGGGGGGGGGGGGGGGGGC
GGGGGGGGGGGGGGGGGGGGGGGGGGGGGGGGGGGGGGGGGGGGGGGGGGGGGGGGGGGGGGGGGGGGGGC


    DK1:GJEDIT2/BL    14.25.39   TUESDAY   9-MAY-78            MINISEM
    EOP



    SHEET 001               GJEDIT2

      000 000                      PAGE 0
      000 000   151 A    START     LFI TITL
      000 001   013 B
      000 002   152 A              LGI <TITL
      000 003   001 B
      000 004   300 A    B2        LDI 0
      000 005   127 A              SNZ
      000 006   046 A              JMR B1
      000 007   150 A              LFI XTRAN
      000 010   020 A
      000 011   175 A              RMON; JMB 1
      000 012   076 A

      000 013   113 A              ISF
      000 014   067 A              JMR B2
      000 015   022 B    B1        JMS INNO
      000 016   074 A
      000 017   261 B              STD M
      000 020   011 A
      000 021   140 A              LXI 116
      000 022   116 A
      000 023   150 A              LFI XTRAN
      000 024   020 A
      000 025   175 A              RMON; JMB 1
      000 026   076 A

      000 027   140 A              LXI 275
      000 030   275 A
      000 031   150 A              LEI XTRAN
      000 032   020 A
      000 033   175 A              RMON; JMB 1
      000 034   076 A

      000 035   022 B              JMS INNO
      000 036   074 A
      000 037   261 B              STD N
      000 040   012 A
      000 041   151 A              LFI IORO
      000 042   035 B
      000 043   152 A              LGI <IORO
      000 044   001 B
      000 045   300 A    B3        LDI 0
      000 046   127 A              SNZ
      000 047   046 A              JMR B4
      000 050   150 A              LFI XTRAN
      000 051   020 A
      000 052   175 A              RMON; JMB 1
      000 053   076 A

      000 054   113 A              ISF
      000 055   067 A              JMR B3
      000 056   150 A    B4        LEI XTRAN; FDC
      000 057   020 A
      000 060   114 A
```

SHEET 002   GJEDIT2

```
000 061   175 A            RMON; JMR 1
000 062   076 A

000 063   153 A            SXD 317
000 064   317 A
000 065   042 A            JMR B5
000 066   114 A            PDC
000 067   042 A            JMR B6
000 070   140 A     B5     LXI 5
000 071   005 A
000 072   261 B     B6     STD CT4
000 073   003 A
000 074   114 A            PDC
000 075   114 A            PDC
000 076   114 A            PDC
000 077   261 B            STD CT1
000 100   000 A
000 101   261 B            STD CT2
000 102   001 A
000 103   261 B            STD CT3
000 104   002 A
000 105   261 B            STD CT5
000 106   004 A
000 107   261 B            STD CT6
000 110   005 A
000 111   114 A            PDC
000 112   140 A            LXI 100; LXI FLUSH+LINE; LEI ASSIGN+4
000 113   100 A
000 114   140 A
000 115   300 A
000 116   150 A
000 117   144 A
000 120   175 A            RMON; EMON
000 121   176 A
000 122   114 A            PDC
000 123   140 A            LXI 120; LXI FLUSH+LINE; LEI ASSIGN+5
000 124   120 A
000 125   140 A
000 126   300 A
000 127   150 A
000 130   145 A
000 131   175 A            RMON; EMON
000 132   176 A
000 133   022 B            JMS PL
000 134   171 A
000 135   022 B            JMS HDG
000 136   000 A
000 137   021 B     B8     JMS RNO
000 140   047 A
000 141   241 B            LDD CT5
000 142   004 A
000 143   144 A            ADI 1
000 144   001 A
000 145   261 B            STD CT5
```

```
000 146   004 A
000 147   112 A            CDN
000 150   241 B            LDD M
000 151   011 A
000 152   135 A            SUB
000 153   127 A            SNZ
000 154   042 A            JMR B7
000 155   000 B            JMD B8
000 156   137 A
000 157   241 B     B7     LDD NO1
000 160   006 A
000 161   150 A            LFI 5
000 162   005 A
000 163   175 A            RMON; JMR 1
000 164   076 A

000 165   241 B            LDD NO2
000 166   007 A
000 167   150 A            LFI 5
000 170   005 A
000 171   175 A            RMON; JMR 1
000 172   076 A

000 173   241 B            LDD NO3
000 174   010 A
000 175   150 A            LFI 5
000 176   005 A
000 177   175 A            RMON; JMR 1
000 200   076 A

000 201   241 B            LDD CT1
000 202   000 A
000 203   144 A            ADI 1
000 204   001 A
000 205   261 B            STD CT1
000 206   000 A
000 207   241 B            LDD CT2
000 210   001 A
000 211   144 A            ADI 1
000 212   001 A
000 213   261 B            STD CT2
000 214   001 A
000 215   112 A            CDN
000 216   153 A            SXD 144
000 217   144 A
000 220   042 A            JMR B9
000 221   000 B            JMD B10
000 222   255 A
000 223   022 B     B9     JMS CRLF
000 224   206 A
000 225   022 B            JMS FL
000 226   171 A
000 227   140 A            LXI 64; LXI 100; LXI REIS+LINE
000 230   064 A
```

```
  000 231   140 A
  000 232   100 A
  000 233   140 A
  000 234   220 A
  000 235   150 A            LEI ASSIGN+4
  000 236   144 A
  000 237   175 A            RMON; EMON
  000 240   176 A
  000 241   140 A            LXI 40; LXI 120; LXI RELS+LINE
  000 242   040 A
  000 243   140 A
  000 244   120 A
  000 245   140 A
  000 246   220 A
  000 247   150 A            LEI ASSIGN+5
  000 250   145 A
  000 251   175 A            RMON; EMON
  000 252   176 A
  000 253   000 B            JMD START
  000 254   000 A
  000 255   241 B    B10     LDD CT1
  000 256   000 A
  000 257   153 A            SXD 6
  000 260   006 A
  000 261   047 A            JMR B11
  000 262   140 A            LXI 254
  000 263   254 A
  000 264   150 A            LEI 5
  000 265   005 A
  000 266   175 A            RMON; JMR 1
  000 267   076 A

  000 270   047 A            JMR B12
  000 271   022 B    B11     JMS CRLF
  000 272   206 A
  000 273   022 B            JMS HDG
  000 274   000 A
  000 275   114 A            PDC
  000 276   261 B            STD CT1
  000 277   000 A
  000 300   021 B    B12     JMS RNO
  000 301   047 A
  000 302   241 B            LDD CT6
  000 303   005 A
  000 304   144 A            ADI 1
  000 305   001 A
  000 306   261 B            STD CT6
  000 307   005 A
  000 310   112 A            CDN
  000 311   241 B            LDD N
  000 312   012 A
  000 313   135 A            SUB
  000 314   127 A            SNZ
  000 315   041 A            JMR B13
```

SHEET 005   GJEDIT2

```
  000 316   061 A          JMR B12
  000 317   114 A   B13    PDC
  000 320   261 B          STD CT6
  000 321   005 A
  000 322   000 B          JMD B7
  000 323   157 A
  001 000                  PAGE
  001 000   000 A   CT1    0
  001 001   000 A   CT2    0
  001 002   000 A   CT3    0
  001 003   000 A   CT4    0
  001 004   000 A   CT5    0
  001 005   000 A   CT6    0
  001 006   000 A   NO1    0
  001 007   000 A   NO2    0
  001 010   000 A   NO3    0
  001 011   000 A   M      0
  001 012   000 A   N      0
  001 013   015 A   TITL   TEXT(15)(12)/ GJEDIT VOA/(15)(12)/M=/(0)
  001 014   012 A
  001 015   040 A
  001 016   107 A
  001 017   112 A
  001 020   105 A
  001 021   104 A
  001 022   111 A
  001 023   124 A
  001 024   040 A
  001 025   126 A
  001 026   060 A
  001 027   101 A
  001 030   015 A
  001 031   012 A
  001 032   115 A
  001 033   075 A
  001 034   000 A
  001 035   040 A   IORO   TEXT/ I OR O?:/(0)
  001 036   111 A
  001 037   040 A
  001 040   117 A
  001 041   122 A
  001 042   040 A
  001 043   117 A
  001 044   077 A
  001 045   072 A
  001 046   000 A
  001 047   000 A   RNO    0
  001 050   000 A          0
  001 051   150 A   A1     LFI 4
  001 052   004 A
  001 053   175 A          RMON; JMR 1
  001 054   076 A

  001 055   261 B          STD NO1
```

SHEET 006 GJFDI12

```
 001 056  006 A
 001 057  112 A         CDN
 001 060  107 A         7SX
 001 061  145 A         SUI 60
 001 062  060 A
 001 063  126 A         SPO
 001 064  064 A   A2    JMR A1
 001 065  145 A         SUI 12
 001 066  012 A
 001 067  125 A         SNE
 001 070  073 A         JMR A2
 001 071  150 A         LFI 4
 001 072  004 A
 001 073  175 A         RMON; JMR 1
 001 074  076 A

 001 075  261 B         STD NO2
 001 076  007 A
 001 077  150 A         LFI 4
 001 100  004 A
 001 101  175 A         RMON; JMR 1
 001 102  076 A

 001 103  261 B         STD NO3
 001 104  010 A
 001 105  001 B         JMD RNO
 001 106  047 A
 002 000                PAGE
 002 000  000 A   HDG   0
 002 001  000 A         0
 002 002  140 A         LXI 261
 002 003  261 A
 002 004  150 A         LFI 5
 002 005  005 A
 002 006  175 A         RMON; JMR 1
 002 007  076 A

 002 010  241 B         LDD CT4
 002 011  003 A
 002 012  022 B         JMS PUN
 002 013  136 A
 002 014  241 B         LDD CT3
 002 015  002 A
 002 016  022 B         JMS PUN
 002 017  136 A
 002 020  151 A         LFI HD
 002 021  064 B
 002 022  152 A         LGI <HD
 002 023  002 B
 002 024  300 A   H1    LDI 0
 002 025  127 A         SNZ
 002 026  046 A         JMR H2
 002 027  150 A         LFI 5
 002 030  005 A
```

```
  002 031  175 A         RMON; JMR 1
  002 032  076 A

  002 033  113 A         ISF
  002 034  067 A         JMR H1
  002 035  241 B   H2    LDD CT3
  002 036  002 A
  002 037  144 A         ADI 1
  002 040  001 A
  002 041  261 B         STD CT3
  002 042  002 A
  002 043  112 A         CDN
  002 044  153 A         SXD 12
  002 045  012 A
  002 046  042 A         JMR H3
  002 047  002 B         JMD HDG
  002 050  000 A
  002 051  241 B   H3    LDD CT4
  002 052  003 A
  002 053  144 A         ADI 1
  002 054  001 A
  002 055  261 B         STD CT4
  002 056  003 A
  002 057  114 A         FDC
  002 060  261 B         STD CT3
  002 061  002 A
  002 062  002 B         JMD HDG
  002 063  000 A
  002 064  060 A   HD    TEXT/O DATA /(O)
  002 065  040 A
  002 066  104 A
  002 067  101 A
  002 070  124 A
  002 071  101 A
  002 072  040 A
  002 073  000 A
  002 074  000 A   INNO  0
  002 075  000 A         0
  002 076  114 A         FDC
  002 077  262 B         STD NO
  002 100  135 A
  002 101  150 A   C1    LFI XTRAN; FDC
  002 102  020 A
  002 103  114 A
  002 104  175 A         RMON; JMR 1
  002 105  076 A

  002 106  107 A         ZSX
  002 107  145 A         SUI 60
  002 110  060 A
  002 111  126 A         SFO
  002 112  044 A         JMR C2
  002 113  145 A         SUI 12
  002 114  012 A
```

```
002 115  126 A           SPO
002 116  044 A           JMR C3
002 117  242 B   C2      LDD NO
002 120  135 A
002 121  002 B           JMD INNO
002 122  074 A
002 123  144 A   C3      ADI 12
002 124  012 A
002 125  242 B           LDD NO
002 126  135 A
002 127  146 A           MUI 12
002 130  012 A
002 131  262 B           STD NO
002 132  135 A
002 133  002 B           JMD C1
002 134  101 A
002 135  000 A   NO      0
002 136  000 A   FUN     0
002 137  000 A           0
002 140  262 B           STD SX
002 141  166 A
002 142  262 B           STD SY
002 143  167 A
002 144  262 B           STD SZ
002 145  170 A
002 146  144 A           ADI 60
002 147  060 A
002 150  022 B           JMS PAR
002 151  226 A
002 152  150 A           LFI 5
002 153  005 A
002 154  175 A           RMON; JMR 1
002 155  076 A

002 156  242 B           LDD SX
002 157  166 A
002 160  242 B           LDD SZ
002 161  170 A
002 162  242 B           LDD SY
002 163  167 A
002 164  002 B           JMD FUN
002 165  136 A
002 166  000 A   SX      0
002 167  000 A   SY      0
002 170  000 A   SZ      0
002 171  000 A   PL      0
002 172  000 A           0
002 173  151 A           LFI 0
002 174  000 A
002 175  114 A   J1      PDC
002 176  150 A           LFI 5
002 177  005 A
002 200  175 A           RMON; JMR 1
002 201  076 A
```

```
SHEET 009                 GJEDIT2

 002 202   113 A           ISF
 002 203   071 A           JMR J1
 002 204   002 B           JMD PL
 002 205   171 A
 002 206   000 A   CRLF    0
 002 207   000 A           0
 002 210   140 A           LXI 215
 002 211   215 A
 002 212   150 A           LFI 5
 002 213   005 A
 002 214   175 A           RMON; JMR 1
 002 215   076 A

 002 216   140 A           LXI 012
 002 217   012 A
 002 220   150 A           LFI 5
 002 221   005 A
 002 222   175 A           RMON; JMR 1
 002 223   076 A

 002 224   002 B           JMD CRLF
 002 225   206 A
 002 226   000 A   PAR     0
 002 227   000 A           0
 002 230   114 A           PDC
 002 231   262 B           STD COUNT
 002 232   265 A
 002 233   151 A           LFI 370
 002 234   370 A
 002 235   121 A   P1      RXL
 002 236   125 A           SNF
 002 237   046 A           JMR P2
 002 240   242 B           LDD COUNT
 002 241   265 A
 002 242   144 A           ADI 1
 002 243   001 A
 002 244   262 B           STD COUNT
 002 245   265 A
 002 246   113 A   P2      ISF
 002 247   065 A           JMR P1
 002 250   242 B           LDD COUNT
 002 251   265 A
 002 252   122 A           RXR
 002 253   111 A           SAX
 002 254   127 A           SNZ
 002 255   044 A           JMR P3
 002 256   100 A           CUP
 002 257   144 A           ADI 200
 002 260   200 A
 002 261   114 A           PDC
 002 262   100 A   P3      CUP
 002 263   002 B           JMD PAR
 002 264   226 A




SHEET 010                 GJEDIT2

 002 265   000 A   COUNT   0
                           END
```

INDEX COMPILED 2/11/76 APPROX
SUPPLEMENTED 19/6/77
NOTES SUPPLEMENTED 22/11/77

MJ DATA	INDEX	P SPEC	NORM P SPEC	XP SPEC	X CON	CJ EDIT CODE	NOTES
MJ 41	I	✓	✓			T4TG(1) 1	80 GRIT WHEEL 30 SEC GRINDING TALYSURF MAGS.
MJ 42	I	✓	✓			T4TG(1) 2	
MJ 43	I	✓	✓			T4TG(1) 3	
MJ 44	I	✓	✓			T4TG(1) 4	
MJ 45	I	✓	✓			T4TG(2) 5	80 GRIT WHEEL 30 SEC GRINDING TALYSURF ×2000, ×100
MJ 46	I	✓	✓			T4TG(2) 6	
MJ 47	I	✓	✓			T4TG(3) 7	80 GRIT WHEEL 5 MIN GRINDING TALYSURF ×1000, ×100
MJ 48	I	✓	✓			T4TG(3) 8	
MJ 49	I	✓	✓			T4TG(4) 9	80 GRIT WHEEL 5 MIN GRINDING TALYSURF ×2000, ×100
MJ 50	I	✓	✓			T4TG(4) 10	
MJ 51	I	✓	✓			T4TG(5) 11	80 GRIT WHEEL 10 MIN GRINDING TALYSURF ×1000, ×100
MJ 52	I	✓	✓			T4TG(5) 12	
MJ 53	I	✓	✓			T4TG(6) 13	80 GRIT WHEEL [illegible] MIN GRINDING TALYSURF ×1000 ×100
MJ 54	I	✓	✓			T4TG(6) 14	
MJ 58	I	✓	✓			T4TS(7) 28	SURFACE GROUND FOR 30 SEC TALYSURF ×20 000, ×100 NO CURVATURE COMPENSATION
MJ 59	I	✓	✓			T4TS(7) 29	
MJ 60	I	✓	✓			T4TS(7) 30	
MJ 61	I	✓	✓			T4TS(8) 31	SURFACE GROUND FOR 5 MIN TALYSURF ×20000, ×100 NO COMPENSATION FOR CURVATURE
MJ 62	I	✓	✓			T4TS(8) 32	
MJ 63	I	✓	✓			T4TS(9) 33	SURFACE GROUND FOR 5 MIN TALYSURF ×20000, ×100 NO COMPENSATION FOR CURVATURE
MJ 64	I	✓	✓			T4TS(9) 34	
MJ 65	I	✓	✓			T4TS(10) 35	SURFACE GROUND FOR 5 MIN TALYSURF: ×20000, ×100 CURVATURE COMPENSATED
MJ 66	I	✓	✓			T4TS(10) 36	
MJ 67	I	✓	✓			T4TS(11) 37	SURFACE GROUND FOR 30 SEC TALYSURF ×20000, ×100 CURVATURE COMPENSATED
MJ 68	I	✓	✓			T4TS(11) 38	
MJ 69	I	✓	✓			T4TS(12) 39	SURFACE PRODUCED BY 80 GRIT WHEEL AFTER 10 MIN GRINDING TALYSURF: ×20000, ×100 CURVATURE COMPENSATED.
MJ 70	I	✓	✓			T4TS(12) 40	
MJ 71	IO			✓	✓	T4TS(1) 1 × T4TS(11) 37	MJ41I/
MJ 72	IO			✓	✓	T4TS(1) 3 × T4TS(11) 38	
MJ 73	IO			✓	✓	T4TG(2) 5 × T4TS(10) 35	
MJ 74	IO			✓	✓	T4TG(2) 6 × T4TS(10) 36	
MJ 75	IO			✓	✓	T4TG(3) 7 × T4TS(12) 39	
MJ 76	IO			✓	✓	T4TG(3) 8 × T4TS(12) 40	

Table 10.1

Table 10.2

Data Tape (input)	Sample Size (ordinates)	M	N	I or O	Output Tape Code
T4TG(1)	300	255	1	I	MJ1IA
"	500	255	1	I	MJ2IA
"	1000	1	1	I	MJ3IA
"	300	1	3	I	MJ4IA
T4TG(2)	300	1	1	I	MJ5IA
"	300	255	1	I	MJ6IA
"	500	1	1	I	MJ7IA
"	1000	1	1	I	MJ8IA
"	300	1	3	I	MJ9IA
T4TG(3)	300	1	1	I	MJ10IA
"	300	255	1	I	MJ11IA
"	500	1	1	I	MJ21IA
"	500	255	1	I	MJ13IA
"	1000	1	1	I	MJ14IA
"	300	1	3	I	MJ15IA
T4TG(4)	300	255	1	I	MJ16IA
"	300	1	1	I	MJ17IA
"	500	1	1	I	MJ18IA
"	500	255	1	I	MJ19IA
"	1000	1	1	I	MJ20IA
"	300	1	3	I	MJ21IA
T4TG(5)	300	255	1	I	MJ22IA
"	300	1	1	I	MJ23IA
"	500	1	1	I	MJ24IA
"	500	255	1	I	MJ25IA
"	1000	1	1	I	MJ26IA
"	300	1	3	I	MJ27IA

(Continued)

Table 10.2 (continued)

T4TG(6)	300	1	1	I	MJ28IA
"	300	255	1	I	MJ29IA
"	500	1	1	I	MJ30IA
"	500	255	1	I	MJ31IA
"	1000	1	1	I	MJ32IA
"	300	1	3	I	MJ33IA
T4TS(7)	300	255	1	I	MJ34IA
"	500	255	1	I	MJ35IA
"	1000	1	1	I	MJ36IA
"	300	1	3	I	MJ37IA
T4TS(10)	300	255	1	I	MJ38IA
"	500	255	1	I	MJ39IA
"	1000	1	1	I	MJ40IA
"	300	1	3	I	MJ41IA
T4TS(11)	300	255	1	I	MJ42IA
"	500	255	1	I	MJ43IA
"	1000	1	1	I	MJ44IA
"	300	1	3	I	MJ45IA
T4TS(12)	300	255	1	I	MJ46IA
"	500	255	1	I	MJ47IA
"	1000	1	1	I	MJ48IA
"	300	1	3	I	MJ49IA
T4TS(7)	300	1	3	0	MJ50IA
T4TS(10)	300	1	3	0	MJ51IA
T4TS(11)	300	1	3	0	MJ52IA
T4TS(12)	300	1	3	0	MJ53IA
T4TS(7)	300	255	1	0	MJ54IA
"	1000	1	1	0	MJ55IA
T4TS(10)	300	255	1	0	MJ56IA
"	1000	1	1	0	MJ57IA
T4TS(11)	300	255	1	0	MJ58IA
"	1000	1	1	0	MJ59IA
T4TS(12)	300	255	1	0	MJ60IA
"	1000	1	1	0	MJ61IA

Table 10.4 Surface profile data for a grinding wheel after 30 seconds wear (MJ3IA)

```
>1000 DATA 152,152,152,152,152,152
1001 DATA 152,152,152,152,152,1>52
100>2 DATA 152,152,152,152,152,152
10>03 DATA 152,152,152,152,152,152
1>004 DATA 152,152,152,152,152,152
1>005 DATA 152,152,151,151,151,151
1>006 DATA 150,150,149,149,149,149
1>007 DATA 149,149,148,148,148,148
1008 DATA >147,147,146,145,143,141
1>009 DATA 133,103,072,037,009,015
1>010 DATA 017,062,098,125,134,143
1011 DATA 143,121,095,071,047,047
1012 DATA> 07>0,087,110,117,113,109
1>013 DATA 105,097,081,070,052,031
1>014 DATA 010,000,000,000,000,000
1>015 DATA 000,000,000,000,000,000
1>016 DATA 000,000,000,000,000,000
1>017 DATA 000,000,000,000,000,000
1>018 DATA 000,034,035,071,122,143
1>019 DATA 170,205,208,212,215,195
1>020 DATA 168,141,137,127,100,058
1>021 DATA 028,023,015,011,000,003
1>022 DATA 001,000,000,000,000,000
1>023 DATA 000,000,000,000,000,061
1>024 DATA 125,171,167,153,126,101
1>025 DATA 085,058,031,010,000,000
1>026 DATA 000,000,000,000,000,000
1>027 DATA 000,000,000,000,000,000
1>028 DATA 000,000,000,000,000,000
1>029 DATA 000,000,000,000,000,000
1>030 DATA 000,000,000,000,000,000
1>031 DATA 000,000,000,000,000,000
1>032 DATA 000,000,000,000,000,000
1>033 DATA 000,000,000,000,000,000
1>034 DATA 000,000,000,000,000,000
1>035 DATA 000,000,000,000,000,000
1>036 DATA 000,000,000,000,000,000
1>037 DATA 000,000,000,000,000,000
1>038 DATA 000,000,000,000,000,000
1>039 DATA 000,000,000,000,000,000
1>040 DATA 000,000,000,000,000,000
1041 DATA 00>0,000,000,032,090,145
1>042 DATA 177,184,213,185,162,138
1>043 DATA 102,066,069,069,037,102
1>044 DATA 117,140,153,160,169,195
1>045 DATA 210,200,183,160,163,154
1046> DATA 148,129,169,189,210,221
104>7 DATA 222,200,198,200,204,194
1>048 DATA 167,139,152,103,055,017
1>049 DATA 000,000,000,000,000,000
1>050 DATA 042,108,173,199,208,215
10>51 DATA 216,216,216,216,222,219
1>052 DATA 220,156,145,102,055,009
1>053 DATA 000,000,000,000,000,000
1>054 DATA 000,000,000,000,000,000
10>55 DATA 000,000,000,000,000,000
1>056 DATA 000,000,000,000,000,000
1>057 DATA 000,000,000,000,000,000
1>058 DATA 000,000,000,000,000,000
1>059 DATA 000,000,000,000,000,000
1>060 DATA 000,000,000,000,000,000
1>061 DATA 000,000,000,000,000,000
1062 D>ATA 000,000,000,000,000,000
1>063 DATA 000,000,000,000,000,000
1064 DATA 000,000,000,000>,000,011
1>065 DATA 033,057,094,078,057,089
1>066 DATA 113,123,149,151,147,139
1>067 DATA 127,119,075,034,000,000
1>068 DATA 000,000,000,000,000,000
1>069 DATA 000,000,000,000,000,000
1>070 DATA 000,000,000,056,103,147
1>071 DATA 189,220,208,197,194,195
1>072 DATA 194,187,181,180,165,145
1>073 DATA 119,092,069,037,015,000
1>074 DATA 000,000,000,000,000,000
1>075 DATA 000,000,000,000,000,000
1>076 DATA 000,000,000,000,016,037
1>077 DATA 046,042,038,035,011,000
1078 DATA 00>0,000,000,000,000,000
107>9 DATA 000,000,000,000,000,000
1080 DAT>A 000,000,000,000,000,000
108>1 DATA 000,000,000,000,000,000
1082> DATA 000,000,000,000,000,000
108>3 DATA 000,000,000,000,000,000
1>084 DATA 000,000,000,000,000,000
10>85 DATA 000,000,000,000,000,000
1086> DATA 000,000,000,000,000,000
1>087 DATA 000,000,015,075,134,193
1>088 DATA 216,228,229,229,222,209
1>089 DATA 228,227,223,202,176,150
10>90 DATA 121,105,081,101,125,127
1>091 DATA 127,127,127,157,171,175
1>092 DATA 194,225,196,168,140,145
10>93 DATA 092,060,035,019,005,000
1094> DATA 000,000,000,000,000,000
1095> DATA 000,000,000,037,076,103
109>6 DATA 112,145,159,159,156,155
1097 DAT>A 176,194,232,233,224,234
1098 DATA 235,242,241>,233,229,218
1099 DATA> 233,233,226,226,227,214
110>0 DATA 193,171,147,125,102,063
11>01 DATA 040,022,000,000,000,001
11>02 DATA 025,041,057,063,069,070
110>3 DATA 085,097,114,127,143,160
110>4 DATA 177,189,191,188,199,199
1105 D>ATA 189,162,121,077,035,000
1106 DAT>A 000,000,000,000,000,000
1107 DATA >000,000,035,056,066,061
1>108 DATA 047,047,037,007,000,000
1>109 DATA 000,009,037,041,060,081
1110 DAT>A 110,130,156,183,202,208
1>111 DATA 220,217,185,159,138,133
1>112 DATA 129,112,091,050,003,000
1>113 DATA 000,000,000,000,000,000
111>4 DATA 000,000,000,000,000,000
1>115 DATA 000,000,000,000,000,001
1>116 DATA 004,016,044,084,123,129
1>117 DATA 129,129,129,116,103,090
1>118 DATA 074,057,049,027,000,000
1119 DATA 000,00>0,000,000,035,095
1>120 DATA 159,191,201,217,228,229
1>121 DATA 226,210,189,182,169,173
1>122 DATA 172,127,086,045,002,000
1>123 DATA 000,000,000,000,000,000
1>124 DATA 000,000,021,063,106,107
1125 DATA 1>15,123,123,124,115,083
11>26 DATA 043,013,000,000,000,000
1>127 DATA 000,000,000,000,000,000
1128 DA>TA 000,000,000,000,000,000
1>129 DATA 000,000,000,000,000,000
1>130 DATA 000,000,000,000,000,000
1>131 DATA 000,000,000,000,000,000
1132> DATA 000,000,000,000,000,000
113>3 DATA 000,000,000,000,000,000
113>4 DATA 000,000,000,000,000,000
11>35 DATA 000,000,000,000,000,000
11>36 DATA 000,000,026,075,101,132
1>137 DATA 134,162,187,221,232,231
113>8 DATA 225,232,218,198,190,205
113>9 DATA 208,209,205,222,223,230
114>0 DATA 226,209,177,148,187,199
1>141 DATA 202,221,228,227,225,215
1>142 DATA 230,229,220,218,207,191
1143 DATA 174,156,13>2,109,079,050
1>144 DATA 015,000,000,000,000,000
1>145 DATA 000,000,000,000,000,000
1>146 DATA 000,000,000,000,000,000
1147 DATA> 000,000,000,000,027,041
1>148 DATA 050,050,052,085,109,089
114>9 DATA 129,167,131,220,227,223
1150 DA>TA 183,148,140,125,109,084
11>51 DATA 050,089,109,109,086,057
1152 D>ATA 015,000,000,000,000,000
1>153 DATA 000,000,000,000,000,000
1>154 DATA 000,000,000,000,000,000
1>155 DATA 000,000,000,000,000,000
1>156 DATA 000,000,000,000,000,000
1>157 DATA 000,000,000,000,000,000
1158 DATA 000,00>0,000,000,000,000
1>159 DATA 000,000,000,000,000,000
1160 D>ATA 000,000,000,000,000,000
1>161 DATA 020,040,066,093,127,179
1>162 DATA 218,197,136,161,118,095
1>163 DATA 066,044,023,000,000,000
1>164 DATA 000,000,000,000,000,000
1165> DATA 000,000,000,000,000,000
1>166 DATA 000,000,000,000
```

Table 10.5 Surface profile data for a ground surface corresponding with 30 seconds grinding (MJ36IA)

```
>1000 DATA 175,197,191,120,130,153
1>001 DATA 186,191,131,210,184,198
1>002 DATA 198,177,135,190,150,157
1>003 DATA 155,197,163,215,195,147
1>004 DATA 129,183,199,173,186,195
1>005 DATA 168,155,149,173,158,152
1>006 DATA 149,131,164,143,158,175
1>007 DATA 159,185,137,146,153,144
1>008 DATA 167,132,166,165,138,136
1>009 DATA 169,170,192,181,202,165
1>010 DATA 136,145,135,146,148,143
1>011 DATA 116,098,106,116,109,086
1>012 DATA 114,133,126,133,159,119
1>013 DATA 127,103,119,108,079,113
1>014 DATA 116,102,067,068,101,155
1>015 DATA 143,140,160,162,155,154
1>016 DATA 105,166,140,144,153,182
1>017 DATA 173,135,145,165,187,178
1>018 DATA 146,152,137,191,140,136
1>019 DATA 163,151,164,141,113,117
1>020 DATA 194,137,129,132,139,149
1>021 DATA 125,169,157,157,156,175
1>022 DATA 173,153,159,140,141,125
1>023 DATA 100,123,143,154,169,151
>1024 DATA 143,117,131,120,157,127
1>025 DATA 142,113,176,172,183,185
1>026 DATA 207,113,106,120,160,162
1>027 DATA 176,193,191,157,151,120
1>028 DATA 144,141,142,134,149,164
1>029 DATA 157,127,150,157,158,130
1>030 DATA 157,156,157,115,127,135
1>031 DATA 143,162,165,176,173,163
1>032 DATA 164,146,144,172,155,172
1>033 DATA 162,142,161,167,163,157
1>034 DATA 168,159,176,164,163,174
1>035 DATA 164,066,158,160,141,145
1>036 DATA 165,174,155,170,154,143
1>037 DATA 154,148,143,152,150,142
1>038 DATA 142,151,145,118,143,143
1>039 DATA 129,117,131,154,157,144
1>040 DATA 136,153,152,147,141,149
1>041 DATA 108,144,130,143,156,146
1>042 DATA 135,149,152,147,152,151
1>043 DATA 148,129,145,000,129,169
1>044 DATA 145,143,164,167,145,141
1>045 DATA 119,120,157,159,126,115
1>046 DATA 142,131,132,126,106,129
1>047 DATA 126,127,118,097,096,097
1>048 DATA 132,116,142,137,111,129
1>049 DATA 105,123,129,127,118,117
1>050 DATA 142,129,132,105,136,142
1>051 DATA 138,137,127,139,121,103
1>052 DATA 121,120,105,094,114,135
1>053 DATA 127,141,132,127,089,131
1>054 DATA 127,097,099,135,112,125
1>055 DATA 132,117,113,124,111,087
1>056 DATA 106,116,106,122,095,051
1>057 DATA 114,114,100,098,100,115
1>058 DATA 122,113,124,116,104,113
1>059 DATA 114,110,095,098,090,109
1>060 DATA 113,036,124,125,118,108
1>061 DATA 125,126,125,146,117,116
1>062 DATA 136,140,143,135,123,118
1>063 DATA 125,120,125,132,120,126
1>064 DATA 127,116,113,127,123,090
1>065 DATA 112,129,047,114,120,107
1>066 DATA 108,105,114,084,088,108
1>067 DATA 102,097,093,100,107,115
1>068 DATA 085,130,115,106,100,104
1>069 DATA 113,127,102,124,107,128
>1070 DATA 129,135,000,173,136,132
1>071 DATA 109,127,145,126,129,136
1>072 DATA 130,114,113,121,130,142
1>073 DATA 116,138,161,130,125,115
1>074 DATA 122,127,123,127,132,143
1>075 DATA 141,131,127,112,113,095
1>076 DATA 092,050,049,059,111,124
1>077 DATA 121,092,099,102,101,115
1>078 DATA 121,095,118,118,117,105
1>079 DATA 119,105,119,100,122,083
1>080 DATA 110,101,108,091,077,068
1>081 DATA 087,095,087,085,081,100
1>082 DATA 057,089,087,087,100,071
1>083 DATA 077,090,104,086,053,093
1>084 DATA 107,108,092,092,103,092
1>085 DATA 110,116,110,105,114,123
1>086 DATA 099,113,122,125,125,072
1>087 DATA 108,119,115,126,104,114
1>088 DATA 134,127,129,130,119,127
1>089 DATA 135,125,139,115,151,145
1>090 DATA 123,139,132,120,133,127
1>091 DATA 129,138,138,135,126,132
1>092 DATA 125,114,122,131,124,137
1>093 DATA 143,128,130,117,122,114
1>094 DATA 116,127,112,107,111,132
1>095 DATA 108,104,079,092,074,057
1>096 DATA 081,093,101,115,120,100
1>097 DATA 108,089,101,122,090,114
1>098 DATA 105,115,109,098,132,133
1>099 DATA 142,134,126,085,103,120
1>100 DATA 110,034,089,123,117,109
1>101 DATA 116,103,110,116,144,119
1>102 DATA 117,109,100,100,131,124
1>103 DATA 123,134,132,117,113,113
1>104 DATA 140,119,133,133,130,113
1>105 DATA 113,122,114,092,073,093
1>106 DATA 073,102,091,093,099,095
1>107 DATA 092,086,097,096,086,075
1>108 DATA 090,000,039,104,103,039
1>109 DATA 127,096,102,112,120,095
1>110 DATA 120,117,112,115,115,106
1>111 DATA 113,413,114,126,119,116
1>112 DATA 127,132,143,121,131,126
1>113 DATA 097,123,092,115,103,132
1>114 DATA 130,133,146,130,155,129
1>115 DATA 119,126,133,126,135,132
>1116 DATA 119,146,144,152,156,149
1>117 DATA 150,163,140,141,149,154
1>118 DATA 134,156,144,140,164,141
1>119 DATA 167,166,110,170,133,124
1>120 DATA 144,145,141,141,149,157
1>121 DATA 160,143,155,165,162,162
1>122 DATA 168,153,167,162,160,146
1>123 DATA 166,181,165,178,170,173
1>124 DATA 155,177,159,171,159,164
1>125 DATA 157,165,165,152,164,156
1>126 DATA 149,162,157,143,160,152
1>127 DATA 150,125,122,143,151,137
1>128 DATA 128,157,161,164,155,163
1>129 DATA 167,152,149,159,148,156
1>130 DATA 168,172,154,156,162,169
1>131 DATA 159,143,165,157,160,137
1>132 DATA 143,160,147,146,140,120
1>133 DATA 120,140,130,130,133,132
1>134 DATA 140,140,133,118,139,115
1>135 DATA 000,010,145,140,118,135
1>136 DATA 146,123,127,131,127,152
1>137 DATA 137,144,132,131,150,132
1>138 DATA 143,157,149,161,139,141
1>139 DATA 154,120,140,110,110,144
1>140 DATA 141,152,132,121,156,164
1>141 DATA 140,150,138,135,117,150
1>142 DATA 133,119,155,159,132,134
1>143 DATA 113,124,127,116,111,130
1>144 DATA 136,143,142,127,100,113
1>145 DATA 126,100,097,100,119,106
1>146 DATA 124,106,141,139,132,124
1>147 DATA 124,140,147,133,136,141
1>148 DATA 155,146,152,168,149,171
1>149 DATA 155,155,159,155,149,161
1>150 DATA 157,166,176,184,185,165
1>151 DATA 171,160,185,172,175,172
1>152 DATA 053,000,000,162,170,177
1>153 DATA 167,167,167,166,165,165
1>154 DATA 167,167,166,166,167,166
1>155 DATA 166,167,167,166,166,165
1>156 DATA 166,167,165,166,166,167
1>157 DATA 165,166,167,167,166,166
1>158 DATA 167,165,166,167,166,167
1>159 DATA 166,167,167,165,166,167
1>160 DATA 167,167,166,166,167,166
1>161 DATA 167,165,166,166,167,167
1>162 DATA 166,168,167,165,167,168
1>163 DATA 167,166,167,167,165,165
1>164 DATA 166,166,167,166,167,166
1>165 DATA 167,165,168,167,166,165
1>166 DATA 166,167,166,167
```

Table 10.6 Profile data for a ground surface corresponding with 30 seconds grinding wheel wear (MJ44IA)

```
LOAD 'MACJJ4'
1000 DATA 076,065,074,075,092,071
1001 DATA 101,065,111,087,087,132
1002 DATA 116,100,099,105,115,098
1003 DATA 089,090,090,109,104,093
1004 DATA 075,077,079,113,100,106
1005 DATA 106,101,101,118,108,112
1006 DATA 111,094,093,095,081,111
1007 DATA 087,102,113,138,109,139
1008 DATA 127,105,112,118,109,106
1009 DATA 095,107,121,108,121,143
1010 DATA 107,081,000,122,127,106
1011 DATA 099,124,147,132,133,114
1012 DATA 126,109,122,127,121,125
1013 DATA 149,125,127,133,145,141
1014 DATA 150,091,100,103,114,101
1015 DATA 122,131,102,108,130,112
1016 DATA 108,125,130,089,108,083
1017 DATA 110,119,111,102,106,095
1018 DATA 074,080,083,057,089,076
1019 DATA 098,093,067,086,080,073
1020 DATA 086,083,083,094,121,113
1021 DATA 108,103,108,117,115,091
1022 DATA 087,088,069,103,079,101
1023 DATA 065,065,109,099,076,105
1024 DATA 125,148,136,098,108,093
1025 DATA 132,138,139,162,135,125
1026 DATA 143,138,155,166,156,169
1027 DATA 157,145,127,133,130,139
1028 DATA 146,148,134,126,137,141
1029 DATA 104,125,121,136,161,153
1030 DATA 108,107,105,101,110,126
1031 DATA 095,124,121,139,140,063
1032 DATA 116,124,132,137,138,132
1033 DATA 141,138,076,075,122,122
1034 DATA 073,093,096,087,093,095
1035 DATA 068,094,034,054,036,044
1036 DATA 031,091,079,085,120,065
1037 DATA 093,059,132,127,104,092
1038 DATA 087,106,085,131,113,139
1039 DATA 059,095,119,138,113,137
1040 DATA 137,133,133,109,132,095
1041 DATA 133,135,125,108,128,134
1042 DATA 120,147,137,156,154,166
1043 DATA 161,161,164,149,155,132
1044 DATA 159,152,148,120,170,143
1045 DATA 163,154,127,146,124,116
1046 DATA 138,143,134,156,141,164
1047 DATA 163,157,150,150,157,155
1048 DATA 152,159,139,167,148,164
1049 DATA 161,168,151,177,150,185
1050 DATA 168,146,162,160,177,159
1051 DATA 162,168,164,157,176,167
1052 DATA 174,159,167,167,171,162
1053 DATA 145,148,163,176,164,167
1054 DATA 152,165,169,164,169,154
1055 DATA 159,152,155,167,115,153
1056 DATA 167,153,153,145,150,159
1057 DATA 163,154,152,157,154,148
1058 DATA 162,151,150,161,140,153
1059 DATA 140,173,166,137,142,135
1060 DATA 148,152,158,163,144,127
1061 DATA 140,187,145,142,146,146
1062 DATA 137,137,139,142,129,126
1063 DATA 116,143,112,109,119,122
1064 DATA 134,151,123,129,145,139
1065 DATA 141,189,151,137,126,100
1066 DATA 050,127,111,134,126,135
1067 DATA 124,127,130,146,145,118
1068 DATA 130,146,145,123,168,153
1069 DATA 139,114,139,149,157,159
1070 DATA 163,148,145,148,138,140
1071 DATA 155,144,143,129,153,148
1072 DATA 163,161,139,148,156,157
1073 DATA 163,154,151,076,000,059
1074 DATA 125,130,144,141,173,178
1075 DATA 164,147,126,152,139,163
1076 DATA 123,124,149,116,156,143
1077 DATA 161,143,142,145,159,133
1078 DATA 146,156,149,143,131,157
1079 DATA [illegible],150,157,173,171,179
1080 DATA 164,167,189,184,170,196
1081 DATA 175,176,188,159,152,111
1082 DATA 155,159,180,178,182,178
1083 DATA 170,161,158,168,159,151
1084 DATA 178,171,159,164,167,173
1085 DATA 167,161,165,156,162,170
1086 DATA 124,149,160,138,138,143
1087 DATA 147,135,113,029,100,121
1088 DATA 184,131,158,154,123,091
1089 DATA 127,136,147,189,126,123
1090 DATA 129,123,140,145,079,079
1091 DATA [illegible],132,123,111,104,029
1092 DATA [illegible],104,122,087,118,115
1093 DATA 120,095,094,084,102,086
1094 DATA 075,062,045,086,133,108
1095 DATA 115,081,057,061,069,086
1096 DATA 085,065,068,028,061,045
1097 DATA 077,029,091,095,110,004
1098 DATA 053,000,000,000,077,106
1099 DATA 121,148,093,094,127,127
1100 DATA 095,126,084,092,076,106
1101 DATA 158,127,069,108,153,118
1102 DATA 141,134,131,127,145,143
1103 DATA 118,085,110,119,121,079
1104 DATA 095,111,115,117,105,135
1105 DATA 132,108,106,132,127,095
1106 DATA 108,124,132,108,112,138
1107 DATA 125,132,177,178,182,188
1108 DATA 156,159,168,152,179,177
1109 DATA 174,173,153,188,147,150
1110 DATA 140,140,151,138,148,147
1111 DATA 180,151,117,150,138,142
1112 DATA 136,150,160,168,136,138
1113 DATA 137,161,148,135,145,110
1114 DATA 113,123,147,124,153,156
1115 DATA 119,105,124,138,133,123
1116 DATA 133,145,131,161,149,162
1117 DATA 146,171,173,171,170,161
1118 DATA 173,177,174,156,168,158
1119 DATA 169,161,158,169,177,180
1120 DATA 181,179,191,189,183,181
1121 DATA 195,176,190,197,185,141
1122 DATA 180,180,164,173,203,161
1123 DATA 169,160,173,159,174,188
1124 DATA 196,174,203,191,191,184
1125 DATA 213,168,191,185,183,151
1126 DATA 199,195,195,181,174,174
1127 DATA 165,186,183,180,197,186
1128 DATA 179,165,187,180,174,097
1129 DATA 069,073,140,176,170,153
1130 DATA 173,157,185,157,155,154
1131 DATA 160,178,189,194,176,178
1132 DATA 170,169,167,176,194,198
1133 DATA 178,175,197,175,168,172
1134 DATA 140,139,156,162,176,162
1135 DATA 173,145,169,175,151,123
1136 DATA 162,141,157,155,169,167
1137 DATA 146,142,162,164,158,168
1138 DATA 154,129,150,172,159,160
1139 DATA 154,146,135,152,171,154
1140 DATA [illegible],155
1141 DATA [illegible],177,[illegible],[illegible],167,165
1142 DATA 159,153,148,133,138,144
1143 DATA 141,131,137,149,159,167
1144 DATA 154,164,149,177,175,167
1145 DATA 170,168,158,145,149,164
1146 DATA 151,160,152,172,182,146
1147 DATA 172,172,178,168,164,157
1148 DATA 145,153,175,184,170,148
1149 DATA 140,152,149,138,133,119
1150 DATA 138,146,158,149,163,159
1151 DATA 138,156,156,119,144,150
1152 DATA 147,135,123,132,139,141
1153 DATA 132,119,125,140,135,113
1154 DATA 144,151,147,134,145,133
1155 DATA 152,146,141,153,130,132
1156 DATA 138,152,155,152,127,140
1157 DATA 143,140,157,188,177,169
1158 DATA 188,182,203,200,193,184
1159 DATA [illegible],215,184,208
1160 DATA [illegible],201,[illegible],194,183,169
1161 DATA 149,168,145,139,164,169
1162 DATA 170,090,000,000,154,169
1163 DATA [illegible],[illegible],162,141,154,153
1164 DATA [illegible],155,155,133,093,113
1165 DATA [illegible],190,145,155,139,127
1166 DATA 131,130,126,152
```

Table 10.7 Surface profile data for a grinding wheel after 5 minutes wear (MJ14IA)

```
>LOAD 'MACJ04'
>1000 DATA 000,000,000,000,000,000
1>001 DATA 000,000,000,000,000,021
1>002 DATA 054,063,079,078,073,049
1>003 DATA 016,000,000,000,000,000
1>004 DATA 000,000,000,000,000,000
1>005 DATA 000,000,000,000,000,000
1>006 DATA 000,000,000,000,000,000
1007> DATA 000,000,000,000,000,000
1>008 DATA 000,000,000,000,000,000
1>009 DATA 000,000,000,000,000,000
1>010 DATA 000,000,000,000,000,000
1>011 DATA 000,000,000,000,000,000
1>012 DATA 000,000,000,000,000,000
1>013 DATA 000,000,000,000,000,000
1>014 DATA 000,000,000,000,000,000
1>015 DATA 000,000,000,000,000,000
1>016 DATA 000,000,000,000,000,000
1>017 DATA 000,000,000,000,000,000
1>018 DATA 000,000,000,000,000,000
1>019 DATA 000,000,000,000,000,000
1>020 DATA 000,000,000,000,000,000
1>021 DATA 000,000,000,000,000,000
1>022 DATA 000,000,000,000,000,000
1023 >DATA 000,000,000,000,000,000
1>024 DATA 000,000,000,000,000,000
1>025 DATA 000,000,000,000,000,000
1>026 DATA 000,000,000,000,000,000
1>027 DATA 000,000,000,000,000,000
1>028 DATA 000,000,000,000,000,000
1>029 DATA 000,000,000,000,000,000
1>030 DATA 000,000,000,000,000,000
1>031 DATA 000,000,000,000,000,043
1>032 DATA 059,100,117,125,149,176
1>033 DATA 211,230,229,230,228,228
1>034 DATA 227,217,207,198,191,171
1>035 DATA 162,143,125,105,069,022
1>036 DATA 000,000,000,000,000,000
1>037 DATA 000,000,000,000,000,000
1>038 DATA 000,022,080,140,199,227
1>039 DATA 228,209,186,180,175,165
1>040 DATA 148,139,145,145,145,150
1>041 DATA 146,146,142,164,174,177
1>042 DATA 174,170,168,164,157,138
1>043 DATA 095,045,000,000,000,000
1>044 DATA 000,000,000,000,000,000
1>045 DATA 000,000,000,042,094,155
1>046 DATA 208,230,230,223,202,180
1047 DATA 154>,113,066,021,000,000
1>048 DATA 000,000,000,000,000,000
1>049 DATA 000,000,000,000,000,000
1>050 DATA 000,000,000,000,000,000
1>051 DATA 000,000,000,000,000,000
1>052 DATA 000,000,000,000,000,049
1>053 DATA 063,060,056,051,045,039
1>054 DATA 020,000,000,000,000,000
1>055 DATA 000,000,000,000,000,000
1>056 DATA 036,063,076,081,063,071
1>057 DATA 072,058,036,005,000,000
1>058 DATA 000,000,000,000,000,000
1>059 DATA 000,000,000,000,000,000
1>060 DATA 000,000,000,000,000,000
1>061 DATA 000,000,000,000,000,000
1>062 DATA 000,000,034,092,143,141
1>063 DATA 166,193,191,186,183,184
106>4 DATA 193,205,183,146,101,063
1>065 DATA 023,000,000,000,000,000
1>066 DATA 000,000,000,000,000,000
10>67 DATA 000,000,000,035,091,143
1>068 DATA 196,217,217,212,203,177
1>069 DATA 150,148,202,203,217,213
1>070 DATA 211,185,167,139,092,050
1>071 DATA 009,000,000,000,000,000
1>072 DATA 000,000,000,000,000,000
1>073 DATA 000,000,000,000,000,000
1>074 DATA 000,000,000,000,000,000
1>075 DATA 000,000,000,000,000,000
1>076 DATA 000,000,000,000,000,000
1>077 DATA 000,000,000,000,000,000
1>078 DATA 000,000,000,000,000,000
107>9 DATA 000,000,000,000,000,000
1>080 DATA 000,000,000,000,000,000
1>081 DATA 000,000,000,000,000,000
1>082 DATA 000,000,000,000,000,000
1>083 DATA 000,000,000,000,000,000
1>084 DATA 000,000,000,000,000,000
1>085 DATA 000,000,034,059,084,106
1>086 DATA 109,109,110,110,102,083
1>087 DATA 066,065,130,163,161,157
1>088 DATA 153,141,110,080,058,036
1>089 DATA 022,014,000,000,000,000
1>090 DATA 000,000,018,075,114,132
1>091 DATA 146,159,169,176,180,180
1>092 DATA 175,161,135,121,115,094
1>093 DATA 058,021,000,000,003,015
1>094 DATA 024,029,037,034,036,051
1095> DATA 079,108,132,161,207,217
1>096 DATA 224,229,229,230,230,230
1>097 DATA 230,219,179,151,148,156
1>098 DATA 171,175,183,196,206,214
1>099 DATA 216,224,229,229,229,226
1>100 DATA 229,229,191,150,101,056
>1101 DATA 013,000,000,002,013,019
1>102 DATA 020,042,045,045,045,059
1>103 DATA 070,079,105,113,114,114
1>104 DATA 114,114,114,114,100,059
1>105 DATA 014,000,000,000,000,000
1>106 DATA 000,000,000,000,000,000
1>107 DATA 000,000,000,000,000,000
1>108 DATA 000,000,000,000,000,000
1>109 DATA 000,000,000,000,000,000
1>110 DATA 000,000,011,063,108,156
1>111 DATA 211,232,231,231,231,232
1>112 DATA 231,222,202,221,214,231
1>113 DATA 231,231,231,231,231,231
11>14 DATA 231,230,227,228,230,231
1>115 DATA 231,231,231,231,231,216
1>116 DATA 206,172,146,115,066,036
1117 >DATA 023,000,037,069,108,116
1>118 DATA 150,168,206,230,231,232
1>119 DATA 233,233,228,214,219,206
11>20 DATA 168,122,074,028,000,000
1>121 DATA 000,000,000,000,000,000
1>122 DATA 000,000,000,000,000,000
1>123 DATA 000,000,009,021,043,059
1>124 DATA 071,071,071,071,063,050
1125 DATA> 041,032,021,007,000,000
1>126 DATA 000,000,000,000,000,000
11>27 DATA 000,000,000,000,000,000
1>128 DATA 044,072,095,077,059,031
1>129 DATA 001,000,000,000,000,000
1>130 DATA 000,000,000,000,000,000
1>131 DATA 000,000,000,000,000,000
1>132 DATA 000,000,000,000,000,000
1>133 DATA 000,000,000,000,000,000
1134 >DATA 000,000,000,000,000,000
113>5 DATA 000,000,003,017,046,062
11>36 DATA 090,118,151,179,200,217
113>7 DATA 225,228,229,229,229,224
1>138 DATA 212,187,179,194,184,149
113>9 DATA 124,107,104,105,095,095
1140 DAT>A 095,095,094,079,047,002
1141 DATA 026,0>87,124,133,151,169
1142 >DATA 189,205,221,232,220,196
1143 D>ATA 177,157,136,114,087,061
114>4 DATA 039,018,000,000,000,000
1>145 DATA 000,000,000,000,000,000
1>146 DATA 000,000,000,000,000,000
1>147 DATA 000,000,000,000,000,000
1>148 DATA 000,000,000,000,000,005
1>149 DATA 032,037,029,023,036,041
1150 DATA 06>0,060,061,061,061,059
115>1 DATA 023,000,000,000,000,000
1152> DATA 000,000,000,000,000,000
1>153 DATA 000,000,000,000,000,000
11>54 DATA 000,000,000,000,000,000
115>5 DATA 000,000,000,000,000,000
115>6 DATA 000,000,000,000,000,000
1>157 DATA 000,000,000,040,061,083
1>158 DATA 102,126,147,151,151,151
1>159 DATA 137,100,063,026,000,000
1160 D>ATA 000,000,000,000,000,000
1>161 DATA 000,000,000,000,000,000
1>162 DATA 000,000,047,101,133,155
11>63 DATA 178,199,201,207,219,231
1>164 DATA 231,226,232,213,211,203
1>165 DATA 209,224,218,195,152,109
11>66 DATA 074,029,018,075
```

Table 10.8 Surface profile data for a grinding wheel after 5 minutes wear (MJ20IA)

```
0>02 DATA 000,000,000,000,000,001
1>003 DATA 185,224,232,196,223,232
1>004 DATA 233,233,211,183,127,101
1>005 DATA 109,103,093,053,020,001
1>006 DATA 000,000,000,000,000,000
1>007 DATA 000,000,000,000,000,000
1>008 DATA 000,000,000,000,000,000
1>009 DATA 000,000,031,141,139,130
1>010 DATA 151,210,233,235,222,183
1>011 DATA 116,068,030,004,000,000
1>012 DATA 000,000,000,000,000,000
1>013 DATA 000,000,000,000,000,000
1>014 DATA 000,000,019,124,212,238
1>015 DATA 223,157,098,031,000,000
1>016 DATA 000,000,000,000,000,000
1>017 DATA 000,000,000,000,000,000
1>018 DATA 000,000,000,000,000,000
1>019 DATA 000,000,000,000,000,000
1>020 DATA 000,000,000,000,000,000
1>021 DATA 000,000,000,000,000,000
1>022 DATA 000,000,000,000,000,000
1>023 DATA 000,000,000,000,000,000
1>024 DATA 000,000,000,000,000,000
1>025 DATA 000,000,000,000,000,000
1>026 DATA 000,000,000,000,000,000
1>027 DATA 000,000,000,000,000,000
1>028 DATA 000,000,000,000,000,000
1>029 DATA 000,000,000,000,000,000
1>030 DATA 000,000,000,000,000,000
1>031 DATA 000,000,000,000,000,000
1>032 DATA 000,000,021,045,033,000
1>033 DATA 000,000,000,000,000,000
1>034 DATA 000,000,000,000,000,000
1>035 DATA 000,000,000,000,000,000
1>036 DATA 000,000,000,000,000,000
1>037 DATA 000,000,000,000,000,000
1>038 DATA 000,000,000,000,000,000
1>039 DATA 000,000,000,000,000,000
1>040 DATA 000,000,000,000,000,000
1>041 DATA 000,000,000,000,000,000
1>042 DATA 000,000,000,000,000,000
1>043 DATA 000,000,000,000,000,000
1>044 DATA 000,000,000,000,000,000
1>045 DATA 000,000,000,000,000,000
1>046 DATA 000,000,000,000,000,000
1>047 DATA 000,000,000,000,000,000
1>048 DATA 000,000,000,000,000,000
1>049 DATA 000,000,000,000,000,017
>1050 DATA 057,068,035,003,034,012
1>051 DATA 000,000,000,000,000,001
1>052 DATA 187,161,091,001,052,001
1>053 DATA 000,000,000,031,077,121
1>054 DATA 155,231,222,189,234,234
1>055 DATA 158,114,049,000,000,000
1>056 DATA 000,000,000,000,000,000
1>057 DATA 000,000,000,000,000,000
1>058 DATA 000,000,000,000,000,000
>1059 DATA 000,000,000,000,000,000
1>060 DATA 000,000,000,000,000,000
1>061 DATA 000,000,000,000,000,000
1>062 DATA 000,000,000,000,000,000
10>63 DATA 000,000,000,000,000,000
1>064 DATA 000,000,000,000,000,000
1>065 DATA 000,000,014,115,211,232
1>066 DATA 232,232,233,233,233,214
1>067 DATA 185,103,014,000,000,000
1>068 DATA 000,000,000,000,000,000
1>069 DATA 000,000,000,000,000,000
1>070 DATA 000,000,000,000,000,000
1>071 DATA 000,000,000,000,000,000
1>072 DATA 000,000,000,000,000,000
1>073 DATA 000,000,000,000,000,000
1>074 DATA 000,000,000,000,000,000
1>075 DATA 000,000,000,000,000,000
1>076 DATA 000,000,000,103,208,234
1>077 DATA 212,141,064,000,000,065
1>078 DATA 169,222,233,233,233,213
1>079 DATA 157,149,136,095,109,091
1>080 DATA 029,060,059,043,030,000
1>081 DATA 000,000,000,000,000,000
>1082 DATA 000,000,000,000,000,000
1>083 DATA 000,000,000,000,000,000
1>084 DATA 000,000,000,000,000,000
1>085 DATA 000,000,000,000,000,000
1>086 DATA 000,000,000,000,000,000
1>087 DATA 000,000,000,000,000,000
>1088 DATA 000,000,000,000,000,000
1>089 DATA 000,000,000,000,000,000
1>090 DATA 000,000,000,000,000,000
1>091 DATA 000,000,000,000,000,000
>1092 DATA 000,000,000,000,000,000
1>093 DATA 000,000,000,000,000,000
1>094 DATA 000,000,000,000,000,000
1>095 DATA 000,000,000,000,000,000
1>096 DATA 000,000,000,000,000,000
1>097 DATA 000,000,000,000,000,000
1>098 DATA 000,000,000,000,000,000
1>099 DATA 000,000,000,000,000,009
1>100 DATA 019,005,000,000,000,000
1>101 DATA 000,000,000,000,000,000
1>102 DATA 000,000,000,000,000,000
1>103 DATA 000,000,000,000,000,000
1>104 DATA 000,000,000,000,000,000
1>105 DATA 000,000,000,000,002,113
1>106 DATA 221,222,232,223,233,229
1>107 DATA 231,234,234,235,230,217
1>108 DATA 179,190,212,147,099,011
1>109 DATA 000,000,000,000,000,000
1>110 DATA 000,000,000,000,000,000
1>111 DATA 000,000,000,000,000,000
1>112 DATA 000,000,000,000,000,000
1>113 DATA 000,000,000,000,000,000
1>114 DATA 000,000,000,000,000,000
1>115 DATA 000,000,000,000,000,000
1>116 DATA 000,000,000,000,000,050
1>117 DATA 156,139,200,202,221,234
1>118 DATA 233,222,199,111,045,000
1>119 DATA 004,050,039,127,194,231
1>120 DATA 182,224,217,163,140,115
1>121 DATA 108,069,016,002,035,050
1>122 DATA 055,046,055,045,037,014
1>123 DATA 000,000,000,000,000,000
1>124 DATA 000,000,000,000,000,000
1>125 DATA 000,000,000,000,000,000
1>126 DATA 000,000,000,000,000,000
>1127 DATA 000,000,000,000,000,000
1>128 DATA 000,000,000,000,000,000
1>129 DATA 000,000,000,000,000,000
1>130 DATA 000,000,000,000,000,000
1>131 DATA 000,000,000,000,000,000
1>132 DATA 000,000,000,000,000,000
1>133 DATA 000,000,055,045,036,025
1>134 DATA 017,000,000,000,000,000
1>135 DATA 000,000,000,000,014,111
11>36 DATA 061,093,102,112,114,141
1>137 DATA 097,023,000,000,000,000
1>138 DATA 000,000,000,000,000,000
1>139 DATA 000,000,000,000,000,000
1>140 DATA 000,000,000,000,000,000
1>141 DATA 000,000,000,000,000,000
1>142 DATA 000,000,000,000,000,000
1>143 DATA 000,000,000,000,000,000
1>144 DATA 000,000,000,000,000,000
1>145 DATA 000,000,000,000,000,000
1>146 DATA 000,000,000,000,000,000
1>147 DATA 000,000,000,000,000,000
1>148 DATA 000,000,000,000,000,000
1>149 DATA 000,000,000,000,000,000
1>150 DATA 000,000,000,000,000,000
1>151 DATA 000,000,000,000,000,000
1>152 DATA 000,000,000,000,000,000
1>153 DATA 000,000,000,000,000,000
1>154 DATA 000,000,000,000,000,000
1155 >DATA 000,000,000,000,000,000
11>56 DATA 000,000,000,000,000,000
11>57 DATA 068,056,032,015,000,000
1>158 DATA 000,000,000,000,000,000
11>59 DATA 000,000,000,000,000,000
116>0 DATA 000,000,000,000,000,000
1>161 DATA 000,000,000,000,000,000
116>2 DATA 000,000,000,000,000,000
1166DATA000,000,000,000,000,000
```

Table 10.9 Profile data for a ground surface corresponding with 5 minutes grinding wheel wear (MJ40IA)

```
    LOGIN STHUMP
STHUMP (4) LOGGED IN AT  10'27 07090
WELCOME STHUMP

OK, LBASIC
GO
>LOAD 'MACJ04'
>1000 DATA 158,161,160,161,148,140
1000 DATA 158,161,160,161,148,140
↑AD
>1001 DATA 129,163,145,161,175,187
1>002 DATA 189,164,173,161,161,178
1>003 DATA 180,188,164,167,177,156
1>004 DATA 181,176,195,184,179,194
1>005 DATA 215,201,186,209,198,188
1>006 DATA 181,200,191,186,181,162
1>007 DATA 191,196,190,194,172,154
1>008 DATA 195,207,194,187,184,180
1>009 DATA 163,145,179,184,159,179
1>010 DATA 180,196,187,216,201,182
1>011 DATA 188,162,199,206,221,156
1>012 DATA 196,163,175,188,173,185
1>013 DATA 166,160,174,148,185,182
1>014 DATA 164,143,176,181,187,188
1>015 DATA 177,160,161,176,186,199
1>016 DATA 155,183,157,171,173,192
1>017 DATA 207,202,194,194,187,178
1>018 DATA 170,189,191,194,198,193
1>019 DATA 203,173,191,161,188,188
1>020 DATA 196,186,178,197,187,209
1>021 DATA 212,191,205,190,202,201
1>022 DATA 184,205,221,191,188,190
10>23 DATA 229,197,198,173,197,145
1>024 DATA 184,190,193,213,209,211
1>025 DATA 216,203,217,217,228,221
1>026 DATA 193,203,204,209,191,208
1>027 DATA 202,209,212,203,223,205
1>028 DATA 198,187,161,172,174,178
1>029 DATA 185,205,188,190,219,219
1>030 DATA 165,192,218,198,202,211
1>031 DATA 216,205,204,213,162,186
1>032 DATA 225,213,184,181,181,188
1>033 DATA 205,230,195,187,204,163
1>034 DATA 196,161,153,162,157,156
1>035 DATA 176,209,207,201,195,202
1036 DATA 159,1>72,205,146,177,146
1>037 DATA 151,188,188,181,183,180
1>038 DATA 189,195,223,209,201,224
1>039 DATA 198,213,195,221,171,203
1>040 DATA 052,165,197,013,102,000
1>041 DATA 099,123,148,150,162,191
1>042 DATA 195,206,191,199,198,186
1>043 DATA 199,192,208,190,193,216
1>044 DATA 197,203,156,217,204,167
1>045 DATA 207,213,176,211,195,164
1>046 DATA 202,195,178,190,179,180
1>047 DATA 196,188,188,191,187,167
1>048 DATA 191,191,199,190,201,190
1>049 DATA 175,200,194,180,189,184
1>050 DATA 201,184,216,200,159,173
1>051 DATA 188,186,177,194,182,183
1>052 DATA 190,182,174,168,187,179
1>053 DATA 181,216,180,184,179,203
1>054 DATA 202,191,189,176,168,177
1>055 DATA 189,187,188,181,182,175
1>056 DATA 167,186,176,191,169,200
1>057 DATA 189,182,198,191,187,176
1>058 DATA 175,196,059,177,178,173
1>059 DATA 176,197,141,191,173,170
1>060 DATA 189,183,187,194,185,173
1>061 DATA 116,192,164,170,194,194
1>062 DATA 203,206,191,205,196,200
1>063 DATA 170,184,187,180,177,198
1>064 DATA 186,182,198,181,162,170
1>065 DATA 149,191,180,181,199,194
1>066 DATA 180,169,139,191,202,193
1>067 DATA 188,181,184,175,172,156
1>068 DATA 202,189,191,168,184,180
1>069 DATA 188,195,189,186,180,139
>1070 DATA 180,185,178,191,191,200
1>071 DATA 183,201,186,208,194,186
1>072 DATA 182,191,187,199,181,174
1>073 DATA 184,198,193,204,199,191
1>074 DATA 189,181,212,189,158,196
1>075 DATA 165,168,178,183,188,197
1>076 DATA 183,173,185,191,191,191
1>077 DATA 185,199,191,189,179,172
1>078 DATA 193,197,191,191,191,177
1>079 DATA 176,190,186,175,184,168
1>080 DATA 048,019,000,146,211,201
1>081 DATA 197,181,197,186,215,205
1>082 DATA 213,215,202,187,193,213
1>083 DATA 189,192,195,208,230,192
1>084 DATA 217,216,187,203,189,193
1>085 DATA 187,183,187,187,186,183
1>086 DATA 186,157,155,174,178,167
1>087 DATA 178,208,189,166,204,178
1>088 DATA 191,191,201,181,200,193
1>089 DATA 201,218,203,192,000,149
1>090 DATA 154,177,194,203,191,202
1>091 DATA 186,199,181,195,217,211
1>092 DATA 178,189,195,201,202,197
1>093 DATA 189,195,202,159,186,178
1>094 DATA 186,191,175,189,177,180
1>095 DATA 195,198,205,178,178,155
1>096 DATA 177,189,184,183,187,186
1>097 DATA 177,204,173,190,218,207
1>098 DATA 156,194,201,180,188,145
1>099 DATA 172,143,193,200,192,202
1>100 DATA 210,209,207,187,185,195
1>101 DATA 150,195,188,180,183,161
1>102 DATA 196,189,153,183,193,199
1>103 DATA 192,197,219,204,198,207
1>104 DATA 195,185,195,188,182,173
1>105 DATA 166,188,197,210,173,177
1>106 DATA 189,176,179,208,196,195
1>107 DATA 199,182,180,173,176,197
1>108 DATA 184,187,198,193,204,193
1>109 DATA 197,198,205,208,217,227
1>110 DATA 225,220,213,221,209,227
1>111 DATA 203,207,216,212,183,187
1>112 DATA 193,179,188,219,207,198
1>113 DATA 191,189,198,182,187,204
1>114 DATA 208,210,212,202,203,207
1>115 DATA 218,216,208,180,199,193
>1116 DATA 221,199,181,189,204,212
1>117 DATA 207,197,181,214,198,199
1>118 DATA 200,190,193,189,179,180
1>119 DATA 178,167,186,180,183,187
1>120 DATA 197,207,194,212,201,216
1>121 DATA 180,199,205,205,197,203
1>122 DATA 201,186,187,195,198,210
1>123 DATA 211,215,219,199,212,197
1>124 DATA 179,156,180,209,195,200
1>125 DATA 212,181,194,178,196,159
1>126 DATA 176,175,187,177,196,185
1>127 DATA 191,189,211,185,196,203
1>128 DATA 209,180,193,191,192,170
1>129 DATA 178,209,211,206,198,191
1>130 DATA 195,206,203,202,200,200
1>131 DATA 202,181,180,163,053,113
1>132 DATA 173,180,187,190,201,193
1>133 DATA 196,210,206,202,202,210
1>134 DATA 199,204,195,199,185,207
1>135 DATA 202,201,181,172,223,210
1>136 DATA 183,188,201,191,113,099
1>137 DATA 161,171,191,199,204,205
1>138 DATA 197,197,205,179,181,188
1>139 DATA 196,196,178,187,167,162
1>140 DATA 089,173,197,181,204,188
1>141 DATA 167,174,175,147,181,195
1>142 DATA 182,171,177,160,202,195
1>143 DATA 191,196,212,207,200,211
1>144 DATA 195,204,193,209,196,185
1>145 DATA 183,191,199,186,180,179
1>146 DATA 107,139,184,171,171,173
1>147 DATA 162,171,179,174,181,193
1>148 DATA 175,181,168,189,165,165
1>149 DATA 164,177,191,187,197,199
1>150 DATA 214,204,201,209,203,197
1>151 DATA 181,180,188,194,161,197
1>152 DATA 148,181,156,223,200,222
1>153 DATA 190,211,223,214,199,213
1>154 DATA 196,203,180,174,174,197
1>155 DATA 195,185,181,171,178,172
1>156 DATA 170,181,177,187,185,193
1>157 DATA 197,204,217,197,186,186
1>158 DATA 168,191,177,180,186,197
1>159 DATA 188,180,210,146,212,177
1>160 DATA 164,196,182,191,160,181
1>161 DATA 152,145,132,147,145,161
1>162 DATA 159,161,153,138,072,086
1>163 DATA 130,140,104,103,102,102
1>164 DATA 101,101,101,101,101,101
1>165 DATA 101,101,101,100,100,101
1>166 DATA 101,100,100,100
>1000 DATA 158,161,160,161,148,140
```

Table 10.10 Surface profile data for a grinding wheel after 10 minutes wear (MJ26IA)

```
>1000 DATA 000,000,000,000,000,000
1001> DATA 000,000,000,006,012,020
10>02 DATA 034,044,058,067,082,090
1003> DATA 096,125,137,138,138,121
100>4 DATA 164,223,239,255,211,208
1>005 DATA 180,147,112,075,036,000
100>6 DATA 000,000,000,000,000,000
1>007 DATA 000,000,000,000,000,000
100>8 DATA 000,000,000,000,000,000
10>09 DATA 000,000,000,000,000,000
1010> DATA 000,000,000,003,011,018
10>11 DATA 026,026,026,026,000,000
101>2 DATA 000,000,000,000,000,000
101>3 DATA 000,000,000,000,000,000
1>014 DATA 000,000,000,000,000,000
10>15 DATA 000,000,000,000,000,000
1016 DA>TA 000,000,000,000,000,000
10>17 DATA 000,000,000,000,000,000
101>8 DATA 000,000,000,000,000,000
1>019 DATA 000,000,000,039,034,057
102>0 DATA 078,080,078,074,070,078
1>021 DATA 085,046,031,011,000,000
102>2 DATA 000,000,000,000,000,000
1>023 DATA 000,000,000,000,000,000
10>24 DATA 000,000,000,000,000,000
1025> DATA 000,000,000,000,000,000
102>6 DATA 000,000,000,000,000,000
1>027 DATA 000,000,000,000,000,000
1028> DATA 000,000,000,000,000,000
10>29 DATA 000,000,000,000,000,000
1>030 DATA 000,000,000,000,000,000
103>1 DATA 029,075,083,101,110,105
1>032 DATA 097,091,135,191,182,148
103>3 DATA 110,083,050,011,000,000
1>034 DATA 000,000,000,000,000,000
103>5 DATA 000,000,000,000,000,000
1>036 DATA 000,000,000,000,000,000
1>037 DATA 000,000,000,000,000,000
1038 DATA 000,000,000,000,000,000
1>039> DATA 000,000,000,000,000,000
10>40 DATA 000,000,000,000,000,000
1041> DATA 000,000,000,000,000,000
10>42 DATA 000,000,000,013,028,040
104>3 DATA 052,081,103,121,133,154
1>044 DATA 162,169,183,204,208,221
104>5 DATA 221,211,169,121,076,029
1046> DATA 000,000,000,000,034,081
10>47 DATA 055,009,000,000,000,000
104>8 DATA 000,000,000,000,000,000
1>049 DATA 000,000,000,000,000,000
105>0 DATA 000,000,000,000,000,000
1>051 DATA 000,000,000,000,000,000
105>2 DATA 000,000,000,000,000,000
1>053 DATA 000,000,000,000,000,000
105>4 DATA 000,000,000,000,000,000
1>055 DATA 000,000,000,000,000,000
10>56 DATA 000,000,000,000,000,000
10>57 DATA 000,000,000,000,000,000
105>8 DATA 000,000,000,000,000,000
1>059 DATA 000,000,000,000,000,000
1060 DATA 058,101,125,144,172,202
>1061 >DATA 211,194,173,149,130,087
106>2 DATA 051,010,000,000,000,000
1>063 DATA 000,000,000,000,014,020
1064> DATA 033,021,000,000,000,000
1065> DATA 000,000,000,000,000,000
10>66 DATA 000,000,000,000,000,000
1>067 DATA 000,000,000,000,000,000
10>68 DATA 000,000,060,116,172,206
1>069 DATA 208,208,196,164,127,095
10>70 DATA 085,083,044,031,020,000
10>71 DATA 000,000,000,000,000,000
107>2 DATA 000,000,000,000,000,000
1073 >DATA 000,000,000,000,000,000
107>4 DATA 000,000,000,000,000,000
1>075 DATA 000,000,000,000,000,000
1076> DATA 000,000,000,000,017,076
1077> DATA 111,136,127,109,092,082
1>078 DATA 076,056,052,039,016,012
10>79 DATA 023,040,041,042,042,042
1080 D>ATA 042,035,017,011,011,010
1081> DATA 011,011,000,000,000,000
1>082 DATA 000,000,000,000,000,000
1>083 DATA 000,000,000,000,000,000
1084 DA>TA 000,000,000,000,000,000
108>5 DATA 000,000,000,000,000,000
108>6 DATA 000,000,000,000,000,000
1087 >DATA 000,000,000,000,000,000
1>088 DATA 000,000,000,000,000,000
1>089 DATA 000,000,000,000,000,000
1>090 DATA 000,000,000,000,000,000
10>91 DATA 000,000,000,000,000,000
1092 >DATA 000,000,000,000,000,000
10>93 DATA 000,000,000,000,000,000
1>094 DATA 000,000,032,046,045,021
1095 DA>TA 002,000,000,000,000,000
1>Q96 DATA 000,000,000,000,000,000
1097> DATA 000,000,000,000,000,000
1>098 DATA 000,000,000,000,000,000
1099> DATA 000,000,000,000,000,000
11>00 DATA 000,056,082,101,079,055
11>01 DATA 046,045,038,031,022,000
110>2 DATA 000,000,000,000,000,000
1>103 DATA 000,000,000,000,000,000
110>4 DATA 000,000,000,000,000,000
1>105 DATA 000,000,000,000,000,000
11>06 DATA 000,000,000,000,000,000
110>7 DATA 000,000,000,000,000,000
1>108 DATA 000,000,000,000,000,000
11>09 DATA 000,000,000,000,000,000
1>110 DATA 000,000,000,000,000,000
11>11 DATA 000,000,000,000,000,000
11>12 DATA 051,091,130,188,209,212
1113> DATA 179,135,091,059,023,001
111>4 DATA 000,000,000,000,000,000
1>115 DATA 000,000,000,000,023,050
111>6 DATA 065,075,056,037,031,055
111>7 DATA 122,149,171,196,208,195
1>118 DATA 181,151,104,058,014,000
11>19 DATA 000,000,000,000,000,000
112>0 DATA 000,000,000,000,000,000
1>121 DATA 000,000,000,000,000,000
112>2 DATA 000,000,000,000,000,000
1>123 DATA 000,000,000,000,000,000
11>24 DATA 000,000,000,000,000,000
1125> DATA 000,000,000,000,000,000
11>26 DATA 000,000,000,000,000,000
112>7 DATA 000,000,000,000,000,000
11>28 DATA 000,000,000,000,000,000
1129> DATA 000,000,000,000,000,000
11>30 DATA 000,000,000,000,000,000
1131> DATA 000,000,000,000,035,043
113>2 DATA 042,027,009,000,000,000
1>133 DATA 000,000,000,000,000,000
113>4 DATA 000,000,000,000,000,000
1135> DATA 000,000,000,000,000,000
1>136 DATA 000,000,000,006,068,089
1137 DATA 118,157,195,212,212,206
1138 DATA 184,1>65,1>51,127,090,048
1139 DATA 007,000,000,000,000,000>
1140 DATA 000,000,000,000,000,000
>1141 DATA 000,000,000,000,000,000
11>42 DATA 000,000,000,028,052,074
1143 DATA> 097,104,110,115,108,097
1144 DATA 0>81,055,034,001,000,000
1145 DATA 000,>000,000,000,000,000
1146 DATA 000,000,>000>,000,000,000
1147 DATA 000,000,000,00>0,000,000
11>48 DATA 000,000,000,000,000,000
1149> DATA 000,000,000,000,000,000
1150> DATA 000,000,000,000,000,000
1151 DATA 000,000,000,000,000,000
11>52> DATA 000,000,000,000,000,000
115>3 DATA 000,000,000,000,000,000
1>154 DATA 000,000,000,000,000,000
1155> DATA 000,000,000,000,000,000
1156 DA>TA 000,000,000,000,000,000
115>7 DATA 000,000,000,000,000,000
11>58 DATA 000,000,000,000,000,000
115>9 DATA 000,000,000,000,000,000
11>60 DATA 000,000,000,000,000,000
1161> DATA 000,000,000,000,000,000
11>62 DATA 000,013,077,141,190,196
1>163 DATA 202,181,177,188,193,193
116>4 DATA 200,205,215,215,215,214
1>165 DATA 215,215,214,181,164,151
11>66 DATA 108,062,020,000
```

Table 10.11 Surface profile data for a grinding wheel after 10 minutes wear (MJ32IA)

```
>1000 DATA 000,045,133,132,146,133
1>001 DATA 120,109,101,090,078,067
1>002 DATA 057,047,039,035,036,051
1>003 DATA 077,041,003,000,000,000
1>004 DATA 000,000,000,000,000,000
>1005 DATA 000,000,000,000,000,000
1>006 DATA 000,000,000,000,000,000
1>007 DATA 095,188,194,194,160,122
1>008 DATA 091,067,050,033,018,001
1>009 DATA 000,000,000,000,000,000
1>010 DATA 000,001,058,134,177,172
1>011 DATA 171,131,087,049,016,000
1>012 DATA 000,000,000,000,000,000
1>013 DATA 000,000,000,000,000,000
1>014 DATA 000,000,000,000,000,000
1>015 DATA 000,000,000,000,000,000
1>016 DATA 000,000,000,000,000,000
1>017 DATA 000,000,000,000,000,000
1>018 DATA 000,000,000,045,043,072
1>019 DATA 106,176,199,179,111,031
1>020 DATA 000,000,000,000,044,043
1>021 DATA 036,044,138,194,203,204
1>022 DATA 205,203,203,203,194,144
1>023 DATA 086,021,000,000,000,000
1>024 DATA 000,000,000,000,000,000
1>025 DATA 000,000,000,000,000,000
1>026 DATA 000,000,000,000,000,000
1>027 DATA 000,000,000,000,000,000
1>028 DATA 000,000,000,000,000,000
1>029 DATA 000,000,000,000,000,000
1>030 DATA 000,000,000,000,000,000
1>031 DATA 000,000,000,000,000,000
1>032 DATA 000,000,000,000,000,000
1>033 DATA 000,000,000,000,000,000
1>034 DATA 000,000,000,000,000,000
1>035 DATA 000,000,000,000,000,000
1>036 DATA 000,000,000,000,000,000
1>037 DATA 000,000,000,000,000,000
1>038 DATA 000,000,000,000,000,000
1039> DATA 000,000,000,000,000,000
1>040 DATA 000,000,000,000,000,000
1>041 DATA 000,000,000,000,000,000
1>042 DATA 000,000,000,000,000,000
>1043 DATA 000,000,000,000,000,000
1>044 DATA 000,000,000,000,000,000
1>045 DATA 000,000,000,000,000,000
1>046 DATA 000,000,061,092,107,112
1>047 DATA 151,125,079,035,000,000
1>048 DATA 000,000,000,000,000,000
1>049 DATA 000,000,000,000,000,000
1>050 DATA 000,000,000,000,000,000
1>051 DATA 000,000,000,000,000,000
1>052 DATA 000,000,000,000,000,000
1>053 DATA 000,000,000,000,000,000
1>054 DATA 000,000,000,023,036,036
10>55 DATA 033,010,000,015,081,172
1>056 DATA 201,163,130,052,000,000
1>057 DATA 000,000,000,000,000,000
1>058 DATA 000,000,000,000,000,000
1>059 DATA 000,000,000,000,000,000
1>060 DATA 000,000,000,000,000,000
1>061 DATA 000,000,000,000,000,000
1>062 DATA 000,000,000,000,000,000
1>063 DATA 000,000,000,000,000,000
1>064 DATA 000,000,000,000,000,000
1>065 DATA 000,000,000,000,000,000
1>066 DATA 000,000,000,000,000,000
1>067 DATA 000,000,000,000,000,000
1>068 DATA 000,000,000,000,000,000
1>069 DATA 021,055,091,091,085,055
>1070 DATA 023,000,000,000,000,000
1>071 DATA 000,000,000,000,000,000
1>072 DATA 000,032,042,068,127,131
>1073 DATA 091,048,003,000,000,000
>1074 DATA 000,000,000,000,000,000
>1075 DATA 000,000,000,000,000,000
1>076 DATA 000,000,000,000,000,000
107>7 DATA 000,000,000,000,000,000
10>78 DATA 000,000,000,000,000,000
107>9 DATA 000,000,000,000,000,000
1>080 DATA 000,000,000,000,000,000
1>081 DATA 000,000,000,000,000,000
1>082 DATA 000,000,000,009,015,018
1>083 DATA 007,000,000,000,000,000
1>084 DATA 000,000,000,002,071,154
1>085 DATA 202,187,154,102,073,034
1>086 DATA 038,041,033,025,000,000
1>087 DATA 000,000,000,000,000,033
1>088 DATA 109,145,179,197,196,202
10>89 DATA 204,199,204,205,204,191
1>090 DATA 177,160,117,066,000,000
1>091 DATA 000,000,000,000,000,000
1>092 DATA 000,000,000,000,000,000
1>093 DATA 000,000,000,000,000,000
1>094 DATA 000,000,000,000,000,000
1>095 DATA 000,000,000,000,000,000
1>096 DATA 000,000,000,000,000,000
1>097 DATA 000,000,000,000,000,000
1>098 DATA 000,000,000,000,000,000
1>099 DATA 000,000,000,000,000,000
1>100 DATA 000,000,000,000,000,000
1>101 DATA 000,000,000,000,000,000
1>102 DATA 000,000,000,000,000,000
1>103 DATA 000,000,000,000,000,000
1>104 DATA 043,098,109,120,089,094
1>105 DATA 101,116,117,085,025,000
1>106 DATA 000,000,000,000,000,000
1>107 DATA 000,000,000,000,000,000
1>108 DATA 000,000,000,000,000,000
>1109 DATA 000,000,000,000,000,000
1>110 DATA 000,000,012,021,021,000
1>111 DATA 000,000,000,000,000,000
1>112 DATA 000,000,000,000,000,000
1>113 DATA 073,145,176,204,203,203
1>114 DATA 202,169,127,069,012,000
1>115 DATA 000,000,000,000,000,000
1>116 DATA 000,000,000,000,000,000
1>117 DATA 000,000,000,000,000,000
1>118 DATA 000,000,000,000,000,000
1>119 DATA 000,000,000,000,000,000
1>120 DATA 000,000,000,000,000,000
1>121 DATA 000,000,000,000,000,000
1>122 DATA 000,000,000,000,000,000
1>123 DATA 000,000,000,000,000,000
1>124 DATA 000,000,000,000,000,000
1>125 DATA 000,000,000,000,000,000
1>126 DATA 000,000,000,000,000,000
1>127 DATA 000,000,000,000,000,000
1>128 DATA 000,020,050,074,100,082
1>129 DATA 085,091,097,115,100,013
1>130 DATA 000,000,000,000,000,000
1>131 DATA 000,000,000,000,000,000
1>132 DATA 000,000,000,000,000,000
1>133 DATA 000,000,000,000,000,000
1>134 DATA 000,000,000,000,000,000
1>135 DATA 000,000,000,000,000,000
1>136 DATA 000,000,000,000,000,000
1>137 DATA 000,000,000,000,000,000
1>138 DATA 000,000,000,000,000,000
1>139 DATA 000,000,000,014,087,139
1>140 DATA 201,205,193,136,108,031
1>141 DATA 000,000,000,000,000,000
1>142 DATA 000,000,000,000,000,000
1>143 DATA 000,000,000,000,000,000
1>144 DATA 000,000,000,000,000,000
1>145 DATA 000,000,000,000,000,000
1>146 DATA 000,000,000,000,000,000
1>147 DATA 000,000,000,000,000,000
114>8 DATA 000,000,000,000,000,000
1>149 DATA 000,000,000,000,000,000
1>150 DATA 000,000,000,019,063,061
1>151 DATA 053,044,000,000,000,000
1>152 DATA 000,000,000,000,000,000
1>153 DATA 000,000,000,013,014,011
1>154 DATA 002,017,009,002,000,000
1>155 DATA 000,000,000,000,000,000
1156> DATA 000,000,000,000,000,000
1>157 DATA 000,000,000,000,000,000
115>8 DATA 000,000,000,000,000,000
1>159 DATA 000,000,000,000,000,000
1>160 DATA 000,000,000,000,000,000
1>161 DATA 000,000,000,000,000,000
1>162 DATA 000,000,000,000,000,000
1>163 DATA 000,000,000,000,000,000
1>164 DATA 000,000,000,000,000,000
1>165 DATA 000,000,000,000,000,000
1>166 DATA 000,000,000,000
```

Table 10.12 Profile data for a ground surface corresponding with 10 minutes grinding wheel wear (MJ48IA)

```
LOAD 'MACJ04'
>1000 DATA 098,125,085,127,138,139
1>001 DATA 121,138,133,149,112,111
1>002 DATA 168,144,137,165,157,130
1>003 DATA 165,120,131,153,139,150
1>004 DATA 146,131,143,175,156,167
1>005 DATA 131,149,110,127,154,132
1>006 DATA 143,133,126,143,140,130
1>007 DATA 143,136,163,175,152,141
1>008 DATA 113,129,126,143,100,157
1>009 DATA 133,105,145,139,142,136
1>010 DATA 129,134,160,144,152,151
1>011 DATA 133,130,143,125,125,131
1>012 DATA 106,092,147,163,143,149
1>013 DATA 136,117,127,125,141,130
1>014 DATA 115,127,111,137,134,122
1>015 DATA 114,104,101,114,145,144
1>016 DATA 125,122,129,127,097,143
1>017 DATA 142,122,121,123,109,093
1>018 DATA 085,094,136,124,122,122
1>019 DATA 113,103,106,141,122,120
1>020 DATA 129,133,142,134,135,127
10>21 DATA 135,141,143,130,132,134
1>022 DATA 141,143,146,132,131,129
1>023 DATA 154,140,139,133,125,132
1>024 DATA 146,137,146,133,115,094
10>25 DATA 124,123,135,117,119,122
1>026 DATA 124,123,130,129,134,133
1>027 DATA 124,133,137,149,124,108
1>028 DATA 115,126,122,133,112,097
1>029 DATA 121,122,134,125,133,124
1>030 DATA 127,123,119,121,121,127
1>031 DATA 107,132,132,103,127,139
1>032 DATA 117,130,116,097,116,124
1>033 DATA 112,117,120,122,127,130
1>034 DATA 112,104,112,097,116,129
1>035 DATA 123,119,101,111,113,103
1>036 DATA 132,132,117,121,095,090
1>037 DATA 119,090,096,113,121,103
1>038 DATA 119,121,123,123,123,114
1>039 DATA 120,110,099,083,000,115
1>040 DATA 113,109,122,131,141,098
1>041 DATA 094,101,114,132,118,118
1>042 DATA 137,101,111,123,091,105
1>043 DATA 126,107,108,107,109,117
1>044 DATA 116,114,119,122,117,113
1>045 DATA 095,093,091,084,092,097
1>046 DATA 085,074,099,098,112,111
1>047 DATA 103,106,129,119,128,124
1>048 DATA 118,117,111,097,124,114
1>049 DATA 117,116,119,103,153,136
1>050 DATA 130,142,124,101,120,102
1>051 DATA 125,100,132,139,121,134
1>052 DATA 133,125,129,136,131,114
1>053 DATA 135,129,130,129,132,128
1>054 DATA 143,133,135,132,111,138
1>055 DATA 129,124,137,141,140,148
1>056 DATA 137,117,127,126,136,131
1>057 DATA 130,119,133,137,139,152
1>058 DATA 137,145,122,131,112,129
1>059 DATA 126,131,136,095,114,130
1>060 DATA 132,135,110,136,145,140
1>061 DATA 147,111,122,129,135,133
1>062 DATA 135,143,121,127,117,127
1>063 DATA 135,150,141,135,153,145
1>064 DATA 115,124,104,126,133,130
1>065 DATA 136,141,147,130,137,135
1>066 DATA 142,125,120,113,105,145
1>067 DATA 138,110,104,132,127,139
10>68 DATA 146,121,142,117,127,124
1'>069 DATA 128,129,136,134,111,113
1>070 DATA 107,124,109,139,130,119
1>071 DATA 113,118,135,136,152,136
1>072 DATA 140,138,143,143,141,152
1>073 DATA 151,149,143,123,119,119
1>074 DATA 127,127,121,135,138,141
1>075 DATA 141,114,111,123,135,137
1>076 DATA 141,147,146,153,153,139
1>077 DATA 136,133,150,129,147,144
1>078 DATA 143,160,151,139,126,139
1>079 DATA 139,125,156,140,139,156
1>080 DATA 143,149,144,145,141,150
1>081 DATA 140,154,149,152,143,146
1>082 DATA 154,122,141,121,133,133
1>083 DATA 147,156,133,141,151,139
1>084 DATA 154,147,134,147,123,139
1>085 DATA 141,146,127,149,150,147
1>086 DATA 147,143,149,127,147,140
1>087 DATA 151,141,145,146,122,120
1>088 DATA 122,141,131,140,143,149
1>089 DATA 154,133,144,137,143,142
1>090 DATA 155,148,137,147,151,157
1>091 DATA 140,150,153,149,140,147
1>092 DATA 149,143,138,133,143,150
1>093 DATA 153,136,128,135,131,132
1094> DATA 141,139,143,139,143,152
1>095 DATA 140,131,137,140,149,147
1>096 DATA 139,137,146,153,135,143
1>097 DATA 143,125,157,159,162,149
1>098 DATA 157,154,149,153,140,135
1>099 DATA 136,135,144,133,123,122
1>100 DATA 133,144,143,143,120,143
1>101 DATA 147,123,140,151,161,145
1>102 DATA 140,131,145,133,141,121
1>103 DATA 127,127,134,137,147,149
1>104 DATA 147,140,144,137,141,125
1>105 DATA 132,152,134,141,143,14[illegible]
1>106 DATA 119,141,154,140,164,153
1>107 DATA 139,115,021,000,000,140
1>108 DATA 147,153,152,124,143,135
1>109 DATA 113,164,139,135,124,152
1>110 DATA 124,134,140,149,1[illegible],13[illegible]
1>111 DATA 130,127,139,149,144,143
1>112 DATA 138,160,149,142,147,140
1>113 DATA 165,152,149,149,142,140
1>114 DATA 131,136,134,136,134,126
1>115 DATA 129,137,140,133,143,129
1>116 DATA 135,147,152,135,134,126
1>117 DATA 133,139,121,143,135,125
111>8 DATA 140,143,139,136,120,129
1>119 DATA 121,126,120,127,127,134
1>120 DATA 140,124,127,141,137,129
1121> DATA 127,126,140,138,130,135
1>122 DATA 131,128,121,135,121,122
>1123 DATA 129,132,130,140,149,154
1>124 DATA 155,155,157,148,137,130
1>125 DATA 113,106,133,134,141,150
1>126 DATA 152,150,133,157,151,155
1>127 DATA 133,154,133,134,143,130
1>128 DATA 145,135,149,133,137,127
1>129 DATA 133,152,123,135,134,134
1>130 DATA 134,119,129,127,127,131
1>131 DATA 139,132,139,134,134,127
1>132 DATA 121,131,152,135,145,143
1>133 DATA 135,141,136,130,131,124
1>134 DATA 105,127,120,128,114,129
1>135 DATA 133,132,130,143,135,137
1>136 DATA 133,125,127,120,130,135
1>137 DATA 126,143,132,125,113,140
1>138 DATA 121,122,117,136,133,123
1>139 DATA 135,141,131,130,132,147
1>140 DATA 137,130,136,113,135,128
1>141 DATA 137,135,132,137,134,127
1>142 DATA 126,131,132,110,114,111
1>143 DATA 133,119,130,119,119,125
1>144 DATA 122,123,099,095,099,099
1>145 DATA 120,124,131,109,121,139
1>146 DATA 106,139,109,130,141,129
1>147 DATA 138,127,125,115,123,131
1>148 DATA 116,119,103,114,113,119
1>149 DATA 110,098,119,113,13[illegible],1[illegible]3
1>150 DATA 117,092,125,125,122,115
1>151 DATA 110,120,125,121,063,093
1>152 DATA 135,123,127,110,127,105
1>153 DATA 117,124,118,125,130,115
1>154 DATA 138,142,138,133,140,134
1>155 DATA 140,124,127,123,103,134
1>156 DATA 121,132,139,134,125,121
1>157 DATA 141,119,109,124,120,111
1>158 DATA 117,129,121,127,124,1[illegible]
1>159 DATA 125,145,149,131,119,114
1>160 DATA 111,107,119,101,119,124
1>161 DATA 108,131,141,162,143,130
1>162 DATA 127,125,130,126,140,149
1>163 DATA 133,153,134,132,127,132
1>164 DATA 126,123,117,135,129,13[illegible]
1>165 DATA 132,141,129,135,139,136
1>166 DATA 137,155,132,151
```

```
    SOGIN STHUMP
STHUMP (4) LOGGED IN AT  14'10 06200
WELCOME STHUMP

OK, LBASIC
GO
>LOAD 'MACJ04'
>RUN
SAMPLE POWER SPECTRAL DENSITY FUNCTION F(w)
(22)N(SAMPLE SIZE)= 1000
GIVE LAG NO M
!34
GIVE VALUE FOR L
!67
(1220) LAG NO. M= 34
(1225)F(ANG.FREQ.INTERVAL:PI/(10*F))= 10
(4130)E(VERTICAL SCALE FACTOR:RANGE 50*E)= 319.116
MAX.F(w)= 15955.8 MIN.F(W)= 0
```

```
VALUES OF F(W)
 0  15955.8   17  372.474   34  31.6777   51  7.95159
 1  15554.5   18  356.528   35  30.8748   52  7.43894
 2  14259     19  254.778   36  29.5489   53  6.85978
 3  12499.1   20  216.155   37  27.7346   54  6.29144
 4  10562.9   21  186.429   38  25.3994   55  5.99955
 5  8726.5    22  160.246   39  22.4133   56  5.85423
 6  7132.37   23  134.614   40  18.8518   57  5.67471
 7  5792.69   24  110.098   41  15.1747   58  5.33713
 8  4648.39   25  89.029    42  12.0565   59  4.95267
 9  3639.89   26  72.891    43  10.0549   60  4.54635
10  2748.58   27  61.191    44  9.02738   61  4.38954
11  1994.88   28  52.3096   45  8.73755   62  4.40256
12  1407.76   29  45.0098   46  8.66897   63  4.42432
13  994.018   30  39.1336   47  8.57976   64  4.32796
14  727.856   31  35.096    48  8.4663    65  4.11599
15  563.007   32  32.9752   49  8.37568   66  3.86557
16  454.228   33  32.1544   50  8.25135   67  3.70983

END AT LINE 9999
>QUIT

OK, LO
STHUMP (4) LOGGED OUT AT  14'21 06200
TIME USED=  0'11   5'31   0'12
GOODBYE
NO UFD ATTACHED.
ER!
```

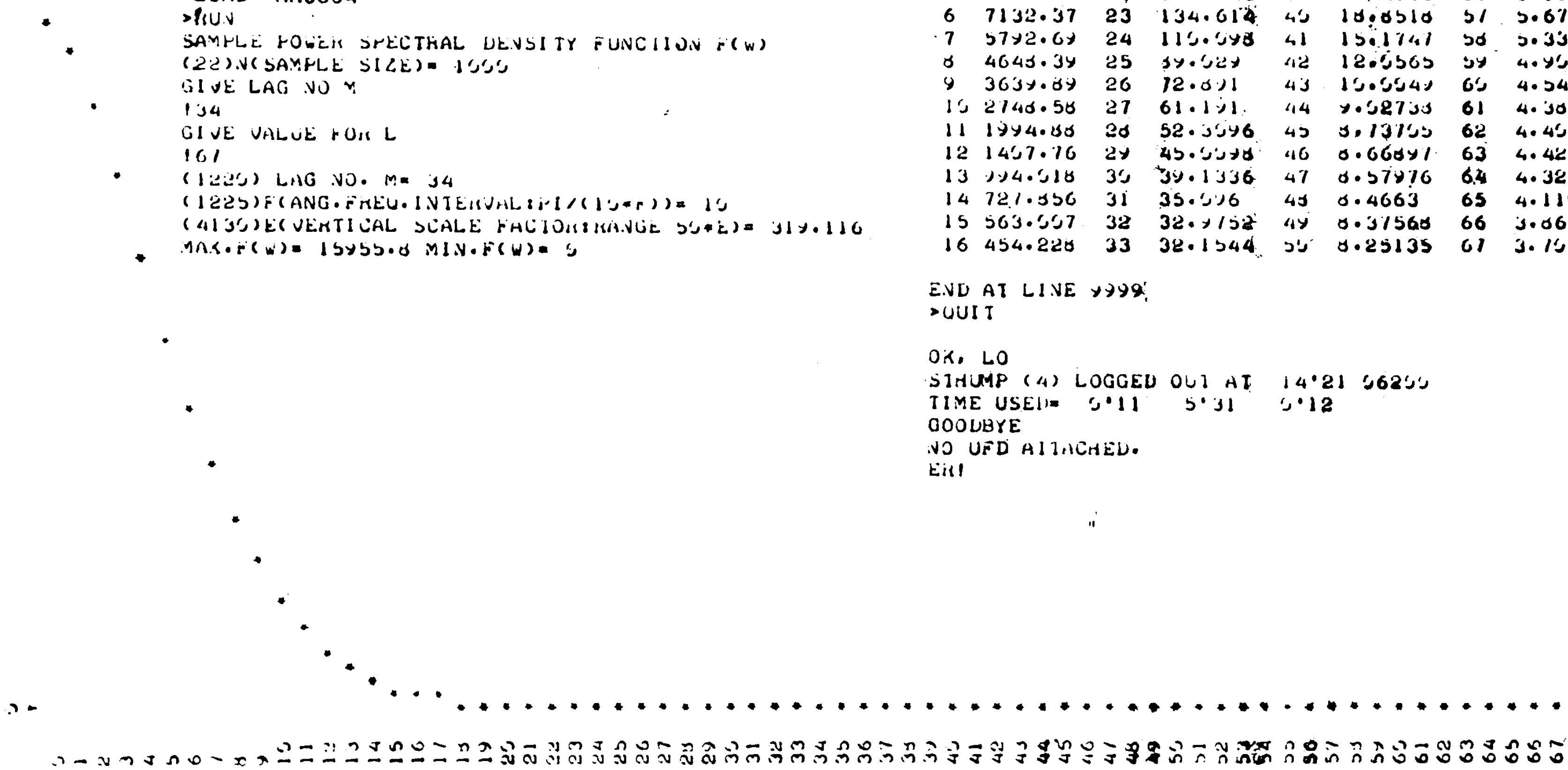

Fig 10.8 Power spectrum for the surface profile of a grinding wheel after 30 seconds wear (MJ3IA)

```
LOGIN PLEASE.
LOGIN STHIMP
STHIMP (5) LOGGED IN AT  14'07 06260
WELCOME STHIMP

OK, LBASIC
GO
>LOAD 'MACJ04'
>RUN
SAMPLE POWER SPECTRAL DENSITY FUNCTION F(W)
(22)N(SAMPLE SIZE)= 1000
GIVE LAG NO M
!22
GIVE VALUE FOR L
!67
(1220) LAG NO. M= 22
(1225)F(ANG.FREQ.INTERVAL:PI/(10*F))= 10
(4130)E(VERTICAL SCALE FACTOR:RANGE 50*E)= 271.616
MAX.F(W)= 13580.8 MIN.F(W)= 0
```

VALUES OF F(W)

0	13580.8	17	445.743	34	33.4092	51	7.95417
1	13371	18	345.134	35	30.9839	52	7.8216
2	12761.8	19	274.485	36	28.0854	53	7.39542
3	11810.9	20	225.617	37	25.0932	54	6.76844
4	10604.5	21	191.392	38	22.3846	55	6.09809
5	9244.11	22	165.822	39	20.1413	56	5.53732
6	7832.84	23	144.433	40	18.3268	57	5.18761
7	6462.25	24	124.528	41	16.749	58	5.04571
8	5203.08	25	105.161	42	15.1825	59	5.03017
9	4100.64	26	86.738	43	13.5123	60	5.02519
10	3174.98	27	70.3605	44	11.766	61	4.93458
11	2424.98	28	57.1366	45	10.1192	62	4.72787
12	1834.65	29	47.6374	46	8.79113	63	4.42556
13	1380.14	30	41.6725	47	7.94329	64	4.10928
14	1035.63	31	38.3929	48	7.60338	65	3.86899
15	777.409	32	36.6081	49	7.64363	66	3.74869
16	585.883	33	35.1994	50	7.84009	67	3.76004

```
END AT LINE 9999
>QUIT

OK, LO
STHIMP (5) LOGGED OUT AT  14'16 06260
TIME USED=  0'09   5'14   0'01
GOODBYE
NO UFD ATTACHED.
ER!
```

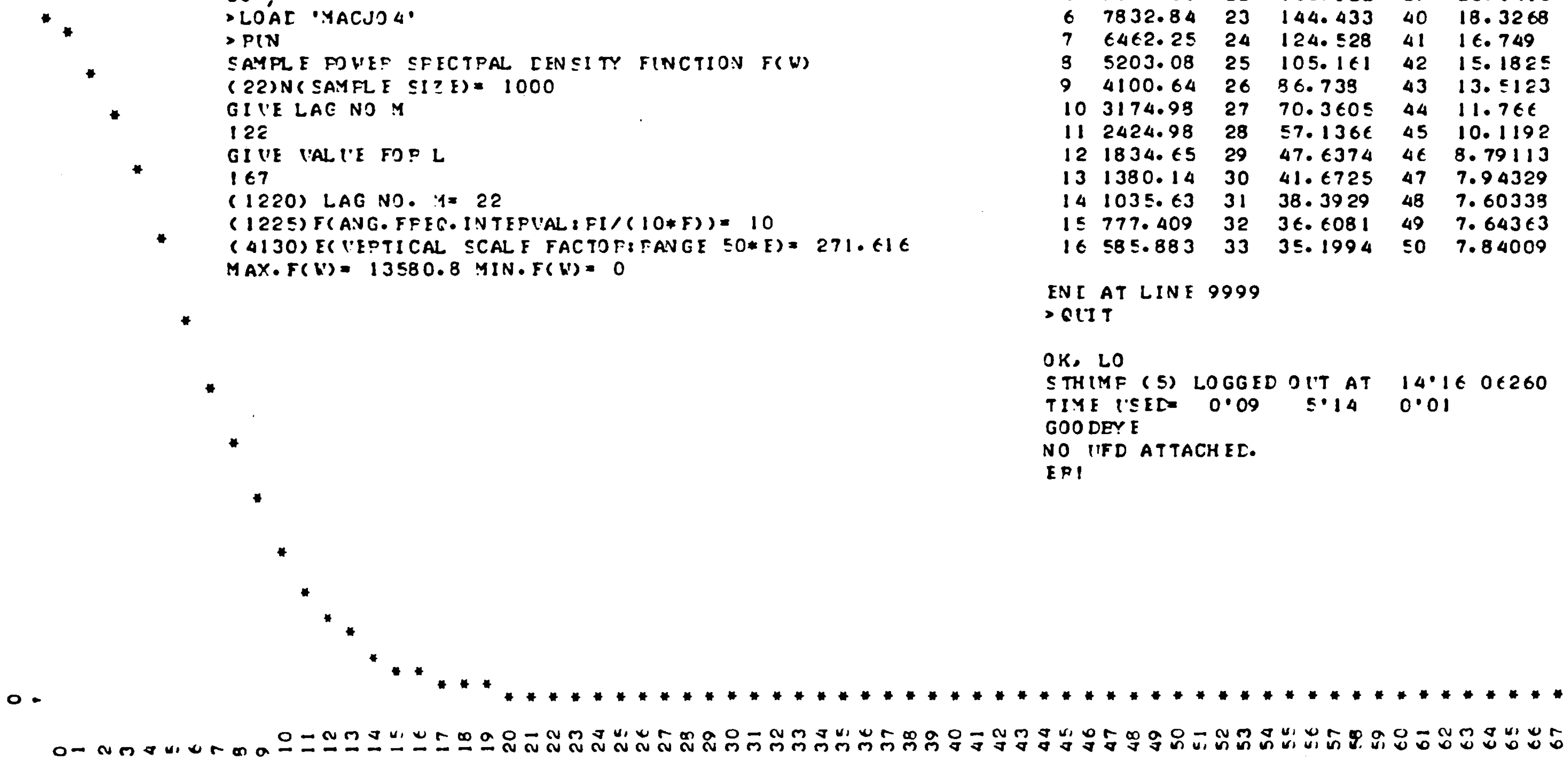

Fig 10.9 Power spectrum for the surface profile of a grinding wheel after 30 seconds wear

(MJ3IA)

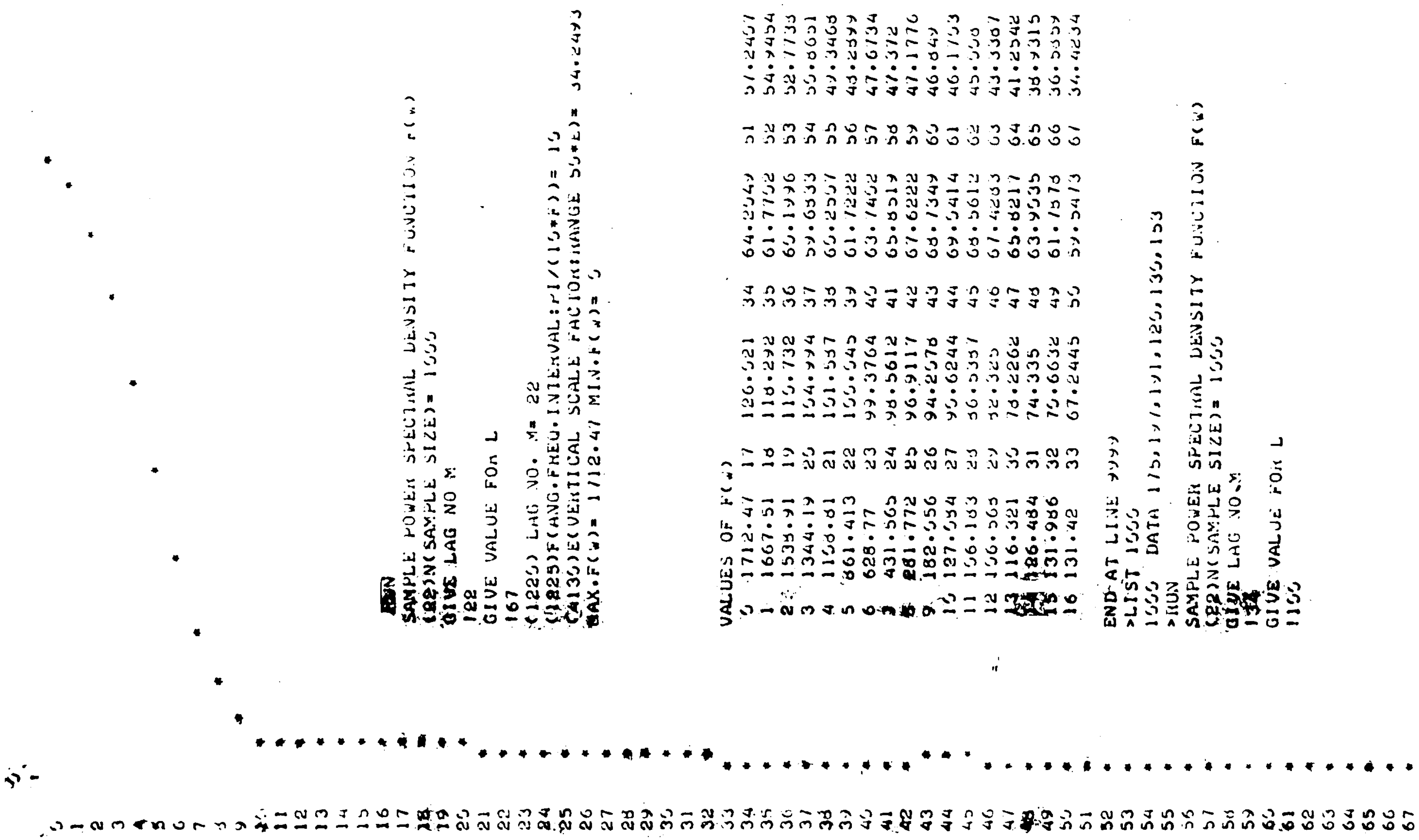

Fig 10.10 Power spectrum for the profile of a ground surface corresponding with 30 seconds grinding wheel wear (MJ36IA)

```
*RUN
SAMPLE POWER SPECTRAL DENSITY FUNCTION F(W)
(220)X(SAMPLE SIZE)= 1000
GIVE LAG NO X
122
GIVE VALUE FOR L
167
(1220) LAG NO. M= 22
(1225)F(ANG.FREQ.INTERVAL:PI/(10*F))= 10
(4130)E(VERTICAL SCALE FACTOR:RANGE 50*E)= 53.8423
MAX.F(W)= 2692.12 MIN.F(W)= 0
```

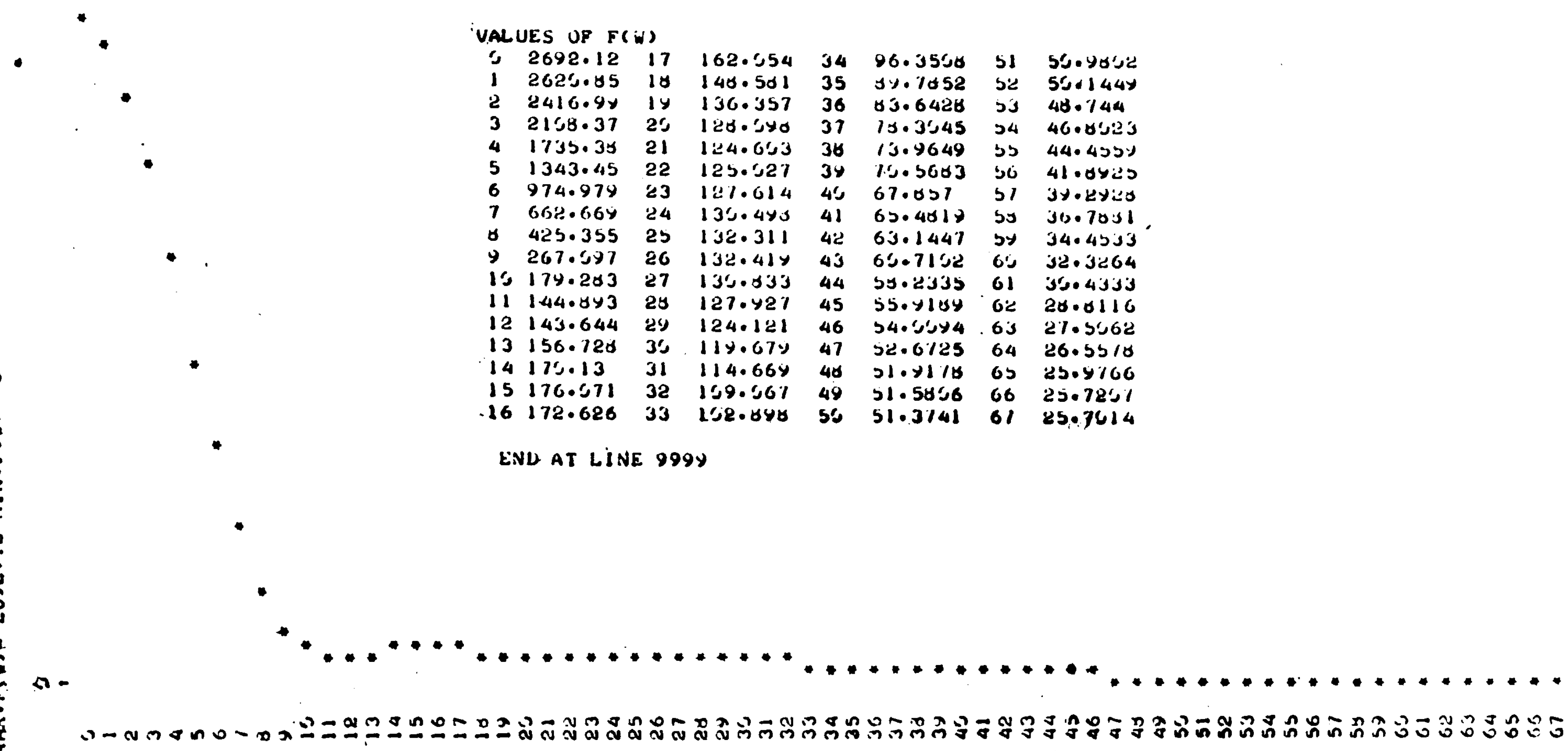

VALUES OF F(W)

0	2692.12	17	162.054	34	96.3508	51	50.9802
1	2620.85	18	148.581	35	89.7852	52	50.1449
2	2416.99	19	136.357	36	83.6428	53	48.744
3	2158.37	20	128.598	37	78.3045	54	46.8023
4	1735.38	21	124.603	38	73.9649	55	44.4559
5	1343.45	22	125.027	39	70.5683	56	41.8925
6	974.979	23	127.614	40	67.857	57	39.2928
7	662.669	24	130.493	41	65.4819	58	36.7831
8	425.355	25	132.311	42	63.1447	59	34.4533
9	267.097	26	132.419	43	60.7102	60	32.3264
10	179.283	27	130.833	44	58.2335	61	30.4333
11	144.893	28	127.927	45	55.9189	62	28.8116
12	143.644	29	124.121	46	54.0094	63	27.5062
13	156.728	30	119.679	47	52.6725	64	26.5578
14	170.13	31	114.669	48	51.9178	65	25.9766
15	176.071	32	109.067	49	51.5856	66	25.7257
16	172.626	33	102.898	50	51.3741	67	25.7014

END AT LINE 9999

Fig 10.11 Power spectrum for the profile of a ground surface corresponding with 30 seconds grinding wheel wear (MJ44IA)

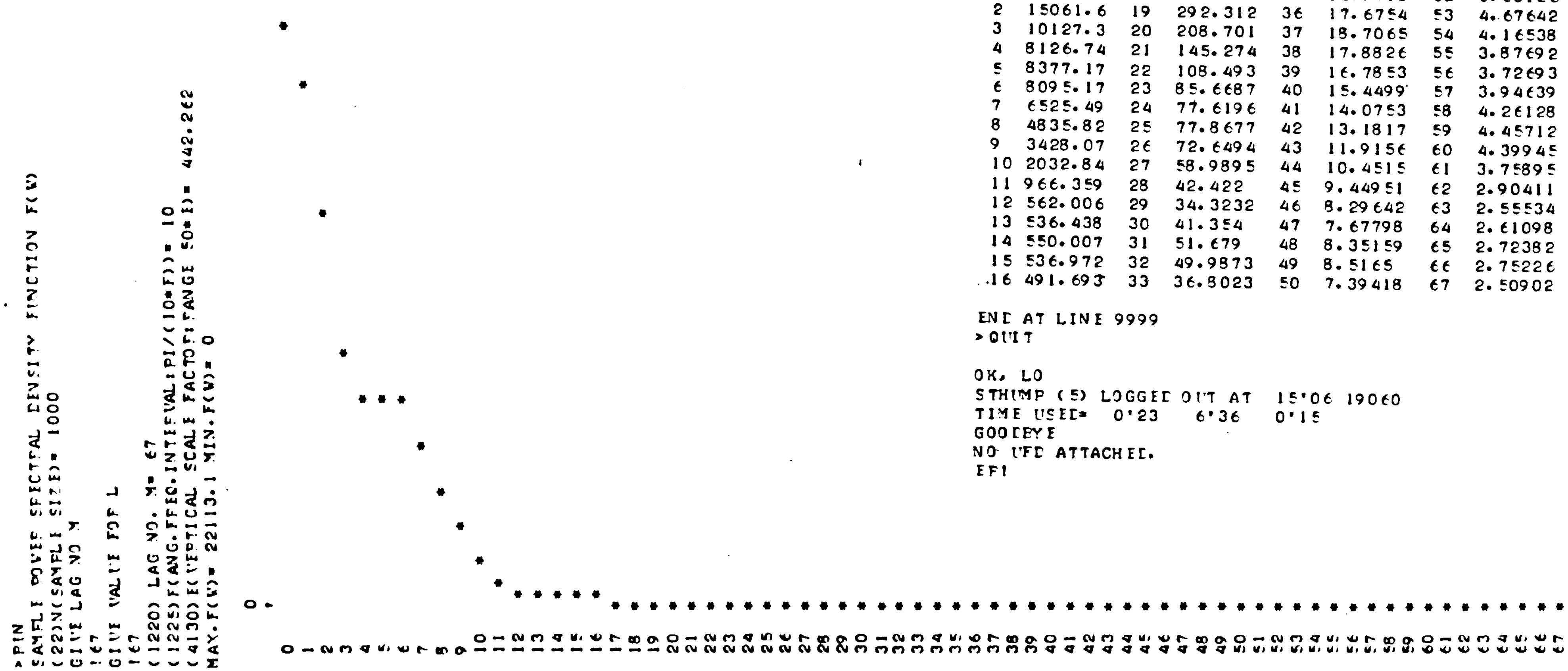

VALUES OF F(W)

0	22113.1	17	423.752	34	23.0302	51	6.30978
1	20085.9	18	362.433	35	16.9713	52	5.50126
2	15061.6	19	292.312	36	17.6754	53	4.67642
3	10127.3	20	208.701	37	18.7065	54	4.16538
4	8126.74	21	145.274	38	17.8826	55	3.87692
5	8377.17	22	108.493	39	16.7853	56	3.72693
6	8095.17	23	85.6687	40	15.4499	57	3.94639
7	6525.49	24	77.6196	41	14.0753	58	4.26128
8	4835.82	25	77.8677	42	13.1817	59	4.45712
9	3428.07	26	72.6494	43	11.9156	60	4.39945
10	2032.84	27	58.9895	44	10.4515	61	3.75895
11	966.359	28	42.422	45	9.44951	62	2.90411
12	562.006	29	34.3232	46	8.29642	63	2.55534
13	536.438	30	41.354	47	7.67798	64	2.61098
14	550.007	31	51.679	48	8.35159	65	2.72382
15	536.972	32	49.9873	49	8.5165	66	2.75226
16	491.693	33	36.8023	50	7.39418	67	2.50902

END AT LINE 9999
>QUIT

OK, LO
STHIMP (5) LOGGED OUT AT 15'06 19060
TIME USED= 0'23 6'36 0'15
GOODBYE
NO UFD ATTACHED.
ER!

Fig 10.12 Power spectrum for the surface profile of a grinding wheel after 5 minutes wear

(MJ14IA)

SAMPLE POWER SPECTRAL DENSITY FUNCTION F(W)
(22)N(SAMPLE SIZE)= 1000
GIVE LAG NO M
122
GIVE VALUE FOR L
167
(03) LAG NO. M= 22
(1225)F(ANG.FREQ.INTERVAL=PI/(10*F))= 10
(4135)E(VERTICAL SCALE FACTOR=RANGE 50*E)= 282.59
MAX.F(W)= 14144.5 MIN.F(W)= 0

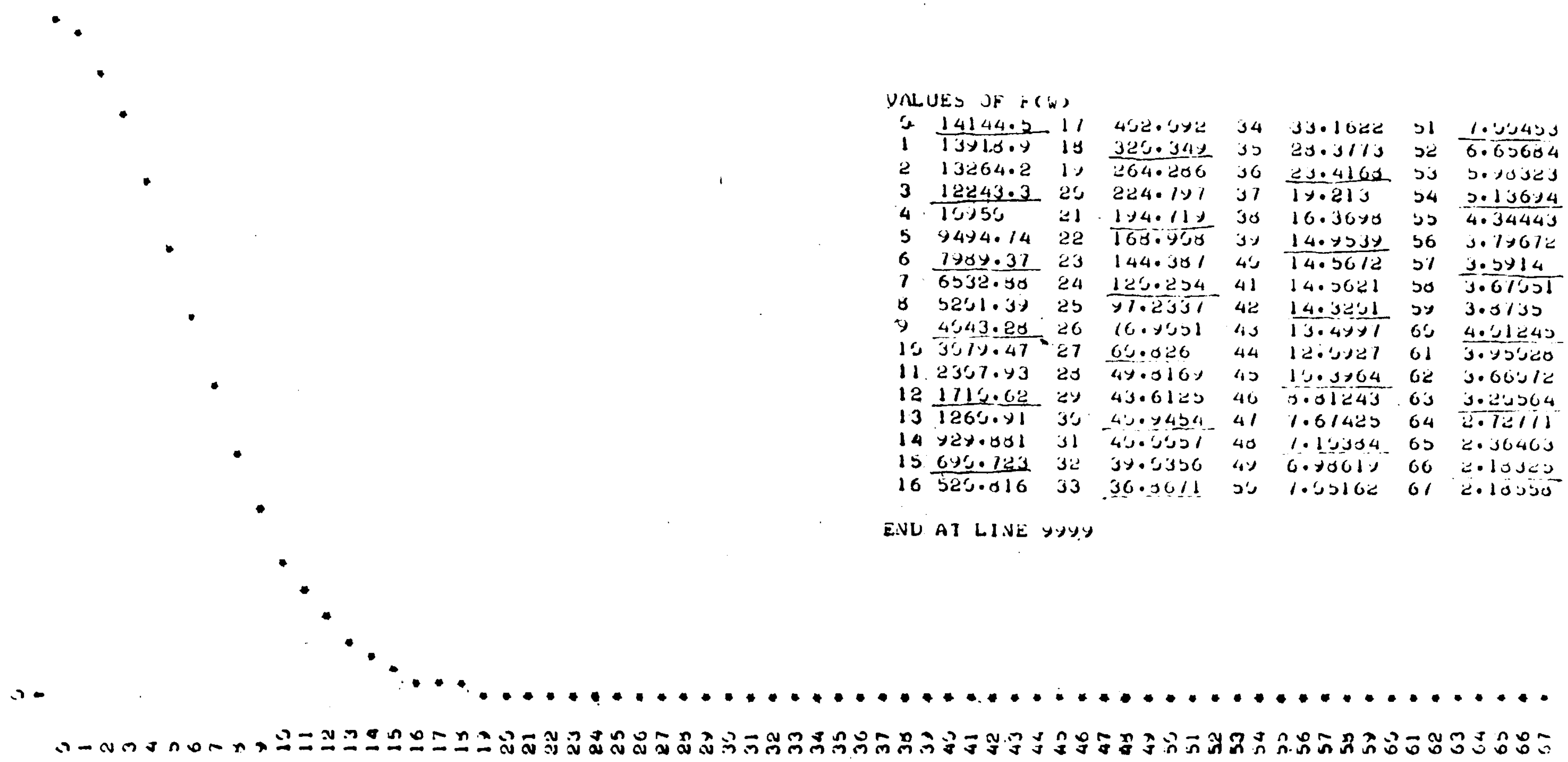

VALUES OF F(W)

0	14144.5	17	402.092	34	33.1622	51	7.00453		
1	13918.9	18	320.349	35	28.3773	52	6.65684		
2	13264.2	19	264.286	36	23.4168	53	5.98323		
3	12243.3	20	224.797	37	19.213	54	5.13694		
4	10950	21	194.719	38	16.3698	55	4.34443		
5	9494.74	22	168.958	39	14.9539	56	3.79672		
6	7989.37	23	144.387	40	14.5672	57	3.5914		
7	6532.88	24	120.254	41	14.5621	58	3.67051		
8	5201.39	25	97.2337	42	14.3201	59	3.8735		
9	4043.28	26	76.9551	43	13.4997	60	4.01245		
10	3079.47	27	60.826	44	12.0927	61	3.95028		
11	2307.93	28	49.8169	45	10.3964	62	3.66072		
12	1710.62	29	43.6125	46	8.81243	63	3.20564		
13	1260.91	30	40.9454	47	7.67425	64	2.72771		
14	929.881	31	40.0557	48	7.19384	65	2.36463		
15	690.723	32	39.0356	49	6.98619	66	2.18325		
16	520.816	33	36.3671	50	7.05162	67	2.18058		

END AT LINE 9999

Fig 10.13 Power spectrum for the surface profile of a grinding wheel after 5 minutes wear

(MJ14IA)

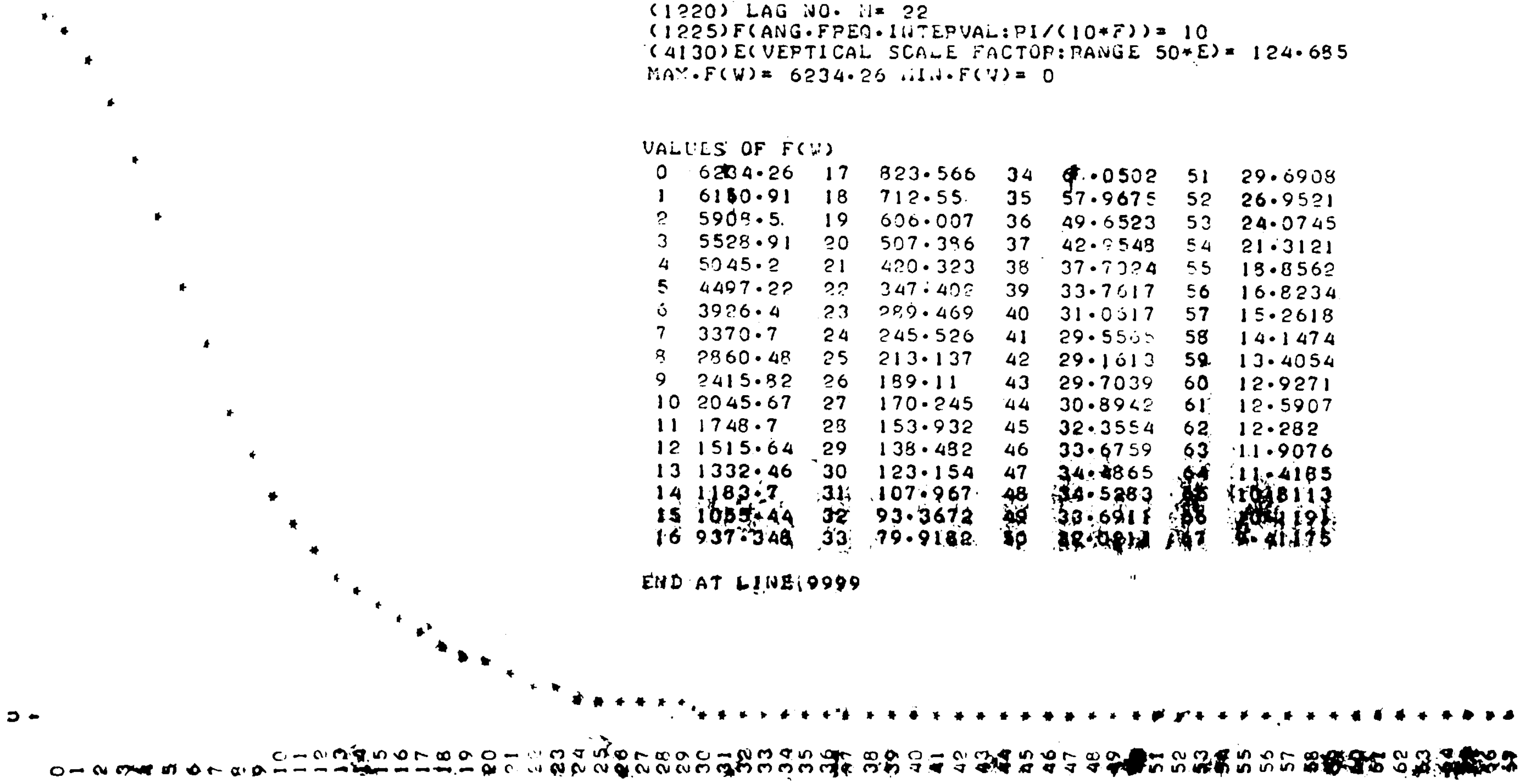

```
>RUN
SAMPLE POWER SPECTRAL DENSITY FUNCTION F(W)
(22)N(SAMPLE SIZE)= 1000
GIVE LAG NO M.
!22
GIVE VALUE FOR L
!67
(1220) LAG NO. M= 22
(1225)F(ANG.FREQ.INTERVAL:PI/(10*F))= 10
(4130)E(VERTICAL SCALE FACTOR:RANGE 50*E)= 124.685
MAX.F(W)= 6234.26 MIN.F(W)= 0
```

VALUES OF F(W)

0	6234.26	17	823.566	34	67.0502	51	29.6908
1	6150.91	18	712.55	35	57.9675	52	26.9521
2	5908.5	19	606.007	36	49.6523	53	24.0745
3	5528.91	20	507.386	37	42.9548	54	21.3121
4	5045.2	21	420.323	38	37.7024	55	18.8562
5	4497.22	22	347.402	39	33.7617	56	16.8234
6	3926.4	23	289.469	40	31.0517	57	15.2618
7	3370.7	24	245.526	41	29.5565	58	14.1474
8	2860.48	25	213.137	42	29.1613	59	13.4054
9	2415.82	26	189.11	43	29.7039	60	12.9271
10	2045.67	27	170.245	44	30.8942	61	12.5907
11	1748.7	28	153.932	45	32.3554	62	12.282
12	1515.64	29	138.482	46	33.6759	63	11.9076
13	1332.46	30	123.154	47	34.4865	64	11.4185
14	1183.7	31	107.967	48	34.5283	65	10.8113
15	1055.44	32	93.3672	49	33.6911	66	[illegible]
16	937.348	33	79.9182	50	[illegible]	67	[illegible]

END AT LINE 9999

Fig 10.14 Power spectrum for the surface profile of a grinding wheel after 5 minutes wear

(MJ20IA)

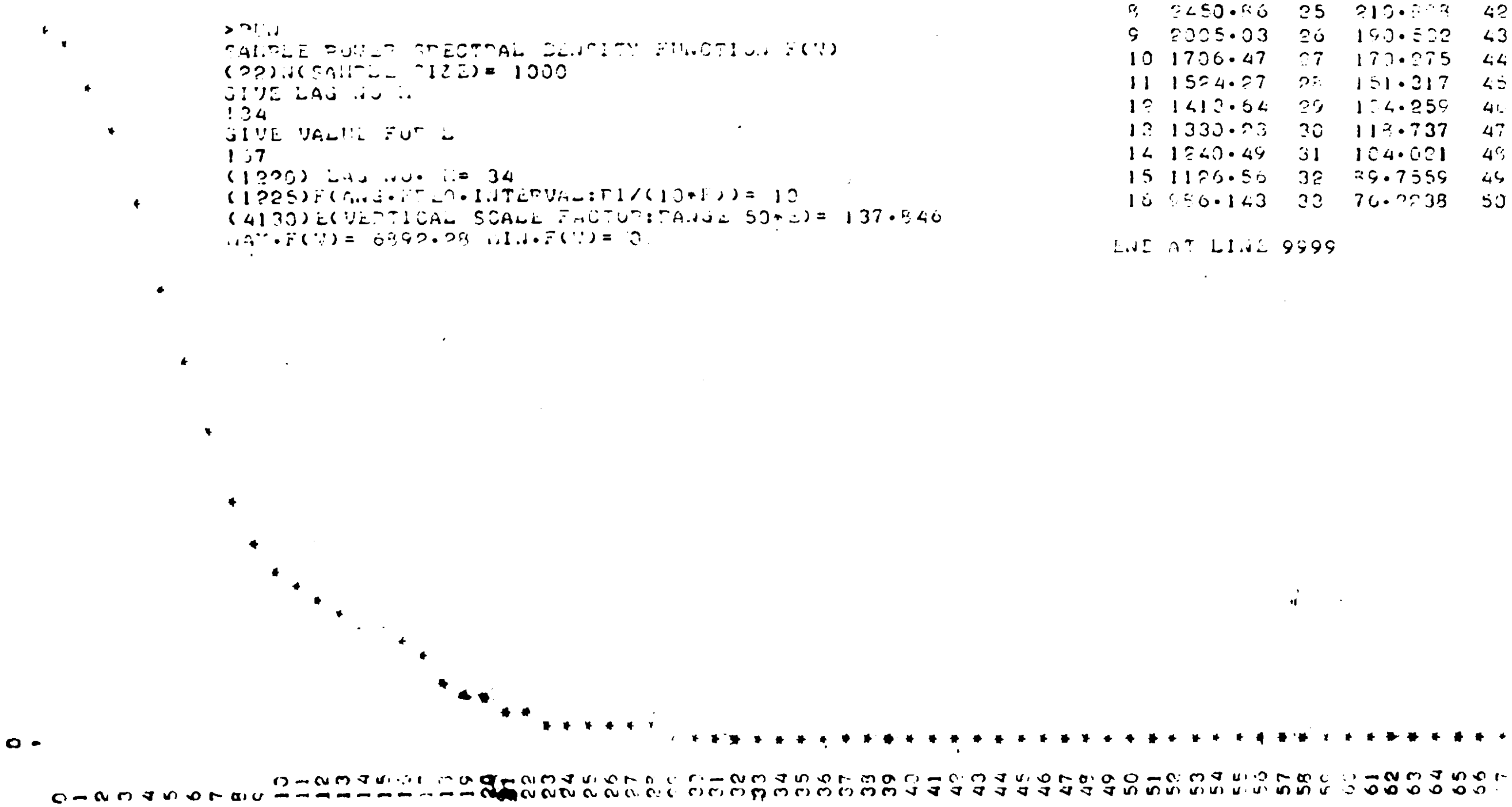

```
LOGIN ST[illegible]
[illegible] (10) LOGGED IN AT 11'37 0[illegible]
WELCOME [illegible]

[illegible] BASIC
[illegible]
>LOAD '[illegible]'

>RUN
SAMPLE POWER SPECTRAL DENSITY FUNCTION F(W)
(22)N(SAMPLE SIZE)= 1000
GIVE LAG NO M
!34
GIVE VALUE FOR L
!37
(1220) LAG NO. M= 34
(1225)F(ANG.FREQ.INTERVAL:PI/(10*F))= 10
(4130)L(VERTICAL SCALE FACTOR:RANGE 50*L)= 137.846
MAX.F(W)= 6892.28 MIN.F(W)= 0
```

VALUES OF F(W)

0	6892.28	17	829.304	34	64.0406	51	31.3469
1	6754.95	18	671.527	35	53.6867	52	27.3044
2	6467.99	19	530.593	36	45.227	53	23.2359
3	5959.56	20	418.175	37	39.4532	54	19.4679
4	5297.04	21	338.171	38	33.0585	55	16.2857
5	4539.96	22	286.482	39	28.9341	56	13.9382
6	3764.24	23	254.036	40	26.1593	57	12.5795
7	3047.51	24	231.193	41	24.5966	58	12.1705
8	2450.86	25	210.[illegible]	42	25.2346	59	12.4639
9	2005.03	26	190.502	43	27.0691	60	13.0764
10	1706.47	27	170.275	44	[illegible].0201	61	13.6115
11	1524.27	28	151.317	45	[illegible].4453	62	13.7772
12	1412.64	29	134.259	46	35.5403	63	13.4195
13	1330.23	30	118.737	47	38.5397	64	12.5361
14	1240.49	31	104.021	48	38.9446	65	11.2465
15	1126.56	32	89.7559	49	37.0603	66	9.76518
16	986.143	33	76.2238	50	34.9665	67	8.07421

END AT LINE 9999

Fig 10.15 Power spectrum for the surface profile of a grinding wheel after 5 minutes wear

(MJ20IA)

```
LOGIN PLEASE.
LOGIN STHIMP
STHIMP (5) LOGGED IN AT  10'07 26060
WELCOME STHIMP

OK, LBASIC
GO
>LOAD 'MACJ04'

>RUN
SAMPLE POWER SPECTRAL DENSITY FUNCTION F(W)
(22)N(SAMPLE SIZE)= 1000
GIVE LAG NO M
!34
GIVE VALUE FOR L
!67
(1220) LAG NO. M= 34
(1225)F(ANG.FREQ.INTERVAL:PI/(10*F))= 10
(4130)E(VERTICAL SCALE FACTOR:RANGE 50*E)= 107.038
MAX.F(W)= 5351.9 MIN.F(W)= 0
```

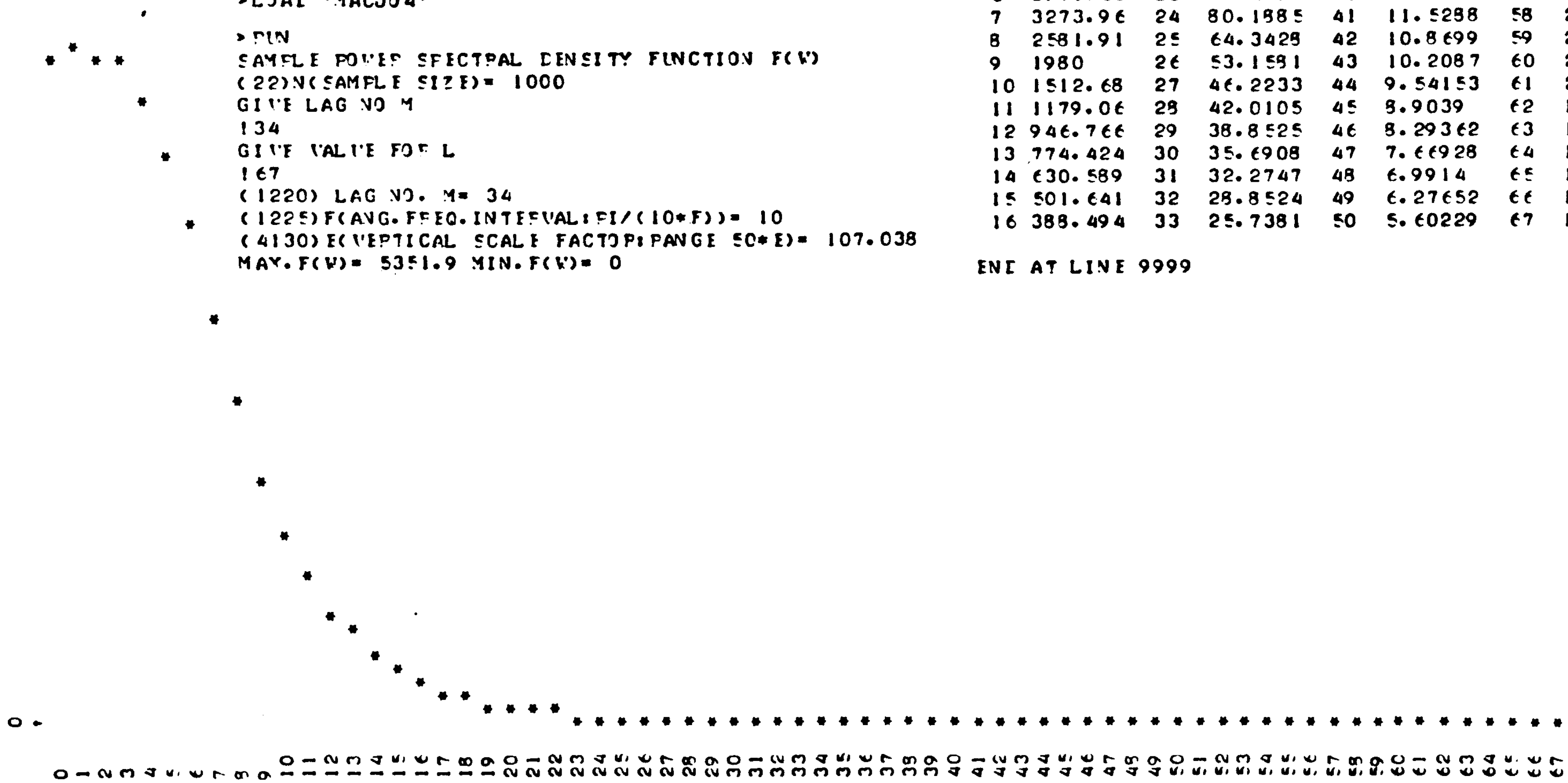

VALUES OF F(W)

0	5344.41	17	297.487	34	23.0275	51	5.04835
1	5351.9	18	232.055	35	20.6235	52	4.64378
2	5346.04	19	189.264	36	18.4034	53	4.34226
3	5257.26	20	161.411	37	16.3627	54	4.07306
4	5012.71	21	140.136	38	14.6126	55	3.7811
5	4576.46	22	119.963	39	13.2548	56	3.4554
6	3971.65	23	99.479	40	12.2704	57	3.12707
7	3273.96	24	80.1885	41	11.5288	58	2.82088
8	2581.91	25	64.3428	42	10.8699	59	2.54244
9	1980	26	53.1581	43	10.2087	60	2.2922
10	1512.68	27	46.2233	44	9.54153	61	2.07453
11	1179.06	28	42.0105	45	8.9039	62	1.91134
12	946.766	29	38.8525	46	8.29362	63	1.81155
13	774.424	30	35.6908	47	7.66928	64	1.77884
14	630.589	31	32.2747	48	6.9914	65	1.79788
15	501.641	32	28.8524	49	6.27652	66	1.84388
16	388.494	33	25.7381	50	5.60229	67	1.91312

END AT LINE 9999

Fig10.16 Power spectrum for the surface profile of a grinding wheel after 10 minutes wear

(MJ26IA)

```
>RUN
SAMPLE POWER SPECTRAL DENSITY FUNCTION F(W)
(22)N(SAMPLE SIZE)= 1000
GIVE LAG NO M
122
GIVE VALUE FOR L
167
(1220) LAG NO. M= 22
(1225)F(ANG.FREQ.INTERVAL:PI/(10*F))= 10
(4130)E(VERTICAL SCALE FACTOR:RANGE 50*E)= 16.5125
MAX.F(W)= 825.624 MIN.F(W)= 0
```

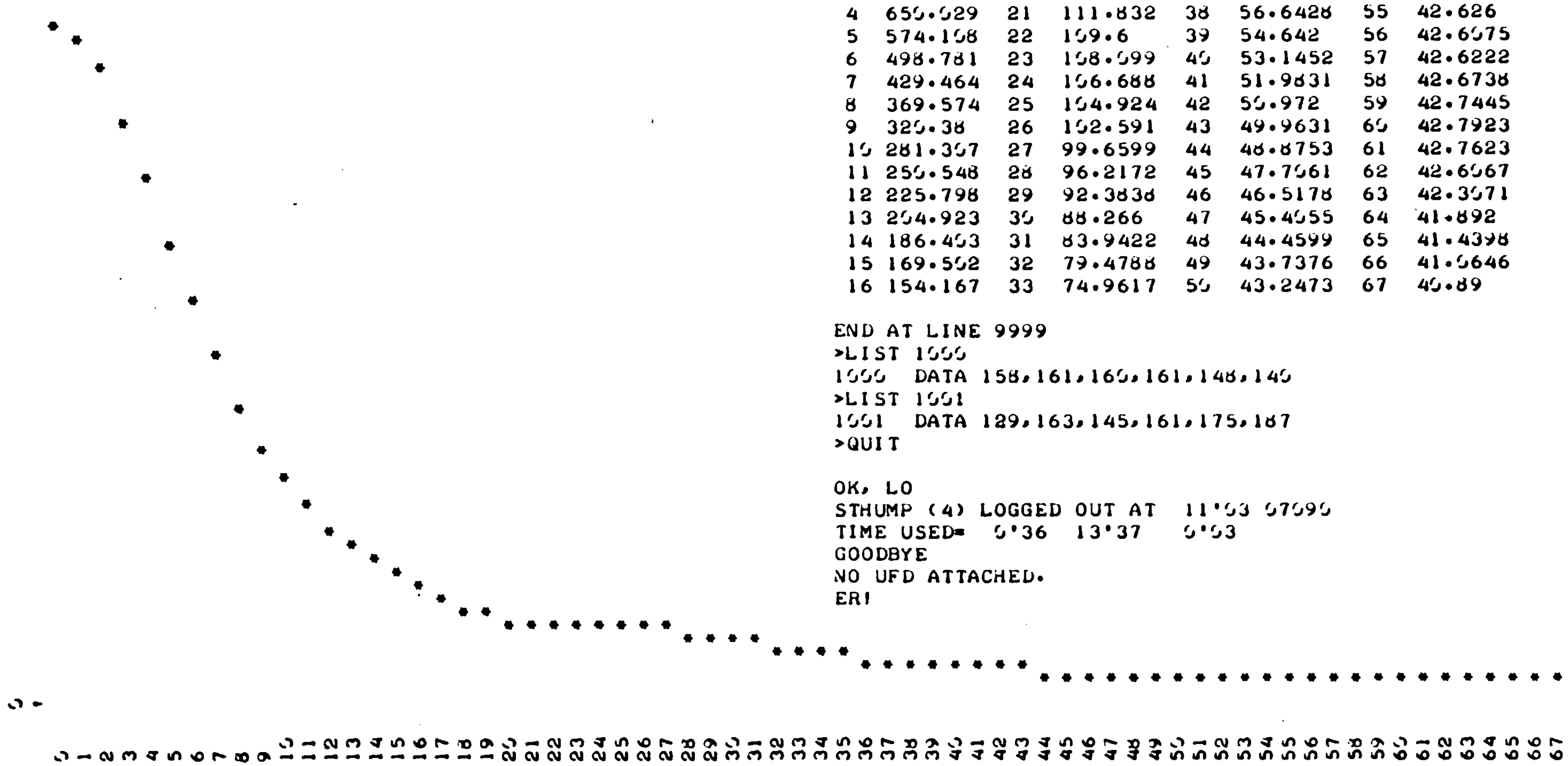

VALUES OF F(W)

0	825.624	17	140.763	34	70.5155	51	42.9541
1	812.867	18	129.739	35	66.3039	52	42.7975
2	776.135	19	121.355	36	62.5023	53	42.7151
3	719.754	20	115.529	37	59.2567	54	42.6637
4	650.029	21	111.832	38	56.6428	55	42.626
5	574.108	22	109.6	39	54.642	56	42.6075
6	498.781	23	108.099	40	53.1452	57	42.6222
7	429.464	24	106.688	41	51.9831	58	42.6738
8	369.574	25	104.924	42	50.972	59	42.7445
9	320.38	26	102.591	43	49.9631	60	42.7923
10	281.307	27	99.6599	44	48.8753	61	42.7623
11	250.548	28	96.2172	45	47.7061	62	42.6067
12	225.798	29	92.3838	46	46.5178	63	42.3071
13	204.923	30	88.266	47	45.4055	64	41.892
14	186.403	31	83.9422	48	44.4599	65	41.4398
15	169.502	32	79.4788	49	43.7376	66	41.0646
16	154.167	33	74.9617	50	43.2473	67	40.89

```
END AT LINE 9999
>LIST 1000
1000  DATA 158,161,160,161,148,140
>LIST 1001
1001  DATA 129,163,145,161,175,187
>QUIT

OK, LO
STHUMP (4) LOGGED OUT AT  11'03 07090
TIME USED=  0'36  13'37   0'03
GOODBYE
NO UFD ATTACHED.
ER!
```

Fig 10.17 Power spectrum for the profile of a ground surface corresponding with 5 minutes grinding wheel wear (MJ40IA)

```
      LOGIN STHUMP
STHUMP (4) LOGGED IN AT  14'44 08275
WELCOME STHUMP

OK, BASIC
GO
>LOAD 'MACJ04'
>RUN
SAMPLE POWER SPECTRAL DENSITY FUNCTION F(W)
(220)N(SAMPLE SIZE)= 1000
GIVE LAG NO M
!22
GIVE VALUE FOR L
!67
(1220) LAG NO. M= 22
(1225)F(ANG.FREQ.INTERVAL:PI/(10*F))= 10
(4130)E(VERTICAL SCALE FACTOR:RANGE 50*E)= 57.3457
MAX.F(J)= 2867.05 MIN.F(W)= 0
```

VALUES OF F(W)

0	2867.05	17	542.718	34	62.7414	51	9.25534
1	2847.11	18	451.558	35	53.0431	52	8.75557
2	2796.63	19	385.58	36	43.636	53	8.17351
3	2713.21	20	326.491	37	35.1583	54	7.52473
4	2603.9[illegible]	21	285.554	38	28.1133	55	6.85577
5	2474.43	22	251.985	39	22.0314	56	6.23735
6	2329.63	23	224.125	40	19.1545	57	5.73315
7	2173.36	24	199.315	41	16.3716	58	5.37125
8	2008.14	25	176.646	42	15.0585	59	5.14513
9	1835.61	26	156.03	43	14.0243	60	4.99535
10	1657.25	27	137.974	44	13.5583	61	4.85275
11	1475.17	28	122.613	45	13.1297	62	4.75556
12	1292.66	29	109.912	46	12.5222	63	4.65329
13	1114.24	30	99.3425	47	11.5248	64	4.42754
14	945.263	31	95.5768	48	10.5595	65	4.25552
15	791.564	32	81.2443	49	10.2137	66	4.12256
16	656.521	33	72.2152	50	9.7149	67	4.53755

END AT LINE 9999

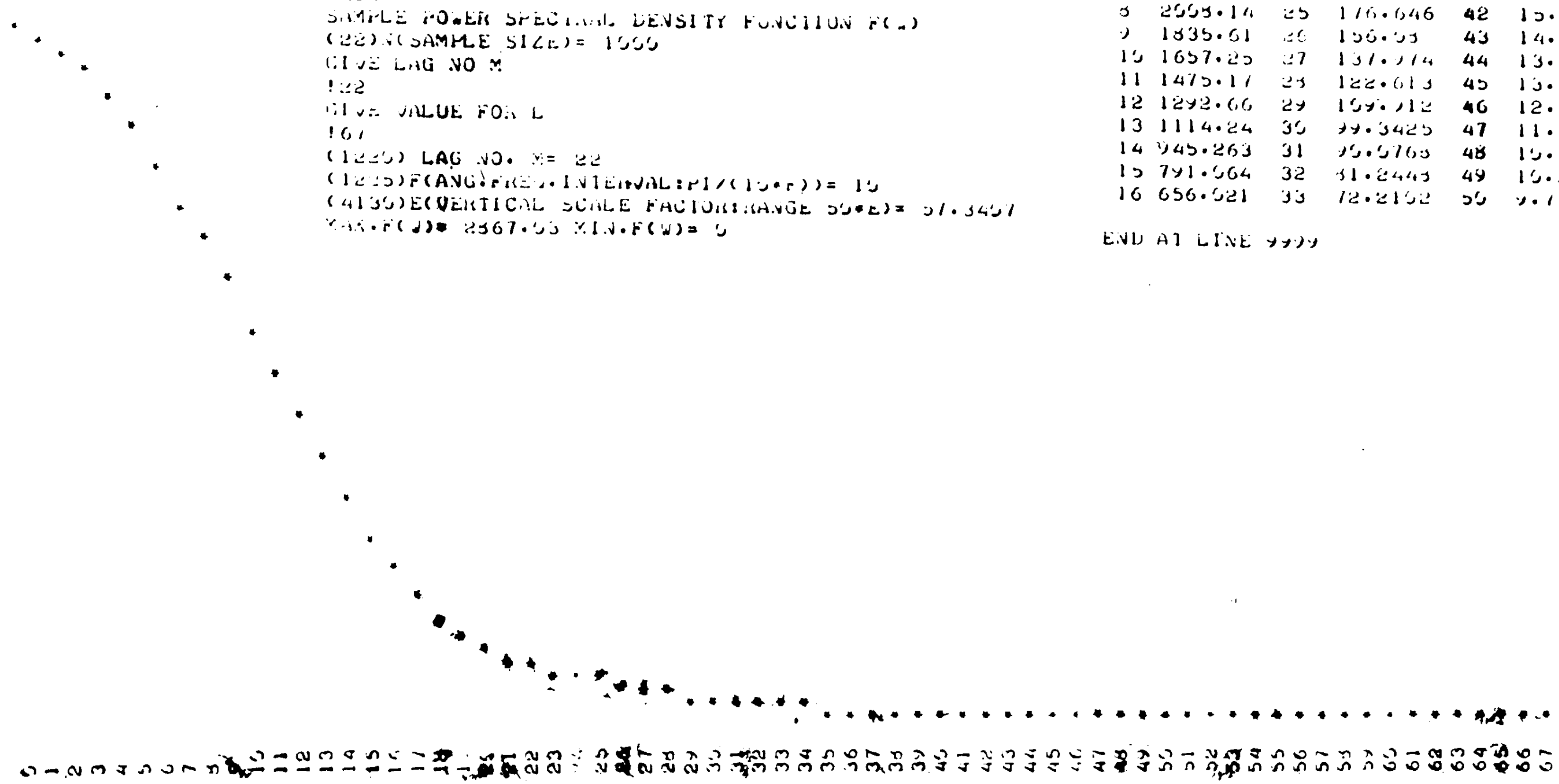

Fig 10.18 Power spectrum for the surface profile of a grinding wheel after 10 minutes wear

(MJ32IA)

[illegible]N

SAMPLE POWER SPECTRAL DENSITY FUNCTION F(.)
(22)N(SAMPLE SIZE)= 1000
GIVE LAG NO M
!22
GIVE VALUE FOR L
!67
(1220) LAG NO. M= 22
(1225)F(ANG.FREQ.INTERVAL:PI/(10*F))= 10
(4130)E(VERTICAL SCALE FACTOR:RANGE 50*E)= 7.1951
MAX.F(W)= 359.505 MIN.F(W)= 0

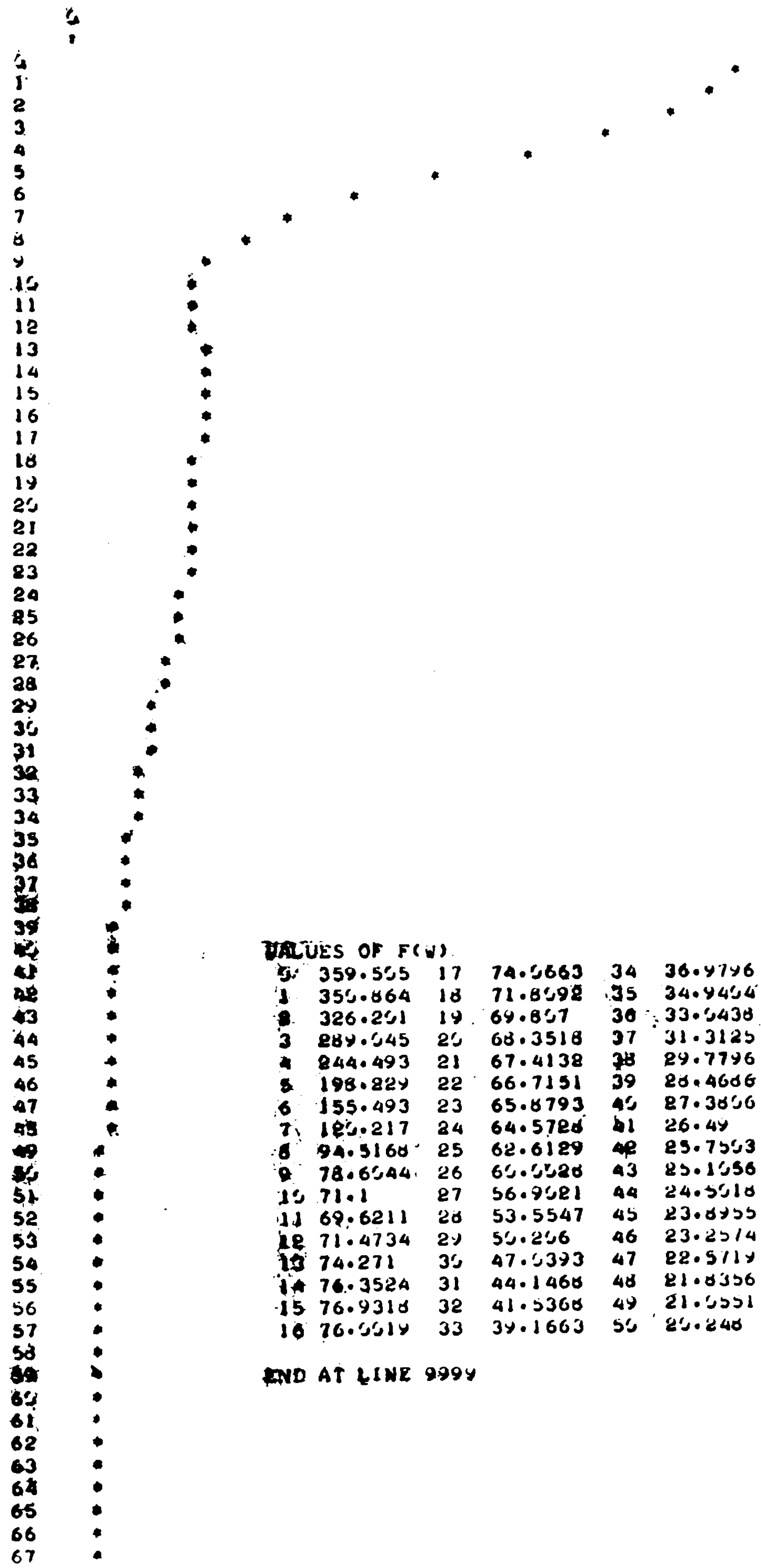

VALUES OF F(W)

0	359.505	17	74.0663	34	36.9796	51	19.4426
1	350.864	18	71.8092	35	34.9404	52	18.6772
2	326.201	19	69.807	36	33.0438	53	17.9968
3	289.045	20	68.3518	37	31.3125	54	17.4469
4	244.493	21	67.4138	38	29.7796	55	17.0645
5	198.229	22	66.7151	39	28.4686	56	16.8695
6	155.493	23	65.8793	40	27.3806	57	16.8602
7	120.217	24	64.5728	41	26.49	58	17.0123
8	94.5168	25	62.6129	42	25.7503	59	17.2831
9	78.6044	26	60.0528	43	25.1056	60	17.6209
10	71.1	27	56.9021	44	24.5018	61	17.9741
11	69.6211	28	53.5547	45	23.8955	62	18.2998
12	71.4734	29	50.206	46	23.2574	63	18.5677
13	74.271	30	47.0393	47	22.5719	64	18.7613
14	76.3524	31	44.1468	48	21.8356	65	18.8741
15	76.9318	32	41.5368	49	21.0551	66	18.905
16	76.0019	33	39.1663	50	20.248	67	18.8538

END AT LINE 9999

Fig 10.19 Power spectrum for the profile of a ground surface corresponding with 10 minutes grinding wheel wear (MJ48IA)

APPENDIX 11

Data MJ3IA

```
LOGIN PLEASE.
LOGIN STHIMP
STHIMP (5) LOGGED IN AT  15'08 06260
WELCOME STHIMP

OK, LBASIC
GO
>LOAD 'MACJO4'
>RUN
SAMPLE POWER SPECTRAL DENSITY FUNCTION F(W)
(22)N(SAMPLE SIZE)= 1000
GIVE LAG NO M
?34
GIVE VALUE FOR L
?100
(1220) LAG NO. M= 34
(1225)F(ANG.FREC.INTERVAL:PI/(10*F))= 10
(4130)F(VERTICAL SCALE FACTOR:RANGE 50*E)= 319.116
MAX.F(W)= 15955.8 MIN.F(W)= 0
```

VALUES OF F(W)

0	15955.8	25.	89.029	50.	8.25135	75.	3.92043		
1	15504.5	26.	72.891	51.	7.95759	76.	3.72709		
2	14259	27.	61.191	52.	7.43894	77.	3.42059		
3	12499.1	28.	52.3096	53.	6.80978	78.	3.07275		
4	10562.9	29.	45.0098	54.	6.29144	79.	2.73237		
5	8726.5	30.	39.1336	55.	5.99955	80.	2.42976		
6	7132.37	31.	35.096	56.	5.85423	81.	2.17548		
7	5792.69	32.	32.9752	57.	5.67471	82.	1.9798		
8	4648.39	33.	32.1544	58.	5.33713	83.	1.86308		
9	3639.89	34.	31.6777	59.	4.90287	84.	1.81863		
10	2748.58	35.	30.8748	60.	4.54633	85.	1.84551		
11	1994.88	36.	29.5489	61.	4.38904	86.	1.91872		
12	1407.76	37.	27.7346	62.	4.40256	87.	1.98011		
13	994.018	38.	25.3994	63.	4.42432	88.	2.02627		
14	727.856	39.	22.4133	64.	4.32796	89.	2.07368		
15	563.007	40.	18.8518	65.	4.11099	90.	2.10927		
16	454.228	41.	15.1747	66.	3.86557	91.	2.12419		
17	372.474	42.	12.0565	67.	3.70983	92.	2.11036		
18	306.522	43.	10.0049	68.	3.67595	93.	2.05969		
19	254.778	44.	9.02738	69.	3.71916	94.	1.98851		
20	216.155	45.	8.73705	70.	3.78382	95.	1.93551		
21	186.429	46.	8.66897	71.	3.84303	96.	1.92261		
22	160.246	47.	8.57976	72.	3.9038	97.	1.95447		
23	134.614	48.	8.4663	73.	3.97048	98.	2.01897		
24	110.098	49.	8.37568	74.	3.99286	99.	2.07523		

END AT LINE 9999

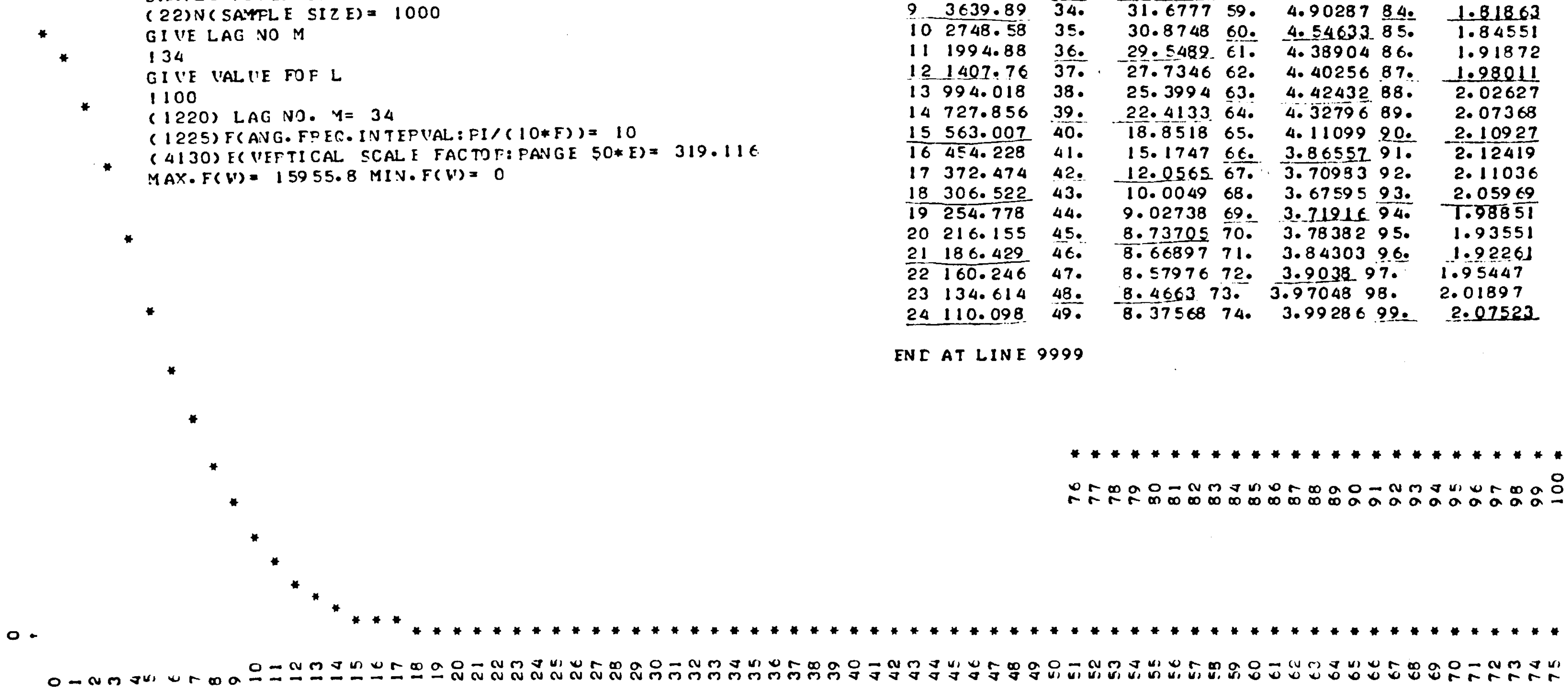

Fig 11.1 Spectrum representing the surface of a grinding wheel after 30 seconds wear

Data MJ36IA

```
ERI LOGIN STHUMP
STHUMP (4) LOGGED IN AT  15'44 56275
WELCOME STHUMP

OK, LBASIC
GO
>LOAD 'MACJ04'

>RUN
SAMPLE POWER SPECTRAL DENSITY FUNCTION F(W)
(22)N(SAMPLE SIZE)= 1000
GIVE LAG NO M
?34
GIVE VALUE FOR L
?100
(1220) LAG NO. M= 34
(1225)F(ANG.FREQ.INTERVAL:PI/(10*F))= 10
(4130)E(VERTICAL SCALE FACTOR:RANGE 50*E)= 48.3657
MAX.F(W)= 2418.29 MIN.F(W)= 0
```

```
VALUES OF F(W)
 0  2418.29   25.   98.7854 50.   66.2685 75.   36.3002
 1  2277.62   26.   91.9423 51.   56.7918 76.   28.9891
 2  1899.27   27.   92.0069 52.   53.4654 77.   27.5508
 3  1394.91   28.   91.651  53.   50.6363 78.   26.402
 4  396.706   29.   89.5393 54.   48.5798 79.   25.3336
 5  506.269   30.   84.9547 55.   47.3379 80.   26.0134
 6  264.74    31.   78.0391 56.   46.7527 81.   26.9957
 7  154.573   32.   69.7423 57.   46.5943 82.   28.6856
 8  125.775   33.   61.5955 58.   46.7156 83.   30.7578
 9  128.025   34.   55.0152 59.   47.5618 84.   32.6989
10  131.326   35.   52.2385 60.   47.5946 85.   33.959
11  128.518   36.   52.7593 61.   48.5755 86.   33.9664
12  124.87    37.   56.154  62.   48.5158 87.   32.8538
13  125.681   38.   60.6678 63.   46.8739 88.   30.9944
14  130.245   39.   64.7754 64.   44.3512 89.   29.5747
15  133.592   40.   67.4377 65.   40.4217 90.   27.7538
16  131.628   41.   68.6243 66.   35.8714 91.   27.1645
17  124.435   42.   68.9635 67.   31.5949 92.   27.3746
18  115.499   43.   69.1377 68.   28.4875 93.   28.568
19  108.495   44.   69.4254 69.   27.5554 94.   29.5447
20  104.753   45.   69.6171 70.   27.2245 95.   30.3033
21  102.878   46.   69.3212 71.   28.4529 96.   31.0354
22  101.529   47.   68.2216 72.   29.9332 97.   33.9199
23  98.2307   48.   66.2448 73.   30.9398 98.   35.9596
24  95.0811   49.   63.514  74.   31.565  99.   37.5311

END AT LINE 9999
>LIST 1000
1000  DATA 175,197,191,120,130,153
>
QUIT

OK,
```

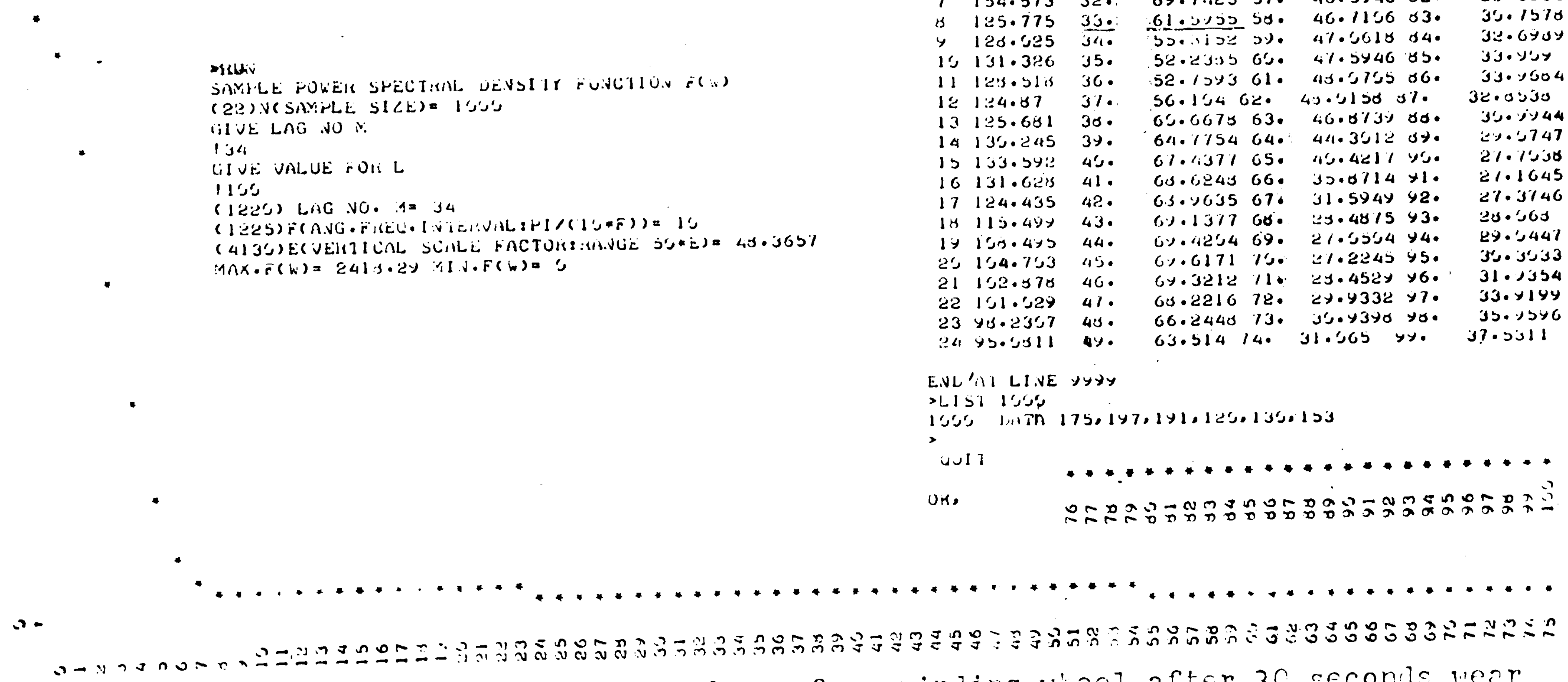

Fig 11.2 Spectrum representing the surface of a grinding wheel after 30 seconds wear

Data MJ44IA

VALUES OF F(W)

0	3817.51	25.25	125.835	50.5	53.9846	75.75	23.6391
1	3593.18	26.25	133.682	51.5	53.1286	76.75	24.9327
2	2989.93	27.25	140.574	52.5	51.3533	77.75	26.7495
3	2186.17	28.25	143.284	53.5	48.9959	78.75	28.3295
4	1393.13	29.25	140.13	54.5	46.5269	79.75	28.9528
5	773.356	30.25	131.547	55.5	44.2814	80.75	28.2933
6	392.619	31.25	119.491	56.5	42.2796	81.75	26.5956
7	222.452	32.25	106.419	57.5	40.2386	82.75	24.5661
8	181.958	33.25	94.5254	58.5	37.8416	83.75	23.5657
9	189.596	34.25	85.4014	59.5	34.9852	84.75	22.7659
10	194.778	35.25	79.8594	60.5	31.8645	85.75	23.9763
11	187.568	36.25	77.7175	61.5	28.8726	86.75	26.7199
12	175.189	37.25	77.731	62.5	26.4176	87.75	30.8523
13	169.442	38.25	77.9643	63.5	24.7779	88.75	35.3999
14	170.826	39.25	76.6061	64.5	24.5553	89.75	41.466
15	172.854	40.25	72.841	65.5	24.1917	90.75	46.6297
16	169.153	41.25	67.1734	66.5	24.9951	91.75	50.3517
17	158.744	42.25	61.5242	67.5	26.1395	92.75	51.5256
18	145.515	43.25	55.8933	68.5	27.2599	93.75	49.9466
19	134.578	44.25	52.6359	69.5	27.8217	94.75	46.1524
20	126.422	45.25	51.2867	70.5	27.6892	95.75	41.2979
21	121.818	46.25	51.3385	71.5	26.7897	96.75	37.5215
22	119.515	47.25	52.1484	72.5	25.4561	97.75	34.2776
23	118.575	48.25	53.1655	73.5	24.5665	98.75	33.1853
24	120.161	49.25	53.9573	74.5	23.3483	99.75	33.559

```
END AT LINE 9999
>QUIT

OK, LO
STRUMP (4) LOGGED OUT AT  12'16 06270
TIME USED=  1'46  42'44   0'18
GOODBYE
NO UFD ATTACHED.
ER!
```

```
>RUN
SAMPLE POWER SPECTRAL DENSITY FUNCTION F(W)
(22)N(SAMPLE SIZE)= 1000
GIVE LAG NO M
!34
GIVE VALUE FOR L
!100
(1220) LAG NO. M= 34
(1225)F(ANG.FREQ.INTERVAL:PI/(10*F))= 10
(4130)E(VERTICAL SCALE FACTOR:RANGE 50*E)= 76.3501
MAX.F(W)= 3817.51 MIN.F(W)= 0
```

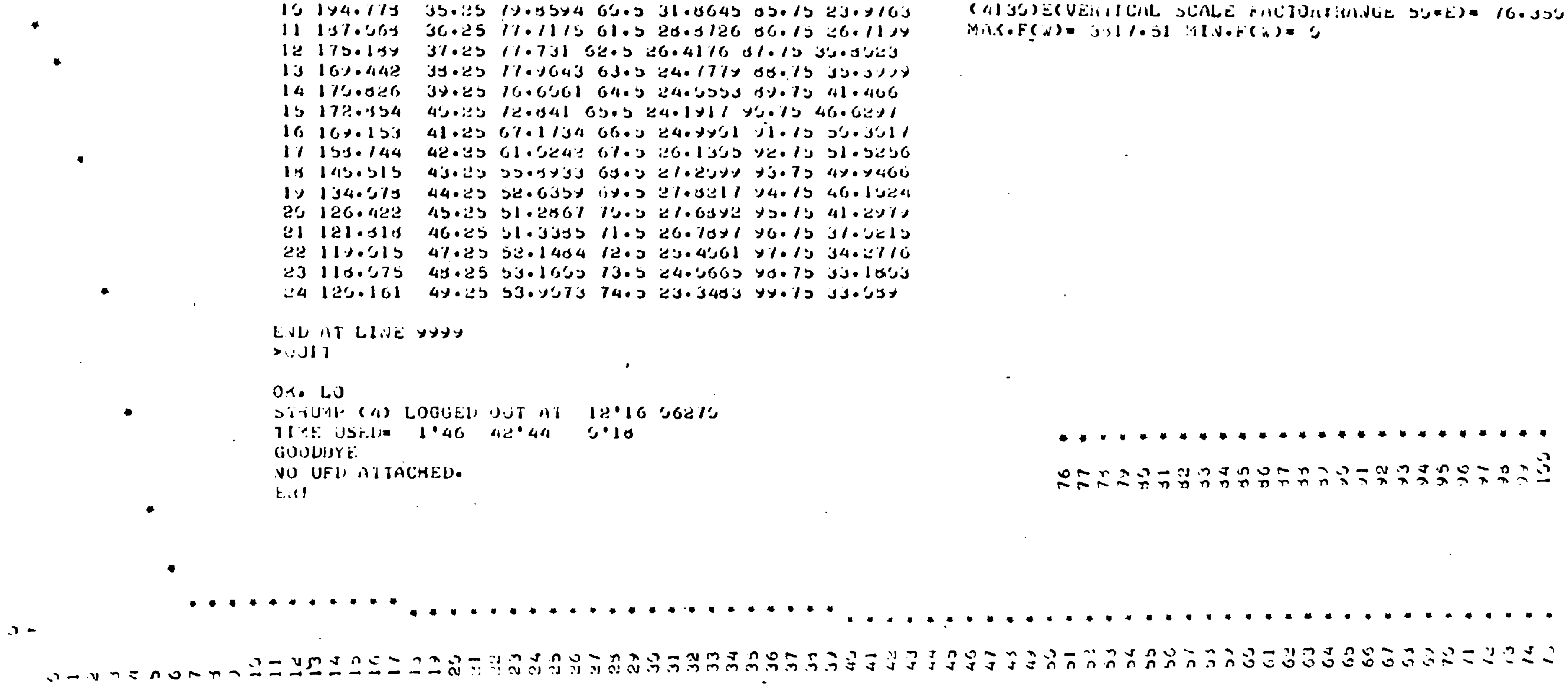

Fig 11.3 Spectrum representing a surface ground for 30 seconds

Data MJ14IA

```
>RUN
SAMPLE POWER SPECTRAL DENSITY FUNCTION F(W)
(22)N(SAMPLE SIZE)= 1000
GIVE LAG NO M
?34
GIVE VALUE FOR L
?100
(1225) LAG NO. M= 34
(1225)F(ANG.FREQ.INTERVAL:PI/(10*F))= 10
(4135)E(VERTICAL SCALE FACTOR:RANGE 50*E)= 339.18
MAX.F(W)= 16959 MIN.F(W)= 0
```

VALUES OF F(W)

0	16959	25.25	71.1715	50.5	6.93692	75.75	2.25195
1	16400.9	26.25	62.9646	51.5	6.62343	76.75	2.1587
2	14885.9	27.25	58.5808	52.5	5.98479	77.75	1.9899
3	12816.4	28.25	54.5042	53.5	5.09747	78.75	1.88763
4	10655.6	29.25	49.3377	54.5	4.33723	79.75	1.91204
5	8739.8	30.25	44.0252	55.5	4.01053	80.75	2.01881
6	7183.33	31.25	39.99	56.5	4.08876	81.75	2.10336
7	5911.08	32.25	37.2998	57.5	4.27133	82.75	2.09031
8	4777.55	33.25	34.5932	58.5	4.25786	83.75	1.98711
9	3688.74	34.25	30.5559	59.5	3.99783	84.75	1.83491
10	2656.44	35.25	25.3394	60.5	3.60799	85.75	1.6904
11	1769.03	36.25	20.4558	61.5	3.43769	86.75	1.57849
12	1116.12	37.25	17.3979	62.5	3.3255	87.75	1.46599
13	724.938	38.25	16.4191	63.5	3.18155	88.75	1.36743
14	546.037	39.25	16.3981	64.5	2.92665	89.75	1.3222
15	436.514	40.25	15.9699	65.5	2.65445	90.75	1.32764
16	459.763	41.25	14.602	66.5	2.34023	91.75	1.33502
17	418.242	42.25	12.7757	67.5	2.22071	92.75	1.45711
18	355.423	43.25	11.3207	68.5	2.19802	93.75	1.52596
19	286.194	44.25	10.5338	69.5	2.15699	94.75	1.57212
20	225.278	45.25	10.0945	70.5	2.05456	95.75	1.60203
21	177.459	46.25	9.55516	71.5	1.94825	96.75	1.60398
22	139.938	47.25	8.63089	72.5	1.94265	97.75	1.58005
23	109.716	48.25	7.76207	73.5	2.06389	98.75	1.54259
24	86.4741	49.25	7.25471	74.5	2.20857	99.75	1.5528

END AT LINE 9999

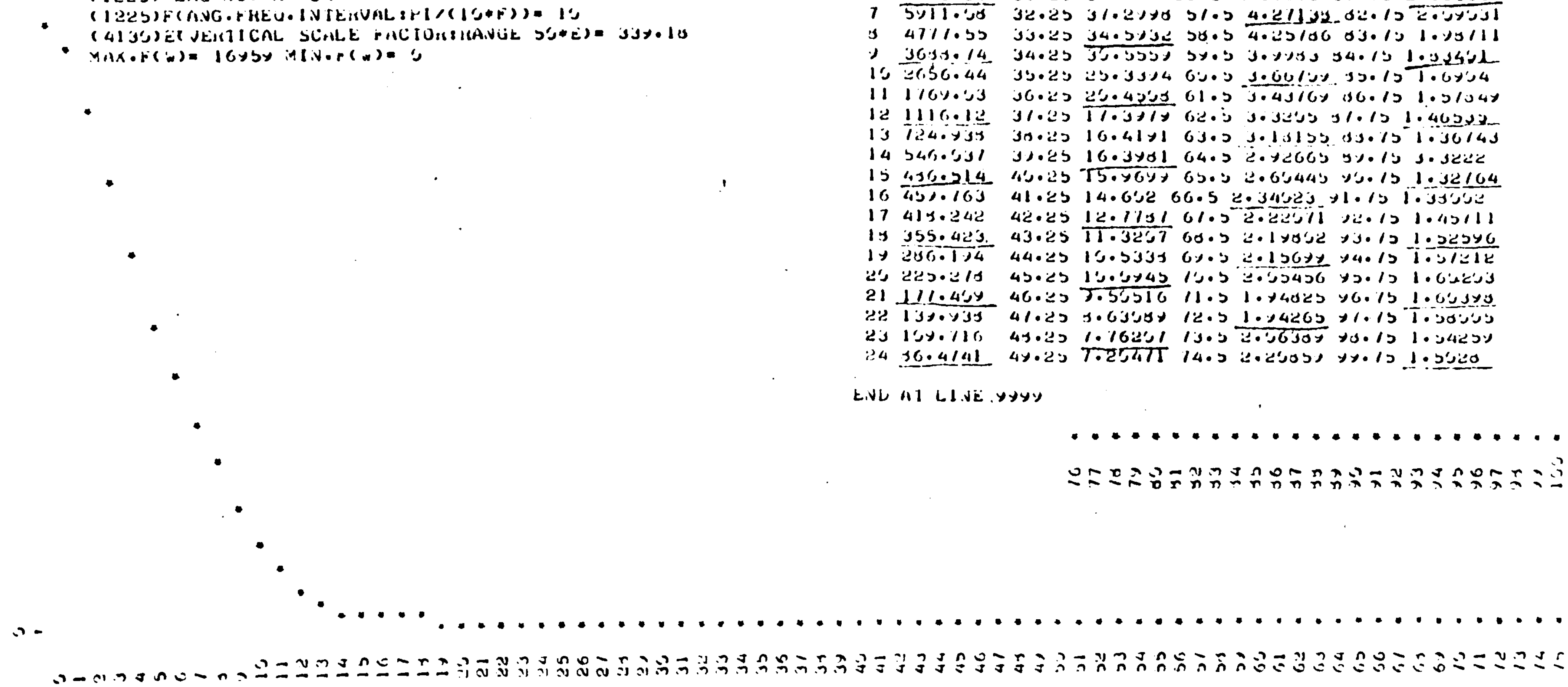

Fig 11.4 Spectrum representing the surface of a grinding wheel after 5 minutes wear

Data MJ20IA

```
*RUN
SAMPLE POWER SPECTRAL DENSITY FUNCTION F(W)
(22)N(SAMPLE SIZE)=1100
GIVE LAG NO M
122
GIVE VALUE FOR L
1100
(1220) LAG NO. M= 22
(1225)F(ANG.FREQ.INTERVAL:PI/(10*F))= 10
(4130)E(VERTICAL SCALE FACTOR:RANGE 50*E)= 124.685
MAX.F(W)= 6234.26 MIN.F(W)= 0
```

VALUES OF F(W)

0	6234.26	2[illegible]	213.137	50.	32.0211[illegible]	7[illegible]	7.[illegible]
1	6[illegible]0.91	2[illegible]	189.11	5[illegible]	29.6908	76.	[illegible]
2	59[illegible].5	27.	170.245	52.	26.9521	7[illegible]	7.730[illegible]
3	5528.91	28.	153.932	53.	24.0745	78.	7.805[illegible]
4	5045.2	29.	13[illegible].482	54.	21.3121	79.	7.915[illegible]
5	4497.2[illegible]	30.	12[illegible].154	55.	16.[illegible]562	80.	8.06025
6	3926.4	31.	107.967	56.	16.[illegible]234	81.	8.21847
7	3370.7	32.	93.3672	57.	15.2618	82.	8.35206
8	2[illegible]0.4[illegible]	33.	79.[illegible]132	58.	14.1474	83.	8.41757
9	2415.82	34.	68.[illegible]	59.	13.4054	84.	8.37001
10	2[illegible]45.67	35.	57.[illegible]75	60.	12.9271	85.	8.1856
11	1748.7	36.	49.[illegible]523	61.	12.5907	86.	7.86418
12	1515.64	37.	42.[illegible]548	62.	12.282	87.	7.41236
13	1[illegible]2.46	38.	37.7[illegible]24	63.	11.9076	88.	6.86783
14	11[illegible]3.7	39.	33.7617	64.	11.4185	89.	6.27535
15	1055.44	40.	31.[illegible]17	65.	10.8113	90.	5.67176
16	927.348	41.	29.[illegible]65	66.	10.1191	91.	5.09412
17	8[illegible]3.566	42.	29.1[illegible]13	67.	9.41175	92.	4.56762
18	71[illegible].55	43.	29.7[illegible]39	68.	8.76192	93.	4.10632
19	6[illegible].007	44.	30.8942	69.	8.23339	94.	3.7152
20	507.336	45.	32.3554	70.	7.86263	95.	3.39308
21	42[illegible].323	46.	33.67[illegible]9	71.	7.649	96.	3.13484
22	347.40[illegible]	47.	34.4[illegible]65	72.	7.56243	97.	2.9378[illegible]
23	289.469	48.	34.5[illegible]	73.	7.55978	98.	2.8005[illegible]
24	245.526	49.	33.6911	74.	7.59359	99.	2.7183[illegible]

END AT LINE 9999

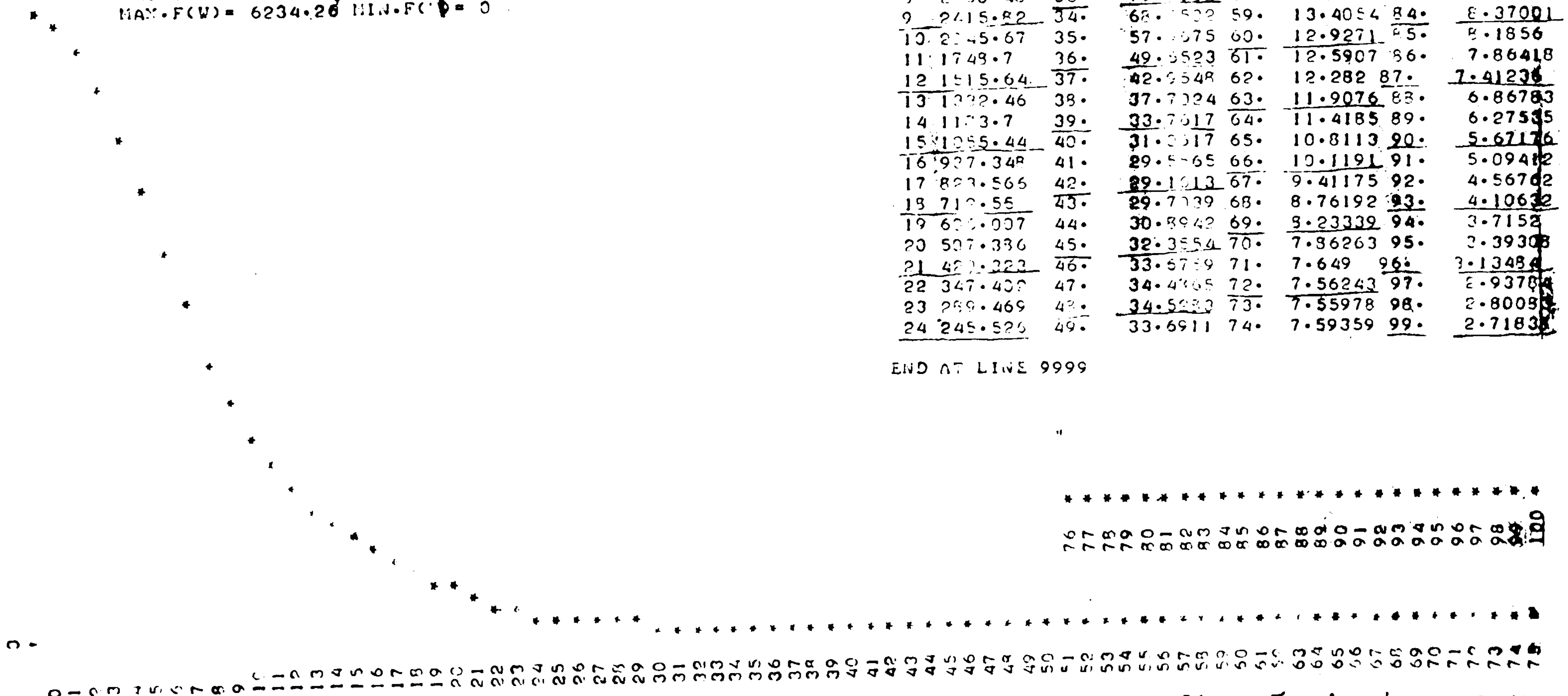

Fig 11.5 Spectrum representing the surface of a grinding wheel after 5 minutes wear

Data MJ40IA

```
>RUN
SAMPLE POWER SPECTRAL DENSITY FUNCTION F(W)
(22)N(SAMPLE SIZE)= 1000
GIVE LAG NO M
!34
GIVE VALUE FOR L
!100
(1220) LAG NO. M= 34
(1225)F(ANG.FREQ.INTERVAL:PI/(10*F))= 10
(4130)E(VERTICAL SCALE FACTOR:RANGE 50*E)= 19.8857
MAX.F(W)= 994.284 MIN.F(W)= 0
```

VALUES OF F(W)

0	994.284	25.25	102.914	50.5	42.0185	75.75	51.7312
1	962.185	26.25	100.84	51.5	42.4582	76.75	51.8393
2	874.222	27.25	99.3496	52.5	43.2086	77.75	48.8981
3	752.082	28.25	97.6642	53.5	43.7767	78.75	43.8526
4	622.489	29.25	95.2011	54.5	43.7592	79.75	38.7266
5	507.989	30.25	91.7221	55.5	43.1023	80.75	35.7651
6	420.876	31.25	87.207	56.5	42.1591	81.75	36.4225
7	362.271	32.25	81.7147	57.5	41.4863	82.75	40.6911
8	325.475	33.25	75.4204	58.5	41.4932	83.75	47.0987
9	300.988	34.25	68.7726	59.5	42.1771	84.75	53.3533
10	280.556	35.25	62.546	60.5	43.1186	85.75	57.323
11	259.054	36.25	57.626	61.5	43.7489	86.75	57.8769
12	234.515	37.25	54.605	62.5	43.7113	87.75	55.2204
13	207.381	38.25	53.4547	63.5	43.0672	88.75	50.6298
14	179.713	39.25	53.5165	64.5	42.2096	89.75	45.7649
15	154.454	40.25	53.843	65.5	41.5483	90.75	41.9351
16	134.523	41.25	53.6628	66.5	41.2034	91.75	39.6663
17	121.721	42.25	52.685	67.5	40.9498	92.75	38.7151
18	115.902	43.25	51.0829	68.5	40.4664	93.75	38.4353
19	114.964	44.25	49.229	69.5	39.7165	94.75	38.2356
20	115.81	45.25	47.4169	70.5	39.161	95.75	37.8649
21	115.777	46.25	45.7542	71.5	39.5871	96.75	37.4064
22	113.701	47.25	44.2571	72.5	41.6016	97.75	37.069
23	110.033	48.25	43.0066	73.5	45.0884	98.75	36.9593
24	106.07	49.25	42.1975	74.5	49.0053	99.75	37.0033

```
END AT LINE 9999
```

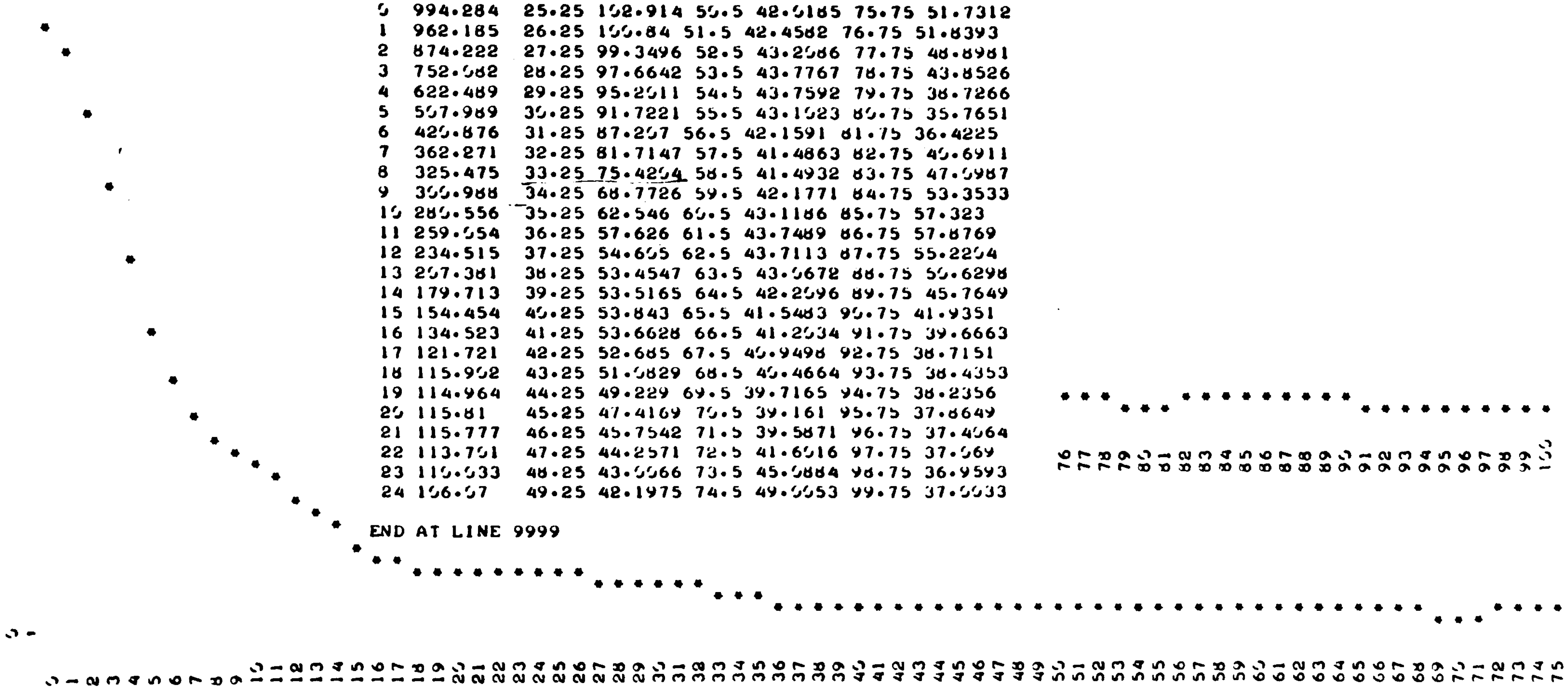

Fig 11.6 Spectrum representing a surface ground for 5 minutes

Data MJ26IA

```
>RUN
SAMPLE POWER SPECTRAL DENSITY FUNCTION F(W)
(22)N(SAMPLE SIZE)= 1000
GIVE LAG NO M
!22.
GIVE VALUE FOR L
!100
(1220) LAG NO. M= 22
(1225)F(ANG.FREQ.INTERVAL:PI/(10*F))= 10
(4130)E(VERTICAL SCALE FACTOR:RANGE 50*E)= 105.598
MAX.F(W)= 5279.92 MIN.F(W)= 0
```

VALUES OF F(W)

0	5279.92	25.	70.8155	50.	5.85019	75.	2.25304
1	5231.92	26.	61.0608	51.	5.14363	76.	2.18038
2	5089.37	27.	53.8864	52.	4.60197	77.	2.07298
3	4856.85	28.	48.0879	53.	4.23999	78.	1.96006
4	4542.54	29.	42.8353	54.	4.01579	79.	1.86176
5	4158.8	30.	37.7777	55.	3.8435	80.	1.7908
6	3722.24	31.	32.9688	56.	3.63974	81.	1.74596
7	3253.19	32.	28.6726	57.	3.36168	82.	1.71426
8	2774.24	33.	25.15	58.	3.01151	83.	1.6803
9	2308.16	34.	22.4915	59.	2.63632	84.	1.63048
10	1875.41	35.	20.5787	60.	2.30192	85.	1.56629
11	1491.87	36.	19.1317	61.	2.06365	86.	1.49853
12	1167.26	37.	17.8324	62.	1.94607	87.	1.42968
13	904.514	38.	16.4518	63.	1.92968	88.	1.37201
14	700.406	39.	14.9149	64.	1.97288	89.	1.33199
15	547.035	40.	13.3038	65.	2.0293	90.	1.30044
16	433.942	41.	11.7926	66.	2.05891	91.	1.27083
17	350.273	42.	10.5523	67.	2.05713	92.	1.23742
18	286.542	43.	9.67201	68.	2.037	93.	1.19553
19	235.695	44.	9.1183	69.	2.02511	94.	1.14991
20	193.367	45.	8.76378	70.	2.0457	95.	1.10414
21	157.477	46.	8.43661	71.	2.10127	96.	1.0652
22	127.409	47.	7.99746	72.	2.17649	97.	1.03785
23	103.126	48.	7.38664	73.	2.24426	98.	1.02433
24	84.4713	49.	6.63695	74.	2.27363	99.	1.01803

```
END AT LINE 9999
>QUIT

OK, LO
STHIMP (5) LOGGED OUT AT  11'10 26060
TIME USED=  1'03  13'36   0'11
GOODBYE
NO UFD ATTACHED.
ER!
```

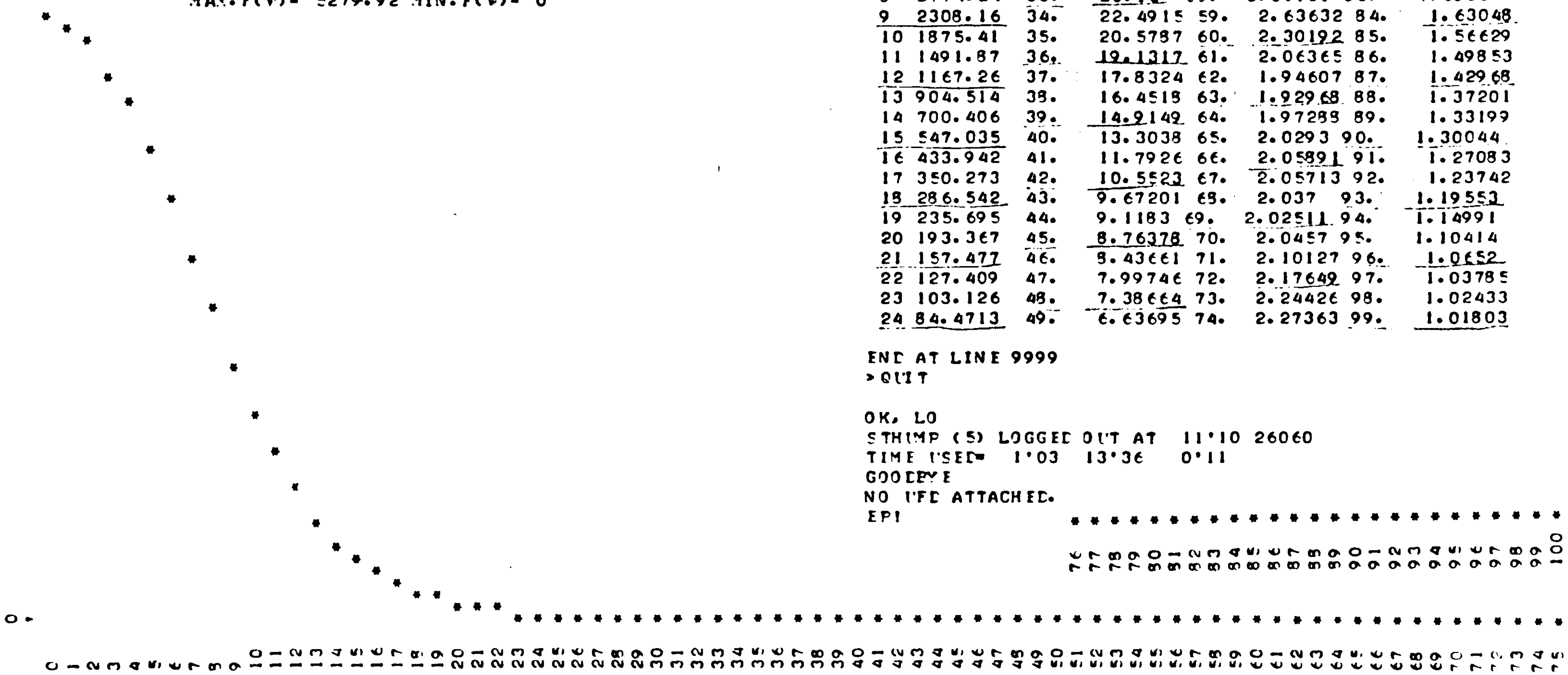

Fig 11.7 Spectrum representing the surface of a grinding wheel after 10 minutes wear

Data MJ32IA

```
     LOGIN STHIMP
STHIMP (5) LOGGEE IN AT  11'11 26060
WELCOME STHIMP

OK, LBASIC
GO
>LOAD 'MACJ04'
>RIN
SAMPLE POWER SPECTRAL DENSITY FUNCTION F(W)
(22)N(SAMPLE SIZE)= 1000
GIVE LAG NO M
!34
GIVE VALUE FOR L
!100
(1220) LAG NO. M= 34
(1225)F(ANG.FREQ.INTERVAL:PI/(10*F))= 10
(4130)E(VERTICAL SCALE FACTOR:RANGE 50*E)= 62.0301
MAX.F(W)= 3101.51 MIN.F(W)= 0
```

VALUES OF F(W)

0	3101.51	25.	141.109	50.	10.8689	75.	2.98392
1	3059.33	26.	125.244	51.	9.57137	76.	2.67338
2	2941.23	27.	119.898	52.	8.27318	77.	2.39121
3	2770.67	28.	119.865	53.	7.21249	78.	2.15901
4	2580.28	29.	119.432	54.	6.47873	79.	1.99239
5	2402.35	30.	114.443	55.	6.0475	80.	1.89844
6	2257.69	31.	103.526	56.	5.84156	81.	1.8679
7	2147.47	32.	88.0364	57.	5.76191	82.	1.86595
8	2052.36	33.	70.8999	58.	5.69391	83.	1.8567
9	1941.14	34.	55.0816	59.	5.53444	84.	1.82329
10	1785.57	35.	42.4668	60.	5.23478	85.	1.78016
11	1574.65	36.	33.5425	61.	4.83441	86.	1.76337
12	1320.99	37.	27.7441	62.	4.44305	87.	1.79679
13	1055.98	38.	24.0513	63.	4.17152	88.	1.88647
14	816.59	39.	21.4632	64.	4.06366	89.	2.01501
15	630.598	40.	19.2514	65.	4.08161	90.	2.15341
16	507.374	41.	17.0461	66.	4.13749	91.	2.28187
17	437.703	42.	14.8432	67.	4.16663	92.	2.39152
18	401.061	43.	12.921	68.	4.15101	93.	2.47498
19	375.596	44.	11.6416	69.	4.1071	94.	2.5227
20	345.933	45.	11.2014	70.	4.04656	95.	2.52472
21	306.259	46.	11.4561	71.	3.95517	96.	2.47879
22	259.005	47.	11.9613	72.	3.80503	97.	2.39929
23	211.133	48.	12.1953	73.	3.5827	98.	2.31124
24	170.14	49.	11.8311	74.	3.29757	99.	2.24379

```
END AT LINE 9999
>QUIT

OK, LO
STHIMP (5) LOGGEE OUT AT  11'37 26060
TIME USED=  0'26   8'27   0'01
GOODBYE
```

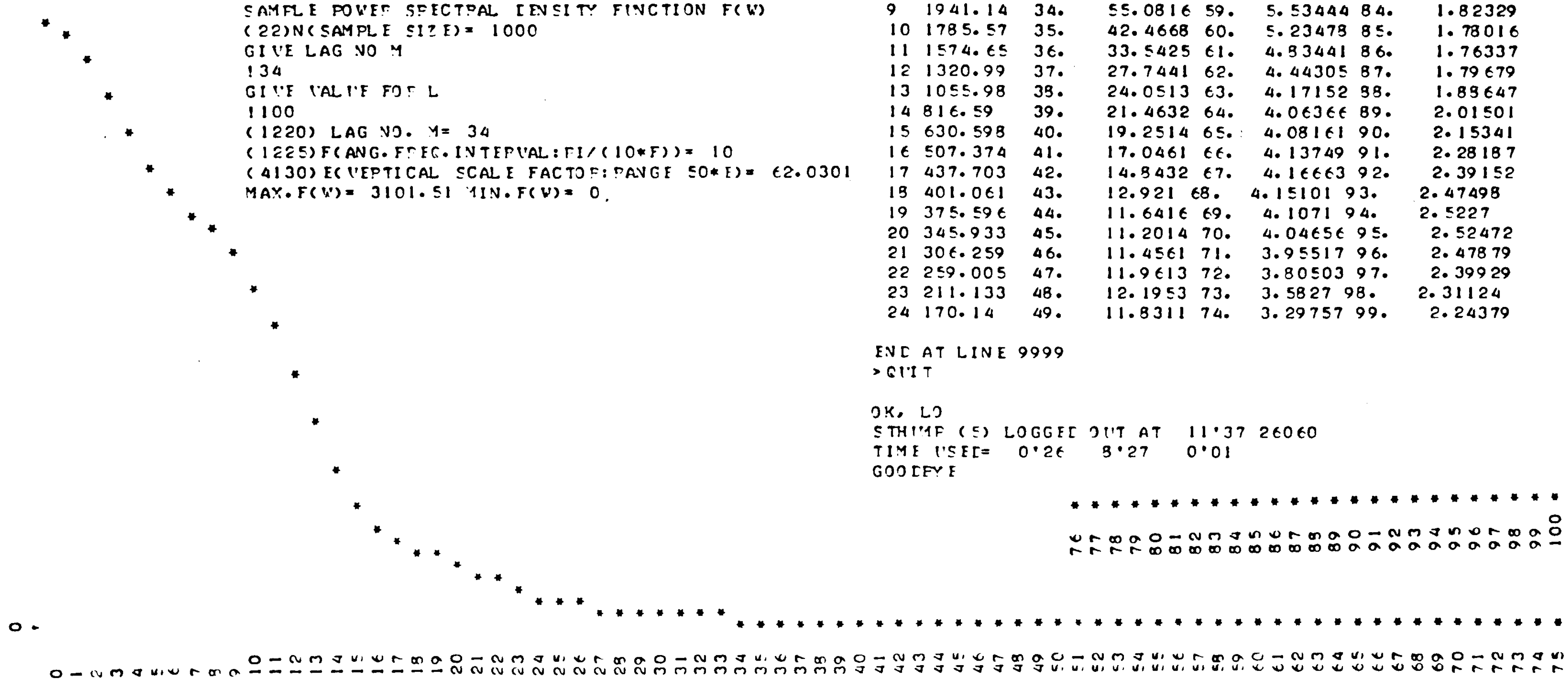

Fig 11.8 Spectrum representing the surface of a grinding wheel after 10 minutes wear

Data MJ48IA

VALUES OF F(W)

0	504.506	25.25	67.2985	50.5	19.3753	75.75	15.5911
1	475.257	26.25	63.512	51.5	19.1048	76.75	15.0928
2	396.989	27.25	58.1481	52.5	18.9654	77.75	14.8426
3	293.888	28.25	52.2927	53.5	18.5932	78.75	14.8529
4	194.363	29.25	47.1583	54.5	17.8562	79.75	15.1467
5	119.843	30.25	43.56	55.5	16.7235	80.75	15.7483
6	78.2619	31.25	41.5779	56.5	15.7149	81.75	16.6419
7	64.6139	32.25	40.6072	57.5	16.2084	82.75	17.7246
8	66.9415	33.25	39.7536	58.5	15.4632	83.75	18.7949
9	73.6084	34.25	38.3236	59.5	16.4275	84.75	19.5958
10	77.9632	35.25	36.1186	60.5	17.7588	85.75	19.9058
11	78.8584	36.25	33.4059	61.5	18.9574	86.75	19.6266
12	78.1695	37.25	30.6645	62.5	19.6513	87.75	18.8193
13	77.7819	38.25	28.316	63.5	19.7054	88.75	17.6697
14	78.0105	39.25	26.5924	64.5	19.2825	89.75	16.3959
15	77.8788	40.25	25.5526	65.5	18.7227	90.75	15.1572
16	76.3581	41.25	25.1398	66.5	18.3527	91.75	14.018
17	73.3478	42.25	25.2014	67.5	18.3251	92.75	12.9778
18	69.7553	43.25	25.4745	68.5	18.5668	93.75	12.0369
19	66.8593	44.25	25.6074	69.5	18.847	94.75	11.2483
20	65.5506	45.25	25.2716	70.5	18.9155	95.75	10.711
21	65.9283	46.25	24.3203	71.5	18.6274	96.75	10.5064
22	67.3462	47.25	22.8884	72.5	17.996	97.75	10.6279
23	68.7319	48.25	21.3439	73.5	17.1617	98.75	10.9502
24	68.9775	49.25	20.0968	74.5	16.3092	99.75	11.2705

```
END AT LINE 9999
>LIST 1000
1000  DATA 98,125,85,127,138,139
>
```

```
>RUN
SAMPLE POWER SPECTRAL DENSITY FUNCTION F(W)
(220)N(SAMPLE SIZE)= 1000
GIVE LAG NO M
?34
GIVE VALUE FOR L
?100
(1220) LAG NO. M= 34
(1285)F(ANG.FREQ.INTERVAL:PI/(10*F))= 10
(4130)E(VERTICAL SCALE FACTOR:RANGE 50*E)= 10.0901
MAX.F(W)= 504.506 MIN.F(W)= 0
```

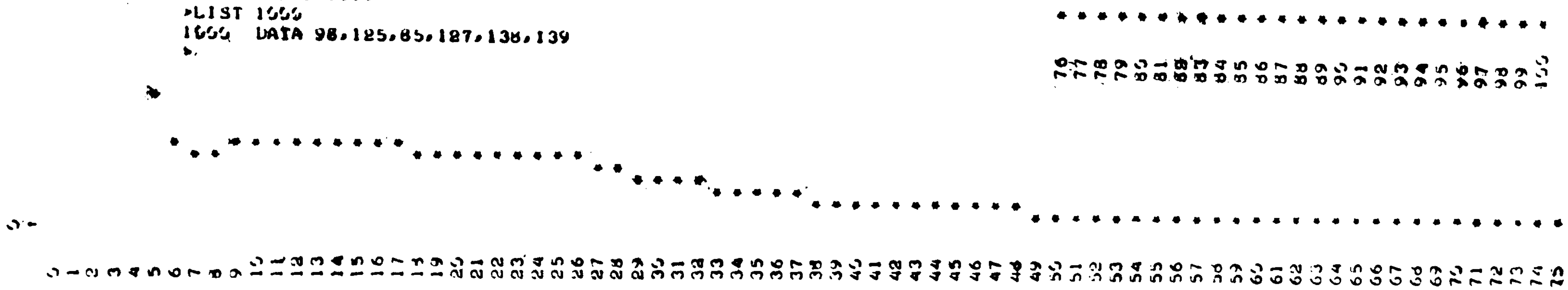

Fig 11.9 Spectrum representing a surface ground for 10 minutes

Table 11.3 Transfer Coefficients (Y^2) relating Spectral Densities of Variance at Frequency X

Frequency mm^{-1} X	Y^2 (F_1/A_1)	Y^2 (M_2/Q_1)	Y^2 (G_1/K_1)	Y^2 (G_1/F_1)	Y^2 (K_1/A_1)
0.0	0.007	0.002	0.003	0.132	0.331
0.5	0.008	0.002	0.003	0.132	0.389
1.0	0.012	0.003	0.003	0.133	0.522
1.5	0.017	0.006	0.004	0.135	0.634
2.0	0.028	0.016	0.005	0.140	0.829
2.5	0.039	0.030	0.006	0.156	0.972
3.0	0.036	0.034	0.008	0.198	0.935
3.5	0.034	0.058	0.012	0.292	0.845
4.0	0.047	0.107	0.022	0.367	0.767
4.5	0.087	0.146	0.039	0.392	0.881
5.0	0.141	0.181	0.058	0.400	0.966
5.5	0.165	0.212	0.090	0.426	0.781
6.0	0.169	0.326	0.115	0.442	0.647
6.5	0.213	0.359	0.148	0.462	0.665
7.0	0.400	0.399	0.208	0.457	0.874
7.5	0.560	0.432	0.251	0.452	1.006
8.0	0.565	0.493	0.291	0.451	0.876
8.5	0.565	0.524	0.408	0.465	0.644
9.0	0.658	0.759	0.494	0.481	0.642
9.5	0.667	0.765	0.563	0.500	0.593
10.0	0.971	0.900	0.795	0.515	0.506
10.5	0.786	1.033	0.973	0.545	0.440
11.0	0.865	1.356	0.923	0.563	0.527
11.5	0.901	1.439	0.949	0.578	0.549
12.0	0.878	1.541	0.902	0.569	0.554
12.5	0.907	1.302	0.837	0.529	0.573
13.0	1.220	1.500	0.919	0.472	0.627
13.5	1.854	1.350	0.939	0.408	0.805
14.0	2.200	1.514	0.903	0.364	0.886
14.5	2.000	1.821	0.926	0.328	0.711
15.0	1.775	2.000	0.960	0.338	0.625
15.5	1.667	1.620	0.957	0.338	0.590
16.0	1.541	1.419	1.100	0.386	0.541
16.5	1.275	1.414	1.105	0.412	0.475
$\Sigma Y^2 =$	23.258	25.063	15.919	12.958	23.208

Table 11.4 $\sqrt{\text{Transfer Coefficient of Variance Density}}$

(see Table 7.3)

X	$\sqrt{F_1/A_1}$ Y	$\sqrt{M_2/Q_1}$ Y	$\sqrt{G_1/K_1}$ Y	$\sqrt{G_1/F_1}$ Y	$\sqrt{K_1/A_1}$ Y
0.0	0.082	0.041	0.052	0.363	0.575
0.5	0.090	0.046	0.053	0.364	0.623
1.0	0.109	0.058	0.055	0.364	0.722
1.5	0.131	0.076	0.060	0.367	0.796
2.0	0.167	0.126	0.069	0.374	0.911
2.5	0.197	0.172	0.079	0.394	0.986
3.0	0.191	0.183	0.088	0.445	0.967
3.5	0.184	0.241	0.108	0.540	0.919
4.0	0.216	0.327	0.150	0.606	0.876
4.5	0.296	0.382	0.197	0.626	0.939
5.0	0.375	0.426	0.242	0.632	0.983
5.5	0.406	0.461	0.300	0.652	0.884
6.0	0.411	0.571	0.340	0.665	0.804
6.5	0.462	0.599	0.385	0.679	0.816
7.0	0.632	0.632	0.457	0.676	0.935
7.5	0.748	0.657	0.501	0.672	1.003
8.0	0.752	0.702	0.539	0.671	0.936
8.5	0.752	0.734	0.639	0.682	0.803
9.0	0.811	0.871	0.703	0.694	0.801
9.5	0.816	0.875	0.750	0.707	0.770
10.0	0.986	0.949	0.892	0.717	0.711
10.5	0.886	1.016	0.986	0.739	0.664
11.0	0.930	1.164	0.961	0.750	0.726
11.5	0.949	1.200	0.974	0.760	0.741
12.0	0.937	1.241	0.950	0.754	0.744
12.5	0.952	1.141	0.915	0.728	0.757
13.0	1.105	1.225	0.958	0.687	0.792
13.5	1.361	1.162	0.969	0.639	0.897
14.0	1.483	1.231	0.950	0.603	0.941
14.5	1.414	1.350	0.962	0.574	0.843
15.0	1.332	1.414	0.980	0.581	0.791
15.5	1.291	1.273	0.978	0.582	0.768
16.0	1.241	1.191	1.048	0.621	0.735
16.5	1.129	1.189	1.051	0.642	0.689
ΣY =	23.824	24.926	19.341	20.550	27.848
$\bar{Y}$ =	0.7007	0.733	0.569	0.604	0.819

Table 11.5 Frequency × Transfer Coefficient

(see Table 7.4)

X	X×Y	X×Y	X×Y	X×Y	X×Y
0.0	0.000	0.000	0.000	0.000	0.000
0.5	0.045	0.023	0.027	0.182	0.312
1.0	0.109	0.058	0.055	0.364	0.722
1.5	0.197	0.114	0.090	0.550	1.194
2.0	0.334	0.252	0.138	0.747	1.821
2.5	0.493	0.430	0.198	0.986	2.464
3.0	0.573	0.549	0.264	1.335	2.901
3.5	0.644	0.844	0.378	1.890	3.217
4.0	0.864	1.308	0.600	2.424	3.504
4.5	1.332	3.690	0.887	2.818	4.223
5.0	1.875	2.130	1.210	3.162	4.915
5.5	2.233	2.536	1.650	3.589	4.862
6.0	2.466	3.426	2.040	3.989	4.824
6.5	3.003	3.894	2.503	4.416	5.301
7.0	4.424	4.424	3.199	4.730	6.544
7.5	5.610	4.928	3.758	5.040	7.523
8.0	6.016	5.616	4.312	5.370	7.487
8.5	6.392	6.239	5.432	5.797	6.825
9.0	7.299	7.839	6.327	6.242	7.209
9.5	7.752	8.313	7.125	6.718	7.313
10.0	9.860	9.490	8.920	7.174	7.111
10.5	9.303	10.668	10.353	7.755	6.969
11.0	10.230	12.804	10.571	8.250	7.986
11.5	10.914	13.800	11.201	8.744	8.523
12.0	11.244	14.892	11.400	9.054	8.932
12.5	11.900	14.263	11.438	9.095	9.465
13.0	14.365	15.925	12.454	8.933	10.295
13.5	18.374	15.687	13.082	8.622	12.112
14.0	20.762	17.234	13.300	8.442	13.176
14.5	20.503	19.575	13.949	8.316	12.222
15.0	19.980	21.210	14.700	8.721	11.859
15.5	20.011	19.732	15.159	9.018	11.903
16.0	19.856	19.056	16.768	9.940	11.763
16.5	18.629	19.619	17.342	10.588	11.372
ΣX×Y =	267.592	280.568	220.830	183.001	226.849

Table 11.6

Spectrum	Σy^2	$(\Sigma y)^2$	$(\Sigma y)^2/n$	S_{yy}	Σxy	$\Sigma x \Sigma y/n$	S_{xy}
$\sqrt{F_1/A_1}$	23.258	567.583	16.694	6.564	267.592	196.548	71.044
$\sqrt{M_2/Q_1}$	25.063	621.305	18.274	6.789	280.568	205.640	74.929
$\sqrt{G_1/K_1}$	15.919	374.074	11.002	4.917	220.830	159.563	61.267
$\sqrt{G_1/F_1}$	12.958	422.303	12.421	0.537	183.001	169.538	13.464
$\sqrt{K_1/A_1}$	23.208	775.511	22.809	0.399	226.849	229.746	-2.897

Table 11.7

Spectrum	$\hat{b}$	$\bar{y}$	$\hat{b}x$	$\hat{a}$	y (x=0)	y (x=16)	$S^2_{y/x}$
$\sqrt{F_1/A_1}$	0.086	0.7007	0.713	-0.012	-0.012	1.364	0.0133
$\sqrt{M_2/Q_1}$	0.091	0.733	0.751	-0.018	-0.018	1.438	-0.0012
$\sqrt{G_1/K_1}$	0.075	0.569	0.619	-0.050	-0.050	1.150	0.0110
$\sqrt{G_1/F_1}$	0.016	0.604	0.135	0.469	0.469	0.725	0.0099
$\sqrt{K_1/A_1}$	-0.0035	0.819	-0.029	0.848	0.848	0.792	0.0120

Table 11.8

Column	1	2	3	4	5	6	7	
	Frequency						95% Confidence Limits	
	x	$S^2_{y/x}$	$S^2_{y/x}\left(1+\frac{1}{n}+\frac{(x-\bar{x})^2}{S_{xx}}\right)$	$\sqrt{\text{Col.3}}$	t_{n-2} (Col.4)	y	y ± (Column 5)	
$\sqrt{F_1/A_1}$	0.0	0.0133	0.015	0.122	0.248	-0.012	0.236	-0.260
	4.0	0.0133	0.014	0.118	0.241	0.332	0.573	0.091
	8.0	0.0133	0.014	0.117	0.237	0.676	0.915	0.439
	16.0	0.0133	0.015	0.121	0.247	1.364	1.611	1.117
$\sqrt{G_1/K_1}$	1.0	0.0110	0.012	0.110	0.224	0.025	0.249	-0.199
	8.0	0.0110	0.011	0.106	0.217	0.550	0.767	0.333
	16.0	0.0110	0.012	0.110	0.225	1.150	1.375	0.925
$\sqrt{G_1/F_1}$	0.0	0.0099	0.011	0.105	0.214	0.469	0.683	0.255
	8.0	0.0099	0.010	0.101	0.206	0.597	0.803	0.391
	16.0	0.0099	0.010	0.101	0.206	0.725	0.931	0.519
$\sqrt{K_1/A_1}$	0.0	0.0120	0.013	0.116	0.236	0.848	1.084	0.612
	8.0	0.0120	0.012	0.111	0.227	0.820	1.047	0.593
	16.0	0.0120	0.013	0.115	0.235	0.792	1.027	0.557

APPENDIX 12

Table 12.3

Frequency

(mm^{-1})

X	Y^2_{FA}	Y^2_{MQ}	Y^2_{GK}	Y^2_{GF}	Y^2_{KA}
0.0	0.001	0.0003	0.0004	0.067	0.229
0.5	0.002	0.0003	0.0004	0.067	0.284
1.0	0.003	0.0004	0.0004	0.068	0.420
1.5	0.004	0.001	0.001	0.069	0.545
2.0	0.009	0.004	0.001	0.073	0.779
2.5	0.013	0.009	0.001	0.084	0.963
3.0	0.012	0.011	0.002	0.115	0.914
3.5	0.011	0.022	0.003	0.194	0.799
4.0	0.017	0.051	0.006	0.263	0.702
4.5	0.039	0.077	0.013	0.287	0.845
5.0	0.073	0.102	0.022	0.295	0.955
5.5	0.090	0.126	0.040	0.321	0.719
6.0	0.093	0.224	0.056	0.337	0.560
6.5	0.127	0.255	0.078	0.357	0.580
7.0	0.295	0.294	0.123	0.352	0.836
7.5	0.462	0.327	0.158	0.347	1.008
8.0	0.467	0.389	0.193	0.346	0.838
8.5	0.467	0.422	0.303	0.360	0.556
9.0	0.572	0.692	0.391	0.377	0.554
9.5	0.583	0.700	0.465	0.397	0.498
10.0	0.962	0.869	0.736	0.413	0.403
10.5	0.725	1.044	0.964	0.445	0.335
11.0	0.824	1.501	0.899	0.465	0.426
11.5	0.870	1.625	0.933	0.481	0.450
12.0	0.841	1.780	0.872	0.472	0.455
12.5	0.878	1.422	0.789	0.428	0.476
13.0	1.304	1.717	0.893	0.367	0.537
13.5	2.278	1.492	0.920	0.303	0.749
14.0	2.861	1.738	0.873	0.260	0.851
14.5	2.520	2.224	0.903	0.226	0.635
15.0	2.149	2.520	0.947	0.235	0.534
15.5	1.977	1.903	0.943	0.235	0.495
16.0	1.780	1.595	1.136	0.281	0.441
16.5	1.383	1.587	1.142	0.307	0.371
ΣY^2 =	24.692	26.724	14.807	9.694	20.742

Table 12.4

Y^2_{KA}	Frequency (mm^{-1}) X	Frequency × Transfer Coefficient XY_{FA}	XY_{MQ}	XY_{GK}	XY_{GF}	XY_{KA}
0.229	0.0	0.000	0.000	0.000	0.000	0.000
0.284	0.5	0.020	0.008	0.011	0.130	0.267
0.420	1.0	0.052	0.025	0.021	0.261	0.648
0.545	1.5	0.099	0.050	0.038	0.395	1.107
0.779	2.0	0.184	0.126	0.058	0.540	1.764
0.963	2.5	0.288	0.243	0.083	0.725	2.453
0.914	3.0	0.327	0.315	0.120	1.020	2.868
0.799	3.5	0.368	0.525	0.182	1.540	3.129
0.702	4.0	0.520	0.900	0.316	2.052	3.352
0.845	4.5	0.882	1.247	0.518	2.412	4.136
0.955	5.0	1.355	1.600	0.750	2.715	4.885
0.719	5.5	1.355	1.600	0.750	2.715	4.885
0.560	6.0	1.836	2.844	1.416	3.480	4.488
0.580	6.5	2.321	3.283	1.820	3.887	4.953
0.836	7.0	3.801	3.794	2.457	4.151	6.398
1.008	7.5	5.093	4.283	2.985	4.418	7.530
0.838	8.0	5.464	4.992	3.512	4.704	7.328
0.556	8.5	5.806	5.525	4.675	5.100	6.341
0.554	9.0	6.813	7.488	5.625	5.526	6.696
0.498	9.5	7.249	7.942	6.479	5.985	6.707
0.403	10.0	9.810	9.320	8.580	6.420	6.350
0.335	10.5	8.946	10.731	10.311	7.004	6.069
0.426	11.0	9.988	13.475	10.428	7.502	7.172
0.450	11.5	10.730	14.663	11.109	7.981	7.705
0.455	12.0	11.004	16.008	11.208	8.244	8.100
0.476	12.5	11.713	14.900	11.100	8.175	8.625
0.537	13.0	14.846	17.030	12.285	7.878	9.529
0.749	13.5	20.[illegible]73	16.484	12.947	7.425	11.678
0.851	14.0	23.688	18.466	13.076	7.140	12.908
0.635	14.5	23.012	21.620	13.775	6.902	11.557
0.534	15.0	21.990	23.805	14.595	7.275	10.965
0.495	15.5	21.793	21.375	15.051	7.518	10.897
0.441	16.0	21.344	20.208	17.056	8.480	10.624
0.371	16.5	19.404	20.790	17.639	9.141	10.049
20.742	ΣXY =	272.774	286.038	211.332	159.239	211.942

Table 12.5

Transfer Function	ΣY^2	$(\Sigma Y)^2$	$(\Sigma Y)^2/n$	ζ_{yy}	ΣXY	$\Sigma X \Sigma Y/n$	ζ_{xy}
Y_{FA}	24.692	534.719	15.727	8.965	272.774	190.773	82.001
Y_{MQ}	26.724	601.328	17.686	9.038	286.038	202.307	83.731
Y_{GK}	14.807	316.520	9.309	5.498	211.332	146.776	64.556
Y_{GF}	9.694	308.143	9.063	0.631	159.239	144.821	14.418
Y_{KA}	20.742	684.136	20.122	0.620	211.942	215.787	-3.845

Table 12.6

Transfer Function	$\hat{b}$	$\bar{Y}$	$\hat{b}\,\bar{X}$	$\hat{a}$	Y (X=0)	Y (X=16)	$\zeta^2_{Y/X}$
Y_{FA}	0.100	0.680	0.825	-0.145	-0.145	1.455	0.0233
Y_{MQ}	0.102	0.721	0.842	-0.121	-0.121	1.511	0.0146
Y_{GK}	0.079	0.523	0.652	-0.129	-0.129	1.135	0.0126
Y_{GF}	0.018	0.516	0.149	0.367	0.367	0.655	0.0118
Y_{KA}	-0.005	0.769	-0.041	0.810	0.810	0.730	0.0188

Table 12.7

X (frequency)	$\frac{(X-\overline{X})^2}{\zeta_{xx}}$	$1+\frac{1}{n}+\frac{(X-\overline{X})^2}{\zeta_{xx}}$
0.0	0.0827	1.1117
4.0	0.0220	1.051
8.0	0.000077	1.029
16.0	0.073	1.102

Table 12.8

Column	1	2	3	4	5	6	95% Confidence Limits	
Transfer Function	X (frequency)	$\zeta^2_{y/x}$	$\zeta^2_{y/x}\left(1+\frac{1}{n}+\frac{(X-\bar{X})^2}{\zeta_{xx}}\right)$	$\sqrt{\text{Col.3}}$	t_{n-2}(Col.4)	Y	Y ± (Column 5)	
Y_{FA}	0.0	0.0233	0.0259	0.161	0.328	-0.145	0.183	-0.473
	4.0	0.0233	0.0245	0.157	0.320	0.255	0.575	-0.065
	8.0	0.0233	0.0240	0.155	0.316	0.655	0.971	0.339
	16.0	0.0233	0.0257	0.160	0.327	1.455	1.782	1.128
Y_{MQ}	0.0	0.0146	0.0162	0.127	0.259	-0.121	0.138	-0.380
	4.0	0.0146	0.0153	0.124	0.253	0.287	0.540	0.034
	8.0	0.0146	0.0150	0.123	0.251	0.695	0.946	0.444
	16.0	0.0146	0.0161	0.127	0.259	1.511	1.770	1.252
Y_{GK}	0.0	0.0126	0.0140	0.118	0.241	-0.129	0.112	-0.370
	8.0	0.0126	0.0130	0.114	0.233	0.503	0.736	0.270
	16.0	0.0126	0.0139	0.118	0.241	1.135	1.376	0.894
Y_{GF}	0.0	0.0118	0.0131	0.114	0.233	0.367	0.600	0.134
	8.0	0.118	0.0121	0.110	0.224	0.511	0.735	0.287
	16.0	0.118	0.0130	0.114	0.233	0.655	0.888	0.422
Y_{KA}	0.0	0.0188	0.0209	0.145	0.296	0.810	1.106	0.514
	8.0	0.0188	0.0193	0.139	0.284	0.770	1.054	0.486
	16.0	0.0188	0.0207	0.144	0.294	0.730	1.024	0.436